Multilevel Collocation with Radial Basis Functions

Patricio Farrell
University of Oxford
Exeter College

Supervisors:
Prof. Dr. Holger Wendland and Dr. Kathryn Gillow

April 2014
A thesis submitted for the degree of
Doctor of Philosophy

Multilevel Collocation with Radial Basis Functions

Patricio Farrell

University of Oxford

Abstract

In this thesis, we analyse multilevel collocation methods involving compactly supported radial basis functions. We focus on linear second-order elliptic boundary value problems as well as Darcy's problem. While in the former case we use scalar-valued positive definite functions for constructing multilevel approximants, in the latter case we use matrix-valued functions that are automatically divergence-free. A similar result is presented for interpolating divergence-free vector fields. Even though it had been observed more than a decade ago that the stationary setting, i. e. when the support radii shrink as fast as the mesh norm, does not lead to convergence [23], it was up to now an open question how the support radii should depend on the mesh norm to ensure convergence. For each case above, we answer this question here thoroughly. Furthermore, we analyse and improve the stability of the linear systems. And lastly, we examine the case when the approximant does not lie in the same space as the solution to the PDE.

Acknowledgments

For their encouragement and advice through the course of this research, I would like to thank my supervisors Kathryn Gillow and Holger Wendland.

Several people must be thanked for their input: Jeremy Levesley and Andy Wathen for examining my thesis; Kathryn Gillow, Chris Farmer and Andy Wathen for their helpful comments when acting as examiners for my transfer or confirmation; Sabine Le Borne, Jennifer Pestana, Rosemary Renault, Endre Süli, Grady Wright, Chris Farmer, Shengxin (Jude) Zhu for discussing my research at various stages throughout my DPhil studies.

This thesis would not have been possible without the support of family. In particular, my parents have nurtured my talents and skills and provided me with all opportunities in life I could wish for. Additionally, I would like to thank the many people who have made my time in Oxford a pleasant one: Cameron Westwood, Thomas White, Eleanore McDonald, Marc Frese, Daniel Morhöfer, Christa Pfafferott, Ingrid von Glehn to name a few.

The staff and faculty at the Mathematical Institute, the Numerical Analysis Group and the Oxford Centre for Collaborative Applied Mathematics have always been extremely helpful. Lastly, I gratefully acknowledge the King Abdullah University of Science and Technology (KAUST) for funding me, the Oxford Centre for Collaborative Applied Mathematics for hosting me and Exeter College for providing research funds to attend conferences.

Contents

Chapter 1

Introduction

Partial differential equations undoubtedly dominate much of applied and pure mathematics. They describe a range of challenging and diverse phenomena in physics, chemistry, biology, meteorology and even economics. However, finding analytic solutions to partial differential equations (PDEs) is often only feasible for very simple cases. Therefore, a great part of the literature in numerical analysis is devoted to solving them computationally [61, 17, 51, 7, 6, 19, 79].

There are several well-established methods to solve PDEs. The most intuitive, but in some sense least flexible, is the finite difference method (FD). It approximates derivatives by differential quotients with a small but finite mesh size. Through Taylor series one often obtains a good estimate for the error, depending on the mesh size. However, finite difference methods are most commonly used on regular grids and domains [61]. Spectral methods need to cluster the grid points near the boundary of the domain. The idea here is to solve a PDE by approximating the solution by a linear translation of globally supported smooth functions (often a Fourier series). Obviously, in order to obtain a reasonable approximation this requires either the solution to be sufficiently smooth or an adaptive strategy [79]. However, when it is possible to apply these methods, one can often achieve exponential convergence.

Finite element (FEM) and finite volume methods (FVM) can be applied to wider problem classes. In both cases, one triangulates the domain of interest (which can be quite arbitrary). In the case of finite element methods, one patches together local polynomial solutions on each triangle to obtain a global approximant. For finite volume methods one considers averages on each triangle (or cell). Apart from triangles, other elements or cells are possible. Either method has its strengths. Finite element methods are applied to weak formulations of a PDE, which allow more general nonclassical solutions [7, 6, 19]. Finite volume methods, on the other hand, are numerically conservative schemes and thus appeal to hyperbolic systems of conservation laws [51, 61].

In this thesis, however, we want to analyse a relatively new numerical method to solve partial differential equations. We focus on collocation with radial basis functions (RBFs) [58, 9, 84, 44, 24, 34, 78, 71, 18, 10, 21, 15, 60], or more generally

positive definite kernels, in combination with a multilevel residual correction scheme. The predominant advantage of this method is its flexibility with respect to the collocation points. These points do not have to be uniformly structured or clustered near the boundary as is often the case for finite difference or spectral methods, but they can be – up to a certain extent – arbitrarily scattered. Unlike for finite volume, finite element or wavelet methods, this approach, however, dispenses with the expensive generation of a mesh. For this reason it is often referred to as *meshless* or *meshfree*.

Radial basis functions have been used in many different ways to numerically solve differential equations [46, 33, 23, 4, 48, 11, 37, 28, 12, 31, 36, 86, 74, 16, 30, 70, 29]. Wendland investigated a Galerkin method using radial basis functions [82]. An advantage of the Galerkin method is that the solution does not need to be as smooth as it has to be for collocation. However, since the basis functions are radial, it requires a numerical integration in order to set up the discretised approximations to the continuous problem and thus introduces an additional error.

There are at least two ways to use collocation to solve differential equations with radial basis functions. One method was proposed by Kansa [46]. The idea is to expand the solution in a linear combination of radial basis functions and then apply the differential equation as well as the corresponding boundary condition, evaluated at given locations. Since in order to obtain the coefficients of the expansion, one needs to solve an unsymmetric linear system. This approach is often referred to as *unsymmetric* collocation. Even though in practice this method is numerically observed to converge quite quickly [54], unfortunately, the invertibility of the collocation matrix is not always guaranteed [43].

Another RBF collocation method includes the differential operator in the expansion of the numerical solution for all interior nodes [23, 50, 33]. Franke and Schaback [32] were the first ones to show that the collocation matrix in this case is symmetric and positive definite (and thus automatically invertible). The idea is to rephrase this *symmetric* collocation method in terms of generalised interpolation [84, Chapter 16], where a general theory is readily available. Due to these reasons, we will focus on symmetric collocation throughout this thesis. We point out that even though in this thesis we look at specific classes of PDEs, both approaches can be used for elliptic, parabolic or hyperbolic PDEs.

In practice, the linear systems one needs to solve to determine the coefficients in the expansion can become quite large. Radial basis functions are known to suffer from conditioning problems, especially when the linear systems are dense [72]. Several improvements have been suggested. Here, we would like to focus on two prominent ones. Firstly, we look at compactly supported radial basis functions, which guarantee that the system we need to solve is sparse. Secondly, we employ multilevel techniques, where we approximate the residual on gradually finer data sets. For interior data, the *residual* refers to the differential operator applied to the difference of the solution to the PDE and its approximant. On the other hand, for Dirichlet boundary data it is simply the difference of solution and approximant.

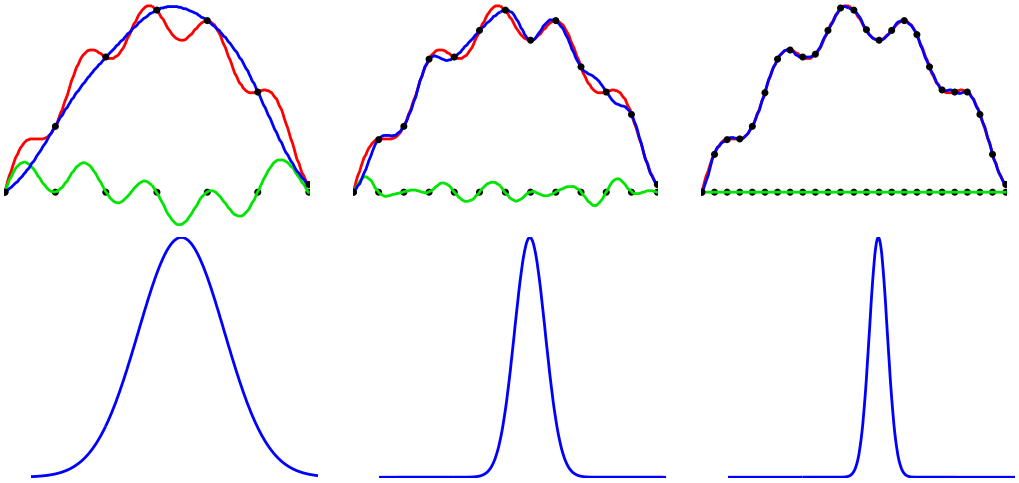

Figure 1.1: *The multilevel collocation approximation (blue) approximates the target solution (red) on denser data sets. For each level the residual (green) is interpolated on the next finer data set, using smaller and smaller support radii (second row). The multilevel approximation is then the sum of these local interpolants.*

These multilevel RBF methods work as follows. Suppose we are given successively denser (but not necessarily nested) data sets, at which the right-hand sides of our PDE are known, as well as a sequence of gradually shrinking support radii, linked to the size of the biggest hole in our data sets. We start by constructing an approximant on the coarsest data set, using a compactly supported basis function having a large support radius. Then on the next finer data set, we approximate the residual through (generalised) interpolation, using compactly supported basis functions with a smaller support radius than the previous one. The sum of the coarse and the finer approximant interpolates the target function on the finer data set. By iterating this process, we are able to capture different scales, that might be incorporated in our target function. Approximants constructed with a large support radius capture large-scale variations whereas approximants with smaller support radii grasp the finer details. The sum of all approximants always interpolates the target function on the finest data set. See Figure 1.1 for a schematic explanation.

Similar multilevel methods have been known to yield excellent results for interpolation problems [27]. But it is only recently that convergence and stability proofs were given [49, 87]. In this thesis, we would like to rigorously prove the corresponding theory for symmetric collocation using radial basis functions. We will focus on two important classes of PDEs: linear second-order elliptic boundary value problems as well as Darcy's problem, a first-order system of PDEs that can be used to model groundwater flow.

In the late nineties, Fasshauer [23] observed numerically that for symmetric RBF collocation there is no convergence in the stationary setting, i. e. when the

support radius at a given level is chosen proportional to the mesh norm of that level. Additionally, he observed that the algorithm converges if the support radii approach zero more slowly than the mesh norms. However, he did not study the precise relationship between mesh norm and support radius needed for convergence. Here, we explain rigorously how the support radii should depend on the mesh norms.

Finally, we present the structure of the thesis. We finish the first chapter by explaining the notation and outlining some of the most important tools. In the second chapter, we explore the theory of positive definite kernels. This includes their characterisation and properties as well as compactly supported positive definite kernels. Moreover, the theory of reproducing kernel Hilbert spaces will be developed, to help analyse the error and the optimality of the interpolation scheme. So-called sampling inequalities will prove to be useful in later chapters.

The third chapter starts with an introduction to generalised interpolation. As a special case RBF collocation is discussed. The following chapter is devoted to multilevel RBF theory. We explain in detail how these multilevel algorithms work. For this we first discuss (inverse) trace theorems as well as the Sobolev norm for functions defined on the boundary of a domain. Then, we look at the convergence theory for the previously studied multilevel interpolation and present new results concerning multilevel collocation. Numerical examples complement the theory.

In order to reduce the condition numbers of the linear systems that have to be solved for each level, three strategies will be discussed in the fifth chapter. Firstly, we prove a smoothing result with several parameters, which extends the one-parameter smoothing theory by Wahba [80] and secondly we show that a diagonal preconditioning strategy significantly improves negative effects on the condition numbers, introduced by the chain rule.

Subsequently, we examine an alternating projection method. The key idea is to further reduce the condition numbers of the level matrices by splitting the interpolant into two new interpolants – one that corresponds to the interior and one that corresponds to the boundary. We adapt a known result [83] that alternating between these two new interpolants will eventually approximate the original interpolant.

Escape theory, which we discuss in the seventh chapter, justifies the use of RBF methods when the numerical solution is actually smoother than the analytical one. The one-shot as well as the multilevel escape theory for second order elliptic boundary value problems will be developed and illustrated with numerical examples. The eighth chapter then gives an introduction to matrix-valued kernels. The multilevel RBF theory for matrix-valued kernels in the case of divergence-free interpolation will be examined.

The ninth chapter builds on the theory of matrix-valued kernels from the previous chapter. Matrix-valued kernels will be employed to construct numerical solutions to Darcy's problem. A multilevel theory as well as an escape theory will be proven. Lastly, the theory is verified with numerical examples. At the very end of the thesis, we summarise what has been achieved and point to areas of future research.

1.1 Notation and Mathematical Tools

Usually, we will denote the space dimension with d, the number of data sites with N, and choose Ω to be a subset of $\mathbb{R}^d$. The natural numbers $\mathbb{N}$ shall not include zero – if we want to include it, we use the notation $\mathbb{N}_0$. Sometimes we denote with i the imaginary unit and sometimes we use it as a summation index. We will use Landau symbols to characterise the growth of a function. That is, if a function $f(x)$ has complexity $\mathcal{O}(g(x))$ for sufficiently large x, we mean there exists a constant $C > 0$ and a real number x_0 such that $|f(x)| < C|g(x)|$ for any $x > x_0$.

We denote with $\lfloor x \rfloor$ the largest integer less than or equal to $x \in \mathbb{R}$ and with $\lceil x \rceil$ the smallest integer bigger than or equal to x. We use $\|\cdot\|_2$ for the Euclidean norm. The L_p norm is given by $\|f\|^p_{L_p(\Omega)} = \int_\Omega |f(\mathbf{x})|^p d\mathbf{x}$ for $1 \le p < \infty$ and by $\|f\|_{L_\infty}(\Omega) = \operatorname{ess\,sup}_{\mathbf{x}\in\Omega} |f(\mathbf{x})|$ for $p = \infty$.

We will abbreviate partial derivatives using the multi-index notation. Let $\boldsymbol{\alpha} = (\alpha_1, \ldots, \alpha_d)^T \in \mathbb{N}^d_{\mathbf{0}}$ and $\mathbf{x} = (x_1, \ldots, x_d)^T \in \mathbb{R}^d$, then

$$D^{\boldsymbol{\alpha}} f(\mathbf{x}) := \frac{\partial^{|\boldsymbol{\alpha}|}}{\partial_1^{\alpha_1} \ldots \partial_d^{\alpha_d}} f(\mathbf{x}) \qquad \text{and} \qquad \boldsymbol{\omega}^{\boldsymbol{\alpha}} = \omega_1^{\alpha_1} \ldots \omega_d^{\alpha_d}$$

where

$$|\boldsymbol{\alpha}| := \|\boldsymbol{\alpha}\|_{\ell_1} = \sum_{j=1}^{d} \alpha_j.$$

For notational convenience, we use *symmetric* factors in the definition of the Fourier transform and the inverse Fourier transform.

Definition 1.1

(i) Let $f \in L_1(\mathbb{R}^d)$, then the **Fourier transform** *of f is given by*

$$\mathcal{F}f(\boldsymbol{\omega}) = \hat{f}(\boldsymbol{\omega}) = \frac{1}{(2\pi)^{d/2}} \int_{\mathbb{R}^d} f(\mathbf{x}) e^{-i\mathbf{x}^T\boldsymbol{\omega}} d\mathbf{x}, \qquad \boldsymbol{\omega} \in \mathbb{R}^d.$$

(ii) Let $g \in L_1(\mathbb{R}^d)$, then we call

$$\mathcal{F}^{-1}g(\mathbf{x}) = \check{g}(\mathbf{x}) = \frac{1}{(2\pi)^{d/2}} \int_{\mathbb{R}^d} g(\boldsymbol{\omega}) e^{i\mathbf{x}^T\boldsymbol{\omega}} d\boldsymbol{\omega}, \qquad \mathbf{x} \in \mathbb{R}^d$$

the **inverse Fourier transform** *of g.*

Sometimes, we will add the space dimension as a subindex $\mathcal{F}_d$ so that it becomes clear which space we integrate over. The definition can be extended to encompass square integrable functions in the following way. If a family of smooth rapidly decreasing functions $\{f_n\}$ converges to some function $f \in L_2(\mathbb{R}^d)$, we define its Fourier transform as the $L_2(\mathbb{R}^d)$ limit of the Fourier transforms $\{\widehat{f_n}\}$. Existence and uniqueness follow from the fact that the Fourier transform is a linear and bounded operator on the set of all smooth rapidly decreasing functions, which is dense in $L_2(\mathbb{R}^d)$.

We note a couple of useful properties of the Fourier transform.

Corollary 1.2 (Properties of the Fourier Transform) *Let $f, g \in L_1(\mathbb{R}^d)$, then:*

1. *The Fourier transform of a function translated by $\mathbf{a} \in \mathbb{R}^d$ is given by*

$$\mathcal{F}[f(\cdot - \mathbf{a})](\boldsymbol{\omega}) = e^{-i\boldsymbol{\omega}^T \mathbf{a}} \mathcal{F}f(\boldsymbol{\omega}).$$

2. *The Fourier transform of a function inversely scaled by $a > 0$ is given by*

$$\mathcal{F}[f(\cdot/a)](\boldsymbol{\omega}) = a^d \mathcal{F}f(a\boldsymbol{\omega}).$$

3. *The Fourier transform of the convolution defined by*

$$(f * g)(\mathbf{x}) := \int_{\mathbb{R}^d} f(\mathbf{y}) g(\mathbf{x} - \mathbf{y}) d\mathbf{y}$$

   is a product of Fourier transforms, namely

$$\mathcal{F}[f * g](\boldsymbol{\omega}) = (2\pi)^{d/2} \mathcal{F}f(\boldsymbol{\omega}) \mathcal{F}g(\boldsymbol{\omega}).$$

4. *We can swap the Fourier transform in the following integral expression*

$$\int_{\mathbb{R}^d} \mathcal{F}f(\mathbf{x}) g(\mathbf{x}) d\mathbf{x} = \int_{\mathbb{R}^d} f(\mathbf{x}) \mathcal{F}g(\mathbf{x}) d\mathbf{x}.$$

5. *If the function $\mathbf{x} \mapsto x_k f(\mathbf{x})$ is L_1 integrable, then the Fourier transform of f is differentiable with respect to its* k*th component and*

$$\mathcal{F}[x_k f(\cdot)](\boldsymbol{\omega}) = i \frac{\partial}{\partial \omega_k} \mathcal{F}f(\boldsymbol{\omega}).$$

6. *If the function $\frac{\partial}{\partial x_k} f$ is L_1 integrable, then its Fourier transform is given by*

$$\mathcal{F}\left[\frac{\partial}{\partial x_k} f\right](\boldsymbol{\omega}) = i\omega_k \mathcal{F}f(\boldsymbol{\omega}).$$

We will use the last statement repeatedly in subsequent chapters, mainly in its multi-index version, i. e.

$$\mathcal{F}\left[D^{\boldsymbol{\alpha}} f\right](\boldsymbol{\omega}) = (i\boldsymbol{\omega})^{\boldsymbol{\alpha}} \mathcal{F}f(\boldsymbol{\omega}).$$

It is possible to recover a function from its Fourier transform under certain conditions.

Theorem 1.3 (Fourier Inversion Theorem) *If both f and $\mathcal{F}f$ lie in $L_1(\mathbb{R}^d)$ and f is continuous, then*

$$f(\mathbf{x}) = \mathcal{F}^{-1}\mathcal{F}(f)(\mathbf{x}) = (2\pi)^{-d/2} \int_{\mathbb{R}^d} \widehat{f}(\boldsymbol{\omega}) e^{i\mathbf{x}^T \boldsymbol{\omega}} d\boldsymbol{\omega}.$$

Proof. See [84, Corollary 5.24]. □

Moreover, for nonnegative integer k, $1 \leq p < \infty$ and $\Omega \subset \mathbb{R}^d$ let $W_p^k(\Omega)$ denote the Sobolev space with differentiability order k and integrability power p. Define for $u \in W_p^k(\Omega)$ the Sobolev (semi-)norms

$$|u|^p_{W_p^k(\Omega)} = \sum_{|\boldsymbol{\alpha}|=k} \|D^{\boldsymbol{\alpha}} u\|^p_{L_p(\Omega)} \quad \text{and} \quad \|u\|^p_{W_p^k(\Omega)} = \sum_{|\boldsymbol{\alpha}|\leq k} \|D^{\boldsymbol{\alpha}} u\|^p_{L_p(\Omega)}.$$

For $p = \infty$ the Sobolev (semi-)norm is given by

$$|u|_{W_\infty^k(\Omega)} = \sup_{|\boldsymbol{\alpha}|=k} \|D^{\boldsymbol{\alpha}} u\|_{L_\infty(\Omega)} \quad \text{and} \quad \|u\|_{W_\infty^k(\Omega)} = \sup_{|\boldsymbol{\alpha}|\leq k} \|D^{\boldsymbol{\alpha}} u\|_{L_\infty(\Omega)}.$$

We will often use the abbreviation $H^k(\Omega) = W_2^k(\Omega)$ for the case $p = 2$ to make clear that we have in fact a Hilbert space. In this case, there is another way to characterise and generalise Sobolev spaces on the whole Euclidean space via Fourier transforms by defining

$$H^\sigma(\mathbb{R}^d) = \left\{ f \in L_2(\mathbb{R}^d) \mid \widehat{f}(\cdot)(1 + \|\cdot\|_2^2)^{\sigma/2} \in L_2(\mathbb{R}^d) \right\},$$

where $0 < \sigma < \infty$ can denote a fractional positive number [20, Chapter 5]. For smooth bounded domains $\Omega \subset \mathbb{R}^d$, one can define $H^\sigma(\Omega)$ as all the functions in $L_2(\Omega)$, which can be extended to a function in $H^\sigma(\mathbb{R}^d)$. Another way to define fractional Sobolev spaces for an open subset Ω is given by

$$H^\sigma(\Omega) = \left\{ \|f\|_{H^{\lfloor\sigma\rfloor}(\Omega)} + \sup_{|\boldsymbol{\alpha}|=\lfloor\sigma\rfloor} [D^{\boldsymbol{\alpha}} f]_{\sigma-\lfloor\sigma\rfloor,2,\Omega} \right\},$$

where the Slobodeckij seminorm $[\cdot]_{\theta,p,\Omega}$ is defined by

$$[f]_{\theta,p,\Omega} := \left(\int_\Omega \int_\Omega \frac{|f(\mathbf{x}) - f(\mathbf{y})|^p}{\|\mathbf{x} - \mathbf{y}\|^{\theta p + d}} \, d\mathbf{x} \, d\mathbf{y} \right)^{\frac{1}{p}}$$

for $\theta \in (0,1)$, $1 \leq p < \infty$ and $f \in L_p(\Omega)$. A very important tool for us will be the Sobolev embedding theorem, which can be found in [7, Theorem 1.4.6 and Corollary 1.4.7].

Theorem 1.4 (Sobolev Embedding Theorem) *Let $\Omega \subseteq \mathbb{R}^d$ be a bounded domain with Lipschitz boundary, let k be a positive integer and m a nonnegative integer with $k > m$. Furthermore let p be a real number $1 \leq p < \infty$ such that*

$$\begin{aligned} k - m &\geq d \quad \textit{when} \quad p = 1, \\ k - m &> d/p \quad \textit{when} \quad p > 1. \end{aligned}$$

Then there is a positive constant C such that for all $u \in W_p^k(\Omega)$

$$\|u\|_{W_\infty^m(\Omega)} \leq C\|u\|_{W_p^k(\Omega)}.$$

Moreover, there is a C^m function in the $L_p(\Omega)$ equivalence class of u.

Due to the last statement in the theorem, we will sometimes abuse notation and write $W_p^k(\Omega) \subseteq C^m(\Omega)$. We will explain what a Lipschitz boundary is in the next chapter.

Finally, we will repeatedly use the Riesz representation theorem, which can be found in standard introductions to linear functional analysis such as [91].

Theorem 1.5 (Riesz Representation Theorem) *Let H be a Hilbert space with real base field and inner product $(\cdot,\cdot)_H$. Denote with H^* its dual. Then the mapping*

$$J(f)(g) := (g, f)_H$$

for $f, g \in H$ defines an isometric isomorphism $J\colon H \to H^*$, i. e. J is bijective, $\|f\|_H = \|J(f)\|_{H^*}$ and $J(\alpha f + g) = \alpha J(f) + J(g)$ for all $f, g \in H$ and $\alpha \in \mathbb{R}$.

Chapter 2

Scattered Data Approximation by Positive Definite Functions

In this chapter, we introduce interpolation with positive definite functions, which serves as an important blueprint for the next chapter, where we turn to generalised interpolation. Most of this introductory chapter is based on the textbook by Wendland [84].

We would like to recover an unknown function $f\colon \mathbb{R}^d \to \mathbb{R}$, of which we know only finitely many samples taken at some discrete data set $X = \{\mathbf{x}_1, \mathbf{x}_2, \dots, \mathbf{x}_N\} \subseteq \mathbb{R}^d$. In order for the interpolation process to work, the least we need to assume regarding its regularity is continuity. We construct an interpolant of the form

$$s_{f,X}(\mathbf{x}) = \sum_{j=1}^{N} \alpha_j \Phi(\mathbf{x} - \mathbf{x}_j), \tag{2.1}$$

for some continuous basis function $\Phi\colon \mathbb{R}^d \to \mathbb{R}$. The real coefficients $\alpha_1, \dots, \alpha_N$ are determined from the interpolation conditions

$$s_{f,X}(\mathbf{x}_j) = f(\mathbf{x}_j) \quad \text{for } 1 \le j \le N \tag{2.2}$$

by solving the linear system

$$\begin{pmatrix} \Phi(\mathbf{x}_1 - \mathbf{x}_1) & \dots & \Phi(\mathbf{x}_1 - \mathbf{x}_N) \\ \vdots & & \vdots \\ \Phi(\mathbf{x}_N - \mathbf{x}_1) & \dots & \Phi(\mathbf{x}_N - \mathbf{x}_N) \end{pmatrix} \begin{pmatrix} \alpha_1 \\ \vdots \\ \alpha_N \end{pmatrix} = \begin{pmatrix} f(\mathbf{x}_1) \\ \vdots \\ f(\mathbf{x}_N) \end{pmatrix}, \tag{2.3}$$

which we abbreviate with

$$A_{\Phi,X}\, \boldsymbol{\alpha} = \mathbf{f}.$$

We would like to explain in more detail how to choose the basis function Φ. For this reason, we will first consider positive definite functions and their properties,

show some examples, and have a closer look at compactly supported ones. At the end of the chapter, we will discuss how these approximation techniques relate to other concepts in functional analysis and how this relationship can be exploited when examining the error of the interpolation method.

Before we start, however, we point out that the multivariate approximation space that our interpolant is taken from $F_{\Phi,X} = \text{span}\{\Phi(\cdot - \mathbf{x}) \mid \mathbf{x} \in X\}$ depends on the data $X = \{\mathbf{x}_1, \mathbf{x}_2, \ldots, \mathbf{x}_N\}$. This is quite different from the univariate case of polynomial interpolation where one can build unique interpolants with the help of the space $\mathcal{P}_{N-1}(\mathbb{R}) = \text{span}\{x^j \mid j = 0, \ldots, N-1\}$, which is independent of the data. Such data-independent spaces have been given a special name.

Definition 2.1 *Let $\Omega \subseteq \mathbb{R}^d$. A linear subspace of continuous functions $V \subseteq C(\Omega)$ is called an N-dimensional* **Haar space** *if for arbitrary data $(X, \mathbf{f})$ for some data set $X = \{\mathbf{x}_1, \mathbf{x}_2, \ldots, \mathbf{x}_N\} \subseteq \Omega$ and $\mathbf{f} = (f_1, \ldots, f_N)^T \in \mathbb{R}^N$ there is exactly one function $p \in V$ with*

$$p(\mathbf{x}_j) = f_j \quad \text{for} \quad 1 \leq j \leq N.$$

One of the reasons why we look at data-dependent approximation spaces in the multivariate case is that there are no higher dimensional Haar spaces.

Theorem 2.2 (Mairhuber-Curtis) *Let $\Omega \subseteq \mathbb{R}^d$ contain an interior point. If $d \geq 2$, then there exists no Haar space of dimension $N \geq 2$.*

The proof of this theorem can be found in the textbook by Wendland [84, Theorem 2.3].

2.1 Positive Definite Functions

It is obvious that the interpolant $s_{f,X}$ needs to be chosen in such a way that the corresponding interpolation matrix $A_{\Phi,X}$ is invertible. From a numerical point of view, however, it would be advantageous to have some additional features such as positive definiteness. This motivates the following definition.

Definition 2.3 *A continuous function $\Phi\colon \mathbb{R}^d \to \mathbb{R}$ is called* **positive semi-definite** *on $\mathbb{R}^d$ if for all $N \in \mathbb{N}$, any finite set $X = \{\mathbf{x}_1, \mathbf{x}_2, ..., \mathbf{x}_N\} \subseteq \mathbb{R}^d$ of pairwise distinct points, and all $\boldsymbol{\alpha} = (\alpha_1, ..., \alpha_N)^T \in \mathbb{R}^N$, the quadratic form*

$$\sum_{j=1}^{N} \sum_{k=1}^{N} \alpha_j \alpha_k \Phi(\mathbf{x}_j - \mathbf{x}_k) \tag{2.4}$$

is nonnegative. It is called **positive definite** *on $\mathbb{R}^d$ if the quadratic form is positive for all $\boldsymbol{\alpha} \in \mathbb{R}^N \backslash \{\mathbf{0}\}$.*

Conveniently, the definition is made in such a way that a function is positive (semi-)definite if the interpolation matrix $A_{\Phi,X}$ is positive (semi-)definite as well. It

is also possible to generalise the definition to complex-valued functions, which has some advantages when employing Fourier transforms. For our purposes, however, it is enough to restrict ourselves to the case of real-valued functions. From the definition one can deduce the following properties of a positive semi-definite function.

Theorem 2.4 (Properties of Positive Definite Functions) *Let Φ be a positive semi-definite function, then the following holds:*

1. $\Phi(\mathbf{0}) \geq 0$.
2. $\Phi(-\mathbf{x}) = \Phi(\mathbf{x})$ *for all* $\mathbf{x} \in \mathbb{R}^d$.
3. Φ *is bounded with* $|\Phi(\mathbf{x})| \leq |\Phi(\mathbf{0})|$ *for all* $\mathbf{x} \in \mathbb{R}^d$.
4. $\Phi(\mathbf{0}) = 0$ *if and only if* Φ *is the zero function.*
5. *If* $\Phi_1, \ldots, \Phi_N$ *are positive semi-definite and* c_j *are nonnegative constants then* $\sum_{j=1}^{N} c_j \Phi_j$ *is also positive semi-definite. If one of the* Φ_j *is positive definite with corresponding coefficient* $c_j > 0$*, then the whole sum is positive definite.*
6. *The product of two positive definite functions is positive definite.*

Proof. See [84, Theorem 6.2]. □

Now we can formulate the well-posedness of the interpolation scheme, see for example [44, Theorem 1].

Theorem 2.5 *Let* $\Phi\colon \mathbb{R}^d \to \mathbb{R}$ *be positive definite. The interpolation problem* (2.2) *has a unique solution of the form* (2.1).

Proof. From the definition of positive definiteness it follows that the matrix in the linear system (2.3) is positive definite and thus invertible. □

2.1.1 Radial Positive Definite Functions

Often the positive semi-definite functions we are interested in have additional properties. A very common one is that they only depend on the norm of the argument, i. e. they are are radial.

Definition 2.6 *A function* $\Phi\colon \mathbb{R}^d \to \mathbb{R}$ *is called* **radial** *if there exists a function* $\phi\colon [0, \infty) \to \mathbb{R}$ *with* $\Phi(\mathbf{x}) = \phi(\|\mathbf{x}\|_2)$ *for all* $\mathbf{x} \in \mathbb{R}^d$.

With the help of univariate radial positive definite functions one can easily describe multivariate positive definite functions for any space dimension d.

Definition 2.7 *A univariate function* $\phi\colon [0, \infty) \to \mathbb{R}$ *is called* **positive semi-definite** *on* $\mathbb{R}^d$ *if* $\Phi\colon \mathbb{R}^d \to \mathbb{R}$*, defined by* $\Phi(\mathbf{x}) = \phi(\|\mathbf{x}\|_2)$ *for all* $\mathbf{x} \in \mathbb{R}^d$*, is positive semi-definite on* $\mathbb{R}^d$.

Now the term, *radial basis function* becomes clear. When characterising positive definite functions their Fourier transform will play an important role. Therefore, we would like to know how the Fourier transform of a radial function behaves. The following theorem states that its Fourier transform is a radial function itself.

Theorem 2.8 *Suppose $\Phi \in L_1(\mathbb{R}^d) \cap C(\mathbb{R}^d)$ is radial with $\Phi(\mathbf{x}) = \phi(\|\mathbf{x}\|_2)$ for all $\mathbf{x} \in \mathbb{R}^d$ and some $\phi\colon [0,\infty) \to \mathbb{R}$. Then its d-variate Fourier transform is radial as well with*

$$\mathcal{F}_d\Phi(\boldsymbol{\omega}) = \mathcal{F}_d\phi(\|\boldsymbol{\omega}\|_2) = \|\boldsymbol{\omega}\|_2^{-\frac{d-2}{2}} \int_0^\infty \phi(t) t^{\frac{d}{2}} J_{\frac{d-2}{2}}(\|\boldsymbol{\omega}\|_2 t) dt,$$

where J_p is the classical Bessel function of the first kind of order $p = \frac{d-2}{2}$ defined as

$$J_p(r) = \sum_{m=0}^{\infty} \frac{(-1)^m \left(\frac{r}{2}\right)^{2m+p}}{m!\Gamma(p+m+1)}.$$

Proof. See [84, Theorem 5.26]. □

The theorem has the nice consequence that testing a radial function for positive definiteness only involves evaluating a one-dimensional integral instead of a multivariate one as we will see in the next section (Theorem 2.10).

2.1.2 Characterisation of Positive Definite Functions

There are two predominant ways to characterise positive semi-definite functions: either through Fourier transforms or through completely monotone functions. The first characterisation is dependent on the space dimension since the Fourier transform consists of $\mathbb{R}^d$-integrals. The second characterisation (often called Bernstein-Hausdorff-Widder characterisation) is achieved with the help of univariate functions that help to describe positive definite functions for any given space dimension. As we will see soon, there exists no compactly supported function that is positive definite for all space dimensions d. Therefore, we will only discuss the characterisation via Fourier transforms, which is known as Bochner's theorem and refer the interested reader to Chapter 7 in Wendland's book [84] for the other option.

Bochner's original result is rather general [84, Theorem 6.6]. It is given for complex-valued positive semi-definite functions. In this thesis, we are only interested in real-valued positive definite functions. Therefore, we cite two special versions of this theorem: one for integrable functions and one for integrable radial functions.

Theorem 2.9 (Bochner's Theorem for Integrable Functions) *Suppose Φ is a continuous function in $L_1(\mathbb{R}^d)$. Then Φ is positive definite on $\mathbb{R}^d$ if and only if Φ is bounded and its Fourier transform is nonnegative and nonvanishing.*

Proof. See [84, Theorem 6.11]. □

Theorem 2.10 (Bochner's Theorem for Radial Functions) *Suppose $\phi \in C([0,\infty))$ satisfies $r \mapsto r^{d-1}\phi(r) \in L_1([0,\infty))$. Then ϕ is positive definite on $\mathbb{R}^d$ if and only if ϕ is bounded and its Fourier transform*

$$\mathcal{F}_d\phi(r) = r^{-\frac{d-2}{2}} \int_0^\infty \phi(t) t^{\frac{d}{2}} J_{\frac{d-2}{2}}(rt)dt$$

is nonnegative and nonvanishing.

Proof. Since the function $r \mapsto r^{d-1}\phi(r)$ is in $L_1([0,\infty))$, we can conclude that $\Phi(\mathbf{x}) := \phi(\|\mathbf{x}\|_2)$ is in $L_1(\mathbb{R}^d)$. Since additionally $\mathcal{F}_d\Phi(\mathbf{x}) = \mathcal{F}_d\phi(\|\mathbf{x}\|_2)$, the result follows from Theorem 2.9. □

2.1.3 Examples

We give three examples of positive definite functions: two globally supported functions and one compactly supported function, which will be of great use when constructing compactly supported positive definite functions. We start by showing that Gaussians

$$\Phi_\alpha(\mathbf{x}) = e^{-\alpha\|\mathbf{x}\|_2^2}$$

for $\alpha > 0$ are positive definite on $\mathbb{R}^d$. If we look at the Fourier transform of $\Phi_{1/2}$, we find

$$\begin{aligned}\mathcal{F}\Phi_{1/2}(\boldsymbol{\omega}) &= \frac{1}{(2\pi)^{d/2}} \int_{\mathbb{R}^d} e^{-\|\mathbf{x}\|_2^2/2} e^{-i\mathbf{x}^T\boldsymbol{\omega}} d\mathbf{x} \\ &= \prod_{k=1}^d \left(\frac{1}{\sqrt{2\pi}} \int_{\mathbb{R}} e^{-x_k^2/2} e^{-ix_k\omega_k} dx_k \right) = \prod_{k=1}^d -e^{\omega_k^2/2} = e^{-\|\boldsymbol{\omega}\|_2^2/2},\end{aligned}$$

where we used and generalised the fact that the Fourier transform of the one-dimensional Gaussian $f(x) = e^{-x^2/2}$ is again a Gaussian, i. e. $f = \hat{f}$. Now since

$$\begin{aligned}\mathcal{F}\Phi_\alpha(\boldsymbol{\omega}) &= \mathcal{F}\left[\Phi_{1/2}(\sqrt{2\alpha}\,\cdot)\right](\boldsymbol{\omega}) \\ &= \left(\frac{1}{2\alpha}\right)^{d/2} \mathcal{F}\Phi_{1/2}\left(\frac{\boldsymbol{\omega}}{\sqrt{2\alpha}}\right) = \left(\frac{1}{2\alpha}\right)^{d/2} e^{-\|\boldsymbol{\omega}\|_2^2/(4\alpha)}\end{aligned}$$

is positive and Φ_α is bounded and continuous, we can deduce that Φ_α is positive definite on $\mathbb{R}^d$.

Another important family of functions are inverse multiquadrics

$$\Phi_\beta(\mathbf{x}) = (1 + \|\mathbf{x}\|_2^2)^{-\beta}, \quad \mathbf{x} \in \mathbb{R}^d. \tag{2.5}$$

They are positive definite on $\mathbb{R}^d$ for $\beta > 0$ [87, Theorem 7.15]. The proof of their positive definiteness for $\beta > d/2$ follows from the fact that the bounded continuous Φ_β is in $L_1(\mathbb{R}^d)$ and the following theorem.

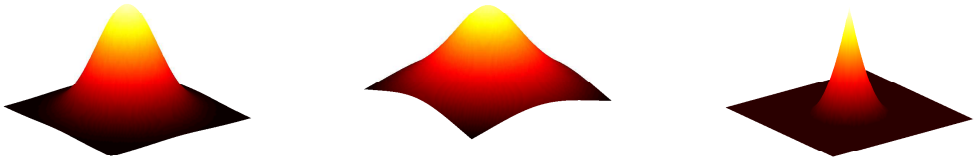

(a) Gaussian (b) Inverse multiquadric (c) Power function

Figure 2.1: Three radial basis functions: Gaussian for $\alpha = 1$, inverse multiquadric for $\beta = 2$, and truncated power function for $\ell = 2$.

Theorem 2.11 *The inverse multiquadrics* (2.5) *possess the nonnegative and non-vanishing Fourier transform*

$$\widehat{\Phi_\beta}(\boldsymbol{\omega}) = \frac{2^{1-\beta}}{\Gamma(\beta)} \|\boldsymbol{\omega}\|_2^{\beta-d/2} K_{d/2-\beta}(\|\boldsymbol{\omega}\|_2),$$

where K_ν is the modified Bessel function which is defined for $\nu, z \in \mathbb{C}$ as

$$K_\nu(z) = \int_0^\infty e^{-z\cosh(t)} \cosh(\nu t) dt$$

for $|\arg(z)| < \pi/2$ and $\cosh(t) = (e^t + e^{-t})/2$.

Proof. See [84, Theorem 6.13]. □

After having seen two examples of globally supported positive definite functions, we have a look at a positive definite function, which is nonzero only inside a bounded domain. With the help of this function we will construct positive definite compactly supported functions of a prescribed smoothness, which automatically have to depend on the space dimension, as we will see in the next section.

Definition 2.12 *Let $l \in \mathbb{N}$. For $r \geq 0$ the* **truncated power function** *is given by*

$$\phi_\ell(r) = (\max\{0, (1-r)\})^\ell .$$

Sometimes we will extend the truncated power function to the whole real line by even extension. We will often make use of the truncation operator $(x)_+ = \max\{0, x\}$ to shorten the notation to $\phi_\ell(r) = (1-r)_+^\ell$. When employing this shortened notation, it is important to remember that the function is first truncated and then raised to the power. These functions will play an important role when constructing compactly supported positive definite functions. It can be shown by employing Bochner's theorem that under certain circumstances the truncated power function is a positive definite function.

Theorem 2.13 *The truncated power function $\phi_\ell(r)$ is positive definite on $\mathbb{R}^d$ if $\ell \geq \lfloor d/2 \rfloor + 1$.*

Proof. See [84, Theorem 6.20]. □

All three radial basis functions are shown in Figure 2.1. The whole next subsection is devoted to a computationally advantageous class of positive definite functions with compact support.

2.1.4 Compactly Supported Positive Definite Functions

If we want to employ the scattered data approximation method to real-life problems, it is necessary to discuss the computational cost. On the one hand, solving a linear system in N unknowns of the form (2.3) leads to a computational complexity of $\mathcal{O}(N^3)$ (at least when employing standard techniques such as Gaussian elimination). On the other hand, evaluating an interpolant of the form (2.1) leads to a computational complexity of $\mathcal{O}(N)$. Since in practice $N \sim 10^6$ or $N \sim 10^7$ is not uncommon, we want to reduce the computational cost of solving the linear system which dominates the complexity. One way to do this is by using *compactly supported* positive definite functions.

Definition 2.14 *The* **support** *of a function* $f\colon \mathbb{R}^d \to \mathbb{R}$ *is defined as*

$$\operatorname{supp} f = \overline{\{\mathbf{x} \in \mathbb{R}^d \mid f(\mathbf{x}) \neq 0\}}^{\|\cdot\|_2}.$$

Since $\operatorname{supp} f \subseteq \mathbb{R}^d$ is closed by definition, the only additional requirement to obtain a compact support is boundedness due to the Heine-Borel theorem. If the positive definite function Φ in our interpolant (2.1) has a sufficiently small support, we can hope for many terms in the sum to be zero. Moreover, the linear system (2.3) becomes sparse and therefore less expensive to solve.

Sadly, it is impossible to find compactly supported functions that are positive definite for any space dimension, as the following theorem shows.

Theorem 2.15 *If* $\phi\colon [0,\infty) \to \mathbb{R}$ *is positive definite on every* $\mathbb{R}^d$*, then* $\phi(r) \neq 0$ *for all* $r \geq 0$*.*

Proof. See [84, Theorem 9.2, Corollary 9.3]. □

From this theorem two consequences arise immediately. A continuous univariate compactly supported function ϕ cannot be positive definite on every $\mathbb{R}^d$. If we want to find a compactly supported positive definite function, it will have to depend on the space dimension d. This in turn implies that we cannot make use of the Bernstein-Hausdorff-Widder characterisation of positive definite functions through completely monotone functions since this theorem describes functions that are positive definite for all space dimensions d. Therefore, Bochner's space-dependent characterisation via nonnegative Fourier transforms (Theorem 2.9 and 2.10) is more appropriate in this context.

Wendland [81] used the truncated power function $\phi_\ell(r) = (1-r)_+^\ell$ to build, with the help of an integral operator, higher dimensional compactly supported positive

definite functions from lower dimensional ones. The main advantage of these functions is that they have minimal degree for a given space dimension and smoothness. This is of computational value because the smaller the degree, the cheaper it is to evaluate the function. Let us introduce some notation.

Definition 2.16 *Using the truncated power function $\phi_\ell(r) = (1-r)_+^\ell$, we define*

$$\phi_{d,k} = \mathcal{I}^k \phi_{\lfloor d/2 \rfloor + k + 1},$$

where $(\mathcal{I}\phi)(r) = \int_r^\infty t\phi(t)dt$ for $r \geq 0$.

We consider the function $\mathcal{I}\phi$ to be evenly extended to the whole real line and note that the integral operator respects functions with compact support. The above defined *Wendland functions* have a lot of useful properties.

Theorem 2.17 (Properties of Wendland's Functions, [84]) *The $\phi_{d,k}$ are radial, positive definite on $\mathbb{R}^d$ and have the form*

$$\phi_{d,k}(r) = \begin{cases} p_{d,k}(r) & 0 \leq r \leq 1, \\ 0 & 1 < r, \end{cases}$$

where $p_{d,k}$ is a univariate polynomial of degree $\lfloor d/2 \rfloor + 3k + 1$. Moreover, the evenly extended $\phi_{d,k} \in C^{2k}(\mathbb{R})$ are unique up to a constant factor and of minimal possible degree to achieve positive definiteness for a given space dimension d and smoothness $2k$.

We state the first four compactly supported functions of minimal degree that are positive definite on $\mathbb{R}^d$ in the following corollary. In Table 2.1, we list some of them for specific space dimensions.

Corollary 2.18 *The functions $\phi_{d,k}$ have for $0 \leq k \leq 3$ the explicit form*

$$\begin{aligned}
\phi_{d,0}(r) &= (1-r)_+^{\lfloor d/2 \rfloor + 1}, \\
\phi_{d,1}(r) &\doteq (1-r)_+^{\ell+1}[(\ell+1)r + 1], \\
\phi_{d,2}(r) &\doteq (1-r)_+^{\ell+2}[(\ell^2 + 4\ell + 3)r^2 + (3\ell+6)r + 3], \\
\phi_{d,3}(r) &\doteq (1-r)_+^{\ell+3}[(\ell^3 + 9\ell^2 + 23\ell + 15)r^3 \\
&\qquad + (6\ell^2 + 36\ell + 45)r^2 + (15\ell + 45)r + 15],
\end{aligned}$$

where $\ell = \lfloor d/2 \rfloor + k + 1$ and $\doteq$ denotes equality up to a constant positive factor.

We note that positive definite kernels can be generalised to *conditionally* positive definite kernels [44, 84], which allow polynomial reproduction. However, since there are no compactly supported functions that are conditionally positive definite of nonvanishing order [84, Theorem 9.1], we do not pursue these functions here any further.

$d = 1$	$\phi_{1,0}(r) = (1-r)_+$	C^0
	$\phi_{1,1}(r) \doteq (1-r)_+^3(3r+1)$	C^2
	$\phi_{1,2}(r) \doteq (1-r)_+^5(8r^2+5r+1)$	C^4
$d \leq 3$	$\phi_{d,0}(r) = (1-r)_+^2$	C^0
	$\phi_{d,1}(r) \doteq (1-r)_+^4(4r+1)$	C^2
	$\phi_{d,2}(r) \doteq (1-r)_+^6(35r^2+18r+3)$	C^4
	$\phi_{d,3}(r) \doteq (1-r)_+^8(32r^3+25r^2+8r+1)$	C^6
	$\phi_{d,4}(r) \doteq (1-r)_+^{10}(429r^4+450r^3+210r^2+50r+5)$	C^8
	$\phi_{d,5}(r) \doteq (1-r)_+^{12}(2048r^5+2697r^4+1644r^3+566r^2+108r+9)$	C^{10}
$d \leq 5$	$\phi_{d,0}(r) = (1-r)_+^3$	C^0
	$\phi_{d,1}(r) \doteq (1-r)_+^5(5r+1)$	C^2
	$\phi_{d,2}(r) \doteq (1-r)_+^7(16r^2+7r+1)$	C^4

Table 2.1: Compactly supported positive definite functions of minimal degree.

2.2 Variational Approach

Previously, we have discussed the basis function $\Phi\colon \mathbb{R}^d \to \mathbb{R}$ which appears in the interpolant of the form (2.1). Now we would like to take a different point of view, well-known in approximation theory as well as functional analysis: the variational approach. We will see that for any positive definite basis function there is a Hilbert space – the so called native space – such that our interpolant (2.1) is the best approximation to a given function f with respect to the native space norm. The first ones to devise this variational setting for (conditionally) positive semi-definite functions were Madych and Nelson [58]. This setting enables us to analyse the error of the interpolation scheme in an elegant way.

In the following, we will look at real-valued *kernels* $\Phi\colon \mathbb{R}^d \times \mathbb{R}^d \to \mathbb{R}$ rather than basis functions of the form $\Phi\colon \mathbb{R}^d \to \mathbb{R}$. Therefore, we adjust our definition of positive definiteness.

Definition 2.19 *A continuous kernel $\Phi\colon \Omega \times \Omega \to \mathbb{R}$ is called* **positive semi-definite** *on $\Omega \subseteq \mathbb{R}^d$ if for all $N \in \mathbb{N}$, any finite set $X = \{\mathbf{x}_1, \mathbf{x}_2, ..., \mathbf{x}_N\} \subseteq \mathbb{R}^d$ of pairwise distinct points, and all $\boldsymbol{\alpha} = (\alpha_1, ..., \alpha_N)^T \in \mathbb{R}^N$ the quadratic form*

$$\sum_{j=1}^{N} \sum_{k=1}^{N} \alpha_j \alpha_k \Phi(\mathbf{x}_j, \mathbf{x}_k) \tag{2.6}$$

is nonnegative. The kernel is called **positive definite** *on $\mathbb{R}^d$ if the above quadratic form is positive for all $\boldsymbol{\alpha} \in \mathbb{R}^N \backslash \{\mathbf{0}\}$.*

2.2.1 Reproducing Kernel Hilbert Spaces

We now introduce Hilbert spaces that automatically lead to positive semi-definite kernels. In the following section, we then discuss the converse, i. e. the fact that

every positive definite kernel leads to a Hilbert space.

Definition 2.20 *Let $\mathcal{F}$ be a real Hilbert space of functions $f\colon \Omega \to \mathbb{R}$. A function $\Phi\colon \Omega \times \Omega \to \mathbb{R}$ is called a* **reproducing kernel** *for $\mathcal{F}$ if*

(1) $\Phi(\cdot, \mathbf{y}) \in \mathcal{F}$ *for all* $\mathbf{y} \in \Omega$,

(2) $f(\mathbf{y}) = (f, \Phi(\cdot, \mathbf{y}))_{\mathcal{F}}$ *for all* $f \in \mathcal{F}$ *and* $\mathbf{y} \in \Omega$.

If there exists a reproducing kernel for some Hilbert space, we refer to it as *reproducing kernel Hilbert space*. There is a useful characterisation of (sufficiently smooth) Hilbert function spaces that have a reproducing kernel. We denote with $\mathcal{F}^*$ the dual space to $\mathcal{F}$.

Theorem 2.21 *Suppose $\mathcal{F}$ is a real Hilbert space of functions $f\colon \Omega \to \mathbb{R}$. Then $\mathcal{F}$ has a reproducing kernel if and only if the point evaluation functionals are continuous, that is $\delta_{\mathbf{y}} \in \mathcal{F}^*$ for all $\mathbf{y} \in \Omega$.*

Proof. See [84, Theorem 10.2]. □

Directly from the definition one obtains the following properties of reproducing kernels.

Theorem 2.22 *Suppose $\mathcal{F}$ is a real Hilbert space of functions $f\colon \Omega \to \mathbb{R}$ with reproducing kernel $\Phi\colon \Omega \times \Omega \to \mathbb{R}$. Then*

(1) Φ *is unique,*

(2) $\Phi(\mathbf{x}, \mathbf{y}) = (\Phi(\cdot, \mathbf{x}), \Phi(\cdot, \mathbf{y}))_{\mathcal{F}} = (\delta_{\mathbf{x}}, \delta_{\mathbf{y}})_{\mathcal{F}^*}$ *for* $\mathbf{x}, \mathbf{y} \in \Omega$,

(3) $\Phi(\mathbf{x}, \mathbf{y}) = \Phi(\mathbf{y}, \mathbf{x})$ *for* $\mathbf{x}, \mathbf{y} \in \Omega$,

(4) Convergence in the Hilbert space norm implies pointwise convergence, i. e. $\lim_{n\to\infty} \|f - f_n\|_{\mathcal{F}} = 0$ *implies* $\lim_{n\to\infty} |f(\mathbf{x}) - f_n(\mathbf{x})| = 0$ *for* $f, f_n \in \mathcal{F}$ *and* $\mathbf{x} \in \Omega$.

Proof. See [84, Theorem 10.3]. □

We conclude this section with the main result, which says that every reproducing kernel is automatically positive semi-definite.

Theorem 2.23 *Suppose $\mathcal{F}$ is a real Hilbert space of functions $f\colon \Omega \to \mathbb{R}$ with reproducing kernel $\Phi\colon \Omega \times \Omega \to \mathbb{R}$. Then Φ is positive semi-definite. It is positive definite if and only if the point evaluation functionals are linearly independent in $\mathcal{F}^*$.*

Proof. See [84, Theorem 10.4]. □

2.2.2 Native Spaces

We have seen that every reproducing kernel is automatically positive semi-definite. In practice, one would usually pick a kernel $\Phi\colon \Omega \times \Omega \to \mathbb{R}$ and then ask if there exists a Hilbert space that has Φ as its reproducing kernel. The following theorem gives us an idea of how this could be achieved.

Theorem 2.24 *Let $\Phi\colon \Omega \times \Omega \to \mathbb{R}$ be a symmetric positive definite kernel. The bilinear form*

$$\left(\sum_{j=1}^{N} \alpha_j \Phi(\cdot, \mathbf{x}_j), \sum_{k=1}^{M} \beta_k \Phi(\cdot, \mathbf{y}_k) \right)_\Phi = \sum_{j=1}^{N} \sum_{k=1}^{M} \alpha_j \beta_k \Phi(\mathbf{x}_j, \mathbf{y}_k)$$

defines an inner product on the $\mathbb{R}$-linear space

$$F_\Phi(\Omega) = \operatorname{span}\{\Phi(\cdot, \mathbf{y}) \mid \mathbf{y} \in \Omega\}$$

Moreover, the pre-Hilbert space $F_\Phi(\Omega)$ has Φ as its reproducing kernel.

Proof. The proof can be found in [84, Theorem 10.7]. Obviously $(\cdot, \cdot)_\Phi$ is bilinear since the summation can be split and merged as needed. It is symmetric as Φ is assumed to be symmetric. It remains to show positive definiteness. For any $f = \sum_{j=1}^{N} \alpha_j \Phi(\cdot, \mathbf{x}_j)$ in $F_\Phi(\Omega) \backslash \{0\}$ we find

$$(f, f)_\Phi = \sum_{j=1}^{N} \sum_{k=1}^{N} \alpha_j \alpha_k \Phi(\mathbf{x}_j, \mathbf{x}_k) > 0,$$

as Φ is positive definite. We have $f \in F_\Phi(\Omega)$ by construction and the reproducing property follows since for all $\mathbf{y} \in \Omega$

$$(f, \Phi(\cdot, \mathbf{y}))_\Phi = \sum_{j=1}^{N} \alpha_j \Phi(\mathbf{x}_j, \mathbf{y}) = \sum_{j=1}^{N} \alpha_j \Phi(\mathbf{y}, \mathbf{x}_j) = f(\mathbf{y})$$

holds. □

So far, we have constructed a pre-Hilbert space. The only ingredient that is missing in order to obtain a Hilbert space is completeness. Therefore, we form the completion of this space. It is well known in functional analysis how to construct the completion of $F_\Phi(\Omega)$ with respect to the space-inherent norm, in this case $\|\cdot\|_\Phi = (\cdot, \cdot)_\Phi^{1/2}$, see for instance the textbook by Yosida [91]. We denote the completion with $\mathcal{F}_\Phi(\Omega)$. The problem, however, is that elements of $\mathcal{F}_\Phi(\Omega)$ being equivalence classes of Cauchy sequences are difficult to work with. However, for our error analysis in the following section we want to understand what the elements in $\mathcal{F}_\Phi(\Omega)$ look like. Fortunately, we can identify these elements with continuous functions in the following sense.

We define the linear mapping

$$R\colon \mathcal{F}_\Phi(\Omega) \to C(\Omega), \qquad R(f)(\mathbf{x}) := (f, \Phi(\cdot, \mathbf{x}))_\Phi,$$

for which the following lemma holds.

Lemma 2.25 *The linear mapping R is well-defined and injective.*

Proof. See [84, Lemma 10.8]. □

Thus, the mapping R is bijective if we restrict the codomain to $R(\mathcal{F}_\Phi(\Omega))$. That means we can identify the space $\mathcal{F}_\Phi(\Omega)$ with a subspace of continuous functions through R. We give this space a special name.

Definition 2.26 *Suppose $\Phi\colon \Omega \times \Omega \to \mathbb{R}$ is a symmetric positive definite kernel. We call the space*

$$\mathcal{N}_\Phi(\Omega) = R(\mathcal{F}_\Phi(\Omega))$$

the **native space** *of Φ.*

Theorem 2.27 *Suppose $\Phi\colon \Omega \times \Omega \to \mathbb{R}$ is a symmetric positive definite kernel. Then its associated native space $\mathcal{N}_\Phi(\Omega)$ carries the inner product*

$$(f, g)_{\mathcal{N}_\Phi(\Omega)} = (R^{-1}f, R^{-1}g)_\Phi$$

and is a Hilbert space of continuous functions with reproducing kernel Φ. Furthermore, the native space is unique.

Proof. See [84, Theorem 10.10 and Theorem 10.11]. □

Even though we identified elements in $\mathcal{F}_\Phi(\Omega)$ with continuous functions, the definition of a native space is still rather abstract. In the special case where Ω is the whole Euclidean space $\mathbb{R}^d$ and Φ is *translation invariant*, i. e. $\Phi(\mathbf{x}, \mathbf{y}) = \Phi(\mathbf{x} - \mathbf{y})$, we can express the native space in terms of Fourier transforms.

Theorem 2.28 *Suppose $\Phi \in C(\mathbb{R}^d) \cap L_1(\mathbb{R}^d)$ is a real-valued positive definite function. The space*

$$\mathcal{G} = \left\{ f \in L_2(\mathbb{R}^d) \cap C(\mathbb{R}^d) \mid \frac{\widehat{f}}{\sqrt{\widehat{\Phi}}} \in L_2(\mathbb{R}^d) \right\}$$

with the bilinear form

$$(f, g)_\mathcal{G} = \frac{1}{(2\pi)^{d/2}} \left(\frac{\widehat{f}}{\sqrt{\widehat{\Phi}}}, \frac{\widehat{g}}{\sqrt{\widehat{\Phi}}} \right)_{L_2(\mathbb{R}^d)} = \frac{1}{(2\pi)^{d/2}} \int_{\mathbb{R}^d} \frac{\widehat{f}(\boldsymbol{\omega})\overline{\widehat{g}(\boldsymbol{\omega})}}{\widehat{\Phi}(\boldsymbol{\omega})} d\boldsymbol{\omega}$$

is a real Hilbert space with inner product $(\cdot, \cdot)_\mathcal{G}$ and reproducing kernel $\Phi(\cdot - \cdot)$. Hence, by the uniqueness result from Theorem 2.27 *we have $\mathcal{G} = \mathcal{N}_{\Phi(\cdot - \cdot)}(\Omega)$ and both inner products coincide.*

Proof. See [84, Theorem 10.12]. □

For convenience we write from now on $\mathcal{N}_\Phi(\Omega)$, instead of $\mathcal{N}_{\Phi(\cdot,-\cdot)}(\Omega)$. The theorem shows that native spaces for Gaussians and inverse multiquadrics are rather small. For Gaussians, for instance, the Fourier transform of a function $f \in \mathcal{N}_\Phi(\mathbb{R}^d)$ must decay faster than the Fourier transform of a Gaussian (another Gaussian). However, the native space contains the space of *band-limited* functions, i. e. functions whose Fourier transforms are compactly supported.

With the previous characterisation of native spaces in mind, even more can be said about native spaces if the Fourier transform of Φ decays only algebraically at a rate σ. In this case, the native space turns out to be a Sobolev space,

$$H^\sigma(\mathbb{R}^d) = \left\{ f \in L_2(\mathbb{R}^d) \mid \widehat{f}(\cdot)(1 + \|\cdot\|_2^2)^{\sigma/2} \in L_2(\mathbb{R}^d) \right\},$$

which by Theorem 1.4 can be embedded into the space of continuous functions if the differentiability order σ is bigger than half the space dimension, i. e. $\sigma > d/2$. We summarise our thoughts in the following corollary.

Corollary 2.29 *Let $\sigma > d/2$. Suppose for $\Phi \in L_1(\mathbb{R}^d) \cap C(\mathbb{R}^d)$ there are constants $c_1, c_2 > 0$ such that*

$$c_1(1 + \|\boldsymbol{\omega}\|_2^2)^{-\sigma} \leq \widehat{\Phi}(\boldsymbol{\omega}) \leq c_2(1 + \|\boldsymbol{\omega}\|_2^2)^{-\sigma}, \tag{2.7}$$

holds for all $\boldsymbol{\omega} \in \mathbb{R}^d$. Then the native space $\mathcal{N}_\Phi(\mathbb{R}^d)$ corresponding to the function Φ coincides with the Sobolev space $H^\sigma(\mathbb{R}^d)$, and the native space norm and the Sobolev norm are equivalent.

Due to the above we will sometimes say that the function Φ *generates* the Sobolev space $H^\sigma(\mathbb{R}^d)$. It will become important to understand how far the above result generalises if we employ a scaled translation-invariant kernel Φ_δ given by

$$\Phi_\delta(\mathbf{x} - \mathbf{y}) = \delta^{-d}\Phi((\mathbf{x} - \mathbf{y})/\delta).$$

The factor δ^{-d} is chosen to simplify the notation when dealing with the Fourier transform. If the Fourier transform of Φ satisfies the algebraic decay condition (2.7), then the Fourier transform $\widehat{\Phi_\delta}(\boldsymbol{\omega}) = \widehat{\Phi}(\delta\boldsymbol{\omega})$ satisfies for $\boldsymbol{\omega} \in \mathbb{R}^d$ the following scaled version of the algebraic decay condition,

$$c_1(1 + \delta^2\|\boldsymbol{\omega}\|_2^2)^{-\sigma} \leq \widehat{\Phi_\delta}(\boldsymbol{\omega}) \leq c_2(1 + \delta^2\|\boldsymbol{\omega}\|_2^2)^{-\sigma}.$$

With this estimate in mind, we can deduce that many differently scaled kernels generate the same Sobolev space, see the following lemma, proven in [87]. It is possible to relax the condition $\delta \in (0, 1]$ to $\delta \in (0, \delta_0]$ for some $\delta_0 > 0$, which would lead to different equivalence constants c_1 and c_2, depending on the support radius δ.

Lemma 2.30 *For every $\delta \in (0,1]$, we have $\mathcal{N}_{\Phi_\delta}(\mathbb{R}^d) = H^\sigma(\mathbb{R}^d)$. Additionally, we have for every $g \in H^\sigma(\mathbb{R}^d)$ the following norm equivalence,*

$$c_1 \|g\|_{\Phi_\delta} \leq \|g\|_{W_2^\sigma(\mathbb{R}^d)} \leq c_2 \delta^{-\sigma} \|g\|_{\Phi_\delta},$$

with $c_1, c_2 > 0$.

As an example, we look at the native spaces of Wendland's compactly supported functions. It can be shown that the Fourier transforms of these functions decay algebraically.

Theorem 2.31 *Let $\Phi_{d,k} = \phi_{d,k}(\|\cdot\|_2)$ denote the function induced by the compactly supported radial basis function of minimal degree that is positive definite on $\mathbb{R}^d$ and in $C^{2k}(\mathbb{R}^d)$, see* Definition 2.16. *In the case of $k = 0$, we need the additional requirement of $d \geq 3$. Then there exist constants $c_1, c_2 > 0$ depending only on d and k such that*

$$c_1(1 + \|\boldsymbol{\omega}\|_2)^{-d-2k-1} \leq \widehat{\Phi_{d,k}}(\boldsymbol{\omega}) \leq c_2(1 + \|\boldsymbol{\omega}\|_2)^{-d-2k-1}$$

for all $\boldsymbol{\omega} \in \mathbb{R}^d$.

Proof. See [84, Theorem 10.35]. □

Note the subtle difference between the two inequalities in Corollary 2.29 and Theorem 2.31. The first inequality uses the square of the Euclidean norm whereas the second does not. In particular this implies

$$\mathcal{N}_{\Phi_{d,k}}(\mathbb{R}^d) = H^{d/2+k+1/2}(\mathbb{R}^d),$$

that is, the native space for these basis functions is a classical Sobolev space.

2.2.3 Error Analysis and Optimality

In this section, we discuss the error of our approximation scheme. When talking about randomly scattered data it is not entirely obvious how to do this. One way is to measure the error in terms of the size of the biggest hole in the data set.

Definition 2.32 *Suppose $\Omega \subseteq \mathbb{R}^d$ and $X = \{\mathbf{x}_1, \ldots, \mathbf{x}_N\}$, then we call*

$$h_{X,\Omega} = \sup_{\mathbf{x} \in \Omega} \min_{\mathbf{x}_j \in X} \|\mathbf{x} - \mathbf{x}_j\|_2$$

the **mesh norm** *or* **fill distance** *of Ω. The smallest distance between two points in X*

$$q_X = \min_{j \neq k} \|\mathbf{x}_j - \mathbf{x}_k\|_2$$

is called the **separation distance**.

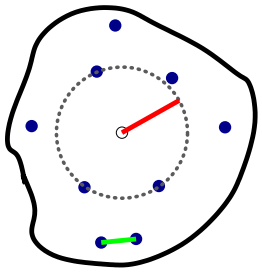

Figure 2.2: For given data sites in a domain (blue dots) the picture shows the mesh norm (red) and the separation distance (green).

The mesh norm measures the radius of the largest data site free ball that is entirely contained in Ω, see Figure 2.2. We shall estimate the error and the convergence order in terms of the fill distance $h_{X,\Omega}$. This is achieved by so called *sampling inequalities*, which were first proven in [3, 67]. We will need a version which allows fractional values on the left-hand side. This can be achieved by interpolation of Sobolev spaces. The following sampling inequality can be found in [86, Theorem 4.6]. It assumes that the domain has a Lipschitz boundary. The definition of a Lipschitz boundary can be found in [7, Definition 1.4.4].

But since we will work a lot with Lipschitz and even smoother boundaries, we give a brief and more intuitive introduction here. The definition below is essentially equivalent to the previously cited one and helps prepare later calculations.

Roughly speaking, we can describe a *Lipschitz boundary* by patching together graphs of Lipschitz continuous functions. More precisely, let us assume that we have a finite cover such that $\partial\Omega = \bigcup_{j=1}^{N} V_j$ for some integer $N > 0$ and relative open sets $V_j \subseteq \partial\Omega \subseteq \mathbb{R}^d$. Then we say Ω has a Lipschitz boundary if there are bijective functions $\psi_j \colon B \to V_j$ such that ψ_j and ψ_j^{-1} are Lipschitz continuous functions. Here B denotes the unit ball in $d-1$ dimensions $B(\mathbf{0},1) \subseteq \mathbb{R}^{d-1}$. The functions ψ_j are referred to as *charts* and the collection $\{\psi_j, V_j\}$ is called an *atlas*. If all functions ψ_j and their inverses are actually smoother, for example in $C^{k,s}$ with $k \in \mathbb{N}_0$ and $s \in [0,1)$, then we say the boundary is $C^{k,s}$ smooth.

Theorem 2.33 (Sampling Inequality for Fractional Norms) *Let $\Omega \subseteq \mathbb{R}^d$ be a bounded domain with a Lipschitz boundary, $1 < p < \infty$, $q < \infty$ and $\sigma > d/p$. Let $X \subseteq \Omega$ be a discrete set with a sufficiently small mesh norm $h_{X,\Omega}$. For each $u \in W_p^\sigma(\Omega)$ with $u|_X = 0$, we have for $0 \le \tau \le \sigma - d(1/p - 1/q)_+$ the estimate*

$$|u|_{W_q^\tau(\Omega)} \le C h_{X,\Omega}^{\sigma-\tau-d(1/p-1/q)_+} |u|_{W_p^\sigma(\Omega)}$$

where $C > 0$ is a constant independent of u and $h_{X,\Omega}$.

To make this theorem a bit more concrete, we present two inequalities that can be proven with its help. Let us suppose we have a kernel Φ that generates the

Sobolev space $H^\sigma(\mathbb{R}^d)$ for $\sigma > d/2$. Then, we have the two special cases

$$\begin{aligned} \|f - s_{f,X}\|_{L_2(\Omega)} &\leq C_1 h_{X,\Omega}^{\sigma} \|f\|_{H^\sigma(\Omega)}, \\ \|f - s_{f,X}\|_{L_\infty(\Omega)} &\leq C_2 h_{X,\Omega}^{\sigma - d/2} \|f\|_{H^\sigma(\Omega)}. \end{aligned} \tag{2.8}$$

The first inequality follows from the previous theorem. Technically, the second inequality cannot be deduced in the same way since we assumed $q < \infty$ when stating the theorem. However, more general results are available to justify this, see for example [84]. To show that both equations hold, we need to extend the domain to the whole Euclidean space with the help of extension operators (details can be found in Chapter 4) and use the norm equivalence between Sobolev space and native space as well as the following best approximation property for $s = 0$.

Theorem 2.34 (Best Approximation Property) *Suppose that $\Phi \in C(\Omega)$ is a positive definite function and that $f \in \mathcal{N}_\Phi(\Omega)$ is known only at $X = \{\mathbf{x}_1, \ldots, \mathbf{x}_N\} \subseteq \Omega \subseteq \mathbb{R}^d$. Then the interpolant $s_{f,X}$ from (2.1) is the best approximation to f from the space $F_{\Phi,X} = \operatorname{span}\{\Phi(\cdot - \mathbf{x}) \mid \mathbf{x} \in X\}$ with respect to the corresponding native space norm. In particular, we have*

$$\|f - s_{f,X}\|_\Phi \leq \|f - s\|_\Phi$$

for all $s \in F_{\Phi,X}$. Hence, $s_{f,X}$ is the orthogonal projection of f onto $F_{\Phi,X}$.

Proof. See [84, Theorem 13.1]. □

Similar to spline interpolants the interpolants of the form (2.1) are optimal among all interpolants in the native space norm.

Theorem 2.35 (Optimality) *Let $\Omega \subseteq \mathbb{R}^d$. Suppose that $\Phi\colon \Omega \to \mathbb{R}$ is a positive definite function. Then the interpolant $s_{f,X}$ from (2.1) for a given function f and a given data set $X = \{\mathbf{x}_1, \mathbf{x}_2, ..., \mathbf{x}_N\} \subseteq \mathbb{R}^d$ is minimal in the Φ norm among all functions $s \in \mathcal{N}_\Phi(\Omega)$ that interpolate the data $f_j = f(\mathbf{x}_j)$ for $1 \leq j \leq N$. That is,*

$$\|s_{f,X}\|_\Phi = \min\{\|s\|_\Phi \mid s \in \mathcal{N}_\Phi(\Omega) \text{ with } s(\mathbf{x}_j) = f_j, 1 \leq j \leq N\}.$$

Proof. See [84, Theorem 13.2]. □

In this chapter, we have given a thorough introduction to the theory of positive definite functions, which included their characterisation, some background on kernel reproducing Hilbert spaces and a discussion of compactly supported radial basis functions. Since we are eventually interested in constructing a collocation method, we will discuss how these results transfer to a more general Hilbert space setting in the next chapter.

Chapter 3

Collocation

Thus far, we have only discussed a numerical scheme for interpolation. In the introduction, however, we already pointed out that there is a way to use approximation techniques with positive definite functions in a broader context. In this chapter, which partially relies on [84, Section 16.1 and Section 16.3], we investigate one way to do this.

3.1 Generalised Interpolation

In order to generalise the interpolation scheme, we start by going back to the interpolant $s_{f,X}$ from (2.1). With the help of the point evaluation functional $\delta_{\mathbf{x}}$ it can be written

$$s_{f,X}(\mathbf{x}) = \sum_{j=1}^{N} \alpha_j \Phi(\mathbf{x} - \mathbf{x}_j) = \sum_{j=1}^{N} \alpha_j \delta_{\mathbf{x}_j}^{\mathbf{y}} \Phi(\mathbf{x} - \mathbf{y}).$$

The superscript here denotes the argument to which the evaluation functional is applied, leaving the other one unaltered. We will frequently use this notation, also for more complicated functionals.

The question now is under which conditions we can still construct a unique and in some sense best approximant to a generalised interpolation problem if we replace the point evaluation functional $\delta_{\mathbf{x}_j}$ by an arbitrary functional λ_j.

The natural environment to discuss best approximation properties are Hilbert spaces. Let $H \subseteq C(\Omega)$ denote a Hilbert space of continuous and real-valued functions and H^* its dual. Furthermore, assume we are given N linearly independent functionals $\lambda_1, \ldots, \lambda_N \in H^*$ as well as some target function $f \in H$, of which we only know $f_j = \lambda_j(f) \in \mathbb{R}$ for $1 \leq j \leq N$. Lastly, let us suppose we are given Riesz representers $\mathbf{v}_j \in H$ such that $\lambda_j = (\cdot, \mathbf{v}_j)_H$. Then, one can show well-posedness of the generalised interpolation problem as well as a minimisation property.

Theorem 3.1 *There is a unique interpolant of the form*

$$s_{f,\Lambda} = \sum_{j=1}^{N} \alpha_j \mathbf{v}_j \in H, \tag{3.1}$$

which solves the generalised interpolation problem,

$$\lambda_j(s_{f,\Lambda}) = f_j, \tag{3.2}$$

and is norm-minimal in the Hilbert space norm, i. e.

$$\|s_{f,\Lambda}\|_H \leq \|s\|_H$$

for all $s \in H$ *with* $\lambda_j(s) = f_j$ *for* $1 \leq j \leq N$.

Proof. See [84, Theorem 16.1]. □

Even though the function $s_{f,\Lambda}$ is not an interpolant in the classical sense, we will sometimes refer to it as an interpolant. This shall remind us of the fact that the generalised interpolation conditions (3.2) hold.

Corollary 3.2 *If* H *is a Hilbert space with reproducing kernel* Φ*, we can write the optimal solution* $s_{f,\Lambda}$ *from* (3.1) *in the following form*

$$s_{f,\Lambda}(\mathbf{x}) = \sum_{j=1}^{N} \alpha_j \lambda_j^{\mathbf{y}} \Phi(\mathbf{x} - \mathbf{y}). \tag{3.3}$$

Proof. This is due to the fact that for $\Phi(\cdot - \mathbf{x}) \in H$, for some fixed $\mathbf{x} \in \Omega$, we find

$$\lambda_j^{\mathbf{y}}(\Phi(\mathbf{y} - \mathbf{x})) = (\Phi(\cdot - \mathbf{x}), \mathbf{v}_j)_H = (\mathbf{v}_j, \Phi(\cdot - \mathbf{x}))_H = \mathbf{v}_j(\mathbf{x}),$$

where the last equality holds by the reproduction property. □

Similar to pure interpolation, we obtain the coefficients of the interpolant (3.3) by applying (3.2) to it and then solving the linear system

$$\begin{pmatrix} \lambda_1^{\mathbf{x}}\lambda_1^{\mathbf{y}}\Phi(\mathbf{x}-\mathbf{y}) & \dots & \lambda_1^{\mathbf{x}}\lambda_N^{\mathbf{y}}\Phi(\mathbf{x}-\mathbf{y}) \\ \vdots & & \vdots \\ \lambda_N^{\mathbf{x}}\lambda_1^{\mathbf{y}}\Phi(\mathbf{x}-\mathbf{y}) & \dots & \lambda_N^{\mathbf{x}}\lambda_N^{\mathbf{y}}\Phi(\mathbf{x}-\mathbf{y}) \end{pmatrix} \begin{pmatrix} \alpha_1 \\ \vdots \\ \alpha_N \end{pmatrix} = \begin{pmatrix} f_1 \\ \vdots \\ f_N \end{pmatrix}. \tag{3.4}$$

We abbreviate the system with

$$A_{\Phi,\Lambda}\, \boldsymbol{\alpha} = \mathbf{f}.$$

Note that this matrix is again symmetric and positive definite, see [84, Theorem 16.1] for details. In the Hilbert space setting, it is also possible to show another optimality property, which we have shown before in a more specific context, namely Theorem 2.34.

Theorem 3.3 (Best Approximation Property for Generalised Interpolants) *The function $s_{f,\Lambda}$ is the best approximation from the space $V = \operatorname{span}\{\mathbf{v}_1, \ldots, \mathbf{v}_N\}$ to $f \in H$ i. e.*

$$\|f - s_{f,\Lambda}\|_H \leq \|f - s\|_H$$

for all $s \in V$.

Proof. By (3.2), we have

$$0 = \lambda_j(f) - \lambda_j(s_{f,\Lambda}) = (f - s_{f,\Lambda}, \mathbf{v}_j)_H$$

for $1 \leq j \leq N$, which is just another characterisation of the best approximation in Euclidean spaces. □

3.1.1 Collocation with Positive Definite Functions

In the previous section, we have discussed a rather general Hilbert space setting. In this thesis we are interested in collocation, which effectively means that we replace the abstract functionals in the preceding section by differential and boundary operators. There are two advantages of such a collocation method with positive definite functions. Firstly, it allows to compute a numerical solution to a PDE even if some of the boundary data is missing. Then, of course the boundary value problem might not be well-posed anymore. But even though it is analytically not clear to which numerical approximation the method converges (since there might not be a unique solution), one would still obtain a converging method. Secondly, due to the symmetric and positive definite discrete system regardless of the underlying problem, there is some hope that this method even works for convection-dominated problems, where the standard finite element method produces unwanted oscillatory solutions, see for example [47, Chapter 9].

3.1.2 Elliptic Boundary Value Problems of Second Order

Finally, we wish to prepare the theoretical background for the multiscale collocation algorithm, that we wish to prove in the next chapter of this thesis, where we consider elliptic problems of second order with Dirichlet boundary conditions. We want to approximate a solution $u\colon \overline{\Omega} \to \mathbb{R}$ to an elliptic partial differential equation of the form

$$\begin{aligned} Lu &= f \qquad \text{in} \quad \Omega \\ u &= F \qquad \text{on} \quad \partial\Omega, \end{aligned} \tag{3.5}$$

where L is an elliptic linear differential operator of second order

$$Lu(\mathbf{x}) = \sum_{i,j=1}^{d} a_{ij}(\mathbf{x}) \frac{\partial^2}{\partial x_i \partial x_j} u(\mathbf{x}) + \sum_{i=1}^{d} b_i(\mathbf{x}) \frac{\partial}{\partial x_i} u(\mathbf{x}) + c(\mathbf{x}) u(\mathbf{x}), \tag{3.6}$$

which is strictly elliptic on Ω. This means that there exists a constant $c_E > 0$ such that

$$c_E \|\boldsymbol{\xi}\|_2^2 \leq \sum_{i,j=1}^{d} a_{ij}(\mathbf{x}) \xi_i \xi_j$$

for all $\mathbf{x} \in \Omega$ and $\boldsymbol{\xi} = (\xi_1, \ldots, \xi_d)^T \in \mathbb{R}^d$.

If we assume that $u \in H^\sigma(\Omega)$ with $\sigma > 2 + d/2$, then Lu is in fact well-defined since we know by the Sobolev embedding theorem (Theorem 1.4) that $H^\sigma(\Omega) \subseteq C^2(\Omega)$. We choose a point set $X = X_1 \cup X_2$, consisting of the union of interior points $X_1 = \{\mathbf{x}_1, \ldots, \mathbf{x}_n\}$ in Ω and boundary points $X_2 = \{\mathbf{x}_{n+1}, \ldots, \mathbf{x}_N\}$ on $\partial\Omega$. Then, we can define linear functionals

$$\lambda_j = \begin{cases} \delta_{\mathbf{x}_j} \circ L, & 1 \leq j \leq n, \\ \delta_{\mathbf{x}_j}, & n+1 \leq j \leq N. \end{cases} \tag{3.7}$$

Assuming these functionals $\Lambda = \{\lambda_1, \ldots, \lambda_N\}$ are linearly independent, we can construct (according to Theorem 3.1) a unique Φ norm-minimal interpolant of the form

$$s_{u,\Lambda} = \sum_{j=1}^{N} \alpha_j \lambda_j^{\mathbf{y}} \Phi(\cdot, \mathbf{y}) = \sum_{j=1}^{n} \alpha_j L^{\mathbf{y}} \Phi(\cdot, \mathbf{x}_j) + \sum_{j=n+1}^{N} \alpha_j \Phi(\cdot, \mathbf{x}_j),$$

that satisfies the generalised interpolation conditions

$$\begin{aligned} L s_{u,\Lambda}(\mathbf{x}_j) &= f(\mathbf{x}_j) \qquad 1 \leq j \leq n, \\ s_{u,\Lambda}(\mathbf{x}_j) &= g(\mathbf{x}_j) \qquad n+1 \leq j \leq N. \end{aligned}$$

The superscript in $L^{\mathbf{y}}$ denotes action with respect to the second argument. These conditions yield a block matrix system of the form

$$\begin{pmatrix} A_{LL} & A_{LB} \\ A_{BL} & A_{BB} \end{pmatrix} \begin{pmatrix} \boldsymbol{\alpha}_L \\ \boldsymbol{\alpha}_B \end{pmatrix} = \begin{pmatrix} \mathbf{f} \\ \mathbf{F} \end{pmatrix}$$

which needs to be solved in order to determine the coefficients. The different parts of the system are given by

$$\begin{aligned} A_{LL} &= \left((\delta_{\mathbf{x}_j} \circ L)^{\mathbf{x}} (\delta_{\mathbf{x}_k} \circ L)^{\mathbf{y}} \Phi(\mathbf{x}, \mathbf{y}) \right)_{1 \leq j,k \leq n}, & A_{BB} &= \left(\Phi(\mathbf{x}_j, \mathbf{y}_k) \right)_{n+1 \leq j,k \leq N}, \\ A_{LB} &= \left((\delta_{\mathbf{x}_j} \circ L)^{\mathbf{x}} \Phi(\mathbf{x}, \mathbf{x}_k) \right)_{\substack{1 \leq j \leq n \\ n+1 \leq k \leq N}}, & A_{BL} &= A_{LB}^T, \\ \boldsymbol{\alpha}_L &= (\alpha_j)_{1 \leq j \leq n}, & \boldsymbol{\alpha}_B &= (\alpha_j)_{n+1 \leq j \leq N}, \\ \mathbf{f} &= (f(\mathbf{x}_j))_{1 \leq j \leq n}, & \mathbf{F} &= (F(\mathbf{x}_j))_{n+1 \leq j \leq N}. \end{aligned}$$

In the following chapters, we will often drop the Λ and denote the collocation approximation with s_u.

We need to make sure that the functionals defined in (3.7) are linearly independent for this system to be uniquely solvable. We introduce the notion of a singular point of a differential operator.

Definition 3.4 *Let L be defined as in* (3.6)*. The point $\mathbf{x} \in \mathbb{R}^d$ is called a* **singular point** *of L if $\delta_x \circ L = 0$, i. e. $a_{ij}(\mathbf{x}) = b_i(\mathbf{x}) = c(\mathbf{x}) = 0$ for all $1 \leq i, j \leq d$.*

With this definition one can prove the following theorem, which is taken from [37, Proposition 3.8].

Theorem 3.5 *Let L be defined as in* (3.6)*. Let $X_1 = \{\mathbf{x}_1, \ldots, \mathbf{x}_n\} \subseteq \Omega$ and $X_2 = \{\mathbf{x}_{n+1}, \ldots, \mathbf{x}_N\} \subseteq \partial\Omega$ be two sets of pairwise distinct points such that X_1 contains no singular point of L. Then the functionals defined in* (3.7) *are linearly independent over $H^\sigma(\mathbb{R}^d)$ with $\sigma > 2 + d/2$.*

Due to this theorem, we will assume in the following chapters that the interior collocation points never contain a singular point of the differential operator L.

So far we have not imposed any restrictions on the coefficients. If we assume that $a_{ij}, b_i, c \in W_\infty^{k-1}(\Omega)$ for $k := \lfloor \sigma \rfloor$, then one can verify that L is a bounded operator from $W_2^\sigma(\Omega)$ to $W_2^{\sigma-2}(\Omega)$, see Lemma 3.6. However, since $(k-1) - 1 > d/2$, we can again use the Sobolev embedding theorem to conclude that $W_\infty^{k-1} \subseteq W_2^{k-1}(\Omega) \subseteq C^1(\Omega)$. The proof of the following lemma can be found in a more general context in [37, Lemma 3.4].

Lemma 3.6 *Let $\sigma \in \mathbb{R}$ with $k := \lfloor \sigma \rfloor > 2 + d/2$. Suppose that the coefficients a_{ij}, b_i and c of the operator defined in* (3.6) *are in $W_\infty^{k-1}(\Omega)$. Then L is a bounded operator from $W_2^\sigma(\Omega)$ to $W_2^{\sigma-2}(\Omega)$, i. e.*

$$\|Lu\|_{W_2^{\sigma-2}(\Omega)} \leq C \|u\|_{W_2^\sigma(\Omega)}$$

for $u \in W_2^\sigma(\Omega)$.

Note that since the principal coefficients a_{ij} of the operator L are differentiable, we can write the operator in *divergence* form

$$Lu(\mathbf{x}) = \sum_{i,j=1}^{d} \frac{\partial}{\partial x_j} \left(a_{ij}(\mathbf{x}) \frac{\partial}{\partial x_i} u(\mathbf{x}) \right) + \sum_{i=1}^{d} \tilde{b}_i(\mathbf{x}) \frac{\partial}{\partial x_i} u(\mathbf{x}) + c(\mathbf{x}) u(\mathbf{x}), \tag{3.8}$$

where the coefficients $\tilde{b}_i$ are not the same as the b_i in (3.6). The divergence form of the elliptic operator has the advantage that it can be applied in a *weak* sense to more functions than twice continuously differentiable ones, see for instance [38, Chapter 8]. For our purposes this is not so important as we will work with functions in $H^\sigma(\Omega)$, which can be embedded in $C^2(\Omega)$.

3.1.3 Applying the Differential Operator to a Kernel

When discretising the operator L with the help of a positive definite kernel $\Phi(\mathbf{x} - \mathbf{y}) = \phi(\|\mathbf{x} - \mathbf{y}\|)$, we need to compute the two expressions $L^{\mathbf{y}} \Phi(\mathbf{x} - \mathbf{y})$ as well as

$L^{\mathbf{x}}L^{\mathbf{y}}\Phi(\mathbf{x}-\mathbf{y})$. First we note the relationships

$$\begin{aligned}
\partial_j^{\mathbf{x}}\Phi(\mathbf{x}-\mathbf{y}) =& -\partial_j^{\mathbf{y}}\Phi(\mathbf{x}-\mathbf{y}),\\
\partial_j^{\mathbf{y}}\partial_k^{\mathbf{y}}\Phi(\mathbf{x}-\mathbf{y}) =& \ \ \partial_j^{\mathbf{x}}\partial_k^{\mathbf{x}}\Phi(\mathbf{x}-\mathbf{y}),\\
\partial_j^{\mathbf{x}}\partial_k^{\mathbf{y}}\Phi(\mathbf{x}-\mathbf{y}) =& -\partial_j^{\mathbf{x}}\partial_k^{\mathbf{x}}\Phi(\mathbf{x}-\mathbf{y}),\\
\partial_j^{\mathbf{x}}\partial_k^{\mathbf{y}}\partial_\ell^{\mathbf{y}}\Phi(\mathbf{x}-\mathbf{y}) =& -\partial_j^{\mathbf{x}}\partial_k^{\mathbf{x}}\partial_\ell^{\mathbf{y}}\Phi(\mathbf{x}-\mathbf{y}).
\end{aligned}$$

Now we apply the operator L to the kernel. We use the nondivergence form (3.6) for computing this expression. We obtain

$$L^{\mathbf{y}}\Phi(\mathbf{x}-\mathbf{y}) = \left[\sum_{i,j=1}^{d} a_{ij}(\mathbf{y})\partial_i^{\mathbf{y}}\partial_j^{\mathbf{y}} + \sum_{i=1}^{d} b_i(\mathbf{y})\partial_i^{\mathbf{y}} + c(\mathbf{y})\right]\Phi(\mathbf{x}-\mathbf{y})$$

as well as

$$\begin{aligned}
L^{\mathbf{x}}L^{\mathbf{y}}\Phi(\mathbf{x}-\mathbf{y}) =& \Bigg[\sum_{i,j,k,\ell=1}^{d} a_{ij}(\mathbf{y})a_{k\ell}(\mathbf{x})\partial_i^{\mathbf{y}}\partial_j^{\mathbf{y}}\partial_k^{\mathbf{x}}\partial_\ell^{\mathbf{x}}\\
&+ \sum_{i,j,k=1}^{d}\left\{a_{ij}(\mathbf{x})b_k(\mathbf{y}) - a_{jk}(\mathbf{y})b_i(\mathbf{x})\right\}\partial_i^{\mathbf{x}}\partial_j^{\mathbf{x}}\partial_k^{\mathbf{y}}\\
&+ \sum_{i,j=1}^{d}\left\{a_{ij}(\mathbf{y})c(\mathbf{x}) + a_{ij}(\mathbf{x})c(\mathbf{y}) - b_i(\mathbf{x})b_j(\mathbf{y})\right\}\partial_i^{\mathbf{x}}\partial_j^{\mathbf{x}}\\
&+ \sum_{i=1}^{d}\left\{b_i(\mathbf{x})c(\mathbf{y}) - b_i(\mathbf{y})c(\mathbf{x})\right\}\partial_i^{\mathbf{x}} + c(\mathbf{y})c(\mathbf{x})\Bigg]\Phi(\mathbf{x}-\mathbf{y}).
\end{aligned}$$

We look at two simplifications of the last expressions. Firstly, assume that the differential operator only has constant coefficients, then

$$\begin{aligned}
&L^{\mathbf{x}}L^{\mathbf{y}}\Phi(\mathbf{x}-\mathbf{y}) =\\
&\left[\sum_{i,j,k,\ell=1}^{d} a_{ij}a_{k\ell}\partial_i^{\mathbf{x}}\partial_j^{\mathbf{x}}\partial_k^{\mathbf{x}}\partial_\ell^{\mathbf{x}} + \sum_{i,j=1}^{d}\left\{2a_{ij}c - b_ib_j\right\}\partial_i^{\mathbf{x}}\partial_j^{\mathbf{x}} + c^2\right]\Phi(\mathbf{x}-\mathbf{y})
\end{aligned}$$

and in the even more special case where the differential operator is given by the Laplacian, $L = \Delta$, we find

$$L^{\mathbf{x}}L^{\mathbf{y}}\Phi(\mathbf{x}-\mathbf{y}) = \sum_{i,j=1}^{d}\partial_i^{\mathbf{x}}\partial_i^{\mathbf{x}}\partial_j^{\mathbf{x}}\partial_j^{\mathbf{x}}\Phi(\mathbf{x}-\mathbf{y}).$$

Finally, we compute the partial derivatives of a scaled radial function. However, since for higher dimensions several different cases would need to be considered, we restrict ourselves to functions of two dimensional arguments here. This already

yields eight different cases for all derivatives up to fourth order. Setting $r = \|\mathbf{x}\| = \sqrt{x^2+y^2}$, we obtain

$$
\begin{aligned}
\partial_x \Phi(\varepsilon\mathbf{x}) &= \varepsilon\phi'(\varepsilon r)\frac{\partial r}{\partial x},\\
\partial_{xx} \Phi(\varepsilon\mathbf{x}) &= \varepsilon^2\phi''(\varepsilon r)\left(\frac{\partial r}{\partial x}\right)^2 + \varepsilon\phi'(\varepsilon r)\frac{\partial^2 r}{\partial x^2},\\
\partial_{xy} \Phi(\varepsilon\mathbf{x}) &= \varepsilon^2\phi''(\varepsilon r)\frac{\partial r}{\partial x}\frac{\partial r}{\partial y} + \varepsilon\phi'(\varepsilon r)\frac{\partial^2 r}{\partial x\partial y},\\
\partial_{x^3} \Phi(\varepsilon\mathbf{x}) &= \varepsilon^3\phi'''(\varepsilon r)\left(\frac{\partial r}{\partial x}\right)^3 + 3\varepsilon^2\phi''(\varepsilon r)\frac{\partial r}{\partial x}\frac{\partial^2 r}{\partial x^2} + \varepsilon\phi'(\varepsilon r)\frac{\partial^3 r}{\partial x^3},\\
\partial_{x^2y} \Phi(\varepsilon\mathbf{x}) &= \varepsilon^3\phi'''(\varepsilon r)\left(\frac{\partial r}{\partial x}\right)^2\frac{\partial r}{\partial y}\\
&\quad + \varepsilon^2\phi''(\varepsilon r)\left\{2\frac{\partial r}{\partial x}\frac{\partial^2 r}{\partial x\partial y} + \frac{\partial r}{\partial y}\frac{\partial^2 r}{\partial y^2}\right\} + \varepsilon\phi'(\varepsilon r)\frac{\partial^3 r}{\partial x^2\partial y},\\
\partial_{x^4} \Phi(\varepsilon\mathbf{x}) &= \varepsilon^4\phi''''(\varepsilon r)\left(\frac{\partial r}{\partial x}\right)^4 + 6\varepsilon^3\phi'''(\varepsilon r)\left(\frac{\partial r}{\partial x}\right)^2\frac{\partial^2 r}{\partial x^2}\\
&\quad + \varepsilon^2\phi''(\varepsilon r)\left\{3\left(\frac{\partial^2 r}{\partial x^2}\right)^2 + 4\frac{\partial r}{\partial x}\frac{\partial^3 r}{\partial x^3}\right\} + \varepsilon\phi'(\varepsilon r)\frac{\partial^4 r}{\partial x^4},\\
\partial_{x^3y} \Phi(\varepsilon\mathbf{x}) &= \varepsilon^4\phi''''(\varepsilon r)\left(\frac{\partial r}{\partial x}\right)^3\frac{\partial r}{\partial y} + 3\varepsilon^3\phi'''(\varepsilon r)\left\{\left(\frac{\partial r}{\partial x}\right)^2\frac{\partial^2 r}{\partial x\partial y} + \frac{\partial r}{\partial x}\frac{\partial r}{\partial y}\frac{\partial^2 r}{\partial x^2}\right\}\\
&\quad + \varepsilon^2\phi''(\varepsilon r)\left\{3\frac{\partial^2 r}{\partial x\partial y}\frac{\partial^2 r}{\partial x^2} + 3\frac{\partial r}{\partial x}\frac{\partial^3 r}{\partial x^2\partial y} + \frac{\partial r}{\partial y}\frac{\partial^3 r}{\partial x^3}\right\} + \varepsilon\phi'(\varepsilon r)\frac{\partial^4 r}{\partial x^3\partial y},\\
\partial_{x^2y^2} \Phi(\varepsilon\mathbf{x}) &= \varepsilon^4\phi''''(\varepsilon r)\left(\frac{\partial r}{\partial x}\right)^2\left(\frac{\partial r}{\partial y}\right)^2\\
&\quad + \varepsilon^3\phi'''(\varepsilon r)\left\{4\frac{\partial r}{\partial x}\frac{\partial r}{\partial y}\frac{\partial^2 r}{\partial x\partial y} + \left(\frac{\partial r}{\partial x}\right)^2\frac{\partial^2 r}{\partial y^2} + \left(\frac{\partial r}{\partial y}\right)^2\frac{\partial^2 r}{\partial x^2}\right\}\\
&\quad + \varepsilon^2\phi''(\varepsilon r)\left\{2\left(\frac{\partial^2 r}{\partial x\partial y}\right)^2 + 2\frac{\partial r}{\partial x}\frac{\partial^3 r}{\partial x\partial y^2} + 2\frac{\partial r}{\partial y}\frac{\partial^3 r}{\partial x^2\partial y} + \frac{\partial^2 r}{\partial x^2}\frac{\partial^2 r}{\partial y^2}\right\}\\
&\quad + \varepsilon\phi'(\varepsilon r)\frac{\partial^4 r}{\partial x^2\partial y^2},
\end{aligned}
$$

where we have repeatedly used the chain rule.

The partial derivatives of the Euclidean norm are also easily computed.

$$\frac{\partial r}{\partial x} = \frac{x}{r}, \qquad \frac{\partial r}{\partial y} = \frac{y}{r},$$
$$\frac{\partial^2 r}{\partial x^2} = \frac{y^2}{r^3}, \qquad \frac{\partial^2 r}{\partial y^2} = \frac{x^2}{r^3}, \qquad \frac{\partial^2 r}{\partial x \partial y} = -\frac{xy}{r^3},$$
$$\frac{\partial^4 r}{\partial x^4} = -3\frac{y^2}{r^5} - 15\frac{x^2 y^2}{r^7}, \quad \frac{\partial^4 r}{\partial x^2 \partial y^2} = \frac{2}{r^3} - 15\frac{y^2}{r^5} + 15\frac{y^4}{r^7}, \quad \frac{\partial^4 r}{\partial x^3 \partial y} = -6\frac{xy}{r^5} + 15\frac{xy^3}{r^7}.$$

After having presented the necessary tools in the previous chapters, we can turn our attention to multilevel radial basis functions techniques to solve partial differential equations. We start with elliptic boundary value problems.

Chapter 4

Elliptic Boundary Value Problems

Even though one-shot RBF methods are successfully used in practice, they suffer from ill-conditioning. Let us for example consider Franke's two dimensional test function [34] for scattered data,

$$f(x,y) = \frac{3}{4}e^{-1/4((9x-2)^2+(9y-2)^2)} + \frac{3}{4}e^{-1/49(9x+1)^2-1/10(9y+1)^2} + \frac{1}{2}e^{-1/4((9x-7)^2+(9y-3)^2)} - \frac{1}{5}e^{-(9x-4)^2-(9y-7)^2},$$

which is depicted in Figure 4.1.

We use Gaussians to reconstruct Franke's functions from uniformly sampled data. One would expect that this is a sensible choice since Franke's test function consists of a linear combination of Gaussians. Even though Gaussians are in theory globally supported radial basis functions, for practical purposes they decay so fast that they can be considered to be compactly supported if the domain is sufficiently large. We will scale the Gaussian basis functions with a shape parameter ε by setting $\Phi_\varepsilon = \Phi(\varepsilon\cdot)$. That is, roughly speaking the shape parameter acts like the inverse of the previously introduced support radius.

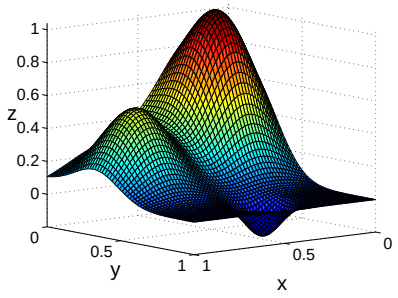

Figure 4.1: Franke's test function

N	$\varepsilon = 2$	$\varepsilon = 4$	$\varepsilon = 8$	$\varepsilon = 16$	$\varepsilon = 32$
25	1.13e-01	4.06e-02	1.20e-01	2.78e-01	3.53e-01
289	5.26e-02	1.64e-02	4.48e-03	3.46e-02	1.64e-01
1089	6.37e-02	4.76e-04	3.65e-05	3.56e-03	2.95e-02

Table 4.1: L_2 errors for RBF interpolation of Franke's function using Gaussians as basis functions for different uniform grids and shape parameters.

N	$\varepsilon = 2$	$\varepsilon = 4$	$\varepsilon = 8$	$\varepsilon = 16$	$\varepsilon = 32$
25	4.42e+05	1.74e+02	2.74e+00	1.05e+00	1.00e+00
289	3.87e+20	1.72e+17	9.68e+06	1.83e+02	5.19e+00
1089	3.22e+20	1.48e+19	1.36e+18	3.37e+07	4.59e+02

Table 4.2: Condition numbers for RBF interpolation matrices $A_{\Phi,X}$ when approximating Franke's function with Gaussians as basis functions for different uniform grids and shape parameters.

Tables 4.1 and 4.2 list the L_2 errors and condition numbers for different uniform grids and shape parameters for this simple test problem. Several problems become apparent. The reconstruction depends highly on the shape parameter ε. In fact, a great part of the RBF literature focuses on how to find the optimal shape parameter, see [24] for example. Moreover, the condition numbers grow drastically when the amount of data points grows. This has a negative effect on our approximation. If $\varepsilon = 2$, we can see that the condition numbers have become so large that we cannot compute accurately any longer. Comparing the L_2 error for $N = 289$ and $N = 1089$ for instance, we see that the computed errors worsen even though we would expect them to decrease. Lastly, we note that when the L_2 error is low, the condition numbers are very large.

This last statement is a general concept. Schaback [72] showed for interpolation problems that it is impossible to keep the condition numbers as well as the error between interpolant and target function small at the same time. This relationship is often referred to as *trade-off principle*. Since for larger and larger systems the cost to achieve a certain tolerance can be unbearably high, we turn to multilevel strategies for compactly supported radial basis functions in this chapter to help resolve this issue.

The convergence proof of the multilevel interpolation algorithm is due to Wendland [87]. Previous work has been done on the sphere [49, 50]. Consequently, we present our convergence proof of a multilevel collocation variant, which was published in [22].

4.1 Multilevel Interpolation Algorithm

Unlike Narcowich, Schaback and Ward in [64], we would like the basis functions to have the same smoothness for each level and not become smoother for finer

data sets. The multilevel algorithm we study here relies on two things: gradually denser data sets $X_1, X_2, \ldots$, and corresponding scaled positive definite functions. In our setting, these functions or translation-invariant kernels, will eventually consist of scaled versions of the previously introduced compactly supported radial basis functions Φ. For given scaling parameters $\delta_j > 0$ and a basis function $\Phi = \Phi_{d,k}$ we define the *scaled* radial basis function $\Phi_j : \mathbb{R}^d \to \mathbb{R}$ through

$$\Phi_j(\mathbf{x} - \mathbf{y}) = \delta_j^{-d} \Phi \left(\frac{\mathbf{x} - \mathbf{y}}{\delta_j} \right). \tag{4.1}$$

It follows that if Φ has support radius one, the Φ_j have support radius δ_j. Using these scaled and translation-invariant Φ_j as basis functions, we can construct interpolants s_j from the spaces

$$V_j = \operatorname{span}\{\Phi_j(\cdot - \mathbf{x}) \mid \mathbf{x} \in X_j\},$$

just as we have done before, compare with (2.1). In the context of pure interpolation, we will choose the support radius δ_j proportional to the corresponding mesh norm, $h_j = h_{X_j,\Omega}$, since in this case convergence is guaranteed as we will see soon. Now the multilevel algorithm is nothing else than a residual correction scheme.

Algorithm 4.1 (Multilevel Algorithm for Pure Interpolation)

Input: Right-hand side f, number of levels n

Set $f_0 = 0, e_0 = f$
for $j = 1, \ldots, n$ **do**

(i) Determine the local correction $s_j \in V_j$ to e_{j-1}

$$s_j(\mathbf{x}) = e_{j-1}(\mathbf{x}), \qquad \mathbf{x} \in X_j$$

(ii) Update the global approximation and the error

$$f_j = f_{j-1} + s_j$$
$$e_j = e_{j-1} - s_j$$

end

Output: Approximate solution f_n

The algorithm produces a numerical solution by adding residuals on finer data sets to the first coarse local interpolant. Consequently, we present a collocation version of this algorithm. It is worth clarifying the notation. The local interpolant denoted with s_j is actually given by the interpolant to the error of the previous level, i. e. $s_j = s_{e_{j-1},X_j} = s_{Ee_{j-1},X_j}$ in our previous notation.

Though numerical evidence for the convergence of Algorithm 4.1 had been given a long time ago by Floater and Iske [27], convergence was not proven until very recently – first on a sphere [49] and later for bounded domains [87]. We will cite the latter one here. We point out that similar algorithms have been developed in the context of globally supported thin plate splines [41, 45].

Theorem 4.2 (Convergence of Multilevel Interpolation Algorithm) *Let $\Omega \subseteq \mathbb{R}^d$ be a Lipschitz-bounded domain. Let $X_1, X_2, \ldots$ be a sequence of point sets in Ω with mesh norms $h_1, h_2, \ldots$ satisfying*

$$c\mu h_j \leq h_{j+1} \leq \mu h_j \qquad \text{for} \quad j \in \mathbb{N} \tag{4.2}$$

with $\mu \in (0,1)$, $c \in (0,1]$ and h_1 sufficiently small. Let Φ be a positive definite kernel that decays algebraically, i. e. (2.7) holds for some $\sigma > d/2$, which implies $\mathcal{N}_\Phi(\mathbb{R}^d) = H^\sigma(\mathbb{R}^d)$. Let the functions Φ_j be defined by (4.1) with scale factors $\delta_j = \nu h_j$. Furthermore assume $1/h_1 \geq \nu \geq \gamma/\mu$ with $\gamma > 0$. Let the target function f belong to $H^\sigma(\Omega)$. Then, there exists a constant $C_1 = C_1(\gamma) > 0$ such that for $\alpha = C_1\mu^\sigma$

$$\|Ee_j\|_{\Phi_{j+1}} \leq \alpha \|Ee_{j-1}\|_{\Phi_j} \qquad \text{for} \quad j \in \mathbb{N}$$

and hence there exists a constant $C > 0$ such that

$$\|f - f_n\|_{L_2(\Omega)} \leq C\alpha^n \|f\|_{H^\sigma(\Omega)} \qquad \text{for} \quad n \in \mathbb{N}.$$

Thus, the multilevel approximation f_n converges linearly to f in the L_2 norm if μ is chosen so small that $\alpha = C_1\mu^\sigma < 1$.

Proof. See [87, Theorem 1]. □

Note that in the statement of the theorem we make use of an extension operator E, which we properly define in Section 4.2.1. We also assume the boundary to be Lipschitz.

The proportional dependence between mesh norms and support radii, $\delta_j = \nu h_j$, has the nice consequence that we can find a bound for the condition numbers of the different interpolation matrices [49] if we assume the data sets to be *quasi-uniform*. That is, mesh norm and separation distance are comparable to each other in the sense that

$$q_{X_j} \leq h_{X_j,\Omega} \leq c q_{X_j}$$

for all level j and some constant $c > 1$.

Theorem 4.3 *For quasi-uniform data sets X_j the condition numbers of the interpolation matrices A_{Φ_j,X_j} are independent of the level.*

Proof. See [87] for the statement and [49] for the proof. □

4.2 Multilevel Collocation Algorithm

In the previous section, we explained the multilevel algorithm for pure interpolation. After having introduced in the previous chapter a generalised interpolation scheme, which can be used to solve partial differential equations of the form (3.5) numerically, we want to combine the multiscale idea now with the collocation method for elliptic problems of second order as discussed in Section 3.1.2.

In order to set up the multiscale approximation scheme for elliptic problems, we define two (not necessarily nested) point set sequences. Firstly, let $X_1, X_2, X_3, \ldots$ be a sequence of point sets in the bounded domain Ω and secondly let $Y_1, Y_2, Y_3, \ldots$ be a sequence of point sets on the boundary $\partial\Omega$.

Again, using scaled basis functions Φ_j, given by (4.1) for some scaling parameters $\delta_j > 0$ and a compactly supported radial basis function Φ, we can construct interpolants s_j – this time from the space

$$LV_{X_j} + V_{Y_j} = \operatorname{span}\{L_2\Phi_j(\cdot - \mathbf{x}) \mid \mathbf{x} \in X_j\} + \operatorname{span}\{\Phi_j(\cdot - \mathbf{y}) \mid \mathbf{y} \in Y_j\}.$$

The differential operator L is defined as in (3.6) and applied to the second variable, hence the subscript. In this setting, we obtain a multilevel algorithm of the following form.

Algorithm 4.4 (Multilevel Algorithm for Collocation)

Input: Right-hand sides f and F, number of levels n

Set $u_0 = 0, f_0 = f, F_0 = F$
for $j = 1, \ldots, n$ **do**

(i) Determine the local correction $s_j \in LV_{X_j} + V_{Y_j}$ to f_{j-1} and F_{j-1}

$$\begin{aligned} Ls_j(\mathbf{x}) &= f_{j-1}(\mathbf{x}), \qquad \mathbf{x} \in X_j \\ s_j(\mathbf{y}) &= F_{j-1}(\mathbf{y}), \qquad \mathbf{y} \in Y_j \end{aligned}$$

(ii) Update the global approximation and the residuals

$$\begin{aligned} u_j &= u_{j-1} + s_j \\ f_j &= f_{j-1} - L(s_j|_\Omega) \\ F_j &= F_{j-1} - s_j|_{\partial\Omega} \end{aligned}$$

end

Output: Approximate solution u_n

We define the error at level j to be the difference between the exact solution and the global approximant at level j, i. e. $e_j = u - u_j$. From this definition and the algorithm one can easily establish the following identities

$$u_j = \sum_{k=1}^{j} s_k \quad \text{and} \quad e_j = u - \sum_{k=1}^{j} s_k = e_{j-1} - s_j.$$

Moreover, we find

$$f_j = f - L(u_j|_\Omega) \quad \text{and} \quad F_j = F - u_j|_{\partial\Omega}. \tag{4.3}$$

The first equation follows by applying the linear operator L to $u_j|_\Omega$ and then adding it to the interior residual at level j and the second by adding $u_j|_{\partial\Omega}$ to the boundary residual at level j. Similar to interpolation, the local interpolant denoted with s_j is actually given by the interpolant to the error of the previous level since $f_{j-1}(\mathbf{x}) = Le_{j-1}(\mathbf{x})$ and $F_{j-1}(\mathbf{y}) = e_{j-1}(\mathbf{y})$.

Now, we analyse the convergence of the multilevel collocation algorithm. In order to prove the result presented in Section 4.2.3, we need two tools that help us deal with the boundary: an extension operator and (inverse) trace theorems.

4.2.1 Extension Operator

From Theorem 2.28 we know that the native space of a translation-invariant kernel, whose Fourier transform decays algebraically is norm-equivalent to a Sobolev space defined on the whole Euclidean space. One trick to cope with Sobolev spaces defined on bounded domains, instead of the whole Euclidean space, is to introduce an extension operator. The following result can be found in [87, Proposition 1] and comes originally from [77, Theorem 5, Section 5.3]. Again, we need to assume the boundary to be Lipschitz.

Lemma 4.5 *Suppose $\Omega \subseteq \mathbb{R}^d$ is open and has a Lipschitz boundary. Let $\sigma \geq 0$. Then, there exists a linear operator $E\colon W_2^\sigma(\Omega) \to W_2^\sigma(\mathbb{R}^d)$, such that, for all $f \in W_2^\sigma(\Omega)$ the two conditions hold*

(1) $Ef|_\Omega = f|_\Omega$,

(2) $\|Ef\|_{W_2^\sigma(\mathbb{R}^d)} \leq C_\sigma \|f\|_{W_2^\sigma(\Omega)}$

for some constant $C_\sigma > 0$.

4.2.2 Sobolev Norm of Functions Defined on the Boundary

It is obvious that when discussing boundary value problems we need to treat the boundary differently from the interior. In particular, we need to define the Sobolev norm on the boundary of Ω. In order to be able to do this, we need to impose some smoothness restrictions on the boundary. In particular we want Ω to have a $C^{k,s}$ boundary with $k \in \mathbb{N}_0$ and $s \in [0, 1)$. We introduced the definition for smooth boundaries in Section 2.32. An equivalent definition can be found in [89, Definition 2.7].

For smooth boundaries we are able to define the Sobolev norm of a function on the boundary via charts. If we assume that Ω has a $C^{k,s}$ boundary, then we are able to represent the boundary $\partial\Omega$ by a finite number of $C^{k,s}$ diffeomorphisms

$$\psi_j\colon B \to V_j \qquad \text{for} \qquad 1 \leq j \leq K,$$

where $B = B(\mathbf{0}, 1)$ is the unit ball in $\mathbb{R}^{d-1}$ and the V_j are open sets in $\mathbb{R}^d$ such that $\partial\Omega \subset \bigcup_{j=1}^K V_j$. With the help of a partition of unity $\{\omega_j\}$ with respect to $\{V_j\}$ we

can then define the Sobolev norm on the boundary to be

$$\|u\|_{W_p^k(\partial\Omega)} = \sum_{j=1}^{K} \|(u\omega_j) \circ \psi_j\|_{W_p^k(B)}.$$

The Sobolev space $W_p^k(\partial\Omega)$ (all functions for which the above norm is finite) is independent of the chosen atlas $\{V_j, \psi_j\}$ and the partition of unity $\{\omega_j\}$. Even though the norm depends on these choices, it can be shown that two norms constructed with different sets of charts are equivalent. Introducing the Sobolev norm on the boundary via charts enables us to define the mesh norm on the boundary. For some point set $Y \subseteq \partial\Omega$, we define

$$h_{Y,\partial\Omega} = \max_{1\leq j\leq K} h_{T_j,B}, \tag{4.4}$$

where $T_j = \psi_j^{-1}(Y \cap V_j) \subseteq B$, compare with [37]. If we fixed a different atlas, we would get an $\widetilde{h}_{Y,\partial\Omega}$ which is equivalent to $h_{Y,\partial\Omega}$. However, since we are mostly interested in the convergence rates, the equivalence constant would drop out as can be seen in (4.14).

In order to prove error bounds in the subsequent section, we need two results, well known in the theory of weak solutions to elliptic PDEs that establish a relationship between Sobolev norms for the domain Ω as well as Sobolev norms for the boundary $\partial\Omega$. The first result, taken from [89, Theorem 8.7], shows how restricting a function in $W_2^\sigma(\Omega)$, only defined almost everywhere, to the boundary $\partial\Omega$ is feasible.

Lemma 4.6 (Trace Theorem) *Suppose $\Omega \subseteq \mathbb{R}^d$ is a bounded region with a $C^{k,s}$ boundary $\partial\Omega$ and $1/2 < \sigma \leq k + s$. Then, there exists a continuous linear operator*

$$T\colon W_2^\sigma(\Omega) \to W_2^{\sigma-1/2}(\partial\Omega)$$

such that $Tu = u|_{\partial\Omega}$ for all $u \in W_2^\sigma(\Omega)$. This means in particular that the restriction of $u \in W_2^\sigma(\Omega)$ to $\partial\Omega$ is well-defined, belongs to $W_2^{\sigma-1/2}(\partial\Omega)$ and satisfies

$$\|u\|_{W_2^{\sigma-1/2}(\partial\Omega)} \leq C\|u\|_{W_2^\sigma(\Omega)} \tag{4.5}$$

for some positive constant C, that is independent of u.

Roughly speaking one could think of the so called *trace* operator T as a generalisation of the restriction mapping $f \mapsto f|_{\partial\Omega}$, which in the case of Sobolev functions f is not well-defined since $\partial\Omega$ is a null set in $\mathbb{R}^d$. It is also possible to generalise the notion of the extension mapping $f|_{\partial\Omega} \mapsto f$ in a similar fashion with the help of an *inverse* operator Z [89, Theorem 8.8].

Lemma 4.7 (Inverse Trace Theorem) *Suppose $\Omega \subseteq \mathbb{R}^d$ is a bounded region with a $C^{k,s}$ boundary $\partial\Omega$ and $1/2 < \sigma \leq k + s$. Then, there exists a continuous linear operator*

$$Z\colon W_2^{\sigma-1/2}(\partial\Omega) \to W_2^\sigma(\Omega)$$

such that $T \circ Zu = u$ for all $u \in W_2^{\sigma-1/2}(\partial\Omega)$, where T is the trace operator from Lemma 4.6.

4.2.3 Convergence Result

Before we start looking at the multilevel convergence result, we need an auxiliary result for the L_2 error of the solution to the boundary value problem (3.5) and its collocation approximation (Theorem 4.9).

One important step in the proof of this lemma is to use the solution's continuous dependence on the data. We cite the L_2 analogue of the maximum principle taken from [38, Corollary 8.7] here.

Lemma 4.8 (Continuous Dependence on Data in L_2 norm) *Let $u \in W_2^1(\Omega)$ satisfy (3.5) in the weak sense. Define with the help of an inverse trace operator Z the function $\phi = ZF \in W_2^1(\Omega)$ for boundary data $F \in W_2^{1/2}(\partial\Omega)$. Then we have for some $\widetilde{C} > 0$ the following estimate*

$$\|u\|_{W_2^1(\Omega)} \leq \widetilde{C} \left\{ \|f\|_{L_2(\Omega)} + \|\phi\|_{W_2^1(\Omega)} \right\}. \tag{4.6}$$

Now bearing in mind that the inverse trace operator is a continuous and thus bounded operator, we have

$$\|\phi\|_{W_2^1(\Omega)} = \|ZF\|_{W_2^1(\Omega)} \leq c\|F\|_{W_2^{1/2}(\partial\Omega)}$$

for some positive constant c so that we can rewrite (4.6) to find

$$\|u\|_{L_2(\Omega)} \leq C \left\{ \|f\|_{L_2(\Omega)} + \|F\|_{W_2^{1/2}(\partial\Omega)} \right\}, \tag{4.7}$$

for some $C > 0$. Here we also employed the trivial estimate $\|u\|_{L_2(\Omega)} \leq \|u\|_{W_2^1(\Omega)}$.

In order to prove our main result in this section, it is also possible to directly use the maximum principle. However, as we will see in the proof of Theorem 4.10, it is more favourable to have such a bound for the solution to (3.5) in the L_2 norm than in the L_∞ norm since the sampling inequality would in the latter case yield an extra factor of $h^{-d/2}$, see for example Corollary 2.8.

With estimate (4.7) we can now bound the L_2 error between the solution u and its approximation s_u. Let $h_{X,\Omega}$ denote the mesh norm corresponding to the interior of the domain Ω and $h_{Y,\partial\Omega}$ denote the mesh norm corresponding to its boundary $\partial\Omega$. Then, the following result for the L_2 error holds.

Theorem 4.9 (L_2 Error) *Assume that $\delta \in (0, 1]$ and $u \in W_2^\sigma(\Omega)$ solves (3.5). Let the domain Ω have a $C^{k,s}$ boundary for $s \in [0, 1)$ such that $\sigma = k + s$ and $k := \lfloor \sigma \rfloor > 2 + d/2$. Let the differential operator L from (3.6) be strictly elliptic and its interior collocation points not contain a singular point. Then the error between the solution u and its collocation approximation s_u can be bounded in the L_2 norm by*

$$\begin{aligned} \|u - s_u\|_{L_2(\Omega)} &\leq C\delta^{-\sigma}\{h_{X,\Omega}^{\sigma-2} + h_{Y,\partial\Omega}^{\sigma-1}\}\|Eu\|_{\Phi_\delta} \\ &\leq C\delta^{-\sigma}\left\{h_{X,\Omega}^{\sigma-2} + h_{Y,\partial\Omega}^{\sigma-1}\right\}\|u\|_{W_2^\sigma(\Omega)} \\ &\leq C\delta^{-\sigma}h^{\sigma-2}\|u\|_{W_2^\sigma(\Omega)}, \end{aligned}$$

where $h = \max\{h_{X,\Omega}, h_{Y,\partial\Omega}\}$.

Proof. First, we note that by (4.7) we have

$$\|u - s_u\|_{L_2(\Omega)} \leq C \left\{ \|Lu - Ls_u\|_{L_2(\Omega)} + \|u - s_u\|_{W_2^{1/2}(\partial\Omega)} \right\}.$$

Now we estimate the two terms on the right-hand side separately. With the help of the sampling inequality, the boundedness of L as well as the norm equivalence for scaled kernels we obtain for the term corresponding to the interior of the domain the following bound:

$$\begin{aligned}
\|Lu - Ls_u\|_{L_2(\Omega)} &\leq C h_{X,\Omega}^{\sigma-2} \|Lu - Ls_u\|_{W_2^{\sigma-2}(\Omega)} && \text{by Theorem 2.33} \\
&\leq C h_{X,\Omega}^{\sigma-2} \|u - s_u\|_{W_2^{\sigma}(\Omega)} && \text{by Lemma 3.6} \\
&\leq C h_{X,\Omega}^{\sigma-2} \|Eu - s_{Eu}\|_{W_2^{\sigma}(\mathbb{R}^d)} && \text{since } s_u = s_{Eu} \\
&\leq C h_{X,\Omega}^{\sigma-2} \delta^{-\sigma} \|Eu - s_{Eu}\|_{\Phi_\delta} && \text{by Lemma 2.30} \\
&\leq C h_{X,\Omega}^{\sigma-2} \delta^{-\sigma} \|Eu\|_{\Phi_\delta} && \text{by optimality.}
\end{aligned}$$

For the boundary term we use the definition of a Sobolev norm on a boundary, introduced in Section 4.2.2. The procedure is very similar to the proof of Theorem 3.10 in [37]. For $B = B(\mathbf{0}, 1) \subseteq \mathbb{R}^{d-1}$ we set $u_j = ((u - s_u)w_j) \circ \psi_j \in W_2^{\sigma-1/2}(B)$. Since we want to employ the sampling inequality, it is important to note that the u_j vanish on the T_j. Thus, we find

$$\begin{aligned}
\|u - s_u\|_{W_2^{1/2}(\partial\Omega)}^2 &= \sum_{j=1}^{K} \|u_j\|_{W_2^{1/2}(B)}^2 \\
&\leq C \sum_{j=1}^{K} h_{T_j,B}^{2(\sigma-1)} \|u_j\|_{W_2^{\sigma-1/2}(B)}^2 && \text{by Theorem 2.33} \\
&\leq C h_{Y,\partial\Omega}^{2(\sigma-1)} \|u - s_u\|_{W_2^{\sigma-1/2}(\partial\Omega)}^2 \\
&\leq C h_{Y,\partial\Omega}^{2(\sigma-1)} \|u - s_u\|_{W_2^{\sigma}(\Omega)}^2 && \text{by Lemma 4.6.}
\end{aligned}$$

From this we can deduce

$$\begin{aligned}
\|u - s_u\|_{W_2^{1/2}(\partial\Omega)} &\leq C h_{Y,\partial\Omega}^{\sigma-1} \|u - s_u\|_{W_2^{\sigma}(\Omega)} \\
&\leq C h_{Y,\partial\Omega}^{\sigma-1} \delta^{-\sigma} \|Eu\|_{\Phi_\delta},
\end{aligned}$$

where we used for the second inequality exactly the same last three steps as for the term $\|Lu - Ls_u\|_{L_2(\Omega)}$. Thus, by combining both results we can conclude

$$\begin{aligned}
\|u - s_u\|_{L_2(\Omega)} &\leq C\delta^{-\sigma} \{h_{X,\Omega}^{\sigma-2} + h_{Y,\partial\Omega}^{\sigma-1}\} \|Eu\|_{\Phi_\delta} \\
&\leq C\delta^{-\sigma} \{h_{X,\Omega}^{\sigma-2} + h_{Y,\partial\Omega}^{\sigma-1}\} \|Eu\|_{W_2^{\sigma}(\mathbb{R}^d)} && \text{by Lemma 2.30} \\
&\leq C\delta^{-\sigma} \{h_{X,\Omega}^{\sigma-2} + h_{Y,\partial\Omega}^{\sigma-1}\} \|u\|_{W_2^{\sigma}(\Omega)} && \text{by Lemma 4.5} \\
&\leq C\delta^{-\sigma} h^{\sigma-2} \|u\|_{W_2^{\sigma}(\Omega)}.
\end{aligned}$$

□

The above result would mean that ideally δ should be fixed if the mesh norm tends to zero. In this case, however, the band widths of the collocation matrices grow for smaller grids since there will be more and more points in the support radius of each basis function. With the help of this error estimate, we are now able to prove convergence of the multilevel approximation scheme for elliptic partial differential equations of second order.

Theorem 4.10 (Convergence of the Multilevel Collocation Algorithm) *Assume $u \in W_2^\sigma(\Omega)$ solves (3.5). Let $k := \lfloor \sigma \rfloor > 2 + d/2$. We define two point set sequences. Let $X_1, X_2, \ldots$ be a sequence of point sets in Ω with mesh norms $h_{X_1,\Omega}, h_{X_2,\Omega}, \ldots$ such that the X_j contain no singular point of the operator L and let $Y_1, Y_2, \ldots$ be a sequence of point sets in $\partial\Omega$ with mesh norms $h_{Y_1,\partial\Omega}, h_{Y_2,\partial\Omega}, \ldots$. Set $h_j = \max\{h_{X_j,\Omega}, h_{Y_j,\partial\Omega}\}$ and assume*

$$\gamma\mu h_j \le h_{j+1} \le \mu h_j \tag{4.8}$$

for $j = 1, 2, \ldots$ and some fixed $\mu \in (0,1)$ and $\gamma \in (0,1)$. Let the domain Ω have a $C^{k,s}$ boundary for $s \in [0,1)$ such that $\sigma = k + s$ and let Φ be a kernel satisfying

$$c_1(1 + \|\boldsymbol{\omega}\|_2^2)^{-\sigma} \le \widehat{\Phi}(\boldsymbol{\omega}) \le c_2(1 + \|\boldsymbol{\omega}\|_2^2)^{-\sigma}, \quad \boldsymbol{\omega} \in \mathbb{R}^d,$$

with two fixed constants $0 < c_1 \le c_2$. Define $\delta_j = \left(\frac{h_j}{\mu}\right)^{1-\frac{2}{\sigma}}$ and

$$\Phi_j(\mathbf{x}, \mathbf{y}) = \Phi_{\delta_j}(\mathbf{x}, \mathbf{y}) = \delta_j^{-d}\Phi((\mathbf{x} - \mathbf{y})/\delta_j).$$

Lastly, let $h_1 \le \mu$ be sufficiently small. Then, there exists a constant C independent of μ, j and u such that

$$\|Ee_j\|_{\Phi_{j+1}} \le \alpha \|Ee_{j-1}\|_{\Phi_j},$$

for $j = 1, 2, \ldots$ with $\alpha = C\mu^{\sigma-2}$. Thus, we have the estimate

$$\|u - u_n\|_{L_2(\Omega)} \le C\alpha^n \|u\|_{W_2^\sigma(\Omega)} \tag{4.9}$$

and the multilevel approximation u_k converges to u in the L_2 norm if we choose μ so small that $\alpha = C\mu^{\sigma-2} < 1$.

Note that condition (4.8) guarantees that the grids become finer. The parameter μ can be thought of as the rate at which the grid size decreases.

Proof. First we see that

$$\delta_j = \left(\frac{h_j}{\mu}\right)^{1-\frac{2}{\sigma}} \le \left(\frac{h_j h_{j-1}}{h_j}\right)^{1-\frac{2}{\sigma}} < \left(\frac{h_{j-1}}{\mu}\right)^{1-\frac{2}{\sigma}} = \delta_{j-1}.$$

That is, $\delta_j < \delta_1 \leq 1$ since $h_1 \leq \mu$ and $1 - \frac{2}{\sigma} > 0$ due to our assumptions. Hence, we can apply Lemma 2.30. We use the definition of the native space norm to obtain

$$\begin{aligned}
\|Ee_j\|^2_{\Phi_{j+1}} &= \frac{1}{(2\pi)^{d/2}} \int_{\mathbb{R}^d} \frac{|\widehat{Ee_j}(\boldsymbol{\omega})|^2}{\widehat{\Phi_{j+1}}(\boldsymbol{\omega})} d\boldsymbol{\omega} = C \int_{\mathbb{R}^d} \frac{|\widehat{Ee_j}(\boldsymbol{\omega})|^2}{\widehat{\Phi}(\delta_{j+1}\boldsymbol{\omega})} d\boldsymbol{\omega} \\
&\leq \frac{C}{c_1} \int_{\|\boldsymbol{\omega}\|_2 \leq 1/\delta_{j+1}} |\widehat{Ee_j}(\boldsymbol{\omega})|^2 (1 + \delta_{j+1}^2 \|\boldsymbol{\omega}\|_2^2)^\sigma d\boldsymbol{\omega} \\
&+ \frac{C}{c_1} \int_{\|\boldsymbol{\omega}\|_2 \geq 1/\delta_{j+1}} |\widehat{Ee_j}(\boldsymbol{\omega})|^2 (1 + \delta_{j+1}^2 \|\boldsymbol{\omega}\|_2^2)^\sigma d\boldsymbol{\omega} \\
&=: C(I_1 + I_2).
\end{aligned}$$

For the first term I_1, we obtain

$$\begin{aligned}
I_1 &\leq 2^\sigma \int_{\mathbb{R}^d} |\widehat{Ee_j}(\boldsymbol{\omega})|^2 d\boldsymbol{\omega} = 2^\sigma \|Ee_j\|^2_{L_2(\mathbb{R}^d)} && \text{by Parseval's identity} \\
&\leq C\|e_j\|^2_{L_2(\Omega)} = C\|e_{j-1} - s_j\|^2_{L_2(\Omega)} && \text{by Lemma 4.5} \\
&= C\|e_{j-1} - s_{e_{j-1}}\|^2_{L_2(\Omega)} && \\
&\leq C h_j^{2(\sigma-2)} \delta_j^{-2\sigma} \|Ee_{j-1}\|^2_{\Phi_j} && \text{by Theorem 4.9.}
\end{aligned}$$

Here we have used that s_j is in fact equal to s_{Ee_{j-1},X_j}. This follows by observing that for $\mathbf{x} \in X_j$ and $\mathbf{y} \in Y_j$, we have

$$\begin{aligned}
Ls_j(\mathbf{x}) = f_{j-1}(\mathbf{x}) = f(\mathbf{x}) - Lu_{j-1}(\mathbf{x}) = L[u - u_{j-1}](\mathbf{x}) = Le_{j-1}(\mathbf{x}), \\
s_j(\mathbf{y}) = F_{j-1}(\mathbf{y}) = F(\mathbf{y}) - u_{j-1}(\mathbf{y}) = u(\mathbf{y}) - u_{j-1}(\mathbf{y}) = e_{j-1}(\mathbf{y}),
\end{aligned}$$

using the algorithm as well as (4.3). Since

$$\mu^{2(\sigma-2)} = \frac{h_j^{2(\sigma-2)}}{\delta_j^{2\sigma}},$$

we then have

$$I_1 \leq C\mu^{2(\sigma-2)} \|Ee_{j-1}\|^2_{\Phi_j}.$$

For the second term I_2, we obtain

$$\begin{aligned}
I_2 &\leq 2^\sigma \delta_{j+1}^{2\sigma} \int_{\|\boldsymbol{\omega}\|_2 \geq 1/\delta_{j+1}} |\widehat{Ee_j}(\boldsymbol{\omega})|^2 \|\boldsymbol{\omega}\|_2^{2\sigma} d\boldsymbol{\omega} \\
&\leq 2^\sigma \delta_{j+1}^{2\sigma} \int_{\|\boldsymbol{\omega}\|_2 \geq 1/\delta_{j+1}} |\widehat{Ee_j}(\boldsymbol{\omega})|^2 (1 + \|\boldsymbol{\omega}\|_2^2)^\sigma d\boldsymbol{\omega} \\
&\leq 2^\sigma \delta_{j+1}^{2\sigma} \|Ee_j\|^2_{W_2^\sigma(\mathbb{R}^d)} \\
&\leq C\delta_{j+1}^{2\sigma} \|e_j\|^2_{W_2^\sigma(\Omega)} \\
&= C\delta_{j+1}^{2\sigma} \|e_{j-1} - s_j\|^2_{W_2^\sigma(\Omega)}.
\end{aligned}$$

Now, using again that $s_j = s_{Ee_{j-1},X_j}$, this leads to

$$\begin{aligned} I_2 &\leq C\delta_{j+1}^{2\sigma}\|Ee_{j-1} - s_{Ee_{j-1}}\|_{W_2^\sigma(\Omega)}^2 \\ &\leq C\delta_{j+1}^{2\sigma}\|Ee_{j-1} - s_{Ee_{j-1}}\|_{W_2^\sigma(\mathbb{R}^d)}^2 \\ &\leq C\delta_{j+1}^{2\sigma}\delta_j^{-2\sigma}\|Ee_{j-1} - s_{Ee_{j-1}}\|_{\Phi_j}^2 \\ &\leq C\delta_{j+1}^{2\sigma}\delta_j^{-2\sigma}\|Ee_{j-1}\|_{\Phi_j}^2 \qquad \text{by optimality} \\ &\leq C\mu^{2(\sigma-2)}\|Ee_{j-1}\|_{\Phi_j}^2, \end{aligned}$$

where in the last step we have used

$$\left(\frac{\delta_{j+1}}{\delta_j}\right)^{2\sigma} = \left(\frac{h_{j+1}}{h_j}\right)^{2(\sigma-2)} \leq \mu^{2(\sigma-2)}.$$

Thus, in total we have

$$\|Ee_j\|_{\Phi_{j+1}} \leq C\mu^{\sigma-2}\|Ee_{j-1}\|_{\Phi_j} = \alpha\|Ee_{j-1}\|_{\Phi_j}, \tag{4.10}$$

for $\alpha := C\mu^{\sigma-2}$. From this we can conclude

$$\begin{aligned} \|u - u_n\|_{L_2(\Omega)} &= \|e_n\|_{L_2(\Omega)} \\ &\leq Ch_n^{\sigma-2}\delta_{n+1}^{-\sigma}\|Ee_n\|_{\Phi_{n+1}} \qquad \text{by Theorem 4.9} \\ &\leq C\|Ee_n\|_{\Phi_{n+1}}, \end{aligned}$$

where we have used in the last step that

$$\frac{h_n^{\sigma-2}}{\delta_{n+1}^\sigma} = \frac{h_n^{\sigma-2}}{h_{n+1}^{\sigma-2}}\mu^{\sigma-2} = \left(\frac{h_n}{h_{n+1}}\mu\right)^{\sigma-2} \leq \gamma^{2-\sigma}.$$

Now applying (4.10) n times, we find

$$\|u - u_n\|_{L_2(\Omega)} \leq C\|Ee_n\|_{\Phi_{n+1}} \leq C\alpha^n\|Eu\|_{W_2^\sigma(\mathbb{R}^d)} \leq C\alpha^n\|u\|_{W_2^\sigma(\Omega)}$$

for $\alpha = C\mu^{\sigma-2}$.

□

4.3 Numerical Examples

In this section, we provide numerical examples to illustrate the theory. We choose nested point sets $\{X_i\} \subseteq \Omega$ in the domain as well as nested point sets $\{Y_i\} \subseteq \partial\Omega$ on the boundary, i. e.

$$\begin{aligned} X_1 \subseteq X_2 \subseteq X_3 \subseteq \ldots \subseteq X_F \\ Y_1 \subseteq Y_2 \subseteq Y_3 \subseteq \ldots \subseteq Y_F, \end{aligned}$$

where we specify $F \in \mathbb{N}$ for each of problem separately. The total number of data sites at level j is given by the sum of the cardinalities of the point sets for that level, i. e.

$$N_j = |X_j| + |Y_j|, \quad \text{for} \quad 1 \leq j \leq F.$$

The sets X_F and Y_F are the finest sets that are used for computing the error. We examine the stationary as well as the nonstationary case. That is, we choose support radii proportional to the mesh norm as well as nonproportional to it (as suggested by the convergence theorem), namely

$$\delta_j = \nu \left(h_j/\mu\right)^{1-2/\sigma}, \tag{4.11}$$

for $h_j = \max\{h_{X_j,\Omega}, h_{Y_j,\partial\Omega}\}$ with $j \in \mathbb{N}$. Also, we included a proportionality constant $\nu > 0$ and will investigate its influence on the algorithm. These constants have been chosen by trial and error, bearing in mind that a large constant yields a large support radius and thus a relatively good approximation at the cost of having to solve a more ill-conditioned problem (and vice versa). The code used here and in subsequent chapters partially relies on the code provided by Fasshauer in his textbook [24]. Since the condition numbers become quite large, they are estimated via the `condest` routine in Matlab.

For all examples, we will choose $\mu = 0.5$ and specify ν accordingly in each of the following subsections. We determine the mesh norm on the new level mostly by choosing it to be equal to half the mesh norm of the previous level – thus automatically satisfying (4.8), i. e. we have

$$h_j = \frac{h_{j-1}}{2}. \tag{4.12}$$

In Section 4.3.2, however, we also look at unstructured grids. On the finest level, we approximate the error e_n between the exact solution u evaluated at the data sites

$$U = (u|_{X_F}, u|_{Y_F})^T \in \mathbb{R}^{N_F},$$

and its multilevel approximation $\widetilde{U}_k \in \mathbb{R}^{N_F}$ at level k with the root-mean-square error, a weighted ℓ_2 error of the form

$$E_k = \|u - u_k\|_{L_2(\Omega)} \approx \frac{\|U - \widetilde{U}_k\|_{\ell_2}}{\sqrt{N_F}}. \tag{4.13}$$

When computing the error on the boundary we adjust the equation above by taking the difference of the boundary vectors in the ℓ_2 norm and dividing it by the square root of $|Y_F|$. We point out that even though analytically there is no difference between the $L_p(\Omega)$ and the $L_p(\overline{\Omega})$ norm, it is still interesting to see how big the numerically computed difference (which analytically should be zero) is. Therefore, we include both norms in the following tables.

We proved convergence of the multilevel algorithm with respect to the mesh norm if $\alpha = C\mu^{\sigma-2} < 1$, see Theorem 4.10. The assumption that the constant α is less than one, is important since in the inequality (4.9) it is raised to the power k, where k denotes the level. Theoretically, this is not a problem since we can choose the discretisation parameter μ to meet this requirement, e. g. $\mu < (1/C)^{1/(\sigma-2)}$. In practice, however, we do not know the constant C. Therefore we try to verify the order of convergence numerically. Assuming there exists a $\beta > 0$ such that

$$E_k = Ch_k^\beta \|u\|_{W_2^\sigma(\Omega)}$$

for some $C > 0$, we can estimate β from two consecutive errors

$$\frac{E_{k+1}}{E_k} = \left(\frac{h_{k+1}}{h_k}\right)^\beta,$$

from which we obtain

$$\beta = \frac{\log\left(\frac{E_{k+1}}{E_k}\right)}{\log\left(\frac{h_{k+1}}{h_k}\right)}. \tag{4.14}$$

We compute the convergence order β with the error given on the domain including its boundary $\overline{\Omega}$. Additionally, it will be of interest to separate the error in the interior from the error on the boundary.

4.3.1 1D Laplace Problem

We start with a simple 1D Laplace problem with Dirichlet boundary conditions,

$$\begin{aligned} u'' &= 0, && \text{in } \Omega = (0,1) \\ u(0) &= 0, \\ u(1) &= 1. \end{aligned} \tag{L1}$$

Its analytic solution is given by the identity $u(x) = x$. We form nested point sets

$$X_j = \left\{ \frac{1}{2^j}\ell \colon \ell = 1, \dots, 2^j - 1 \right\} \qquad \text{and} \qquad Y_j = \{0, 1\}$$

and choose the support radii according to Theorem 4.10. Note that for this one dimensional problem the boundary nodes cannot be refined.

We compute the multilevel approximation to the Laplace problem, using two different basis functions: $\phi_{1,2} \in C^4$ and $\phi_{1,6} \in C^{12}$. The errors measured in different norms are given in Table 4.3 and Table 4.7, respectively. The orders of convergence can be found in Table 4.4 and Table 4.8, respectively. We remark that throughout this thesis the condition numbers are estimated values only since the matrices become quite large.

N	h	$\|e\|_{L_2(\overline{\Omega})}$	$\|e\|_{H^1(\overline{\Omega})}$	$\|e\|_{L_\infty(\overline{\Omega})}$	cond(A)
5	2^{-3}	8.22e-3	5.31e-2	1.45e-2	5.3e1
9	2^{-4}	1.92e-3	1.44e-2	3.16e-3	1.9e2
17	2^{-5}	4.34e-4	3.42e-3	6.66e-4	7.6e2
33	2^{-6}	1.05e-4	7.63e-4	1.60e-4	3.1e3
65	2^{-7}	2.71e-5	1.69e-4	4.15e-5	1.2e4
129	2^{-8}	7.28e-6	3.83e-5	1.12e-5	5.6e4
257	2^{-9}	1.95e-6	9.13e-6	3.01e-6	2.6e5
513	2^{-10}	5.16e-7	2.27e-6	8.01e-7	1.3e6
1025	2^{-11}	1.35e-7	5.74e-7	2.10e-7	6.5e6

Table 4.3: Convergence study for the Laplace problem (L1) with basis function $\phi_{1,2}$ and support radii of the form (4.11) for $\nu = 5$.

N	h	$\|e\|_{L_2(\overline{\Omega})}$	$\|e\|_{H^1(\overline{\Omega})}$	$\|e\|_{L_\infty(\overline{\Omega})}$	cond(A)
9	2^{-4}	2.10	1.88	2.20	-1.83
17	2^{-5}	2.14	2.07	2.25	-2.00
33	2^{-6}	2.05	2.16	2.09	-2.04
65	2^{-7}	1.95	2.17	1.94	-1.98
129	2^{-8}	1.90	2.14	1.89	-2.17
257	2^{-9}	1.90	2.07	1.90	-2.22
513	2^{-10}	1.92	2.01	1.91	-2.32
1025	2^{-11}	1.93	1.98	1.93	-2.34

Table 4.4: Convergence orders for the Laplace problem (L1) with basis function $\phi_{1,2}$ and support radii of the form (4.11) for $\nu = 5$.

N	h	$\|e\|_{L_2(\overline{\Omega})}$	$\|e\|_{H^1(\overline{\Omega})}$	$\|e\|_{L_\infty(\overline{\Omega})}$	cond(A)
5	2^{-3}	1.82e-3	1.31e-2	1.82e-3	2.8e1
9	2^{-4}	3.41e-4	3.05e-3	5.92e-4	5.6e1
17	2^{-5}	5.88e-5	6.39e-4	9.54e-5	1.9e2
33	2^{-6}	1.04e-5	1.27e-4	1.61e-5	6.0e2
65	2^{-7}	2.05e-6	2.44e-5	3.22e-6	1.9e3
129	2^{-8}	4.53e-7	4.71e-6	7.28e-7	7.1e3
257	2^{-9}	1.08e-7	9.31e-7	1.76e-7	2.7e4
513	2^{-10}	2.67e-8	1.93e-7	4.38e-8	1.0e5
1025	2^{-11}	6.75e-9	4.24e-8	1.11e-8	4.8e5

Table 4.5: Convergence study for the Laplace problem (L1) with basis function $\phi_{1,2}$ and support radii of the form (4.11) for $\nu = 10$.

N	h	$\|e\|_{L_2(\overline{\Omega})}$	$\|e\|_{H^1(\overline{\Omega})}$	$\|e\|_{L_\infty(\overline{\Omega})}$	cond(A)
9	2^{-4}	2.41	2.10	2.43	-1.00
17	2^{-5}	2.54	2.25	2.65	-1.73
33	2^{-6}	2.49	2.34	2.56	-1.68
65	2^{-7}	2.35	2.37	2.31	-1.68
129	2^{-8}	2.18	2.37	2.15	-1.90
257	2^{-9}	2.07	2.34	2.05	-1.94
513	2^{-10}	2.01	2.27	2.00	-1.92
1025	2^{-11}	1.99	2.18	1.98	-2.15

Table 4.6: Convergence orders for the Laplace problem (L1) with basis function $\phi_{1,2}$ and support radii of the form (4.11) for $\nu = 10$.

N	h	$\|e\|_{L_2(\overline{\Omega})}$	$\|e\|_{H^1(\overline{\Omega})}$	$\|e\|_{L_\infty(\overline{\Omega})}$	cond(A)
5	2^{-3}	2.16e-2	1.79e-1	4.45e-2	4.5e2
9	2^{-4}	3.99e-3	4.44e-2	8.60e-3	9.8e3
17	2^{-5}	6.38e-4	9.80e-3	1.40e-3	1.5e5
33	2^{-6}	8.20e-5	1.76e-3	1.80e-4	1.9e6
65	2^{-7}	8.31e-6	2.51e-4	1.82e-5	2.5e7
129	2^{-8}	6.63e-7	2.85e-5	1.45e-6	3.6e8
257	2^{-9}	4.20e-8	2.61e-6	9.14e-8	5.0e9
513	2^{-10}	2.14e-9	1.98e-7	4.64e-9	7.0e10
1025	2^{-11}	8.86e-11	1.28e-8	1.90e-10	1.0e12

Table 4.7: Convergence study for the Laplace problem (L1) with basis function $\phi_{1,6}$ and support radii of the form (4.11) for $\nu = 5$.

N	h	$\|e\|_{L_2(\overline{\Omega})}$	$\|e\|_{H^1(\overline{\Omega})}$	$\|e\|_{L_\infty(\overline{\Omega})}$	cond(A)
9	2^{-4}	2.43	2.01	2.37	-4.43
17	2^{-5}	2.64	2.18	2.62	-3.90
33	2^{-6}	2.96	2.48	2.96	-3.68
65	2^{-7}	3.30	2.81	3.31	-3.76
129	2^{-8}	3.65	3.14	3.65	-3.81
257	2^{-9}	3.98	3.45	3.98	-3.81
513	2^{-10}	4.30	3.72	4.30	-3.81
1025	2^{-11}	4.59	3.95	4.61	-3.84

Table 4.8: Convergence orders for the Laplace problem (L1) with basis function $\phi_{1,6}$ and support radii of the form (4.11) for $\nu = 5$.

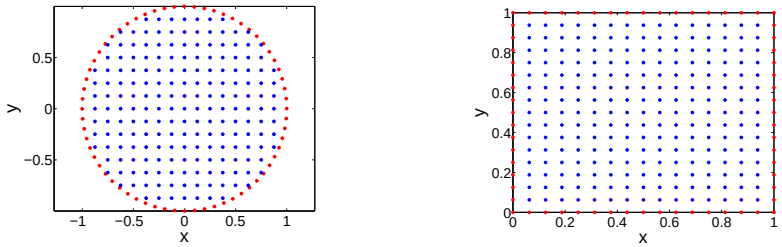

(a) (P1) with $N = 257$ (b) (P2) with $N = 289$

Figure 4.2: Point sets for the interior (blue) and boundary (red) for Poisson problems (P1) and (P2).

It can be observed that the smoother the basis function, the faster the convergence (in all three norms examined here), but also the faster the condition number of the level matrices grows. The first observation makes sense, given that the solution to the ordinary differential equation (L1) is infinitely many times differentiable. The second observation we examine more closely in Chapter 5, where we discuss preconditioning strategies.

Somewhat surprising is the fact that the H_1 error diminishes as fast as the L_∞ and L_2 error, when using $\phi_{1,2}$ as basis function. For $\phi_{1,6}$, the H_1 error is diminishing slightly slower – but still faster than one would expect for gradually finer one-shot solutions [37]. In these cases one usually expects the order for the H_1 error to be reduced by one compared to the L_2 convergence order.

Doubling the proportionality constant ν (see Tables 4.5 and 4.6) yields initially better errors and convergence rates. This reflects the fact that the initial support radius is bigger and thus we can expect better results. In the long run, however, these effects seem to level out. The convergence orders for $\nu = 5$ on the finest level seem to be comparable to the convergence orders for $\nu = 10$ on the finest level.

This numerical example, however, is a rather artificial example as the boundary consists only of two points. Therefore, we look at two-dimensional problems in the next section.

4.3.2 2D Poisson Problem

We will look at two different 2D examples to illustrate the convergence of the multilevel collocation algorithm. More specifically we will look at two Poisson problems – on a disk and on a square. We will see that both multilevel approximations for these domains converge quite fast. Technically, only the first example is in the setting of the theorem since its boundary is sufficiently smooth. However, examining the convergence proof, we note that the boundary is handled using charts. Therefore, it is not too surprising that we still achieve convergence on a square domain.

For both examples we compare the convergence obtained through a nonpropor-

N	H	$\|e\|_{L_2(\overline{\Omega})}$	$\|e\|_{L_2(\Omega)}$	$\|e\|_{L_2(\partial\Omega)}$	$\|e\|_{H^1(\overline{\Omega})}$	$\|e\|_{L_\infty(\overline{\Omega})}$	cond(A)
9	1	6.21e-2	6.28e-2	8.41e-7	1.80e-1	8.94e-1	1.0e3
25	2^{-1}	1.24e-2	1.25e-2	8.44e-5	5.69e-2	1.86e-2	6.3e4
77	2^{-2}	2.05e-3	2.07e-3	3.56e-5	1.45e-2	4.06e-3	1.0e7
257	2^{-3}	3.13e-4	3.16e-4	1.06e-6	3.10e-3	7.06e-4	9.7e8
921	2^{-4}	3.91e-5	3.95e-5	3.11e-7	5.69e-4	1.01e-4	7.7e10
3461	2^{-5}	4.49e-6	4.53e-6	2.04e-8	9.33e-5	1.20e-5	1.9e13
13361	2^{-6}	4.26e-7	4.30e-7	1.68e-9	1.38e-5	1.20e-6	6.7e14

Table 4.9: Convergence study for the Poisson problem (P1) with basis function $\phi_{2,3}$ and support radii of the form (4.11) for $\nu = 3.5$.

N	H	$\|e\|_{L_2(\overline{\Omega})}$	$\|e\|_{L_2(\Omega)}$	$\|e\|_{L_2(\partial\Omega)}$	$\|e\|_{H^1(\overline{\Omega})}$	$\|e\|_{L_\infty(\overline{\Omega})}$	cond(A)
25	2^{-1}	1.55	1.55	-4.43	1.11	1.51	-3.97
77	2^{-2}	2.60	2.60	1.25	1.98	2.19	-7.32
257	2^{-3}	2.71	2.71	5.08	2.22	2.53	-6.59
921	2^{-4}	3.00	3.00	1.76	2.45	2.80	-6.30
3461	2^{-5}	3.13	3.13	3.93	2.61	3.07	-7.94
13361	2^{-6}	3.40	3.40	3.60	2.76	3.32	-5.15

Table 4.10: Convergence order for the Poisson problem (P1) with basis function $\phi_{2,3}$ and support radii of the form (4.11) for $\nu = 3.5$.

tional relation between support radii and mesh norms as suggested by the convergence theorem to the effect of a proportional relation. In the latter case, we will see that the algorithm does not converge. This lack of convergence is rather unfortunate because in the fast-convergent, nonstationary case the condition numbers of the generalised interpolation matrices are considerably higher than in the stationary case. Thus, we obtain convergence at the expense of efficiency. Fasshauer observed this in [23].

We will use $\phi_{2,3} \in C^6$ as our basis function for both examples. Other basis function have been tried as well. As in the 1D case smoother functions yield faster convergence but also systems with larger condition numbers.

Poisson Problem on a Disk

The first Poisson problem we look at is defined on the unit disk and has zero boundary conditions, that is

$$\begin{aligned} \Delta u &= -1 \quad \text{on} \quad \Omega = B(0,1) \\ u &= \quad 0 \quad \text{on} \quad \partial\Omega = \{(x,y)^T \in \mathbb{R}^2 \mid x^2 + y^2 = 1\}. \end{aligned} \tag{P1}$$

N	H	$\|e\|_{L_2(\overline{\Omega})}$	$\|e\|_{L_2(\Omega)}$	$\|e\|_{L_2(\partial\Omega)}$	$\|e\|_{H^1(\overline{\Omega})}$	$\|e\|_{L_\infty(\overline{\Omega})}$	cond(A)
9	1	4.38e-2	4.42e-2	2.60e-7	1.28e-1	6.23e-2	3.4e3
25	2^{-1}	1.23e-2	1.24e-2	8.95e-5	5.13e-2	1.73e-2	3.4e4
77	2^{-2}	7.04e-3	7.10e-3	8.95e-5	2.60e-2	1.12e-2	1.3e6
257	2^{-3}	6.60e-3	6.66e-3	8.73e-6	1.95e-2	1.14e-2	2.7e7
921	2^{-4}	6.56e-3	6.62e-3	4.47e-6	1.81e-2	1.15e-2	3.9e8
3461	2^{-5}	6.56e-3	6.62e-3	8.88e-7	1.78e-2	1.15e-2	8.4e9
13361	2^{-6}	6.56e-3	6.62e-3	2.51e-7	1.77e-2	1.15e-2	1.8e11

Table 4.11: Convergence study for the Poisson problem (P1) with basis function $\phi_{2,3}$ and support radii $\delta = \nu\,(h/\mu)$ for $\mu = 0.5$ and $\nu = 3.5$.

Its C^∞ solution is given by $u(x, y) = (1 - x^2 - y^2)/4$. We choose support radii of the form (4.11) with $\nu = 3.5$ and cover the disk with nested uniform point sets

$$X_j = \Omega \cap H_j\mathbb{Z}^2, \quad \text{where} \quad H_j = \frac{1}{2^{j-1}}$$

for $j \in \mathbb{N}$. This leads to mesh norms

$$h_{X_1,\Omega} = 1 \quad \text{and} \quad h_{X_j,\Omega} = \frac{H_j}{\sqrt{2}}$$

for $j \in \mathbb{N} \setminus \{1\}$. The boundary is covered at level j by 2^{j+2} uniformly distributed points given by

$$Y_j = \left\{ (\cos(\theta_k), \sin(\theta_k))^T \in \mathbb{R}^2 \mid \theta_k = 0.1 + k\frac{2\pi + 0.1}{2^{j+2}}, 0 \le k \le 2^{j+2} - 1 \right\},$$

see Figure 4.2a. We chose to offset the interval $[0, 2\pi]$ by 0.1 to add some asymmetry to the problem. With these two point sets we find for $j \in \mathbb{N}$

$$h_{Y_j,\partial\Omega} = \frac{2\pi}{2^{j+3}} = \frac{\pi}{4}\frac{1}{2^j} < \frac{1}{2^j} < h_{X_j,\Omega},$$

where we computed $h_{Y_j,\partial\Omega}$ to be half the geodesic distance between two adjacent points. Computing the mesh norm on the boundary like this yields an equivalent norm to the boundary mesh norm defined in (4.4). The previous inequality shows that (4.12) holds with $h_j = h_{X_j,\Omega}$ for $j \in \mathbb{N} \setminus \{1\}$.

In Figure 4.3, one sees the approximation for the first seven levels – we compute the error on level $F = 8$. For each level the absolute error is also plotted separately along with the residual $|\Delta u_k - \Delta s_{u_k}|$. Where the distance between interior and boundary nodes is greatest (see Figure 4.2a) four spikes can be observed. This could be easily mended by putting additional points in these regions.

Tables 4.9 and 4.10 then summarises all necessary parameters and gives an overview of the errors. The results seem to verify our theoretical convergence result. We have an excellent convergence order at the cost of linear systems that are

N	H	$\|e\|_{L_2(\overline{\Omega})}$	$\|e\|_{L_2(\Omega)}$	$\|e\|_{L_2(\partial\Omega)}$	$\|e\|_{H^1(\overline{\Omega})}$	$\|e\|_{L_\infty(\overline{\Omega})}$	cond(A)
25	2^{-1}	1.22	1.22	-5.62	0.88	1.23	-2.22
77	2^{-2}	0.80	0.80	3.79	0.98	0.62	-5.19
257	2^{-3}	0.10	0.10	3.36	0.41	-0.03	-4.41
921	2^{-4}	<1e-2	<1e-2	0.97	0.11	<1e-2	-3.86
3461	2^{-5}	<1e-3	<1e-3	2.33	0.03	<1e-3	-4.42
13361	2^{-6}	<1e-4	<1e-4	1.83	0.01	<1e-3	-4.44

Table 4.12: Convergence order for the Poisson problem (P1) with basis function $\phi_{2,3}$ and support radii $\delta = \nu\,(h/\mu)$ for $\mu = 0.5$ and $\nu = 3.5$.

increasingly more difficult to solve. Additionally, it can be seen that the L_2 error on the boundary is generally lower than in the interior. This is not surprising since the second inequality in Theorem 4.9 suggests that

$$h_{Y_j,\partial\Omega} \approx h_{X_j,\Omega}^{\frac{\sigma-2}{\sigma-1}}$$

is a sensible choice because in that case the interior and the boundary contribute errors of comparable size to the overall error. This implies that the data sites on the boundary need not be chosen as densely as in the interior.

We compare in Tables 4.11 and 4.12 our previous results for a scaling of the form (4.11) with a proportional relationship between the support radii and the mesh norms. Whereas the algorithm stagnates in the interior, it still converges on the boundary which is not so surprising since we use pure interpolation there.

Poisson Problem on a Square

The second Poisson problem is taken from [24, Chapter 39] and given by

$$\begin{aligned} \Delta u(x,y) &= -\frac{5}{4}\pi^2 \sin(\pi x)\cos(\pi y/2) \qquad \text{on} \quad \Omega = (0,1)^2, \\ u(x,y) &= \begin{cases} \sin(\pi x) & \text{on} \quad \Gamma = \{(x,y)^T \in \mathbb{R}^2 \mid 0 \le x \le 1, y = 0\} \\ 0 & \text{on} \quad \partial\Omega \setminus \Gamma. \end{cases} \end{aligned} \tag{P2}$$

Its C^∞ solution is given by

$$u(x,y) = \sin(\pi x)\cos\left(\frac{\pi y}{2}\right).$$

The boundary of the domain is only piecewise smooth and thus technically the convergence result does not apply. However, the smoothness requirement stems from the trace theorem and it is not unlikely that it can be weakened to piecewise smooth boundaries. This is also supported by numerical evidence, which seems to suggest that convergence extends to piecewise smooth domains as well.

N	H	$\|e\|_{L_2(\overline{\Omega})}$	$\|e\|_{L_2(\Omega)}$	$\|e\|_{L_2(\partial\Omega)}$	$\|e\|_{H^1(\overline{\Omega})}$	$\|e\|_{L_\infty(\overline{\Omega})}$	cond(A)
9	2^{-1}	7.98e-2	8.04e-2	2.15e-2	4.31e-1	1.49e-1	1.5e3
25	2^{-2}	2.08e-2	2.10e-2	3.99e-3	1.58e-1	3.45e-2	1.0e5
81	2^{-3}	4.58e-3	4.61e-3	5.80e-4	4.92e-2	7.73e-3	2.3e7
289	2^{-4}	8.80e-4	8.86e-4	6.53e-5	1.32e-2	1.41e-3	2.3e9
1089	2^{-5}	1.44e-4	1.45e-4	6.15e-6	3.02e-3	2.09e-4	1.7e11
4225	2^{-6}	2.00e-5	2.01e-5	4.99e-7	6.07e-4	2.92e-5	1.3e13
16641	2^{-7}	2.41e-6	2.42e-6	3.32e-8	1.12e-4	3.71e-6	9.5e14

Table 4.13: Convergence study for the Poisson problem (P2) with basis function $\phi_{2,3}$ and support radii of the form (4.11) for $\nu = 2.4$.

N	H	$\|e\|_{L_2(\overline{\Omega})}$	$\|e\|_{L_2(\Omega)}$	$\|e\|_{L_2(\partial\Omega)}$	$\|e\|_{H^1(\overline{\Omega})}$	$\|e\|_{L_\infty(\overline{\Omega})}$	cond(A)
25	2^{-2}	1.94	1.94	2.42	1.45	2.11	-6.12
81	2^{-3}	2.19	2.19	2.78	1.68	2.16	-7.78
289	2^{-4}	2.38	2.38	3.15	1.90	2.45	-6.64
1089	2^{-5}	2.62	2.62	3.41	2.13	2.75	-6.25
4225	2^{-6}	2.85	2.85	3.62	2.31	2.84	-6.21
16641	2^{-7}	3.05	3.05	3.91	2.44	2.98	-6.22

Table 4.14: Convergence orders for the Poisson problem (P2) with basis function $\phi_{2,3}$ and support radii of the form (4.11) for $\nu = 2.4$.

N	H	$\|e\|_{L_2(\overline{\Omega})}$	$\|e\|_{L_2(\Omega)}$	$\|e\|_{L_2(\partial\Omega)}$	$\|e\|_{H^1(\overline{\Omega})}$	$\|e\|_{L_\infty(\overline{\Omega})}$	cond(A)
9	2^{-1}	7.01e-2	7.06e-2	1.81e-2	3.80e-1	1.33e-1	1.5e3
25	2^{-2}	2.98e-2	3.01e-2	4.44e-3	1.94e-1	4.85e-2	5.7e4
81	2^{-3}	2.26e-2	2.28e-2	1.02e-3	1.31e-1	3.97e-2	2.1e6
289	2^{-4}	2.19e-2	2.21e-2	2.22e-4	1.14e-1	3.99e-2	3.8e7
1089	2^{-5}	2.18e-2	2.20e-2	4.77e-5	1.10e-1	4.00e-2	6.2e8
4225	2^{-6}	2.18e-2	2.20e-2	1.03e-5	1.09e-1	4.00e-2	9.9e9
16641	2^{-7}	2.18e-2	2.20e-2	2.11e-6	1.09e-1	4.00e-2	1.6e11

Table 4.15: Convergence study for the Poisson problem (P2) with basis function $\phi_{2,3}$ and support radii $\delta = \nu\,(h/\mu)$ for $\mu = 0.5$ and $\nu = 3$.

N	H	$\|e\|_{L_2(\overline{\Omega})}$	$\|e\|_{L_2(\Omega)}$	$\|e\|_{L_2(\partial\Omega)}$	$\|e\|_{H^1(\overline{\Omega})}$	$\|e\|_{L_\infty(\overline{\Omega})}$	cond(A)
25	2^{-2}	1.23	1.23	2.03	0.97	1.46	-5.29
81	2^{-3}	0.40	0.40	2.12	0.56	0.29	-5.19
289	2^{-4}	0.05	0.05	2.20	0.20	0.05	-4.20
1089	2^{-5}	<1e-2	<1e-2	2.21	0.05	<1e-2	-4.02
4225	2^{-6}	<1e-3	<1e-3	2.22	0.01	<1e-3	-4.00
16641	2^{-7}	<1e-4	<1e-4	2.28	<1e-2	<1e-4	-4.00

Table 4.16: Convergence order for the Poisson problem (P2) with basis function $\phi_{2,3}$ and support radii $\delta = \nu\,(h/\mu)$ for $\mu = 0.5$ and $\nu = 3$.

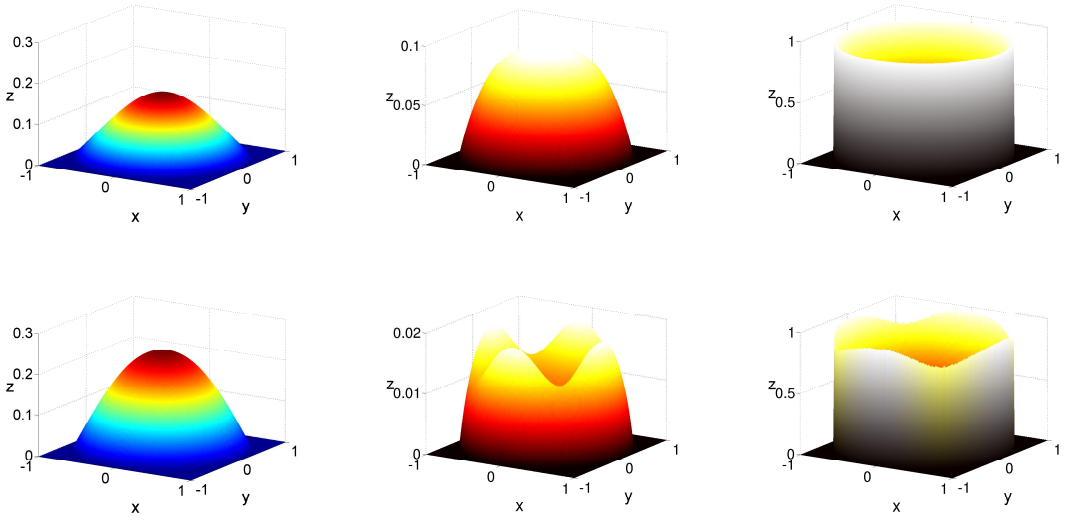

Figure 4.3: The multilevel approximation for seven different levels (left), along with the absolute error (middle) and residual (right) for problem (P1), to be continued on the next page.

Again, we choose support radii of the form (4.11) – this time with $\mu = 0.5$ and $\nu = 2.4$. We cover the closed domain $\overline{\Omega} = [0,1]^2$ with uniformly distributed nested point sets (see Figure 4.2b) such that

$$X_j = \Omega \cap H_j \mathbb{Z}^2 \qquad \text{and} \qquad Y_j = \left[\overline{\Omega} \cap H_j \mathbb{Z}^2\right] \setminus X_j,$$

where $H_j = 1/2^j$ for $j \geq 1$. Hence, we obtain mesh norms that satisfy (4.12) with

$$h_{X_j,\Omega} = \frac{H_j}{\sqrt{2}} \quad \text{and} \quad h_{Y_j,\partial\Omega} = \frac{H_j}{2}.$$

In Figure 4.4, one finds again the approximation, the absolute error $|u_k - s_{u_k}|$ and the residual $|\Delta u_k - \Delta s_{u_k}|$ for the first seven levels. The numerical values are given in Table 4.13 and 4.14, where we computed the error on level $F = 8$. Even though the boundary is only piecewise smooth, the algorithm still converges fast.

Again, the condition numbers show an unbounded growth and the error on the boundary is better than in the interior. Similar to (P1), the algorithm converges on the boundary but not in the interior when choosing the support radii proportional to the mesh norm, see Table 4.15 and 4.16.

Comparison with Other Numerical Methods

We briefly discuss how our previous results compare with other methods. In particular, we focus on the finite element method (FEM). Since multigrid techniques

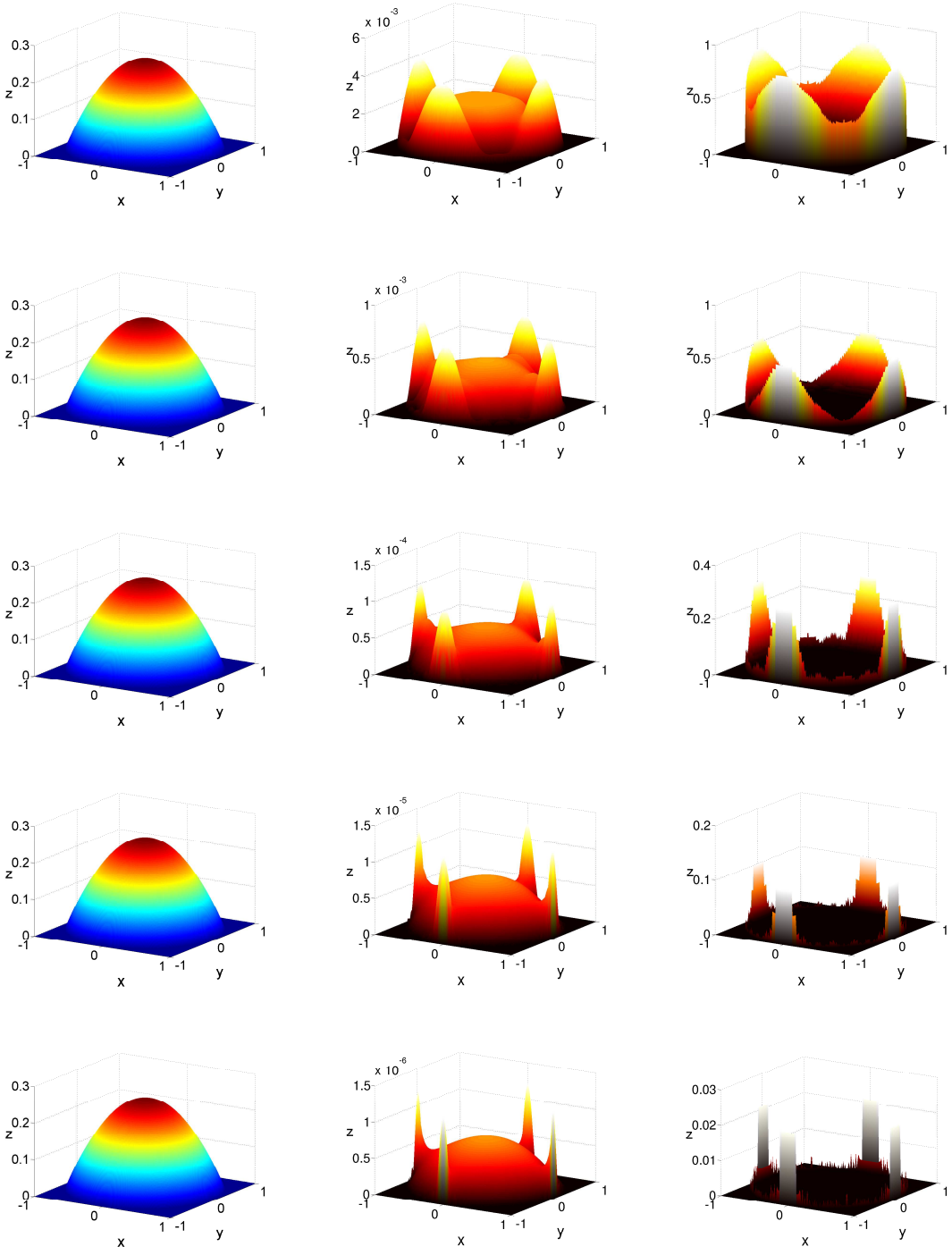

Figure 4.3: The multilevel approximation for seven different levels (left), along with the absolute error (middle) and residual (right) for problem (P1).

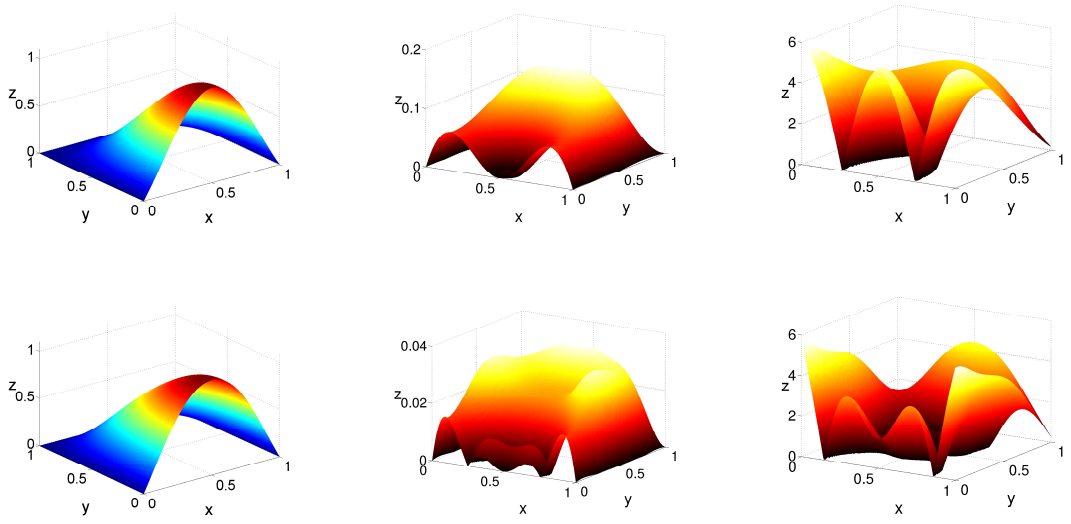

Figure 4.4: The multilevel approximation for seven different levels (left), along with the absolute error (middle) and residual (right) for problem (P2), to be continued on the next page.

for the finite element method only increase the efficiency but not the accuracy of the numerical solution (see [7, Chapter 6]), we employ the finite element method for finer and finer triangulations without transferring information between the different levels.

We solve (P2), discretising the unit square with a regular triangulation. Hence, if N again denotes the number of interior and boundary data points, then there are $2(\sqrt{N}-1)^2$ triangles. The boundary nodes are known exactly, therefore, we only need to solve for the interior nodes. On each triangle we approximate the solution with a piecewise linear polynomial. Though these basis functions are significantly less smooth than the basis function we have used for the multilevel RBF collocation method, they yield systems that have the same number of unknowns. For smoother finite element basis functions, we would need to solve larger systems.

The finite element method can also be interpreted as a finite difference method, that approximates the Laplacian by a quotient, namely

$$\Delta u(x,y) \approx \frac{u(x-H,y)+u(x+H,y)+u(x,y-H)+u(x,y+H)-4u(x,y)}{H^2},$$

where H corresponds to the length of the triangles.

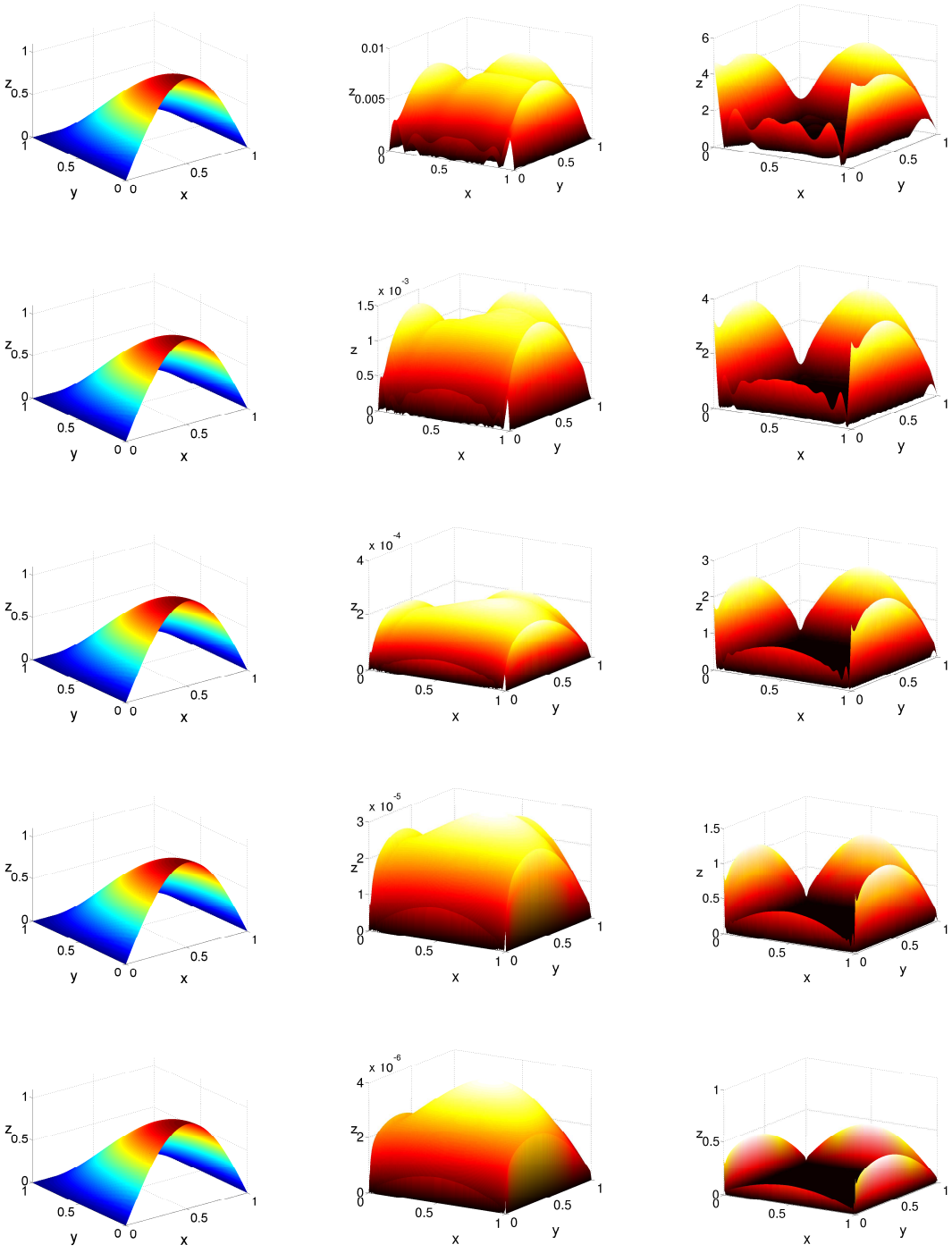

Figure 4.4: The multilevel approximation for seven different levels (left), along with the absolute error (middle) and residual (right) for problem (P2).

N	H	$\|e\|_{L_2(\overline{\Omega})}$	$\|e\|_{L_\infty(\overline{\Omega})}$	cond(A)
9	2^{-1}	1.22e-2	3.65e-2	5
25	2^{-2}	4.58e-3	1.11e-2	15
81	2^{-3}	1.33e-3	3.04e-3	3.7e1
289	2^{-4}	3.54e-4	7.74e-4	1.5e2
1089	2^{-5}	9.14e-5	1.94e-4	6.0e2
4225	2^{-6}	2.32e-5	4.86e-5	2.4e3
16641	2^{-7}	5.85e-6	1.22e-5	9.7e3

Table 4.17: FEM convergence study for Poisson problem (P2) with piecewise linear basis functions.

N	H	$\|e\|_{L_2(\overline{\Omega})}$	$\|e\|_{L_\infty(\overline{\Omega})}$	cond(A)
25	2^{-2}	1.41	1.72	-1.59
81	2^{-3}	1.79	1.86	-1.31
289	2^{-4}	1.90	1.97	-2.01
1089	2^{-5}	1.95	1.99	-2.00
4225	2^{-6}	1.98	2.00	-2.00
16641	2^{-7}	1.99	2.00	-2.00

Table 4.18: FEM orders for Poisson problem (P2) with piecewise linear basis functions.

The results are shown in Tables 4.17 and 4.18. The L_2 and L_∞ errors diminish quadratically and the condition numbers grow quadratically. These results agree with the theory [7]. On the one hand, the multilevel RBF collocation method yields faster convergence rates. On the other hand, the condition numbers also grow considerably faster. It has to be noted that for smoother basis functions, the finite element method can also achieve faster convergence rates. It seems not unlikely that smoother FEM basis functions would actually yield similar convergence rates and lower condition numbers (for bigger systems) than the presented RBF collocation method – at least for simple problems on uniform grids. And this is not even taking into account how the efficiency can be improved via preconditioning and multigrid strategies.

The main advantage of the (multilevel) RBF collocation is that it can deal with unstructured data, without needing to generate a mesh. We will demonstrate this in the next subsection.

Results for Unstructured Grids

Even though the previous results were given on structured grids, they also hold on unstructured grids that still satisfy inequality (4.8). An example of such a grid can be constructed with quasi-random (i. e. seemingly random but actually deterministic) Halton points [42]. The following explanation of Halton points is taken from Fasshauer's textbook [24, Appendix A].

h	$\|e\|_{L_2(\overline{\Omega})}$	$\|e\|_{L_2(\Omega)}$	$\|e\|_{L_2(\partial\Omega)}$	$\|e\|_{H^1(\overline{\Omega})}$	$\|e\|_{L_\infty(\overline{\Omega})}$	cond(A)
3.54e-1	7.45e-2	7.51e-2	2.29e-2	3.90e-1	1.42e-2	1.5e3
1.77e-1	2.12e-2	2.14e-2	4.06e-3	1.38e-1	3.64e-2	1.7e5
8.84e-2	2.83e-3	2.85e-3	1.50e-3	3.11e-2	7.43e-3	2.3e7
4.42e-2	4.13e-4	4.16e-4	9.44e-5	5.92e-3	6.55e-4	2.9e9
2.21e-2	5.16e-5	5.20e-5	8.67e-6	1.02e-3	8.66e-5	2.6e11
1.10e-2	6.38e-6	6.43e-6	5.34e-7	1.81e-4	1.07e-5	2.7e13
5.52e-3	9.25e-7	9.32e-7	4.16e-8	2.94e-5	1.62e-6	1.3e15

Table 4.19: Convergence study for the Poisson problem (P2) with basis function $\phi_{2,3}$ and support radii of the form (4.11) for $\nu = 2.4$ and data sets constructed from Halton points.

h	$\|e\|_{L_2(\overline{\Omega})}$	$\|e\|_{L_2(\Omega)}$	$\|e\|_{L_2(\partial\Omega)}$	$\|e\|_{H^1(\overline{\Omega})}$	$\|e\|_{L_\infty(\overline{\Omega})}$	cond(A)
3.54e-1	1.81	1.81	2.49	1.50	1.96	-6.74
1.77e-1	2.90	2.91	1.44	2.14	2.29	-7.45
4.42e-2	2.78	2.78	3.99	2.39	3.50	-6.65
2.21e-2	3.00	3.00	3.44	2.53	2.92	-6.50
1.10e-2	3.02	3.02	4.02	2.50	3.02	-6.69
5.52e-3	2.79	2.79	3.68	2.62	2.72	-5.55

Table 4.20: Convergence study for the Poisson problem (P2) with basis function $\phi_{2,3}$ and support radii of the form (4.11) for $\nu = 2.4$ and data sets constructed from Halton points.

Every nonnegative integer n can be decomposed uniquely with a prime base p in the following form

$$n = \sum_{i=0}^{k} a_i p^i$$

for some $k \in \mathbb{N}_0$, where each coefficient $a_i \in \mathbb{N}$ satisfies $0 \leq a_i < p$. For example, for $n = 10$ and $p = 3$, we have

$$10 = 1 \cdot 3^0 + 0 \cdot 3^1 + 1 \cdot 3^2.$$

That is, $k = 2$, $a_0 = a_2 = 1$ and $a_1 = 0$. Next we map the nonnegative number n to the interval $[0, 1)$ via the function

$$h_p(n) = \sum_{i=0}^{k} \frac{a_i}{p^{i+1}}.$$

In our example that means

$$h_3(10) = \frac{1}{3} + \frac{1}{3^3} = \frac{10}{27} \in [0, 1).$$

This expression can be used to define a sequence, which is known as a *van der Corput* sequence. It is given by

$$h_{p,N} := \{h_p(n) \mid n = 0, 1, 2, \ldots, N\}.$$

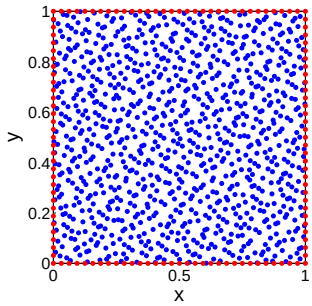

Figure 4.5: Blue interior Halton points and red uniform boundary points, 961 and 128 points respectively.

For example

$$h_{3,10} = \{0, 1/3, 2/3, 1/9, 4/9, 7/9, 2/9, 5/9, 8/9, 1/27, 10/27\}.$$

To construct a Halton point set in the d-dimensional unit cube $[0,1)^d$, we take d (usually distinct) primes $p_1, \ldots, p_d$ and use the resulting van der Corput sequences $h_{p_1,N}, \ldots, h_{p_d,N}$ as the coordinates of the d-dimensional Halton points. That is the set of $N+1$ Halton points in the unit cube $[0,1)^d$ is given by

$$H_{d,N} = \{(h_{p_1}(n), \ldots, h_{p_d}(n)) \mid n = 0, \ldots, N\}.$$

Since we have $d = 2$, we need to specify two primes. We choose $p_1 = 2$ and $p_2 = 3$. Since Halton points in 1D behave quite regularly, we use equidistant points on the boundary. See Figure 4.5 for an example of a data set, consisting of interior Halton and uniform boundary points. We construct Halton points in the interior as well as equidistant points on the boundary on the finest level and obtain a sequence of nested sets using the farthest point algorithm [26]. For each level we double the mesh norm, starting with the smallest. We obtain relatively well-behaved data sets.

The results are displayed in Tables 4.19 and 4.20 for the Poisson problem on a square (P2). They are relatively comparable to our previous results on regular grids, see Tables 4.13 and 4.14. They even seem to perform slightly better. This comes, however, at the expense of a slightly higher condition number. To compute the errors, we use Halton points on the finest level (F=8). This seems to have an impact on the errors as the results on the last level seem to deviate from the pattern. The finest level which we use for evaluation is not automatically as well-behaved as the previous sets as it is not constructed with the farthest point algorithm. Another possible explanation for this is that the condition number is too large at the highest level.

Comparison with One Shot Method

Lastly, we demonstrate the advantage of the multilevel approximation compared to using simply a symmetric one-shot RBF collocation approach. In Table 4.21, we

N	H	$\|e\|_{L_2(\overline{\Omega})}$	$\|e\|_{L_2(\Omega)}$	$\|e\|_{L_2(\partial\Omega)}$	$\|e\|_{H^1(\overline{\Omega})}$	$\|e\|_{L_\infty(\Omega)}$	cond(A)
16641	2^{-7}	9.58e-3	9.66e-3	1.10e-6	4.44e-2	1.92e-2	9.5e14

Table 4.21: Symmetric one-shot RBF collocation method for (P2) with $\nu = 2.4$, $\delta = 0.20$ and $\phi_{2,3}$ as basis function.

compute a one-shot approximation to the Poisson problem (P2) and give the errors evaluated on the next finest level, consisting of equispaced 66049 data points. We use $\phi_{2,3}$ as basis function and the same support radius as for the finest level of the multilevel approximation in Table 4.13. It has to be noted that it is likely that we would achieve better results with a larger support radius. However, then the condition numbers become too large to solve the system.

Even though the condition numbers are obviously exactly the same (since the matrix has not changed), the errors are significantly worse than for the multilevel approximation of the same level. This naturally comes at the expense of having to solve six additional but smaller systems.

We have given a rigorous convergence proof of the multilevel collocation algorithm, which was introduced to overcome some of the shortages of the one-shot method. Nevertheless, the numerical examples in this chapter show that there is still room for improvement because the condition numbers of the multilevel collocation approximation still grow relatively quickly. Therefore, the next two chapters are dedicated to regularisation and preconditioning as well as an operator splitting technique in an effort to improve the conditioning of the problem.

Chapter 5

Regularisation, Preconditioning and Alternating Projections

As we have seen in the previous chapter, the multilevel collocation algorithm suffers from stability problems in the sense that the condition numbers grow for each level. That means, if we use an iterative method like the conjugate gradient method, that the number of iteration steps needed to achieve a certain tolerance grows accordingly. Also for direct methods a low condition number is beneficial. Therefore, we discuss in this chapter how to improve the condition number based on two strategies: regularisation, preconditioning and operator splittling.

The regularisation technique is due to Wahba [80]. In this thesis, her result will be extended to several regularisation parameters and generalised error theory will be presented, which builds on previous results in [85]. The numerical advantages of a Jacobi preconditioner have been observed by Fasshauer [23]. Here, we will present a sound numerical proof for the efficiency of the preconditioner. This work has been published in [22]. The operator splitting is achieved via the alternating projection method [76], which was first applied to RBFs by Beatson, Light and Billings in the context of interpolation [2] and by Wendland in the context of generalised interpolation [83]. We adapt the alternating projection method here to collocation.

5.1 Regularisation

So far we have made the implicit assumption that all the data we use as input for the multilevel algorithm are exact. In practice, however, this might not be a very sensible idea as measured data surely contain errors. In this case (generalised) interpolation is not desirable. To avoid this problem, a promising idea is to minimise the difference between approximation and exact solution at the data points in some norm plus an additional penalty constraint. In her book [80], Grace Wahba investigates *spline smoothing*, a Tikhonov-type regularisation technique. The idea is that as long as the penalty constant is small enough, the additional error in solving the system might be negligible.

Let us be a bit more precise (and introduce the necessary notation) along the way. Instead of an interpolation problem we would like to consider for some $\varepsilon > 0$ a penalised least-squares problem of the form

$$\operatorname{argmin}\left\{\sum_{j=1}^{N}(\lambda_j(s)-f_j)^2+\varepsilon\|s\|_\Phi^2 \big| s\in\mathcal{N}_\Phi(\mathbb{R}^d)\right\}, \tag{5.1}$$

using the same notation as in Section 3.1. Setting the constant ε to zero would yield the standard interpolation solution. Unlike for standard Tikhonov regularisation, the additional term is measured in the native space norm (instead of the Euclidean norm), which simplifies the analysis. If we think of the native space as a Sobolev space, the constant ε helps to control how smooth we allow the solution to be. However, smoothness comes at a price. The bigger ε, the higher the risk of not being able to approximately satisfy the least-square part. There is a unique minimiser to this problem.

Theorem 5.1 (One Smoothing Parameter) *The unique solution to the minimisation problem* (5.1) *is given by*

$$s_\varepsilon(\mathbf{x})=\sum_{j=1}^{N}\alpha_j^*\lambda_j^{\mathbf{y}}\Phi(\mathbf{x},\mathbf{y}), \tag{5.2}$$

where the coefficients $\boldsymbol{\alpha}^*=(\alpha_j^*)\in\mathbb{R}^N$ *are determined by*

$$[A+\varepsilon I]\boldsymbol{\alpha}^*=\mathbf{f},$$

where $\mathbf{f}=(f_j)$.

Now it becomes clear how the regularisation works from a linear algebra point of view. If the smallest eigenvalue of the matrix A is so small that solving the standard interpolation problem is not feasible, this Tikhonov approach helps stabilise the system by adding ε to the eigenvalues. Even though the proof of this theorem is well-known (see for example [80, Theorem 1.3.1]), we present it here as we shall generalise it in the following section.

Proof. We first claim that a solution to the minimisation problem (5.1) comes from the finite-dimensional space

$$V_\Lambda:=\operatorname{span}\left\{\lambda_j^{\mathbf{y}}\Phi(\cdot,\mathbf{y})\mid 1\le j\le N\right\}.$$

To see this let $\mathfrak{s}\in\mathcal{N}_\Phi(\mathbb{R}^d)$. Since V_Λ is a finite-dimensional (and thus closed) subspace of the Hilbert space $\mathcal{N}_\Phi(\mathbb{R}^d)$, there exists an orthogonal projection which helps us decompose the native space into V_Λ and its orthogonal complement. That is, we can find $s\in V_\Lambda$ and $s^\perp\in V_\Lambda^\perp$ such that $\mathfrak{s}=s+s^\perp$.

On the one hand, we deduce, due to the kernel reproduction property and the fact that $s^\perp \in V_\Lambda^\perp$, that

$$\begin{aligned}\lambda_j(\mathfrak{s}) &= (\mathfrak{s}, \lambda_j^{\mathbf{y}}\Phi(\cdot,\mathbf{y}))_\Phi = (s, \lambda_j^{\mathbf{y}}\Phi(\cdot,\mathbf{y}))_\Phi + (s^\perp, \lambda_j^{\mathbf{y}}\Phi(\cdot,\mathbf{y}))_\Phi \\ &= (s, \lambda_j^{\mathbf{y}}\Phi(\cdot,\mathbf{y}))_\Phi = \lambda_j(s).\end{aligned}$$

On the other hand, we see that

$$\|\mathfrak{s}\|_\Phi^2 = (s,s)_\Phi + 2(s,s^\perp)_\Phi + (s^\perp,s^\perp)_\Phi = \|s\|_\Phi^2 + \|s^\perp\|_\Phi^2.$$

Hence,

$$\sum_{j=1}^N (\lambda_j(\mathfrak{s}) - f_j)^2 + \varepsilon\|\mathfrak{s}\|_\Phi^2 \geq \sum_{j=1}^N (\lambda_j(s) - f_j)^2 + \varepsilon\|s\|_\Phi^2,$$

which shows that the orthogonal complement does not contribute to the minimiser and thus $\mathfrak{s} = s$. This insight has the useful consequence that the minimisation problem is actually of finite nature. We know now that the solution has to be of the form

$$s = \sum_{j=1}^N \alpha_j \lambda_j^{\mathbf{y}}\Phi(\cdot,\mathbf{y}).$$

Defining $\boldsymbol{\alpha} = (\alpha_j), \mathbf{f} = (f_j)$ and $A = (\lambda_j^{\mathbf{x}}\lambda_k^{\mathbf{y}}\Phi(\mathbf{x},\mathbf{y}))$, problem (5.1) can be written in terms of vectors and matrices. We would like to minimise

$$g(\boldsymbol{\alpha}) := \|A\boldsymbol{\alpha} - \mathbf{f}\|_2^2 + \varepsilon\boldsymbol{\alpha}^T A\boldsymbol{\alpha}.$$

Forming the normal equations by taking the gradient with respect to $\boldsymbol{\alpha}$ and setting the resulting equation to zero, we find that the coefficient vector $\boldsymbol{\alpha}^*$ of the minimiser s_ε needs to satisfy

$$\nabla_{\boldsymbol{\alpha}} g(\boldsymbol{\alpha}^*) = 2(A^T A\boldsymbol{\alpha}^* - A^T\mathbf{f}) + 2\varepsilon A\boldsymbol{\alpha}^* = \mathbf{0},$$

or

$$(A + \varepsilon I)\boldsymbol{\alpha}^* = \mathbf{f},$$

where we have used the fact that $A^T = A$ is invertible. Therefore, the penalised least-square solution (5.2) is an optimiser. Moreover, it is even a minimiser since

$$\mathrm{Hess}(g)(\boldsymbol{\alpha}) = 2A^T A + 2\varepsilon A$$

is positive definite. This follows from the fact that the sum of two positive definite matrices is again positive definite. The product of invertible matrices $A^T A$ is positive definite and εA is positive definite since Φ is a positive definite function and ε is assumed to be a positive constant. □

5.1.1 General Regularisation Results

The problem with the standard way of smoothing the data is that it allows little flexibility. If the matrix has intrinsically different blocks (like in our case due to the interior and boundary part of the PDE) it might be beneficial to add different smoothing parameters to each block. To develop the theory for this case is the objective of this section.

Instead of (5.1), let us consider the minimisation problem

$$\operatorname{argmin}\left\{\sum_{k=1}^{N}\left(\sum_{j=1}^{N} p_{kj}\left[\lambda_j(s)-f_j\right]\right)^2+\varepsilon\|s\|_\Phi^2\,\middle|\, s\in\mathcal{N}_\Phi(\mathbb{R}^d)\right\}, \tag{5.3}$$

for some $p_{kj}\in\mathbb{R}$. Again, there exists a unique minimiser to this problem.

Theorem 5.2 (Different Smoothing Parameters) *The unique solution to the minimisation problem* (5.3) *is given by*

$$s_\varepsilon(\mathbf{x})=\sum_{j=1}^{N}\alpha_j^*\lambda_j^{\mathbf{y}}\Phi(\mathbf{x},\mathbf{y}), \tag{5.4}$$

where the coefficients $\boldsymbol{\alpha}^*=(\alpha_j^*)\in\mathbb{R}^d$ *are determined by*

$$(A+\varepsilon P^{-1}P^{-T})\boldsymbol{\alpha}^*=\mathbf{f}.$$

Here the matrix $P=(p_{kj})_{1\le k,j\le N}$ *is assumed to be invertible.*

Note that for convenience we have used the same notation as before for the solution to the minimisation problem. Even though it would be more accurate to use s_ε^P, we prefer to keep the notation simple and drop the superscript P here. This should not cause problems since the following theory is based on (5.4) exclusively except when explicitly stated otherwise.

Proof. As in the proof of Theorem 5.1, we can deduce that the minimiser lies in the finite-dimensional space $V_\Lambda=\operatorname{span}\left\{\sum_{j=1}^{N}\alpha_j\lambda_j^{\mathbf{y}}\Phi(\cdot,\mathbf{y})\right\}$, i. e. it is of the form (5.4).

If we exploit again the finite dimensionality, the minimisation problem (5.3) reduces to finding the minimum of

$$g(\boldsymbol{\alpha}):=\|P(A\boldsymbol{\alpha}-\mathbf{f})\|_2^2+\varepsilon\boldsymbol{\alpha}^TA\boldsymbol{\alpha}.$$

We introduce the abbreviations $\widetilde{A}=PA$ and $\widetilde{\mathbf{f}}=P\mathbf{f}$. Taking the gradient with respect to $\boldsymbol{\alpha}$ and setting the resulting equation to zero, we find that the coefficient vector of the minimiser s_ε needs to satisfy

$$\nabla_{\boldsymbol{\alpha}}g(\boldsymbol{\alpha}^*)=2\left(\widetilde{A}^T\widetilde{A}\boldsymbol{\alpha}^*-\widetilde{A}^T\widetilde{\mathbf{f}}\right)+2\varepsilon A\boldsymbol{\alpha}^*=\mathbf{0}.$$

Note we have

$$A = A^T P^T P^{-T} = (PA)^T P^{-T} = \widetilde{A}^T P^{-T}.$$

Therefore, we obtain after dividing by two and applying $\widetilde{A}^{-T}$ from the left

$$\widetilde{A}\boldsymbol{\alpha}^* - \widetilde{\mathbf{f}} + \varepsilon P^{-T}\boldsymbol{\alpha}^* = \mathbf{0},$$

or in other words

$$(PAP^T + \varepsilon I)P^{-T}\boldsymbol{\alpha}^* = P\mathbf{f}.$$

After left multiplication by P^{-1} this yields the desired result,

$$(A + \varepsilon P^{-1}P^{-T})\boldsymbol{\alpha}^* = \mathbf{f}.$$

Since

$$\mathrm{Hess}(g)(\boldsymbol{\alpha}) = 2\widetilde{A}^T\widetilde{A} + 2\varepsilon A$$

is positive definite, we have indeed found the unique minimiser. □

This result can now be used to regularise different parts of the matrix A in different ways. For example, in the case of a diagonal matrix P, the following corollary holds.

Corollary 5.3 *Let P be a diagonal matrix with*

$$P = \sqrt{\varepsilon}\,\mathrm{diag}(1/\sqrt{\varepsilon_1}, \ldots, 1/\sqrt{\varepsilon_N}) \tag{5.5}$$

for some $\varepsilon_i > 0$. Then problem (5.3) is equivalent to solving

$$\mathrm{argmin}\left\{ \sum_{j=1}^{N} \frac{1}{\varepsilon_j}\left[\lambda_j(s) - f_j\right]^2 + \|s\|_\Phi^2 \,\middle|\, s \in \mathcal{N}_\Phi(\mathbb{R}^d) \right\} \tag{5.6}$$

and the solution is given by

$$s_\varepsilon(\mathbf{x}) = \sum_{j=1}^{N} \alpha_j^* \lambda_j^{\mathbf{y}} \Phi(\mathbf{x}, \mathbf{y}),$$

where the coefficients α^* are determined from the linear system

$$(A + \mathrm{diag}(\varepsilon_1, \ldots, \varepsilon_N))\boldsymbol{\alpha}^* = \mathbf{f}.$$

5.1.2 Error of the Regularised Interpolant

After proving the general regularisation result, we turn our attention to error estimates. For a one-shot approximation to the solution of a partial differential equation with just one smoothing parameter this has been analysed by Wendland, see [85]. Here we extend the result to a scale-dependent kernel and various smoothing parameters, more specifically to the case where P is given by (5.5).

We need an approximate sampling inequality, namely

$$|u|_{L_p(\Omega)} \leq C \left\{ h_{X,\Omega}^{\sigma - d(1/q - 1/p)_+} |u|_{W_q^\sigma(\Omega)} + \max_{\mathbf{x} \in X} |u(\mathbf{x})| \right\}, \tag{5.7}$$

where u is the solution to the PDE. This result can be found in [85] and applies to approximate interpolation, unlike Theorem 2.33. It holds for $1 \leq p, q \leq \infty$ and $\sigma > d/2$. The domain Ω needs to satisfy an interior cone condition (see [84, Definition 3.6]), which is automatically satisfied if we assume the boundary to be Lipschitz. Earlier results on approximate sampling inequalities can be found in [88]. Using the extension operator E from the previous chapter, we can prove the following theorem.

Lemma 5.4 *Let Φ_δ be a scale-dependent translation-invariant kernel that generates $H^\sigma(\mathbb{R}^d)$ and $\{\lambda_j\}_{j=1}^N$ be a family of linearly independent functionals over $H^\sigma(\mathbb{R}^d)$. For s_ε, the solution to (5.6), we have for any $1 \leq j \leq N$*

$$|\lambda_j(s_\varepsilon) - \lambda_j(u)| \leq \max_{1 \leq k \leq N} \sqrt{\varepsilon_k} \|Eu\|_{\Phi_\delta} \qquad \text{and} \qquad \|Eu - s_\varepsilon\|_{\Phi_\delta} \leq 2\|Eu\|_{\Phi_\delta}$$

where $u \in H^\sigma(\Omega)$ is the solution to (3.6).

Proof. The proof is similar to [85, Lemma 5.1]. Since $Eu \in H^\sigma(\mathbb{R}^d) = \mathcal{N}_{\Phi_\delta}(\mathbb{R}^d)$, we can substitute it into (5.6). However, the minimiser s_ε of the penalised least-squares problem must yield a value that is smaller or equal. Therefore, we deduce

$$\begin{aligned}
&\max \left\{ \min_{1 \leq k \leq N} \frac{1}{\varepsilon_k} |\lambda_j(s_\varepsilon) - \lambda_j(u)|^2, \|s_\varepsilon\|_{\Phi_\delta}^2 \right\} \\
&\qquad \leq \left(\sum_{j=1}^N \frac{1}{\varepsilon_j} |\lambda_j(s_\varepsilon) - \lambda_j(u)| \right)^2 + \|s_\varepsilon\|_{\Phi_\delta}^2 \\
&\qquad \leq \left(\sum_{j=1}^N \frac{1}{\varepsilon_j} |\lambda_j(s) - \lambda_j(u)| \right)^2 + \|s\|_{\Phi_\delta}^2
\end{aligned}$$

for all $s \in H^\sigma(\mathbb{R}^d)$. In particular, the last inequality holds for the choice $s = Eu$. Thus, we have

$$|\lambda_j(s_\varepsilon) - \lambda_j(u)|^2 \leq \frac{1}{\min_{1 \leq k \leq N} 1/\varepsilon_k} \|Eu\|_{\Phi_\delta}^2 = \max_{1 \leq k \leq N} \varepsilon_k \|Eu\|_{\Phi_\delta}^2$$

as well as

$$\|s_\varepsilon\|_{\Phi_\delta} \leq \|Eu\|_{\Phi_\delta}.$$

The assertion follows by taking the square root in the former case and using the triangle inequality in the latter. □

Now we can prove the following error estimates for regularised RBF collocation, which generalise the one-shot results in [85, Theorem 5.2]. We will use the notation from Section 3.1.1.

Theorem 5.5 *Let the domain $\Omega \subseteq \mathbb{R}^d$ have a $C^{k,s}$ boundary for $s \in [0,1)$ such that $\sigma = k + s$ and $k := \lfloor \sigma \rfloor > 2 + d/2$. Let L be the strictly elliptic differential operator defined in* (3.6)*. Then, we have for $1 \leq p \leq \infty$ the following error estimates*

$$\|Lu - Ls_\varepsilon\|_{L_p(\Omega)} \leq C \left\{ \delta^{-\sigma} h_{X_1,\Omega}^{\sigma-2-(d/2-d/p)_+} + \max_{1\leq k\leq n} \sqrt{\varepsilon_k} \right\} \|u\|_{H^\sigma(\Omega)},$$
$$\|u - s_\varepsilon\|_{L_p(\partial\Omega)} \leq C \left\{ \delta^{-\sigma} h_{X_2,\partial\Omega}^{\sigma-1/2-(d-1)(1/2-1/p)_+} + \max_{n+1\leq k\leq N} \sqrt{\varepsilon_k} \right\} \|u\|_{H^\sigma(\Omega)}.$$

Proof. We start with the first inequality corresponding to the interior part. Using the approximate sampling inequality (5.7), we find

$$\|Lu - Ls_\varepsilon\|_{L_p(\Omega)} \leq C h_{X_1,\Omega}^{\sigma-2-(d/2-d/p)_+} \|Lu - Ls_\varepsilon\|_{W_2^{\sigma-2}(\Omega)} + \max_{1\leq j\leq n} |\lambda_j(s_\varepsilon - u)|.$$

Estimating the first term separately, we see that

$$\begin{aligned}
\|Lu - Ls_\varepsilon\|_{W_2^{\sigma-2}(\Omega)} &\leq C\|u - s_\varepsilon\|_{W_2^\sigma(\Omega)} && \text{by Lemma 3.6} \\
&= C\|Eu - s_\varepsilon\|_{W_2^\sigma(\Omega)} \\
&\leq C\|Eu - s_\varepsilon\|_{W_2^\sigma(\mathbb{R}^d)} \\
&\leq C\delta^{-\sigma}\|Eu - s_\varepsilon\|_{\Phi_\delta} && \text{by Lemma 2.30} \\
&\leq 2C\delta^{-\sigma}\|Eu\|_{\Phi_\delta} && \text{by Lemma 5.4.}
\end{aligned}$$

Note, that we had to use Lemma 5.4 as unlike before no optimality condition holds. The second term yields by Lemma 5.4

$$\max_{1\leq j\leq n} |\lambda_j(u - s_\varepsilon)| \leq \max_{1\leq k\leq n} \sqrt{\varepsilon_k} \|Eu\|_{\Phi_\delta}.$$

Thus, in total we have

$$\begin{aligned}
\|Lu - Ls_\varepsilon\|_{L_p(\Omega)} &\leq C \left\{ \delta^{-\sigma} h_{X_1,\Omega}^{\sigma-2-(d/2-d/p)_+} + \max_{1\leq k\leq n} \sqrt{\varepsilon_k} \right\} \|Eu\|_{\Phi_\delta} \\
&\leq C \left\{ \delta^{-\sigma} h_{X_1,\Omega}^{\sigma-2-(d/2-d/p)_+} + \max_{1\leq k\leq n} \sqrt{\varepsilon_k} \right\} \|u\|_{W_2^\sigma(\Omega)}.
\end{aligned}$$

For the boundary part we need an atlas, just as in Section 4.2.2. Using the same notation as there, we set for simplicity $u_j = ((u - s_\varepsilon)w_j) \circ \psi_j \in W_2^{\sigma-1/2}(B)$. For $T_j = \psi_j^{-1}(X_2 \cap V_j) \subset B = B(\mathbf{0}, 1) \subset \mathbb{R}^{d-1}$ define $T = \bigcup_{j=1}^K T_j$. This time the approximate sampling inequality yields

$$\|u_j\|_{L_p(B)} \leq C \left\{ h_{T_j,B}^{\sigma-1/2-(d-1)(1/2-1/p)_+} \|u_j\|_{W_2^{\sigma-1/2}(B)} + \max_{\mathbf{t}\in T} |u_j(\mathbf{t})| \right\}.$$

In order to estimate the second term on the left-hand side, choose some arbitrary $\mathbf{t}^* \in T$ and define a boundary node through $\mathbf{y}^* = \psi_j(\mathbf{t}^*) \in X_2$. We have

$$\begin{aligned} |u_j(\mathbf{t}^*)| = |(u - s_\varepsilon)(\mathbf{y}^*)w_j(\mathbf{y}^*)| &\leq |(u - s_\varepsilon)(\mathbf{y}^*)| \leq \max_{n+1\leq k\leq N} \sqrt{\varepsilon_k} \|Eu\|_{\Phi_\delta} \\ &\leq C \max_{n+1\leq k\leq N} \sqrt{\varepsilon_k} \|u\|_{W_2^\sigma(\Omega)}. \end{aligned}$$

The last step follows again from Lemma 2.30. The second to last step follows from Lemma 5.4 for the point evaluation functional $\delta_{\mathbf{x}^*}$. Thus we have the estimate

$$\max_{\mathbf{t}\in T} |u_j(\mathbf{t})| \leq C \max_{n+1\leq k\leq N} \sqrt{\varepsilon_k} \|u\|_{W_2^\sigma(\Omega)}. \tag{5.8}$$

Using the definition of the Sobolev norm on the boundary (again as defined in Section 4.2.2) of the domain Ω and setting $M = \max_{n+1\leq k\leq N} \sqrt{\varepsilon_k}$, we can now see for $1 \leq p < \infty$ that

$$\begin{aligned} \|u - s_\varepsilon\|_{L_p(\partial\Omega)}^p &= \sum_{j=1}^K \|u_j\|_{L_p(B)}^p \\ &\leq C \sum_{j=1}^K \left\{ h_{T_j,B}^{\sigma-1/2-(d-1)(1/2-1/p)_+} \|u_j\|_{W_2^{\sigma-1/2}(B)} + \max_{\mathbf{t}\in T} |u_j(\mathbf{t})| \right\}^p \\ &\leq C \left\{ h_{X_2,\partial\Omega}^{(\sigma-1/2-(d-1)(1/2-1/p)_+)} \|u - s_\varepsilon\|_{W_2^{\sigma-1/2}(\partial\Omega)} + M\|u\|_{W_2^\sigma(\Omega)} \right\}^p \\ &\leq C \left\{ h_{X_2,\partial\Omega}^{(\sigma-1/2-(d-1)(1/2-1/p)_+)} \|u - s_\varepsilon\|_{W_2^\sigma(\Omega)} + M\|u\|_{W_2^\sigma(\Omega)} \right\}^p \\ &\leq C \left\{ \delta^{-\sigma} h_{X_2,\partial\Omega}^{(\sigma-1/2-(d-1)(1/2-1/p)_+)} \|u - s_\varepsilon\|_{\Phi_\delta} + M\|u\|_{W_2^\sigma(\Omega)} \right\}^p \\ &\leq 2C \left\{ \delta^{-\sigma} h_{X_2,\partial\Omega}^{(\sigma-1/2-(d-1)(1/2-1/p)_+)} \|u\|_{\Phi_\delta} + M\|u\|_{W_2^\sigma(\Omega)} \right\}^p \\ &\leq C \left\{ \delta^{-\sigma} h_{X_2,\partial\Omega}^{(\sigma-1/2-(d-1)(1/2-1/p)_+)} + \max_{n+1\leq k\leq N} \sqrt{\varepsilon_k} \right\}^p \|u\|_{W_2^\sigma(\Omega)}^p, \end{aligned}$$

where we have used the general sampling inequality (5.7), the Minkowski inequality, the norm equivalence between the ℓ_p and ℓ_1 norm, the trace theorem, Lemma 2.30 and inequality (5.8). The case $p = \infty$ is treated similarly. □

We can simplify the above theorem by just looking at the L_2 error and a uniform regularisation of interior and boundary.

N	H	$\|e\|_{L_2(\overline{\Omega})}$	$\|e\|_{L_2(\Omega)}$	$\|e\|_{L_2(\partial\Omega)}$	$\|e\|_{H^1(\overline{\Omega})}$	$\|e\|_{L_\infty(\overline{\Omega})}$	$\mathrm{cond}(\widetilde{A})$
9	2^{-1}	1.04e-1	1.05e-1	6.05e-2	5.07e-1	1.56e-1	1.1e1
25	2^{-2}	2.37e-2	2.39e-2	1.13e-2	1.94e-1	3.81e-2	4.4e1
81	2^{-3}	5.00e-3	5.03e-3	2.82e-3	6.27e-2	1.02e-2	1.2e2
289	2^{-4}	9.01e-4	9.02e-4	7.95e-4	1.82e-2	3.46e-3	4.5e2
1089	2^{-5}	1.36e-4	1.34e-4	2.53e-4	4.97e-3	1.44e-3	2.4e3
4225	2^{-6}	2.08e-5	1.82e-5	8.21e-5	1.48e-3	5.60e-4	1.1e4
16641	2^{-7}	4.57e-6	3.33e-6	2.52e-5	5.03e-4	2.05e-6	5.0e4

Table 5.1: Convergence study for the regularised Poisson problem (P2) with basis function $\phi_{2,3}$ and support radii of the form (4.11) for $\nu = 2.4$. The regularisation parameters are $\varepsilon_1 = 0$ and $\varepsilon_2 =$1e-1.

Corollary 5.6 (L_2 Error) *Let s_ε solve (5.6). Suppose $\varepsilon_k = \varepsilon_I$ for $1 \le k \le n$ and $\varepsilon_k = \varepsilon_B$ for $n+1 \le k \le N$. The L_2 error is given by*

$$\|Lu - Ls_\varepsilon\|_{L_2(\Omega)} \le C \left\{ h_{X_1,\Omega}^{\sigma-2} \delta^{-\sigma} + \sqrt{\varepsilon_I} \right\} \|u\|_{H^\sigma(\Omega)},$$
$$\|u - s_\varepsilon\|_{L_2(\partial\Omega)} \le C \left\{ h_{X_2,\partial\Omega}^{\sigma-1/2} \delta^{-\sigma} + \sqrt{\varepsilon_B} \right\} \|u\|_{H^\sigma(\Omega)}.$$

5.1.3 Numerical Examples

Finally, we examine the influence of regularisation parameters. Theorem 5.7 shows that the asymptotic behaviour of the smallest eigenvalue is dictated by the boundary operator, the identity. We focus on stabilising the smallest eigenvalue since perturbing the largest eigenvalue by adding a small enough constant (so that the approximation error does not become too big) will be negligible. Therefore, we consider the preconditioned and regularised collocation matrix

$$\widetilde{A} = PA_\Lambda P + \begin{pmatrix} \varepsilon_1 I_{n,n} & \mathbf{0} \\ \mathbf{0}^T & \varepsilon_2 I_{N-n,N-n} \end{pmatrix}$$

with $\varepsilon_1 = 0$ and different choices for ε_2. The matrix $I_{k,k}$ denotes the k-dimensional identity and P is diagonal preconditioner from (5.13). We give numerical results for the multilevel collocation algorithm for the test problem (P2) from Chapter 4 using $\widetilde{A}$. Tables 5.1-5.6 state the errors and condition numbers as well as the corresponding order for $\varepsilon_1 = 0$ and different choices of ε_2.

Not surprisingly, once the boundary error becomes as small as the parameter ε_2 the boundary error is affected first. On the other hand, the effect on the condition numbers is impressive. Even small boundary parameters lead to a considerable improvement.

N	H	$\|e\|_{L_2(\overline{\Omega})}$	$\|e\|_{L_2(\Omega)}$	$\|e\|_{L_2(\partial\Omega)}$	$\|e\|_{H^1(\overline{\Omega})}$	$\|e\|_{L_\infty(\overline{\Omega})}$	$\mathrm{cond}(\widetilde{A})$
25	2^{-2}	2.13	2.13	2.43	1.38	2.03	-2.06
81	2^{-3}	2.24	2.25	2.00	1.63	1.91	-1.49
289	2^{-4}	2.47	2.48	1.83	1.79	1.55	-1.88
1089	2^{-5}	2.72	2.76	1.65	1.87	1.27	-2.40
4225	2^{-6}	2.71	2.87	1.63	1.75	1.36	-2.14
16641	2^{-7}	2.19	2.45	1.70	1.56	1.45	-2.26

Table 5.2: Convergence orders for the regularised Poisson problem (P2) with basis function $\phi_{2,3}$ and support radii of the form (4.11) for $\nu = 2.4$. The regularisation parameters are $\varepsilon_1 = 0$ and ε_2 =1e-1.

N	H	$\|e\|_{L_2(\overline{\Omega})}$	$\|e\|_{L_2(\Omega)}$	$\|e\|_{L_2(\partial\Omega)}$	$\|e\|_{H^1(\overline{\Omega})}$	$\|e\|_{L_\infty(\overline{\Omega})}$	$\mathrm{cond}(\widetilde{A})$
9	2^{-1}	8.00e-2	8.06e-2	2.17e-2	4.32e-1	1.49e-1	1.5e1
25	2^{-2}	2.09e-2	2.11e-2	4.14e-3	1.59e-1	2.09e-2	1.7e2
81	2^{-3}	4.60e-3	4.63e-3	6.57e-4	4.97e-2	7.73e-3	3.2e3
289	2^{-4}	8.85e-4	8.92e-4	1.04e-5	1.34e-2	1.41e-3	1.5e4
1089	2^{-5}	1.44e-4	1.46e-4	1.84e-5	3.10e-3	2.09e-4	3.7e4
4225	2^{-6}	2.00e-5	2.02e-5	3.19e-6	6.31e-4	3.19e-5	9.0e4
16641	2^{-7}	2.41e-6	2.42e-6	6.02e-7	1.19e-4	6.14e-6	1.9e5

Table 5.3: Convergence study for the regularised Poisson problem (P2) with basis function $\phi_{2,3}$ and support radii of the form (4.11) for $\nu = 2.4$. The regularisation parameters are $\varepsilon_1 = 0$ and ε_2 =1e-3.

N	H	$\|e\|_{L_2(\overline{\Omega})}$	$\|e\|_{L_2(\Omega)}$	$\|e\|_{L_2(\partial\Omega)}$	$\|e\|_{H^1(\overline{\Omega})}$	$\|e\|_{L_\infty(\overline{\Omega})}$	$\mathrm{cond}(\widetilde{A})$
25	2^{-2}	1.94	1.94	2.40	1.44	2.11	-3.47
81	2^{-3}	2.18	2.18	2.65	1.67	2.16	-4.28
289	2^{-4}	2.38	2.38	2.65	1.89	2.45	-2.17
1089	2^{-5}	2.62	2.62	2.50	2.11	2.76	-1.36
4225	2^{-6}	2.85	2.85	2.53	2.30	2.71	-1.27
16641	2^{-7}	3.06	3.06	2.40	2.40	2.38	-1.11

Table 5.4: Convergence orders for the regularised Poisson problem (P2) with basis function $\phi_{2,3}$ and support radii of the form (4.11) for $\nu = 2.4$. The regularisation parameters are $\varepsilon_1 = 0$ and ε_2 =1e-3.

N	H	$\|e\|_{L_2(\overline{\Omega})}$	$\|e\|_{L_2(\Omega)}$	$\|e\|_{L_2(\partial\Omega)}$	$\|e\|_{H^1(\overline{\Omega})}$	$\|e\|_{L_\infty(\overline{\Omega})}$	cond$(\widetilde{A})$
9	2^{-1}	7.98e-2	8.04e-2	2.15e-2	4.31e-1	1.49e-1	1.5e1
25	2^{-2}	2.08e-2	2.10e-2	3.99e-3	1.58e-1	3.45e-2	1.7e2
81	2^{-3}	4.58e-3	4.61e-3	5.81e-4	4.92e-2	7.73e-3	4.6e3
289	2^{-4}	8.80e-4	8.87e-4	6.60e-5	1.32e-2	1.41e-3	7.9e4
1089	2^{-5}	1.44e-4	1.45e-4	6.66e-6	3.02e-3	2.09e-4	9.3e5
4225	2^{-6}	2.00e-5	2.01e-5	7.55e-7	6.09e-4	2.93e-5	4.6e6
16641	2^{-7}	2.41e-6	2.43e-6	1.05e-7	1.13e-4	3.72e-6	1.2e7

Table 5.5: Convergence study for the regularised Poisson problem (P2) with basis function $\phi_{2,3}$ and support radii of the form (4.11) for $\nu = 2.4$. The regularisation parameters are $\varepsilon_1 = 0$ and ε_2 =1e-5.

N	H	$\|e\|_{L_2(\overline{\Omega})}$	$\|e\|_{L_2(\Omega)}$	$\|e\|_{L_2(\partial\Omega)}$	$\|e\|_{H^1(\overline{\Omega})}$	$\|e\|_{L_\infty(\overline{\Omega})}$	cond$(\widetilde{A})$
25	2^{-2}	1.94	1.94	2.43	1.45	2.11	-3.51
81	2^{-3}	2.19	2.19	2.78	1.68	2.16	-4.74
289	2^{-4}	2.38	2.38	3.14	1.90	2.45	-4.12
1089	2^{-5}	2.61	2.61	3.31	2.13	2.75	-3.55
4225	2^{-6}	2.85	2.85	3.14	2.31	2.84	-2.30
16641	2^{-7}	3.05	3.05	2.84	2.43	2.98	-1.43

Table 5.6: Convergence orders for the regularised Poisson problem (P2) with basis function $\phi_{2,3}$ and support radii of the form (4.11) for $\nu = 2.4$. The regularisation parameters are $\varepsilon_1 = 0$ and ε_2 =1e-5.

5.2 Preconditioning the Level Matrices

In this section, we investigate how the condition numbers of the level collocation matrices depend on the support radius as well as the separation distance. Throughout this section, we will use the separation distance rather than the mesh norm since it is more natural in the context of condition numbers. Hence, if we want to have statements on both convergence and conditioning we will implicitly assume that the data sets are quasi-uniform, i.e. that the separation distance and the mesh norm are of comparable size.

In the case of pure interpolation choosing the support radii proportional to the corresponding mesh norms had the positive side effect that the condition numbers of each interpolation matrix could be bounded independently of the level, see Theorem 4.3. Unfortunately, this does not hold for the collocation matrices, where the support radii are no longer proportional to the mesh norms to achieve convergence. Moreover, even if we look at a proportional dependence, the condition numbers of the collocation matrices cannot be bounded independently of the level either. However, in both cases a simple diagonal preconditioner significantly improves the bounds on the condition numbers, see Section 5.2.2.

To simplify the analysis, we will drop the index for the current level. We will continue to use the notation introduced at the beginning of Section 3.1.1. We will denote the interior collocation points by $\mathbf{x}_1, \dots, \mathbf{x}_n \in \Omega$ and the boundary collocation points by $\mathbf{x}_{n+1}, \dots, \mathbf{x}_N \in \partial\Omega$. The set of *all* collocation points will now be denoted by $X = \{\mathbf{x}_1, \dots, \mathbf{x}_N\}$ and its separation distance by q_X. The functionals λ_j are then given by (3.7). Remember that the operator L, which we use to construct the interior functionals, is a second-order strictly elliptic differential operator. The collocation matrix is given by

$$A_\Lambda = (\lambda_j^{\mathbf{x}} \lambda_k^{\mathbf{y}} \Phi_\delta(\mathbf{x} - \mathbf{y})) \in \mathbb{R}^{N \times N}.$$

Since any constant factor in the definition of the scaled basis function will cancel out when it comes to the order of the condition number, from now on, we simply define the scaled basis function by

$$\Phi_\delta := \Phi(\cdot/\delta).$$

for $\delta > 0$.

It will turn out that a linear relationship between support radius and separation distance leads to condition numbers that are not independent of the level – unlike for pure interpolation [87, Theorem 4]. For this reason, we investigate also a simple diagonal preconditioner as suggested in [23].

To follow up the ideas of that paper, we will derive estimates for general scalings and then specify the results for the two specific choices $\delta = cq_X$ (stationary setting) and $\delta = cq_X^{1-2/\sigma}$ (nonstationary setting). While the first choice does not lead to a convergent scheme, it is still interesting in itself since Fasshauer observed that the simple preconditioning strategy leads to level-independent condition numbers, which

we will prove here. The latter choice corresponds to the nonstationary situation for which we proved convergence of the scheme in Theorem 4.10.

In this section, we will follow ideas developed in [85]. In that paper, a Sobolev space $H^\sigma(\mathbb{R}^d)$ was called *feasible* if it contained a compactly supported function Φ satisfying (2.7). This was necessary at that time. Since then, a series of new compactly supported radial basis functions have emerged, so that, for example, it is now known that every $H^\sigma(\mathbb{R}^d)$ with $\sigma \in \mathbb{N}$, $\sigma > \frac{d+1}{2}$ is norm-equivalent to a native space with a compactly supported reproducing kernel, see [14, Corollary 2.5].

In our context, however, we are only working in Sobolev spaces with a compactly supported reproducing kernel, since we are using this kernel to build our approximation spaces. Nonetheless, we will state and prove our stability estimates more generally also for non-compactly supported radial basis functions, as long as they are reproducing kernels to a native space which is norm-equivalent to $H^\sigma(\mathbb{R}^d)$, which is also norm-equivalent to a native space with a compactly supported reproducing kernel.

5.2.1 Condition Number of the Collocation Matrix

We have the following first result.

Theorem 5.7 (Condition Number of Collocation Matrix) *Consider the Sobolev space $H^\sigma(\mathbb{R}^d)$ with $\sigma > d/2 + 2$. Suppose Φ has a Fourier transform which satisfies (2.7). Let $\Phi_\delta = \Phi(\cdot/\delta)$ with $0 < \delta \leq 1$. Suppose L is a linear, strictly elliptic, bounded, second order differential operator. Then, for sufficiently small δ the condition number of the collocation matrix A_Λ can be bounded by*

$$\operatorname{cond}(A_\Lambda) \leq C\delta^{-4}\left(1 + \frac{2\delta}{q_X}\right)^d \left(\frac{\delta}{q_X}\right)^{2\sigma-d},$$

with a constant $C > 0$ independent of X and δ.

Proof. We estimate the smallest and the largest eigenvalue of A_Λ. We first prove for the smallest eigenvalue that

$$\lambda_{\min}(A_\Lambda) \geq C\left(\frac{q_X}{\delta}\right)^{2\sigma-d}$$

holds for a constant $C > 0$ independent of X and δ. Using the functionals λ_j introduced in (3.7), we are done once we can prove that the following bound for the quadratic form exists

$$\boldsymbol{\beta}^T A_\Lambda \boldsymbol{\beta} = \sum_{j,k=1}^{N} \beta_j \beta_k \lambda_j^{\mathbf{x}} \lambda_k^{\mathbf{y}} \Phi_\delta(\mathbf{x} - \mathbf{y}) \geq C\left(\frac{q_X}{\delta}\right)^{2\sigma-d} \|\boldsymbol{\beta}\|_2^2$$

for all $\boldsymbol{\beta} \in \mathbb{R}^N$.

Due to the discussion before the beginning of this section we know there exists a function Ψ with compact support in the unit ball $B(\mathbf{0},1) \subseteq \mathbb{R}^d$, whose Fourier transform satisfies for some $c_1, c_2 > 0$ the decay condition

$$c_1(1+\|\boldsymbol{\omega}\|_2^2)^{-\sigma} \leq \widehat{\Psi}(\boldsymbol{\omega}) \leq c_2(1+\|\boldsymbol{\omega}\|_2^2)^{-\sigma}$$

for all $\boldsymbol{\omega} \in \mathbb{R}^d$. If we set $\Psi_\varepsilon = \Psi(\cdot/\varepsilon)$, it follows for $0 < \varepsilon \leq 1$ that

$$\widehat{\Psi_\varepsilon}(\boldsymbol{\omega}) = \varepsilon^d \widehat{\Psi}(\varepsilon\boldsymbol{\omega}) \leq c_2\varepsilon^d(1+\|\varepsilon\boldsymbol{\omega}\|_2^2)^{-\sigma} \leq c_2\varepsilon^{d-2\sigma}(1+\|\boldsymbol{\omega}\|_2^2)^{-\sigma}.$$

Combining this result with (2.7), we obtain

$$\widehat{\Phi}(\boldsymbol{\omega}) \geq \frac{c_1(\Phi)}{c_2(\Psi)}\varepsilon^{2\sigma-d}\widehat{\Psi_\varepsilon}(\boldsymbol{\omega}). \tag{5.9}$$

Now we compute by Theorem 1.3

$$\begin{aligned}
\boldsymbol{\beta}^T A_\Lambda \boldsymbol{\beta} &= \sum_{j,k=1}^N \beta_j\beta_k\lambda_j^{\mathbf{x}}\lambda_k^{\mathbf{y}}\Phi_\delta(\mathbf{x}-\mathbf{y}) \\
&= \frac{1}{(2\pi)^{d/2}}\sum_{j,k=1}^N \beta_j\beta_k\lambda_j^{\mathbf{x}}\lambda_k^{\mathbf{y}}\int_{\mathbb{R}^d}\widehat{\Phi_\delta}(\boldsymbol{\omega})e^{i(\mathbf{x}-\mathbf{y})^T\boldsymbol{\omega}}d\boldsymbol{\omega} \\
&= \frac{1}{(2\pi)^{d/2}}\sum_{j,k=1}^N \delta^d\beta_j\beta_k\lambda_j^{\mathbf{x}}\lambda_k^{\mathbf{y}}\int_{\mathbb{R}^d}\widehat{\Phi}(\delta\boldsymbol{\omega})e^{i(\mathbf{x}-\mathbf{y})^T\boldsymbol{\omega}}d\boldsymbol{\omega} \\
&= \frac{1}{(2\pi)^{d/2}}\sum_{j,k=1}^N \beta_j\beta_k\lambda_j^{\mathbf{x}}\lambda_k^{\mathbf{y}}\int_{\mathbb{R}^d}\widehat{\Phi}(\boldsymbol{\eta})e^{i(\mathbf{x}-\mathbf{y})^T\boldsymbol{\eta}/\delta}d\boldsymbol{\eta} \\
&= \frac{1}{(2\pi)^{d/2}}\int_{\mathbb{R}^d}\widehat{\Phi}(\boldsymbol{\eta})\left|\sum_{j=1}^N \beta_j\lambda_j^{\mathbf{x}}e^{i\frac{\mathbf{x}^T\boldsymbol{\eta}}{\delta}}\right|^2 d\boldsymbol{\eta}.
\end{aligned}$$

Using estimate (5.9), we can derive the bound:

$$\begin{aligned}
\boldsymbol{\beta}^T A_\Lambda \boldsymbol{\beta} &\geq \frac{1}{(2\pi)^{d/2}} \frac{c_1(\Phi)}{c_2(\Psi)} \varepsilon^{2\sigma-d} \int_{\mathbb{R}^d} \widehat{\Psi_\varepsilon}(\boldsymbol{\eta}) \left| \sum_{j=1}^N \beta_j \lambda_j^{\mathbf{x}} e^{i\frac{\mathbf{x}^T\boldsymbol{\eta}}{\delta}} \right|^2 d\boldsymbol{\eta} \\
&= \frac{1}{(2\pi)^{d/2}} \frac{c_1(\Phi)}{c_2(\Psi)} \varepsilon^{2\sigma-d} \sum_{j,k=1}^N \beta_j \beta_k \lambda_j^{\mathbf{x}} \lambda_k^{\mathbf{y}} \int_{\mathbb{R}^d} \widehat{\Psi_\varepsilon}(\boldsymbol{\eta}) e^{i\frac{(\mathbf{x}-\mathbf{y})^T\boldsymbol{\eta}}{\delta}} d\boldsymbol{\eta} \\
&= \frac{1}{(2\pi)^{d/2}} \frac{c_1(\Phi)}{c_2(\Psi)} \varepsilon^{2\sigma-d} \delta^d \sum_{j,k=1}^N \beta_j \beta_k \lambda_j^{\mathbf{x}} \lambda_k^{\mathbf{y}} \int_{\mathbb{R}^d} \widehat{\Psi_\varepsilon}(\delta\boldsymbol{\omega}) e^{i(\mathbf{x}-\mathbf{y})^T\boldsymbol{\omega}} d\boldsymbol{\omega} \\
&= \frac{1}{(2\pi)^{d/2}} \frac{c_1(\Phi)}{c_2(\Psi)} (\varepsilon\delta)^d \varepsilon^{2\sigma-d} \sum_{j,k=1}^N \beta_j \beta_k \lambda_j^{\mathbf{x}} \lambda_k^{\mathbf{y}} \int_{\mathbb{R}^d} \widehat{\Psi}(\varepsilon\delta\boldsymbol{\omega}) e^{i(\mathbf{x}-\mathbf{y})^T\boldsymbol{\omega}} d\boldsymbol{\omega} \\
&= \frac{1}{(2\pi)^{d/2}} \frac{c_1(\Phi)}{c_2(\Psi)} \varepsilon^{2\sigma-d} \sum_{j,k=1}^N \beta_j \beta_k \lambda_j^{\mathbf{x}} \lambda_k^{\mathbf{y}} \int_{\mathbb{R}^d} \widehat{\Psi_{\varepsilon\delta}}(\boldsymbol{\omega}) e^{i(\mathbf{x}-\mathbf{y})^T\boldsymbol{\omega}} d\boldsymbol{\omega} \\
&= \frac{c_1(\Phi)}{c_2(\Psi)} \varepsilon^{2\sigma-d} \sum_{j,k=1}^N \beta_j \beta_k \lambda_j^{\mathbf{x}} \lambda_k^{\mathbf{y}} \Psi_{\varepsilon\delta}(\mathbf{x}-\mathbf{y}).
\end{aligned}$$

If we choose $\varepsilon\delta = q_X$, we only sum over diagonal elements. Thus we find

$$\boldsymbol{\beta}^T A_\Lambda \boldsymbol{\beta} \geq \frac{c_1(\Phi)}{c_2(\Psi)} \left(\frac{q_X}{\delta}\right)^{2\sigma-d} \left\{ \sum_{j=1}^n \beta_j^2 \lambda_j^{\mathbf{x}} \lambda_j^{\mathbf{y}} \Psi_{q_X}(\mathbf{x}-\mathbf{y}) + \sum_{j=n+1}^N \beta_j^2 \Psi_{q_X}(\mathbf{0}) \right\}. \quad (5.10)$$

Let us have a closer look at the first sum. For $1 \leq m \leq n$ we compute

$$\begin{aligned}
\lambda_m^{\mathbf{x}} \lambda_m^{\mathbf{y}} \Psi_{q_X}(\mathbf{x}-\mathbf{y}) = q_X^{-4} &\sum_{i,j=1}^d \sum_{k,\ell=1}^d a_{ij}(\mathbf{x}_m) a_{k\ell}(\mathbf{x}_m) \frac{\partial^4 \Psi(\mathbf{0})}{\partial x_i \partial x_j \partial x_k \partial x_\ell} \\
&+ q_X^{-2} \sum_{i,j=1}^d \left[2a_{ij}(\mathbf{x}_m) c(\mathbf{x}_m) - b_i(\mathbf{x}_m) b_j(\mathbf{x}_m) \right] \frac{\partial^2 \Psi(\mathbf{0})}{\partial x_i \partial x_j} \\
&+ c(\mathbf{x}_m)^2 \Psi(\mathbf{0}).
\end{aligned}$$

For the first term on the right-hand side, note that expressing the derivatives using

the inverse Fourier transform and then the strict ellipticity of the operator yields

$$\begin{aligned}
&\sum_{i,j=1}^{d}\sum_{k,\ell=1}^{d} a_{ij}(\mathbf{x}_m)a_{k\ell}(\mathbf{x}_m)\frac{\partial^4\Psi(\mathbf{0})}{\partial x_i\partial x_j\partial x_k\partial x_\ell}\\
&\qquad= \frac{1}{(2\pi)^{d/2}}\int_{\mathbb{R}^d}\widehat{\Psi}(\boldsymbol{\omega})\left(\sum_{i,j=1}^{d} a_{ij}(\mathbf{x}_m)\omega_i\omega_j\right)\left(\sum_{k,\ell=1}^{d} a_{k\ell}(\mathbf{x}_m)\omega_j\omega_k\right)d\boldsymbol{\omega}\\
&\qquad\geq \frac{c_E^2}{(2\pi)^{d/2}}\int_{\mathbb{R}^d}\|\boldsymbol{\omega}\|_2^4\widehat{\Psi}(\boldsymbol{\omega})d\boldsymbol{\omega}\\
&\qquad\geq \frac{c_E^2 c_1(\Psi)}{(2\pi)^{d/2}}\int_{\mathbb{R}^d}\|\boldsymbol{\omega}\|_2^4(1+\|\boldsymbol{\omega}\|_2^2)^{-\sigma}d\boldsymbol{\omega}\\
&\qquad=: C_1 > 0.
\end{aligned}$$

Note that the last integral is indeed finite since $\sigma > d/2+2$. We introduce the abbreviations

$$A := \max_{1\leq i,j\leq d}\|a_{ij}\|_{L_\infty(\Omega)},\quad B := \max_{1\leq k\leq d}\|b_k\|_{L_\infty(\Omega)}\quad\text{and}\quad C := \|c\|_{L_\infty(\Omega)}.$$

Using the inverse triangle inequality, the previous estimates and the boundedness of the coefficients, we obtain

$$\begin{aligned}
&|\lambda_m^{\mathbf{x}}\lambda_m^{\mathbf{y}}\Psi_{q_X}(\mathbf{x}-\mathbf{y})|\\
&\qquad\geq q_X^{-4}C_1 - q_X^{-2}d^2\max_{1\leq i,j\leq d}\left|\frac{\partial^2}{\partial x_i\partial x_j}\Psi(\mathbf{0})\right|\left[2AC+B^2\right] - C\Psi(\mathbf{0}).
\end{aligned}$$

Note that here A denotes a scalar while A_Λ denotes the collocation matrix. For sufficiently small q_X the leading term dominates the rest and we can derive

$$|\lambda_m^{\mathbf{x}}\lambda_m^{\mathbf{y}}\Psi_{q_X}(\mathbf{x}-\mathbf{y})| \geq \widetilde{C_1}q_X^{-4} \tag{5.11}$$

with a $\widetilde{C_1} > 0$, which remains true for all $q_X \in (0,1)$.

Thus, using $\Psi_{q_X}(\mathbf{0}) = \Psi(\mathbf{0})$ and putting everything together we have for q_X small enough

$$\begin{aligned}
\boldsymbol{\beta}^T A_\Lambda\boldsymbol{\beta} &\geq \frac{c_1(\Phi)}{c_2(\Psi)}\min\{\Psi(\mathbf{0}),\widetilde{C_1}q_X^{-4}\}\left(\frac{q_X}{\delta}\right)^{2\sigma-d}\|\boldsymbol{\beta}\|_2^2\\
&= C\Psi(\mathbf{0})\left(\frac{q_X}{\delta}\right)^{2\sigma-d}\|\boldsymbol{\beta}\|_2^2.
\end{aligned}$$

Next, we will investigate the largest eigenvalue $\lambda_{\max} = \lambda_{\max}(A_\Lambda)$ of the collocation matrix. The Gershgorin theorem asserts that we can find at least one index j such that

$$|\lambda_{\max} - \lambda_j^{\mathbf{x}}\lambda_j^{\mathbf{y}}\Phi_\delta(\mathbf{x}-\mathbf{y})| \leq \sum_{\substack{k=1\\k\neq j}}^{N}|\lambda_j^{\mathbf{x}}\lambda_k^{\mathbf{y}}\Phi_\delta(\mathbf{x}-\mathbf{y})|$$

holds, which yields by the inverse triangle inequality for the modulus

$$|\lambda_{\max}| \leq \sum_{k=1}^{N} |\lambda_j^{\mathbf{x}} \lambda_k^{\mathbf{y}} \Phi_\delta(\mathbf{x}-\mathbf{y})|.$$

Now bearing in mind that Φ_δ has support in the ball $B(\mathbf{0},\delta)$, we notice that some of the terms vanish. More precisely we only need to sum over the amount of nonzero entries in the j^{th} row

$$n_j := |\{k \in \mathbb{N} \colon \|\mathbf{x}_j - \mathbf{x}_k\|_2 < \delta\}|\,.$$

In order to find an upper bound on n_j, we define balls with radius $q_X/2$ and centre $\mathbf{x}_k$

$$B(\mathbf{x}_k, q_X/2) = \{\mathbf{x} \in \mathbb{R}^d \colon \|\mathbf{x}-\mathbf{x}_k\|_2 < q_X/2\}.$$

If we only consider k taken from the index set

$$I_j = \{\ell \in \mathbb{N} \colon \|\mathbf{x}_j - \mathbf{x}_\ell\|_2 < \delta\},$$

the balls $B(\mathbf{x}_k, q_X/2)$ are disjoint from one another and

$$\bigcup_{k \in I_j} B(\mathbf{x}_k, q_X/2) \subseteq B(\mathbf{x}_j, \delta + q_X/2).$$

Thus, we can conclude

$$\begin{aligned} n_j (q_X/2)^d \operatorname{vol}(B(\mathbf{0},1)) &= \sum_{k \in I_j} \operatorname{vol}(B(\mathbf{x}_k, q_X/2)) = \operatorname{vol}\left(\bigcup_{k \in I_j} B(\mathbf{x}_k, q_X/2)\right) \\ &\leq \operatorname{vol}(B(\mathbf{x}_j, \delta + q_X/2)) = (\delta + q_X/2)^d \operatorname{vol}(B(\mathbf{0},1))\,. \end{aligned}$$

This leads to the estimate

$$n_j \leq \left(\frac{\delta + q_X/2}{q_X/2}\right)^d = \left(1 + \frac{2\delta}{q_X}\right)^d.$$

Now we can bound the largest eigenvalue by

$$\begin{aligned} |\lambda_{\max}| &\leq \sum_{k=1}^{N} |\lambda_j^{\mathbf{x}} \lambda_k^{\mathbf{y}} \Phi_\delta(\mathbf{x}-\mathbf{y})| \\ &\leq n_j \max_{1 \leq k \leq N} \left\{|\lambda_j^{\mathbf{x}} \lambda_k^{\mathbf{y}} \Phi_\delta(\mathbf{x}-\mathbf{y})|\right\} \\ &\leq \left(1 + \frac{2\delta}{q_X}\right)^d \max\left\{\Phi(\mathbf{0}), \delta^{-2}|L\Phi(\mathbf{0})|, \delta^{-4}|L^2\Phi(\mathbf{0})|\right\}. \end{aligned} \tag{5.12}$$

That is, for sufficiently small support radius δ, the largest eigenvalue can be bounded by

$$|\lambda_{\max}| \leq C\delta^{-4}\left(1+\frac{2\delta}{q_X}\right)^d$$

for some $C > 0$ which is independent of X and δ. Combining the results for the smallest and the largest eigenvalue we find for the condition number

$$\mathrm{cond}(A_\Lambda) = \frac{\lambda_{\max}(A_\Lambda)}{\lambda_{\min}(A_\Lambda)} \leq C\delta^{-4}\left(1+\frac{2\delta}{q_X}\right)^d\left(\frac{\delta}{q_X}\right)^{2\sigma-d}$$

for some $C > 0$ which is independent of X and δ. □

The proof of the previous theorem shows in particular that the asymptotic behaviour of the largest eigenvalue is dictated by the differential operator. On the other hand, the behaviour of the smallest eigenvalue is dictated by the boundary operator, the identity. As a consequence of this general result, we can now discuss the two cases $\delta = cq_X$ and $\delta = cq_X^{1-2/\sigma}$.

Corollary 5.8 *1. In the stationary setting $\delta = cq_X$, where the support radius is proportional to the separation distance, the condition number of the collocation matrix can be bounded by*

$$\mathrm{cond}(A_\Lambda) \leq C\delta^{-4} = Cq_X^{-4}.$$

2. In the nonstationary setting $\delta = cq_X^{1-2/\sigma}$, where the support radius tends to zero more slowly than the separation distance, the condition number of the collocation matrix can be bounded by

$$\mathrm{cond}(A_\Lambda) \leq C\delta^{-4}q_X^{-4} = Cq_X^{-8+\frac{8}{\sigma}}.$$

Even though the collocation method does not converge for the first relationship, it still serves as an important reference case. A condition number growing like q^{-4} for a symmetric collocation matrix is not unexpected since we apply a second order differential operator to the kernel twice. The growth of the condition number in the nonstationary setting, however, is unacceptable since we need $\sigma = d/2 + 2$. Hence, in the next section, we will discuss a simple, but nonetheless to a certain extent successful, preconditioning technique.

5.2.2 Diagonal Preconditioner

In [23], it was suggested that one reason for the ill-conditioning was the different scaling of the different parts of the collocation matrix with respect to the support radius. While the diagonal part corresponding to the inner points scales like $\mathcal{O}(\delta^{-4})$,

the diagonal part corresponding to the boundary points scales like $\mathcal{O}(1)$ and the off-diagonal entries scale like $\mathcal{O}(\delta^{-2})$.

An easy way of resolving this problem is to employ a diagonal preconditioner. Hence, we define the diagonal matrix $P = (p_{jk})_{1\le j,k\le N}$ by

$$\begin{cases} p_{jk} = 0 & j \neq k \\ p_{jj} = p_j = \delta^2 & 1 \le j \le n \\ p_{jj} = p_j = 1 & n+1 \le j \le N. \end{cases} \tag{5.13}$$

This preconditioner leads to notably better condition numbers.

Theorem 5.9 (Condition Number of Preconditioned Collocation Matrix) *Consider the Sobolev space $H^\sigma(\mathbb{R}^d)$ with $\sigma > d/2 + 2$. Suppose Φ has a Fourier transform which satisfies (2.7). Let $\Phi_\delta = \Phi(\cdot/\delta)$ with $0 < \delta \le 1$. Suppose L is a linear, strictly elliptic, bounded, second order differential operator. Assume that $q_X \le \delta$. Then, for sufficiently small δ and q_X, the condition number of the preconditioned collocation matrix can be bounded by*

$$\operatorname{cond}(PA_\Lambda P) \le C \left(1 + \frac{2\delta}{q_X}\right)^d \left(\frac{\delta}{q_X}\right)^{2\sigma-d}$$

with a constant $C > 0$ independent of X, q_X and δ.

Proof. Once again, we estimate the smallest and the largest eigenvalue of the matrix, which this time is given by $PA_\Lambda P$. Noting that

$$\boldsymbol{\beta}^T PA_\Lambda P\boldsymbol{\beta} = \sum_{j,k=1}^N (p_j\beta_j)(p_k\beta_k)\lambda_j^{\mathbf{x}}\lambda_k^{\mathbf{y}}\Phi_\delta(\mathbf{x}-\mathbf{y}),$$

we can directly use most of the computations from the proof of Theorem 5.7.

First of all, if we follow the initial steps to estimate the smallest eigenvalue, (5.10) becomes

$$\begin{aligned} &\boldsymbol{\beta}^T PA_\Lambda P\boldsymbol{\beta} \\ &\quad \ge \frac{c_1(\Phi)}{c_2(\Psi)} \left(\frac{q_X}{\delta}\right)^{2\sigma-d} \left\{ \sum_{j=1}^n p_j^2\beta_j^2\lambda_j^{\mathbf{x}}\lambda_j^{\mathbf{y}}\Psi_{q_X}(\mathbf{x}-\mathbf{y}) + \sum_{j=n+1}^N p_j^2\beta_j^2\Psi_{q_X}(\mathbf{0}) \right\}. \end{aligned}$$

As done previously, we have a closer look at the first sum. Taking into account that we have here $p_j = \delta^2$, we can conclude for $1 \le m \le n$ that

$$\begin{aligned} p_m^2\lambda_m^{\mathbf{x}}\lambda_m^{\mathbf{y}}\Psi_{q_X}(\mathbf{x}-\mathbf{y}) = \left(\frac{\delta}{q_X}\right)^4 &\sum_{i,j=1}^d \sum_{k,\ell=1}^d a_{ij}(\mathbf{x}_m)a_{k\ell}(\mathbf{x}_m) \frac{\partial^4\Psi(\mathbf{0})}{\partial x_i\partial x_j\partial x_k\partial x_\ell} \\ &+ \delta^4 q_X^{-2} \sum_{i,j=1}^d \left[2a_{ij}(\mathbf{x}_m)c(\mathbf{x}_m) - b_i(\mathbf{x}_m)b_j(\mathbf{x}_m)\right] \frac{\partial^2\Psi(\mathbf{0})}{\partial x_i\partial x_j} \\ &+ \delta^4 c(\mathbf{x}_m)^2\Psi(0), \end{aligned}$$

which then leads to the bound

$$p_m^2 |\lambda_m^{\mathbf{x}} \lambda_m^{\mathbf{y}} \Psi_{q_X}(\mathbf{x}-\mathbf{y})| \geq C_1 \left(\frac{\delta}{q_X}\right)^4 - C_2 \delta^2 \left[\left(\frac{\delta}{q_X}\right)^2 + \delta^2\right].$$

If both δ and q_X go to zero, this leads eventually to a bound of the form

$$p_m^2 |\lambda_m^{\mathbf{x}} \lambda_m^{\mathbf{y}} \Psi_{q_X}(\mathbf{x}-\mathbf{y})| \geq \widetilde{C}_1 \left(\frac{\delta}{q_X}\right)^4 \geq \widetilde{C}_1$$

since we assumed $\delta/q_X \geq 1$, which means that δ must not go to zero faster than q_X. In this situation, we find for the quadratic form

$$\begin{aligned}\sum_{j,k=1}^{N} p_j p_k \beta_j \beta_k \lambda_j^{\mathbf{x}} \lambda_k^{\mathbf{y}} \Phi_\delta(\mathbf{x}-\mathbf{y}) &\geq \frac{c_1(\Phi)}{c_2(\Psi)} \min\{\Psi(\mathbf{0}), \widetilde{C_1}\} \left(\frac{q_X}{\delta}\right)^{2\sigma-d} \|\boldsymbol{\beta}\|_2^2 \\ &= C \left(\frac{q_X}{\delta}\right)^{2\sigma-d} \|\boldsymbol{\beta}\|_2^2,\end{aligned}$$

and hence for the smallest eigenvalue:

$$\lambda_{\min}(P A_\Lambda P) \geq C \left(\frac{q_X}{\delta}\right)^{2\sigma-d}.$$

The investigation of the largest eigenvalue $\lambda_{\max} = \lambda_{\max}(P A_\Lambda P)$ is again done as in the proof of Theorem 5.7. Hence, equation (5.12) now becomes

$$\begin{aligned}|\lambda_{\max}| &\leq \sum_{k=1}^{N} p_j p_k |\lambda_j^{\mathbf{x}} \lambda_k^{\mathbf{y}} \Phi_\delta(\mathbf{x}-\mathbf{y})| \\ &\leq n_j \max_{1\leq k\leq N} \left\{p_j p_k |\lambda_j^{\mathbf{x}} \lambda_k^{\mathbf{y}} \Phi_\delta(\mathbf{x}-\mathbf{y})|\right\} \\ &\leq \left(1+\frac{2\delta}{q_X}\right)^d \max_{1\leq k\leq N} \left\{p_j p_k |\lambda_j^{\mathbf{x}} \lambda_k^{\mathbf{y}} \Phi_\delta(\mathbf{x}-\mathbf{y})|\right\}.\end{aligned}$$

We need to distinguish three cases to bound the maximum: Both indices j and k lie between 1 and n, only one of them does and neither of them does. In the first case, since $\Phi \in C^4(\mathbb{R}^d)$ we find a constant $c_{LL} > 0$ such that

$$\begin{aligned}&|\lambda_j^{\mathbf{x}} \lambda_k^{\mathbf{y}} \Phi_\delta(\mathbf{x}-\mathbf{y})| \\ &\quad\leq \delta^{-4} \left| \sum_{\ell,m=1}^{d} \sum_{r,s=1}^{d} a_{\ell m}(\mathbf{x}_j) a_{rs}(\mathbf{x}_k) \frac{\partial^4 \Phi((\mathbf{x}_j-\mathbf{x}_k)/\delta)}{\partial x_\ell \partial x_m \partial x_r \partial x_s} \right| + \mathcal{O}(\delta^{-3}) \\ &\quad\leq \delta^{-4} c_{LL} + \mathcal{O}(\delta^{-3}).\end{aligned}$$

Similarly, in the second case, we find a constant $c_L > 0$ such that

$$|\lambda_j^{\mathbf{x}} \lambda_k^{\mathbf{y}} \Phi_\delta(\mathbf{x} - \mathbf{y})| \leq \delta^{-2} c_L + \mathcal{O}(\delta^{-1}).$$

In the third case, we just need to remember that $|\Phi(\mathbf{x})| \leq \Phi(\mathbf{0})$ for all $\mathbf{x} \in \mathbb{R}^d$, i. e.

$$|\lambda_j^{\mathbf{x}} \lambda_k^{\mathbf{y}} \Phi_\delta(\mathbf{x} - \mathbf{y})| = |\Phi_\delta(\mathbf{x}_j - \mathbf{x}_k)| \leq \Phi(\mathbf{0}).$$

All three bounds on $|\lambda_j^{\mathbf{x}} \lambda_k^{\mathbf{y}} \Phi_\delta(\mathbf{x} - \mathbf{y})|$ are independent of the indices j and k. Thus, we find

$$\begin{aligned}
&|\lambda_{\max}| \\
&\leq \left(1 + \frac{2\delta}{q_X}\right)^d \max\left\{\Phi(\mathbf{0}), \delta^2\left[\delta^{-2} c_L + \mathcal{O}(\delta^{-1})\right], \delta^4\left[\delta^{-4} c_{LL} + \mathcal{O}(\delta^{-3})\right]\right\} \\
&= \left(1 + \frac{2\delta}{q_X}\right)^d \max\left\{\Phi(\mathbf{0}), c_L + \mathcal{O}(\delta), c_{LL} + \mathcal{O}(\delta)\right\}.
\end{aligned}$$

That is, for a sufficiently small support radius δ, the largest eigenvalue can be bounded by

$$|\lambda_{\max}| \leq C\left(1 + \frac{2\delta}{q_X}\right)^d$$

for some $C > 0$ which is independent of X and $\delta \in (0, 1]$. Combining the result for the smallest and the largest eigenvalue we find for the condition number

$$\operatorname{cond}(P A_\Lambda P) = \frac{\lambda_{\max}(P A_\Lambda P)}{\lambda_{\min}(P A_\Lambda P)} \leq C\left(1 + \frac{2\delta}{q_X}\right)^d \left(\frac{\delta}{q_X}\right)^{2\sigma - d}$$

for some $C > 0$ which is independent of X and δ. □

As before, we take a closer look at the two cases $\delta = c q_X$ and $\delta = c q_X^{1-2/\sigma}$. In both cases we can assume that $q_X \leq \delta$ such that we can apply the theorem.

Corollary 5.10 *1. In the stationary setting $\delta = c q_X$, where the support radius is proportional to the separation distance, the condition number of the collocation matrix can be bounded by*

$$\operatorname{cond}(P A_\Lambda P) \leq C.$$

2. In the nonstationary setting $\delta = c q_X^{1-2/\sigma}$, where the support radius tends to zero more slowly than the separation distance, the condition number of the collocation matrix can be bounded by

$$\operatorname{cond}(P A_\Lambda P) \leq C q_X^{-4}.$$

Hence, through the proposed diagonal preconditioner we were able to improve the condition numbers considerably. Whereas they became independent of the scale for the stationary setting, they became at least independent of the smoothness index of the Sobolev space σ for the nonstationary setting. In the latter case, the exponent reflects the fact that we apply the second-order differential operator twice.

N	h	$\kappa(A)$	order	$\kappa(PAP)$	order	$\kappa(\widetilde{P}A\widetilde{P})$	order
5	2^{-3}	5.3e1	—	4.4e3	—	8.9e0	—
9	2^{-4}	1.9e2	-1.83	6.7e3	-0.62	1.8e1	-1.02
17	2^{-5}	7.6e2	-2.00	1.1e4	-0.72	5.2e1	-1.53
33	2^{-6}	3.1e3	-2.04	1.9e4	-0.75	1.5e2	-1.55
65	2^{-7}	1.2e4	-1.98	3.0e4	-0.67	4.2e2	-1.46
129	2^{-8}	5.6e4	-2.17	5.4e4	-0.86	1.3e3	-1.60
257	2^{-9}	2.6e5	-2.22	1.0e5	-0.92	3.9e3	-1.60
513	2^{-10}	1.3e6	-2.32	2.1e5	-1.04	1.1e4	-1.53
1025	2^{-11}	6.5e6	-2.34	4.5e5	-1.12	3.4e4	-1.59
2049	2^{-12}	3.1e7	-2.25	9.6e5	-1.08	7.6e4	-1.17

Table 5.7: Condition numbers and their orders for the multilevel algorithm applied to Laplace problem (L1) on uniform grids for a basis function $\phi_{1,2}$ and proportionality constant $\nu = 5$.

N	$\kappa(A)$	order	$\kappa(PAP)$	order	$\kappa(\widetilde{P}A\widetilde{P})$	order
9	1.5e+03	—	2.2e+04	—	1.5e+01	—
25	1.0e+05	-6.12	3.4e+05	-3.93	1.7e+02	-3.51
81	2.3e+07	-7.78	1.6e+07	-5.57	4.6e+03	-4.74
289	2.3e+09	-6.65	3.4e+08	-4.43	8.3e+04	-4.18
1089	1.7e+11	-6.25	5.6e+09	-4.03	1.4e+06	-4.01
4225	1.3e+13	-6.21	8.9e+10	-3.99	2.1e+07	-3.98
16641	9.5e+14	-6.21	1.4e+12	-3.99	3.4e+08	-3.99
66049	7.1e+16	-6.22	2.3e+13	-3.99	5.4e+09	-3.99

Table 5.8: Condition numbers and their orders for the multilevel algorithm applied to Poisson problem (P2) on uniform grids.

5.2.3 Numerical Examples

We verify the theoretical results for diagonal preconditioners for the previously studied numerical problems (L1) and (P2) from Chapter 4. There have been studies by Fasshauer [23] as well.

We have computed the condition number of the unpreconditioned matrix, $\kappa(A)$ and the corresponding order as well as the condition number of the preconditioned matrix $\kappa(PAP)$ and its order. In the latter case, the actual condition number can further be reduced by using a slightly changed preconditioner $\widetilde{P}$, which is also a diagonal matrix. This time, however, the diagonal entries are given by $p_j = 1/\sqrt{a_{jj}}$. Note that the analysis given in Theorems 5.7 and 5.9 remains valid since this preconditioner differs from the other one just by constant factors. Thus, the order achieved by this preconditioner remains the same as the order achieved by the other one.

The theoretical results from Corollaries 5.8 and 5.10 suggest that the condition

number of the collocation matrix should behave for the one-dimensional Laplace problem (L1) like $q_X^{-8+8/\sigma} = q_X^{-5.\overline{3}}$ since $\sigma = 3$ for the basis function $\Phi_{1,2}$. For the two-dimensional Poisson problem (P2), we expect the behaviour $q_X^{-8+8/\sigma} = q_X^{-6.\overline{2}}$ since $\sigma = 4.5$ for the basis function $\Phi_{2,3}$. In both cases the condition numbers of the diagonally preconditioned collocation matrices should not grow faster than q_X^{-4}.

Table 5.7 shows the results of our computation for the one-dimensional Laplace problem (L1) and Table 5.8 for the two-dimensional Poisson problem (P2). For the one-dimensional problem the condition numbers seem to be better than the bound. For the two dimensional problem, however, they behave according to the bound.

5.3 Combining Regularisation and Preconditioning

In this section, we briefly discuss how smoothing and preconditioning can be combined. We will first precondition and then regularise the system. In theory it is also possible to do it the other way around but then the analysis becomes harder. We will highlight two important special cases, that reduce to regularisation with various penalty parameters. Therefore, the theory of Section 5.1 applies.

Suppose we want to precondition the system

$$A\widetilde{\boldsymbol{\alpha}} = \mathbf{f}$$

with a symmetric and invertible preconditioner $M = M^T$ in the following way

$$MAM\left(M^{-1}\widetilde{\boldsymbol{\alpha}}\right) = M\mathbf{f}$$

and then smooth it with one regularisation parameter $\varepsilon > 0$, i. e. we need to solve

$$(MAM + \varepsilon I)\left(M^{-1}\boldsymbol{\alpha}\right) = M\mathbf{f}.$$

Then premultiplying the equation with M^{-1} shows

$$\left(A + \varepsilon M^{-2}\right)\boldsymbol{\alpha} = \mathbf{f}$$

and the combined problem reduces to a regularisation problem with regularisation matrix $P = M$, see Theorem 5.2. Whereas the second to last equation is more useful from a numerical point of view since the condition number of $MAM + \varepsilon I$ is hopefully low, the last equation helps us to interpret the condition.

Lemma 5.11 *Preconditioning and regularisation with one parameter reduces to generalised regularisation from Section 5.1.*

Let us assume we want to regularise a preconditioned system with an arbitrary diagonal smoothing matrix, for example

$$\widetilde{P} = \operatorname{diag}(\widetilde{\varepsilon}_1, \ldots, \widetilde{\varepsilon}_N),$$

with some $\widetilde{\varepsilon}_i > 0$, that is we want to solve

$$\left(MAM + \widetilde{P}\right)\left(M^{-1}\boldsymbol{\alpha}\right) = M\mathbf{f}.$$

If we additionally assume that M is diagonal and defined through

$$M^{-1} = \operatorname{diag}(\kappa_1, \ldots, \kappa_N)$$

then the combined problem is equivalent to solving

$$\left(A + \operatorname{diag}(\widetilde{\varepsilon}_1\kappa_1^2, \ldots, \widetilde{\varepsilon}_N\kappa_N^2)\right)\boldsymbol{\alpha} = \mathbf{f}.$$

This implies that the combined problem reduces to a regularisation problem with diagonal smoothing matrix with entries $\varepsilon_i = \widetilde{\varepsilon}_i\kappa_i^2$, see Corollary 5.3. Again, we summarise this thought.

Lemma 5.12 *Preconditioning with a diagonal matrix and diagonal regularisation with several parameters is equivalent to diagonal regularisation (with a different regularisation matrix).*

Hence, if we want to have an additional benefit through the combination of preconditioning and regularisation, we need to look at more sophisticated preconditioners.

5.4 Alternating Projection Method

In this section, we discuss another approach to overcome the growing condition numbers of the linear systems that arise in the multilevel collocation algorithm. The key idea is to reduce the computational work by approximating the collocation interpolant by splitting it into its interior and boundary part. Instead of solving a block system once, one then has to solve two systems (several times). The splitting is achieved by adapting the rather general alternating projection algorithm. We need the abstract notion of an angle between closed subspaces of a Hilbert space.

The angle between two closed subspaces U_1 and U_2 of a Hilbert space H is given by

$$\cos\alpha := \sup\left\{(u,v) | u \in U_1 \cap U^\perp, v \in U_2 \cap U^\perp, \|u\|, \|v\| \leq 1\right\},$$

where $U := U_1 \cap U_2$. Smith, Solomon and Wagner proved the following convergence result, [76, Theorem 2.2].

Theorem 5.13 (Alternating Projection Method in Hilbert Spaces) *Suppose we are given orthogonal projections $\mathcal{Q}_1, \ldots, \mathcal{Q}_k$ onto closed subspaces $U_1, \ldots, U_k$ of a Hilbert space H with norm $\|\cdot\| = (\cdot,\cdot)^{1/2}$. Define $U := \bigcap_{j=1}^k U_j$ and let $\mathcal{Q}\colon H \to U$ be the orthogonal projection onto U. Finally, let α_j be the angle between the U_j and $A_j := \bigcap_{i=j+1}^k U_i$. Then for any $f \in H$*

$$\|(\mathcal{Q}_k \ldots \mathcal{Q}_1)^\ell f - \mathcal{Q}f\| \leq c^\ell \|f - \mathcal{Q}f\|,$$

where

$$c \leq \left(1 - \prod_{j=1}^{k-1} \sin^2 \alpha_j\right)^{1/2}. \tag{5.14}$$

We remark that two extreme cases are possible. On the one hand, if all angles are $\pi/2$, then the constant c is zero. In this case, however, we do not have to prove anything. Therefore, we exclude this case. On the other hand, we have the more critical case that one of the angles is zero, which means the constant c is one. In this case, we cannot expect convergence. However, in the particular case we are interested in here, it is possible to show that we have indeed $c < 1$.

Smith et al. applied the general Hilbert space result to computed tomography. Beatson, Billings and Light [2] were the first ones to adapt the algorithm to RBF interpolation. They, however, needed some moderate assumptions on the point sets, which are automatically satisfied when adapting the theory to multilevel RBF collocation. Wendland then extended their result to generalised interpolation in [83]. We study collocation here. Though the algorithm converges theoretically, in practice the convergence is rather slow.

5.4.1 One-Shot Projection Collocation Method

For the one-shot projection collocation method, we consider the two projections

$$\begin{aligned} \mathcal{P}_L &: \mathcal{N}_\Phi(\mathbb{R}^d) \to LV_X := \operatorname{span}\{L\Phi(\cdot, \mathbf{x}) \mid \mathbf{x} \in X\} \\ \mathcal{P}_B &: \mathcal{N}_\Phi(\mathbb{R}^d) \to V_Y := \operatorname{span}\{\Phi(\cdot, \mathbf{y}) \mid \mathbf{y} \in Y\}. \end{aligned}$$

Here $Y \subseteq \partial\Omega$ and $X \subseteq \Omega$ denote the interior collocation points and the boundary points.

It will be useful to dwell on the operator $\mathcal{P}_L$ a bit longer. Let us suppose $s_L = \sum_{i=1}^n \alpha_i L_i^{\mathbf{y}} \Phi(\cdot, \mathbf{y}) \in LV_X$, where $L_i^{\mathbf{y}} = \delta_{\mathbf{x}_j} \circ L$. The unknown coefficients are determined from

$$Ls_L|_X = Lu|_X \tag{5.15}$$

for the solution u to the elliptic boundary value problem (3.5). Then, by Theorem 3.3, we have

$$\|Eu - s_L\|_\Phi \leq \|Eu - w\|_\Phi$$

for all $w \in LV_X$. Another way to express the best approximation in Hilbert spaces is via the projection operator $\mathcal{P}_L$ which is characterised by

$$\mathcal{P}_L Eu = s_L.$$

To simplify the notation in the algorithm below, we write $\mathcal{P}_B F = \mathcal{P}_B(u|_{\partial\Omega})$ instead of $\mathcal{P}_B Eu$ for the projection on V_Y. In order to remind us of the fact that the

coefficients of the best approximation are determined by the generalised interpolation condition (5.15), we will even slightly abuse notation and write $\mathcal{P}_L f = \mathcal{P}_L(Lu)$ instead of $\mathcal{P}_L Eu$ when projecting on LV_X.

Now, we can state the one-shot projection algorithm.

Algorithm 5.14 (One-Shot Alternating Projections Algorithm)

Input: Right-hand sides f and F, number of iterations n

Set $u_0 = 0, f_0 = f, F_0 = F$
for $j = 1, \ldots, n$ **do**

Projection on LV_X

(a) Determine the local correction $s_{2j-1} = \mathcal{P}_L(f_{2j-2}) \in LV_X$ to f_{2j-2} from

$$Ls_{2j-1}|_X = f_{2j-2}|_X$$

(b) Update the global approximation and the residuals

$$\begin{aligned} u_{2j-1} &= u_{2j-2} + s_{2j-1} \\ f_{2j-1} &= f_{2j-2} - L(s_{2j-1}|_\Omega) \\ F_{2j-1} &= F_{2j-2} - s_{2j-1}|_{\partial\Omega} \end{aligned}$$

Projection on V_Y

(c) Determine the local correction $s_{2j} = \mathcal{P}_B(F_{2j-1}) \in V_Y$ to F_{2j-1} from

$$s_{2j}|_Y = F_{2j-1}|_Y$$

(d) Update the global approximation and the residuals

$$\begin{aligned} u_{2j} &= u_{2j-1} + s_{2j} \\ f_{2j} &= f_{2j-1} - L(s_{2j}|_\Omega) \\ F_{2j} &= F_{2j-1} - s_{2j}|_{\partial\Omega} \end{aligned}$$

end

Output: Approximate solution u_{2n}

We define the error at level j to be the difference between the exact solution and the global approximant at level j, i. e. $e_j = Eu - u_j$. From this definition and the algorithm one can easily establish the following identities

$$u_j = \sum_{k=1}^{j} s_k \quad \text{and} \quad e_j = Eu - \sum_{k=1}^{j} s_k = e_{j-1} - s_j = (I - \mathcal{P}_\ell) e_{j-1},$$

where $\ell = L$ if j is odd and $\ell = B$ if j is even. Thus, one obtains for the error of the final approximation

$$e_{2n} = \underbrace{(I - \mathcal{P}_B)(I - \mathcal{P}_L) \dots (I - \mathcal{P}_B)(I - \mathcal{P}_L)}_{2n} Ee_0.$$

That is, for each level we make two errors, one for projecting on LV_X and one for projecting on V_Y. Defining the orthogonal projections

$$\mathcal{Q}_L \colon \mathcal{N}_\Phi(\mathbb{R}^d) \to LV_X^\perp \qquad \text{and} \qquad \mathcal{Q}_B \colon \mathcal{N}_\Phi(\mathbb{R}^d) \to V_Y^\perp$$

through

$$\mathcal{Q}_L = I - \mathcal{P}_L \qquad \text{and} \qquad \mathcal{Q}_B = I - \mathcal{P}_B,$$

we can rewrite the error in the following way,

$$e_{2n} = [\mathcal{Q}_B \mathcal{Q}_L]^n \, Eu$$

since $e_0 = u$. Previously, in the case of RBF collocation, we have worked with a projection of the form

$$\mathcal{P} \colon \mathcal{N}_\Phi(\mathbb{R}^d) \to W := LV_X + V_Y,$$

which is given by our generalised interpolant (see Section 3.1.1), i e.

$$s_{Eu} = \mathcal{P} Eu.$$

Setting $\mathcal{Q} = I - \mathcal{P}$, which yields the projection onto $W^\perp$, we can write the error for RBF collocation as

$$e_c = Eu - s_{Eu} = (I - \mathcal{P})Eu = \mathcal{Q}Eu.$$

Now it becomes obvious what the alternating projection algorithm does. It tries to approximate the collocation error e_c by splitting the error operator $\mathcal{Q}$ into two error operators $\mathcal{Q}_L$ and $\mathcal{Q}_B$. The hope is that for n large enough,

$$\mathcal{Q} \approx \left[\mathcal{Q}_B \mathcal{Q}_L\right]^n. \tag{5.16}$$

Theorem 5.16 will indeed help to justify this hope. But before we state and prove the convergence result, we make a couple of smaller observations.

Lemma 5.15 *Let Φ be a reproducing kernel. Then*

1. $LV_X^\perp = \left\{ g \in \mathcal{N}_\Phi(\mathbb{R}^d) | Lg(\mathbf{x}) = 0 \text{ for } \mathbf{x} \in X \right\}$,
2. $V_Y^\perp = \left\{ g \in \mathcal{N}_\Phi(\mathbb{R}^d) | g(\mathbf{y}) = 0 \text{ for } \mathbf{y} \in Y \right\}$,
3. $W^\perp = LV_X^\perp \cap V_Y^\perp$.

Proof.

1. Take an arbitrary element f from LV_X, that is we can write it in the form $f(\mathbf{x}) = \sum_{k=1}^{N} \alpha_k L\Phi(\mathbf{x}, \mathbf{x}_k)$. Now, for any $g \in \mathcal{N}_\Phi(\mathbb{R}^d)$ we have by the reproducing kernel property

$$(f, g)_\Phi = \sum_{k=1}^{N} \alpha_k (g, L\Phi(\cdot, \mathbf{x}_k))_\Phi = \sum_{k=1}^{N} \alpha_k Lg(\mathbf{x}_k).$$

   If Lg vanishes on X, then the equation implies that $(f, g)_{\Phi_j} = 0$ for all $f \in \mathcal{N}_\Phi(\mathbb{R}^d)$, i. e. $g \in LV_X^\perp$. On the other hand, if $g \in LV_X^\perp$, then for the special choice of $f = L\Phi(\cdot, \mathbf{x}_k)$ the above equation will give $Lg(\mathbf{x}_k) = 0$ for all k.

2. Follows similarly.

3. The space $LV_X + V_Y$ is a direct sum since the functionals generating it are linearly independent. Thus we can define the orthogonal complement on it. Now we readily compute

$$W^\perp = (LV_X + V_Y)^\perp = LV_X^\perp \cap V_Y^\perp.$$

□

We have the following convergence result, which is analogous to the interpolation case, [2, Theorem 3.5].

Theorem 5.16 (Convergence of Algorithm 5.14) *Let $Eu \in H^\sigma(\mathbb{R}^d)$ and Φ be a kernel such that its native space is norm-equivalent to $H^\sigma(\mathbb{R}^d)$. Denote by $u^{(n)} = u_{2n}$ the global approximant of Algorithm 5.14 after n completed cycles. Then there exists a constant $c \in (0, 1)$ such that*

$$\|s_{Eu} - u^{(n)}\|_\Phi \leq c^n \|Eu\|_\Phi,$$

where s_{Eu} is the one-shot RBF collocation approximant from Section 3.1.1.

Proof. As initial values we use $f_0 = L(s_{Eu}|_\Omega)$ and $F_0 = s_{Eu}|_{\partial\Omega}$ for Algorithm 5.14. We set $e^{(n)} := e_{2n} = s_{Eu} - u^{(n)}$ and in particular $e^{(0)} = s_{Eu}$. Using the notation from Theorem 5.13, we have

$$\ell = 2, \quad \mathcal{Q}_1 = \mathcal{Q}_L \quad \text{and} \quad \mathcal{Q}_2 = \mathcal{Q}_B$$

as well as

$$U_1 = LV_X^\perp, \quad U_2 = V_Y^\perp, \quad A_1 = \bigcap_{i=2}^{2} U_i = U_2 \quad \text{and} \quad U = U_1 \cap U_2 = W^\perp,$$

where the last equality follows from Lemma 5.15. Since $\mathcal{Q}$ projects therefore on $W^\perp$ and s_{Eu} lies by definition in W, we know that $\mathcal{Q}s_{Eu} = 0$. Hence, we have by Theorems 5.13 and 3.1,

$$\begin{aligned}\|s_{Eu} - u^{(n)}\|_\Phi &= \|e^{(n)}\|_\Phi = \|\left[\mathcal{Q}_B\mathcal{Q}_L\right]^n s_{Eu}\|_\Phi \\ &= \|\left[\mathcal{Q}_B\mathcal{Q}_L\right]^n s_{Eu} - \mathcal{Q}s_{Eu}\|_\Phi \\ &\leq c^n\|s_{Eu} - \mathcal{Q}s_{Eu}\|_\Phi \\ &= c^n\|s_{Eu}\|_\Phi \\ &\leq c^n\|Eu\|_\Phi,\end{aligned}$$

for c defined as in (5.14). Now it remains to show that the constant c is strictly less than one. To prove this, we first make the observation that it is possible to find nonzero functions in both $LV_X^\perp \cap W$ and $V_Y^\perp \cap W$. Define, for instance, the function $s_L \in W$ by

$$s_L = \sum_j \alpha_j L_2\Phi(\cdot - \mathbf{x}_j) + \Phi(\cdot - \mathbf{y}_1)$$

for some coefficients $\alpha_j \in \mathbb{R}$, $\mathbf{x}_j \in X$ and $\mathbf{y}_1 \in Y$. Here, the subindex denotes to which argument the operator is applied. Then by Lemma 5.15 the statement $s_L \in LV_X^\perp$ is equivalent to Ls_L vanishing on all $\mathbf{x} \in X$, which implies

$$\sum_j \alpha_j L_1L_2\Phi(\mathbf{x} - \mathbf{x}_j) = -L_1\Phi(\mathbf{x} - \mathbf{y}_1)$$

for all $\mathbf{x} \in X$. Since the kernel $L_1L_2\Phi$ leads to a positive definite matrix, we have a unique nonvanishing solution $s_L \in LV_X^\perp \cap W$. A similar approach shows that there exists a nonzero function in $V_Y^\perp \cap W$.

For the angle α_1 between U_1 and A_1, we need to compute the expression

$$(U_1 \cap A_1)^\perp = (LV_X^\perp \cap V_Y^\perp)^\perp = \left(W^\perp\right)^\perp = W.$$

If $\alpha_1 = 0$ (which would imply that $c = 1$), we have $\cos(\alpha_1) = 1$ or

$$1 = \sup\left\{(u,v)_\Phi \middle| u \in LV_X^\perp \cap W, v \in V_Y^\perp \cap W \text{ with } \|u\|_\Phi, \|v\|_\Phi \leq 1\right\}.$$

The set of which the supremum is taken is in fact the closed unit ball in the finite-dimensional space $(LV_X^\perp \cap W) \times (V_Y^\perp \cap W)$. Hence, it is compact. Since additionally the inner product is continuous, we can deduce that the supremum is attained. In other words, there must exist a $u^* \in LV_X^\perp \cap W$ and a $v^* \in V_Y^\perp \cap W$ with $\|u^*\|_\Phi \leq 1$, $\|v^*\|_\Phi \leq 1$ and $(u^*, v^*)_\Phi = 1$. If at least one of the two functions has norm less than one, we have by the Cauchy-Schwarz inequality the contradiction

$$1 = (u^*, v^*)_\Phi \leq \|u^*\|_\Phi\|v^*\|_\Phi < 1.$$

Hence, $\|u^*\|_\Phi = \|v^*\|_\Phi = 1$. Equality in the Cauchy-Schwarz inequality is only achieved when both functions are linearly dependent, or here $u^* = v^*$. That is u^* must lie in

$$(LV_X^\perp \cap W) \cap (V_Y^\perp \cap W) = (LV_X^\perp \cap V_Y^\perp) \cap W = W^\perp \cap W = \{0\}\,.$$

But $u^* = 0$ contradicts $\|u^*\|_\Phi = 1$. Therefore, $c < 1$. □

So we can use this projection algorithm to approximate the local solutions of the collocation RBF algorithm. In this case, each level j would yield a constant $c_j \in (0,1)$ and we would need to iterate, say k_j times to approximate the current projection well enough in the sense of (5.16). It would be advantageous if we can show that these k_j are independent of the level i. e. $k_j = k$ for all j because that implies that the different projection operators do not depend on the point sets. However, the numerical test runs in the next section seem to suggest that this is not the case.

5.4.2 Numerical Examples

The previous results unfortunately only say something about the convergence speed in terms of the unknown constant c. Therefore, we are interested in numerical examples to examine how fast different one-shot solutions are approximated by alternating between the interior and the boundary in the sense of (5.16). We do that for six different one-shot solutions on successively finer grids. Figure 5.1 shows the results for several levels, where the one-shot solutions are taken from Example (P2) in Chapter 4 with proportionality constant $\nu = 2.4$.

The convergence speed of the the L_2 error is estimated via the ansatz $g(n) = ae^{bn}$ for $a, b \in \mathbb{R}$. Whereas the first two approximations of the one-shot collocation solution reach machine precision within one hundred iterations, it becomes gradually more difficult to approximate the one-shot solution via alternating projections for finer grids. However, the condition numbers of the interior matrices A_{LL} and the boundary matrices A_{BB} are considerably lower than the one-shot saddle-point collocation matrices. Also, the condition numbers of the interior are several orders of magnitude lower than the condition numbers of the boundary matrices, see Table 5.10. This is advantageous since the interior matrices are a lot bigger than the boundary matrices but not unexpected. Indeed, these results fit in well with the theoretical observations in [85].

We estimate the constant c from Theorem 5.16 numerically as follows. Let us assume that the kernels $\Phi_j = \delta^{-d}\Phi(\cdot/\delta)$ generate $H^\sigma(\mathbb{R}^d)$. Assuming that the L_2 error behaves according to our ansatz, we deduce for some real constants a and b that

$$g(n) = ae^{bn} \approx \|e^{(n)}\|_{L_2(\Omega)} \leq \|e^{(n)}\|_{L_2(\mathbb{R}^d)} = C_1\|e^{(n)}\|_{H^\sigma(\mathbb{R}^d)},$$

where

$$C_1 := \frac{\|e^{(n)}\|_{L_2(\mathbb{R}^d)}}{\|e^{(n)}\|_{H^\sigma(\mathbb{R}^d)}} \leq 1$$

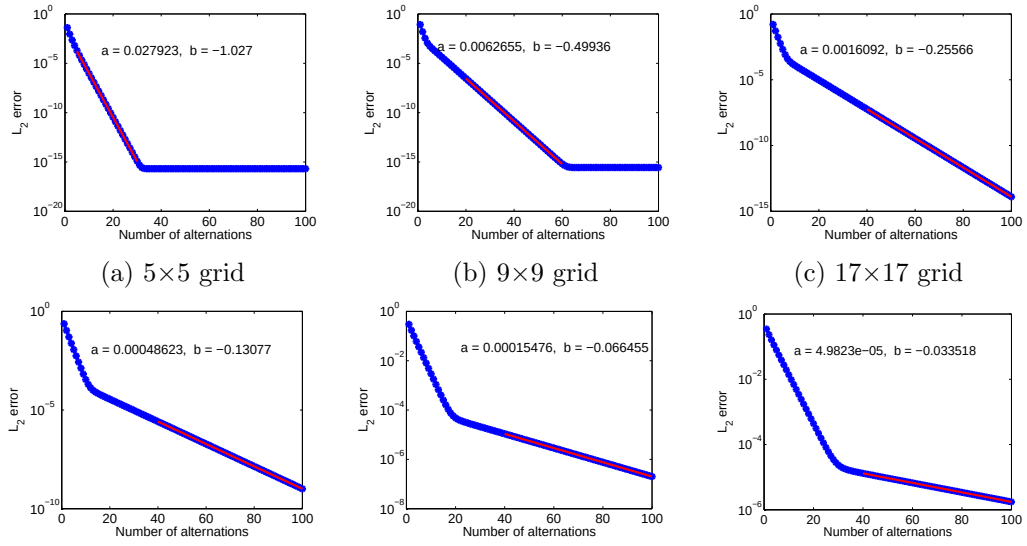

(a) 5×5 grid (b) 9×9 grid (c) 17×17 grid

(d) 33×33 grid (e) 65×65 grid (f) 129×129 grid

Figure 5.1: L_2 errors of the alternating projection approximations to six different one-shot nonstationary approximations. The red lines indicate which parts of the graphs were used for determining a and b.

can be bounded independently of n. Then using the norm equivalence constant C_2 between native space norm and Sobolev space $H^\sigma(\mathbb{R}^d)$, which is also independent of n, we find by Theorem 5.16

$$\begin{aligned} g(n) \leq C_1 C_2 \delta^{-\sigma} \|e^{(n)}\|_{\Phi_j} &= C_1 C_2 \delta^{-\sigma} \|(\mathcal{Q}_B \mathcal{Q}_L)^n s_{Eu} - \mathcal{Q} s_{Eu}\|_{\Phi_j} \\ &\leq C_1 C_2 \delta^{-\sigma} c^n \|s_{Eu}\|_{\Phi_j}. \end{aligned}$$

By taking the logarithm and assuming equality for the above equation, we are able to establish a relationship between our estimates for a and b as well as the unknown constant c. We have

$$\log(g(n)) = \log(a) + bn = \log(C_1 C_2 \delta^{-\sigma} \|s_{Eu}\|_{\Phi_j}) + \log(c) n.$$

That is, we have $a = C_1 C_2 \delta^{-\sigma} \|s_{Eu}\|_{\Phi_j}$ and $c = e^b$.

We have collected the values for the constant c for the nonstationary setting for problem (P2) from Chapter 4 in Table 5.9. Unfortunately, for finer grids the values for c are getting closer to one. This might be due to the fact that we alternate between interpolants which are built from $\mathcal{O}(N^d)$ and $\mathcal{O}(N^{d-1})$ points respectively, assuming that we cover the square domain with $N \times N$ points. This unfortunately seems to lead to spaces $LV_{X_j}^\perp$ and $V_{Y_j}^\perp$ which are not very orthogonal to each other.

grids	5x5	9x9	17x17	33x33	65x65	129x129
c	0.36	0.61	0.77	0.88	0.94	0.97

Table 5.9: Estimated values for the constant c from Theorem 5.16 for several nonstationary one-shot collocation approximations based on Example (P2).

N	$\kappa(A)$	order	$\kappa(A_{LL})$	order	$\kappa(A_{BB})$	order
9	1.5e+03	—	1.0e+00	—	3.7e+02	—
25	1.0e+05	-6.12	5.2e+00	-2.39	9.0e+01	+2.02
81	2.3e+07	-7.78	8.7e+01	-4.05	1.9e+03	-4.40
289	2.3e+09	-6.65	4.7e+02	-2.45	2.7e+04	-3.85
1089	1.7e+11	-6.25	2.3e+03	-2.28	3.3e+05	-3.57
4225	1.3e+13	-6.21	1.1e+04	-2.22	3.8e+06	-3.54
16641	9.5e+14	-6.21	4.8e+04	-2.16	4.4e+07	-3.54

Table 5.10: Comparision of condition numbers.

In this chapter, we have investigated three different ways to reduce the computational cost of the multilevel collocation algorithm: preconditioning, regularisation and the alternating projection method. It turns out that a combination of the first two proved to be particularly powerful. The alternating projection method runs into difficulties probably due to the fact that we alternate between (generalised) interpolants of different size. Throughout the previous chapters, we assumed that the analytic solution to the PDE and its numerical approximation lie in the same spaces. In the next chapter, we consider the case where this is not guaranteed anymore.

Chapter 6

Escape Theory for Elliptic Boundary Value Problems

In this chapter, we discuss the so-called *escape theory* for elliptic boundary value problems [66, 62, 8, 63, 52, 68, 53]. We wish to escape the native space in the sense that the smoothness of the solution of the PDE shall not be necessarily linked to the smoothness of the basis functions. To be a bit more precise, let us assume we have a solution of a second order elliptic boundary value problem, $u \in H^\beta(\Omega)$. However, its approximant s_u shall be in $H^\sigma(\Omega)$ with $\sigma \geq \beta > d/2+2$. In this chapter, we analyse the error $\|u - s_u\|_{L_2(\Omega)}$. Note that because the solution lies in a rougher space, we cannot bound the error by $Ch^{\sigma-2}\|u\|_{H^\sigma(\Omega)}$ as we have done before. However, it is possible to show a corresponding result in the weaker H^β norm. For the proof, we have to make a detour by approximating the solution u with a band-limited function u_ρ for some $\rho > 0$. Band-limited functions allow us to bound stronger Sobolev norms by weaker ones. Whereas the reverse is always true, bounding stronger norms by weaker ones does not work for arbitrary functions. Hence, we focus on functions whose Fourier transform is compactly supported.

We will first establish the escape theory for one-shot collocation and then extend it to multilevel collocation. Both results are original, building on the general escape theory introduced by Narcowich and Ward [66].

6.1 One-Shot Collocation

We turn now to one-shot escape theory for second order elliptic operators. Define the reproducing kernel $\Psi\colon \mathbb{R}^d \to \mathbb{R}$ by its Fourier transform given through

$$\widehat{\Psi}(\boldsymbol{\omega}) = (1 + \|\boldsymbol{\omega}\|_2^2)^{-\beta}.$$

Then, we automatically have $\mathcal{N}_\Psi(\mathbb{R}^d) = H^\beta(\mathbb{R}^d)$. We begin with a relatively abstract result, which is proven in [68]. This result will be the key to proving an error estimate, where the solution of the PDE and its numerical solution lie in different spaces.

Theorem 6.1 *Let $\mathcal{Y}$ be a Banach space over the real or complex numbers, $\mathcal{V}$ be a subspace of $\mathcal{Y}$ and $\mathcal{Z}^*$ a finite dimensional subspace of $\mathcal{Y}^*$, the dual space of $\mathcal{Y}$. If for every $\lambda^* \in \mathcal{Z}^*$ and some $\gamma > 1$ independent of λ^* the inequality*

$$\|\lambda^*\|_{\mathcal{Y}^*} \leq \gamma \|\lambda^*|_{\mathcal{V}}\|_{\mathcal{V}^*}$$

holds, then there exists for $y \in \mathcal{Y}$ a near-best approximation $v \in \mathcal{V}$ such that v interpolates y on $\mathcal{Z}^*$. That is, v possesses the following two properties

1. *$\lambda^*(y) = \lambda^*(v)$ for all $\lambda^* \in \mathcal{Z}^*$ and*
2. *$\|y - v\|_{\mathcal{Y}} \leq (1 + 2\gamma) \min_{v \in \mathcal{V}} \|y - v\|_{\mathcal{Y}}$.*

We want to adjust this abstract result to our particular application. Remember that we want to numerically solve the PDE

$$\begin{aligned} Lu &= f \qquad \text{in} \quad \Omega, \\ u &= F \qquad \text{on} \quad \partial\Omega, \end{aligned}$$

by constructing linear functionals of the form

$$\lambda_j = \begin{cases} \delta_{\mathbf{x}_j} \circ L, & 1 \leq j \leq n, \\ \delta_{\mathbf{x}_j}, & n+1 \leq j \leq N, \end{cases}$$

for a differential operator of the form (3.6). Here, we assume to be given a point set $X = X_1 \cup X_2$ consisting of interior points $X_1 = \{\mathbf{x}_1, \ldots, \mathbf{x}_n\} \subseteq \Omega$ and boundary points $X_2 = \{\mathbf{x}_{n+1}, \ldots, \mathbf{x}_N\} \subseteq \partial\Omega$. Then we have the following spaces

$$\begin{aligned} \mathcal{Z}_\rho^* &= \operatorname{span}\{\rho^{-2}\lambda_1, \ldots, \rho^{-2}\lambda_n, \lambda_{n+1}, \ldots, \lambda_N\}, \\ \mathcal{Y} &= H^\beta(\mathbb{R}^d) = \mathcal{N}_\Psi(\mathbb{R}^d), \\ \mathcal{V} &= B^\rho = \{u \in L_2(\mathbb{R}^d) \mid \operatorname{supp} \widehat{u} \subseteq B(\mathbf{0}, \rho)\}, \end{aligned} \tag{6.1}$$

for some $\rho > 0$. That is, we choose $\mathcal{Z}_\rho^*$ to be the span of the (partially scaled) linear functionals, $\mathcal{Y}$ to be the native space with reproducing kernel Ψ and $\mathcal{V}$ the set of band-limited functions or more precisely the set of functions whose Fourier transform is supported in the ball with radius $\rho > 0$. Indeed the assumptions that Theorem 6.1 needs can be verified in our setting, see Lemma 6.3. For its proof it will be useful to find an expression $\kappa_j(\boldsymbol{\omega})$ such that

$$\mathcal{F}[\lambda_j^{\mathbf{y}} \Psi(\cdot - \mathbf{y})](\boldsymbol{\omega}) = \kappa_j(\boldsymbol{\omega})(\mathcal{F}\Psi)(\boldsymbol{\omega})$$

holds. We compute

$$\begin{aligned} \mathcal{F}[\lambda_j^{\mathbf{y}} \Psi(\cdot - \mathbf{y})](\boldsymbol{\omega}) &= (2\pi)^{-d/2} \int_{\mathbb{R}^d} \lambda_j^{\mathbf{y}} \left[\Psi(\mathbf{x} - \mathbf{y}) e^{-i\mathbf{x}^T\boldsymbol{\omega}} \right] d\mathbf{x} \\ &= (2\pi)^{-d/2} \int_{\mathbb{R}^d} \lambda_j^{\mathbf{y}} \left[\Psi(\mathbf{z}) e^{-i(\mathbf{z}+\mathbf{y})^T\boldsymbol{\omega}} \right] d\mathbf{z} \\ &= \lambda_j^{\mathbf{y}}(e^{-i\mathbf{y}^T\boldsymbol{\omega}})(\mathcal{F}\Psi)(\boldsymbol{\omega}) \\ &=: \kappa_j(\boldsymbol{\omega})(\mathcal{F}\Psi)(\boldsymbol{\omega}). \end{aligned} \tag{6.2}$$

By Corollary 1.2, we find

$$\kappa_j(\boldsymbol{\omega}) = \lambda_j^{\mathbf{y}}(e^{-i\mathbf{y}^T\boldsymbol{\omega}}) = \begin{cases} e^{-i\boldsymbol{\omega}^T\mathbf{x}_j} \sum_{|\boldsymbol{\alpha}|\leq 2} d_{\boldsymbol{\alpha}}(\mathbf{x}_j)(-i\boldsymbol{\omega})^{\boldsymbol{\alpha}} & \text{for} \quad 1 \leq j \leq n, \\ e^{-i\boldsymbol{\omega}^T\mathbf{x}_j} & \text{for} \quad n+1 \leq j \leq N, \end{cases}$$

where we introduced for $1 \leq k, l \leq d$ and $1 \leq j \leq N$ the notation

$$d_{\boldsymbol{\alpha}}(\mathbf{x}_j) = \begin{cases} a_{kl}(\mathbf{x}_j) & \text{if} \quad \boldsymbol{\alpha} = \mathbf{e}_k + \boldsymbol{e}_l, \\ b_k(\mathbf{x}_j) & \text{if} \quad \boldsymbol{\alpha} = \mathbf{e}_k, \\ c(\mathbf{x}_j) & \text{if} \quad \boldsymbol{\alpha} = \mathbf{0}. \end{cases}$$

With this definition, we can prove the following useful lemma.

Lemma 6.2 *We have*

$$\int_{\mathbb{R}^d} \left| \alpha_j \sum_{j=1}^N \kappa_j(\boldsymbol{\omega}) \right|^2 \widehat{\Psi}(\boldsymbol{\omega}) d\boldsymbol{\omega} = (2\pi)^{d/2} \sum_{j,k=1}^N \alpha_j \alpha_k \lambda_j^{\mathbf{x}} \lambda_k^{\mathbf{y}} \Psi(\mathbf{x} - \mathbf{y}).$$

Proof. Using the Fourier inversion theorem, we obtain

$$\begin{aligned} &\sum_{j,k=1}^N \alpha_j \alpha_k \lambda_j^{\mathbf{x}} \lambda_k^{\mathbf{y}} \Psi(\mathbf{x} - \mathbf{y}) \\ &\qquad = \sum_{j,k=1}^N \alpha_j \alpha_k \lambda_j^{\mathbf{x}} \lambda_k^{\mathbf{y}} \left[(2\pi)^{-d/2} \int_{\mathbb{R}^d} e^{i(\mathbf{x}-\mathbf{y})^T\boldsymbol{\omega}} \widehat{\Psi}(\boldsymbol{\omega}) \right] d\boldsymbol{\omega} \\ &\qquad = (2\pi)^{-d/2} \int_{\mathbb{R}^d} \sum_{j,k=1}^N \alpha_j \alpha_k \lambda_j^{\mathbf{x}} \lambda_k^{\mathbf{y}} (e^{i(\mathbf{x}-\mathbf{y})^T\boldsymbol{\omega}}) \widehat{\Psi}(\boldsymbol{\omega}) d\boldsymbol{\omega} \\ &\qquad = (2\pi)^{-d/2} \int_{\mathbb{R}^d} \left(\sum_{k=1}^N \alpha_k \kappa_k(\boldsymbol{\omega}) \right) \overline{\left(\sum_{j=1}^N \alpha_j \kappa_j(\boldsymbol{\omega}) \right)} \widehat{\Psi}(\boldsymbol{\omega}) d\boldsymbol{\omega} \\ &\qquad = (2\pi)^{-d/2} \int_{\mathbb{R}^d} \left| \sum_{j=1}^N \alpha_j \kappa_j(\boldsymbol{\omega}) \right|^2 \widehat{\Psi}(\boldsymbol{\omega}) d\boldsymbol{\omega}. \end{aligned}$$

□

Finally, we can show that the assumption in Theorem 6.1 is true.

Lemma 6.3 *There exists a constant $\rho > 0$ such that the inequality in Theorem 6.1 holds for the spaces defined in* (6.1) *with $\gamma = 2$, i. e. we have*

$$\|\lambda\|_{\mathcal{Y}^*} \leq 2\|\lambda^*|_{\mathcal{V}}\|_{\mathcal{V}^*}. \tag{6.3}$$

Proof. We start by giving meaning to both abstract norms $\|\lambda^*\|_{\mathcal{Y}^*}$ as well as $\|\lambda^*|_{\mathcal{V}}\|_{\mathcal{V}^*}$ when choosing the spaces like in (6.1). Let $\lambda \in \mathcal{Z}_\rho^*$, that means for some $\widetilde{\alpha}_j \in \mathbb{R}$ it can be written as a linear combination,

$$\lambda = \sum_{j=1}^{n} \widetilde{\alpha}_j \rho^{-2} \lambda_j + \sum_{j=n+1}^{N} \widetilde{\alpha}_j \lambda_j = \sum_{j=1}^{N} \alpha_j \lambda_j.$$

In order to keep the notation as simple as possible, we have introduced the abbreviation

$$\alpha_j = \begin{cases} \rho^{-2}\widetilde{\alpha}_j & \text{if} \quad 1 \le j \le n, \\ \widetilde{\alpha}_j & \text{if} \quad n+1 \le j \le N. \end{cases}$$

We introduce the notation $\boldsymbol{\alpha} = P\widetilde{\boldsymbol{\alpha}}$, where $P = (p_{jk})$ is given by

$$\begin{cases} p_{jk} = 0 & \text{if} \quad j \neq k, \\ p_{jj} = \rho^{-2} & \text{if} \quad 1 \le j \le n, \\ p_{jj} = 1 & \text{if} \quad n+1 \le j \le N. \end{cases}$$

By Corollary 3.2, we know that the Riesz representer g_λ of this functional λ can be written as

$$g_\lambda = \sum_{j=1}^{N} \alpha_j \lambda_j^{\mathbf{y}} \Psi(\cdot, \mathbf{y}).$$

That is, by the Riesz representation theorem, we have

$$\|\lambda\|^2_{\mathcal{N}_\Psi(\mathbb{R}^d)^*} = \|g_\lambda\|^2_{\mathcal{N}_\Psi(\mathbb{R}^d)} = \sum_{j,k=1}^{N} \alpha_j \alpha_k \lambda_j^{\mathbf{x}} \lambda_k^{\mathbf{y}} \Psi(\mathbf{x}, \mathbf{y}).$$

In order to understand the norm $\|\lambda^*|_{\mathcal{V}}\|_{\mathcal{V}^*}$, let $f \in B^\rho \subseteq \mathcal{N}_\Psi(\mathbb{R}^d)$ and compute

$$\begin{aligned} \lambda(f) = (f, g_\lambda)_\Psi &= (2\pi)^{-d/2} \int_{\mathbb{R}^d} \frac{\widehat{f}(\omega)\overline{\widehat{g_\lambda}(\omega)}}{\widehat{\Psi}(\omega)} d\omega \\ &= (2\pi)^{-d/2} \int_{\|\omega\|_2 \le \rho} \frac{\widehat{f}(\omega)\overline{\widehat{g_\lambda}(\omega)}}{\widehat{\Psi}(\omega)} d\omega \\ &= (2\pi)^{-d/2} \int_{\mathbb{R}^d} \frac{\widehat{f}(\omega)\overline{\chi_\rho(\omega)\widehat{g_\lambda}(\omega)}}{\widehat{\Psi}(\omega)} d\omega \\ &= (f, g_\lambda^\rho)_\Psi, \end{aligned}$$

where we have introduced the characteristic function $\chi_\rho(\omega) = \chi_{B(\mathbf{0},\rho)}(\omega)$ as well as the band-limited function g_λ^ρ, which is defined so that for its Fourier transform the relation $\widehat{g_\lambda^\rho} = \widehat{g_\lambda}\chi_\rho$ holds. Since B^ρ is a subspace of $\mathcal{N}_\Psi(\mathbb{R}^d)$, it follows that

$$\|\lambda^*|_{B^\rho}\|_{(B^\rho)*} = \sup_{0 \neq f \in B^\rho} \frac{|\lambda(f)|}{\|f\|_\Psi} = \sup_{0 \neq f \in B^\rho} \frac{(f, g_\lambda^\rho)_\Psi}{\|f\|_\Psi} = \|g_\lambda^\rho\|_\Psi,$$

where the last equality holds because for the left-hand side the Cauchy-Schwarz inequality yields an upper bound, which is attained exactly for $f = g_\lambda^\rho \in B^\rho$. Having translated the abstract statement (6.3), we need to show for our concrete example here, that

$$\|g_\lambda\|_\Psi \leq 2\|g_\lambda^\rho\|_\Psi$$

holds for some sufficiently large $\rho > 0$. We will show that

$$\|g_\lambda - g_\lambda^\rho\|_\Psi \leq \frac{1}{2}\|g_\lambda\|_\Psi, \tag{6.4}$$

then the required result follows immediately because

$$\begin{aligned}\|g_\lambda^\rho\|_\Psi &\geq \|g_\lambda\|_\Psi - \|g_\lambda - g_\lambda^\rho\|_\Psi \\ &\geq \|g_\lambda\|_\Psi - \frac{1}{2}\|g_\lambda\|_\Psi = \frac{1}{2}\|g_\lambda\|_\Psi.\end{aligned}$$

By (6.2) and the definition of g_λ, we find

$$\begin{aligned}\|g_\lambda - g_\lambda^\rho\|_\Psi^2 &= \int_{\|\boldsymbol{\omega}\|_2 \geq \rho} \frac{|\widehat{g_\lambda}(\boldsymbol{\omega})|^2}{\widehat{\Psi}(\boldsymbol{\omega})} d\boldsymbol{\omega} \\ &= \int_{\|\boldsymbol{\omega}\|_2 \geq \rho} \left| \sum_{j=1}^N \alpha_j \kappa_j(\boldsymbol{\omega}) \right|^2 \widehat{\Psi}(\boldsymbol{\omega}) d\boldsymbol{\omega} \\ &= \int_{\|\boldsymbol{\omega}\|_2 \geq \rho} \frac{\left| \sum_{j=1}^N \alpha_j \kappa_j(\boldsymbol{\omega}) \right|^2}{(1 + \|\boldsymbol{\omega}\|_2^2)^\beta} d\boldsymbol{\omega} \\ &= \rho^d \int_{\|\boldsymbol{\eta}\|_2 \geq 1} \frac{\left| \sum_{j=1}^N \alpha_j \kappa_j(\rho\boldsymbol{\eta}) \right|^2}{(1 + \rho^2\|\boldsymbol{\eta}\|_2^2)^\beta} d\boldsymbol{\eta}.\end{aligned}$$

Since for $\|\boldsymbol{\eta}\| \geq 1$, we have

$$(1 + \rho^2\|\boldsymbol{\eta}\|_2^2)^{-\beta} \leq 2^\beta \rho^{-2\beta}(1 + \|\boldsymbol{\eta}\|_2^2)^{-\beta},$$

we deduce the bound

$$\begin{aligned}\|g_\lambda - g_\lambda^\rho\|_\Psi^2 &\leq 2^\beta \rho^{d-2\beta} \int_{\|\boldsymbol{\eta}\|_2 \geq 1} \frac{\left| \sum_{j=1}^N \alpha_j \kappa_j(\rho\boldsymbol{\eta}) \right|^2}{(1 + \|\boldsymbol{\eta}\|_2^2)^\beta} d\boldsymbol{\eta} \\ &\leq C\rho^{d-2\beta} \int_{\mathbb{R}^d} \frac{\left| \sum_{j=1}^N \alpha_j \kappa_j(\rho\boldsymbol{\eta}) \right|^2}{(1 + \|\boldsymbol{\eta}\|_2^2)^\beta} d\boldsymbol{\eta} \\ &= C\rho^{d-2\beta} \int_{\mathbb{R}^d} \left| \sum_{j=1}^N \alpha_j \kappa_j(\rho\boldsymbol{\eta}) \right|^2 \widehat{\Psi}(\boldsymbol{\eta}) d\boldsymbol{\eta}.\end{aligned}$$

Now, we can employ Lemma 6.2, to find

$$\begin{aligned}\|g_\lambda - g_\lambda^\rho\|_\Psi^2 &\le C(2\pi)^{d/2}\rho^{d-2\beta}\sum_{j,k=1}^{N}\alpha_j\alpha_k\lambda_j^{\mathbf{x}}\lambda_k^{\mathbf{y}}\Psi(\rho\mathbf{x}-\rho\mathbf{y})\\ &= C\rho^{d-2\beta}\sum_{j,k=1}^{N}\alpha_j\alpha_k\lambda_j^{\mathbf{x}}\lambda_k^{\mathbf{y}}\Psi_{\frac{1}{\rho}}(\mathbf{x}-\mathbf{y}),\end{aligned}$$

where $\Psi_\delta = \Psi(\cdot/\delta)$. If we choose $\frac{1}{\rho} \le q$, we are left with summing over diagonal elements only, i. e.

$$\begin{aligned}&\|g_\lambda - g_\lambda^\rho\|_\Psi^2\\ &\quad\le C\rho^{d-2\beta}\sum_{j=1}^{N}\alpha_j^2\lambda_j^{\mathbf{x}}\lambda_j^{\mathbf{y}}\Psi_{\frac{1}{\rho}}(\mathbf{x}-\mathbf{y})\\ &\quad\le C\rho^{d-2\beta}\left\{\sum_{j=1}^{n}\widetilde{\alpha}_j^2\rho^{-4}\lambda_j^{\mathbf{x}}\lambda_j^{\mathbf{y}}\Psi_{\frac{1}{\rho}}(\mathbf{x}-\mathbf{y}) + \sum_{j=n+1}^{N}\widetilde{\alpha}_j^2\lambda_j^{\mathbf{x}}\lambda_j^{\mathbf{y}}\Psi_{\frac{1}{\rho}}(\mathbf{x}-\mathbf{y})\right\}\\ &\quad\le C\rho^{d-2\beta}\|\widetilde{\boldsymbol{\alpha}}\|_2^2\max\{\rho^{-4}(\rho^4L^2\Psi(\mathbf{0})),\Psi(\mathbf{0})\}\\ &\quad\le C\rho^{d-2\beta}\|\widetilde{\boldsymbol{\alpha}}\|_2^2,\end{aligned}$$

where we have used that $\Psi_{\frac{1}{\rho}}(\mathbf{0}) = \Psi(\mathbf{0})$. Now we are only left with estimating $\|\widetilde{\boldsymbol{\alpha}}\|_2^2$. Since

$$\begin{aligned}\lambda_{\min}(PA_\Lambda P)\|\widetilde{\boldsymbol{\alpha}}\|_2^2 &\le \widetilde{\boldsymbol{\alpha}}^T PA_\Lambda P\widetilde{\boldsymbol{\alpha}}\\ &= (P\widetilde{\boldsymbol{\alpha}})^T A_\Lambda(P\widetilde{\boldsymbol{\alpha}})\\ &= \boldsymbol{\alpha}^T A_\Lambda\boldsymbol{\alpha}\\ &= \|g_\lambda\|_\Psi^2,\end{aligned}$$

we obtain from the proof of Theorem 5.9, which bounds the smallest eigenvalue of a diagonally preconditioned collocation matrix that

$$\|\widetilde{\boldsymbol{\alpha}}\|_2^2 \le \frac{1}{\lambda_{\min}(PA_\Lambda P)}\|g_\lambda\|_\Psi^2 \le Cq^{d-2\beta}\|g_\lambda\|_\Psi^2.$$

Note the matrix $A_\Lambda = (\lambda_j^{\mathbf{x}}\lambda_k^{\mathbf{y}}\Psi(\mathbf{x}-\mathbf{y}))$ is not scaled and thus the support radius does not appear in the inequality. This implies

$$\|g_\lambda - g_\lambda^\rho\|_\Psi^2 \le \widetilde{C}(\rho q)^{d-2\beta}\|g_\lambda\|_\Psi^2$$

for some $\widetilde{C} > 0$. If we now choose $\rho q \ge \max\left\{1, (4\widetilde{C})^{1/(2\beta-d)}\right\} =: m$, we finally end up with

$$\|g_\lambda - g_\lambda^\rho\|_\Psi^2 \le \frac{1}{4}\|g_\lambda\|_\Psi^2,$$

and taking the square root on both sides completes the proof. □

Thus by having verified the assumptions of Theorem 6.1, we can now deduce that for all $v \in \mathcal{N}_\Psi(\mathbb{R}^d) = H^\beta(\mathbb{R}^d)$, there exists a $v_\rho \in B^\rho$ such that for all $1 \leq j \leq N$

$$\lambda_j(v) = \lambda_j(v_\rho) \quad \text{and} \quad \|v - v_\rho\|_\Psi \leq 5 \min_{w_\rho \in B^\rho} \|v - w_\rho\|_\Psi. \tag{6.5}$$

We can use the norm equivalence of the Ψ norm to the Sobolev norm to simplify the inequality. We obtain

$$\lambda_j(v) = \lambda_j(v_\rho) \quad \text{and} \quad \|v - v_\rho\|_{H^\beta(\mathbb{R}^d)} \leq 5 \min_{w_\rho \in B^\rho} \|v - w_\rho\|_{H^\beta(\mathbb{R}^d)}. \tag{6.6}$$

However, we have to bear in mind that for scaled kernels Ψ_δ, one needs to be a bit more careful since the scale δ will appear in the inequality. Also, note that the ρ^{-2} cancels in the case of interior functionals. From the last inequality we can derive by setting $w_\rho = 0$ and using the inverse triangle inequality that

$$\|v_\rho\|_{H^\beta(\mathbb{R}^d)} \leq 6\|v\|_{H^\beta(\mathbb{R}^d)}. \tag{6.7}$$

Note that v_ρ and v are defined on the whole Euclidean space $\mathbb{R}^d$ and not just on Ω. With this result we can now bound the error between analytical and numerical solution when both solutions come from different spaces.

Theorem 6.4 (L_2 Error in Escape Case) *Let Ω have a $C^{k,s}$ boundary with $k \in \mathbb{N}_0$ and $s \in [0, 1)$ and $h = \max\{h_{X,\Omega}, h_{Y,\partial\Omega}\} < 1$. Let the kernel Φ generate the Sobolev space $H^\sigma(\mathbb{R}^d)$. Under the assumptions above we can bound the error for some $C > 0$ independent of ρ, h and q by*

$$\begin{aligned}\|u - s_u\|_{L_2(\Omega)} &\leq Ch^{\beta-2} \left\{1 + \left(\frac{h}{q}\right)^{\sigma-\beta}\right\} \|u\|_{W_2^\beta(\Omega)} \\ &= Ch^{\beta-2}\|u\|_{W_2^\beta(\Omega)}\end{aligned}$$

if the mesh ratio h/q is bounded.

Proof. We employ the L_2 analogue of the maximum principle (4.7) to split the error into an interior and a boundary error

$$\|u - s_u\|_{L_2(\Omega)} \leq C \left\{\|Lu - Ls_u\|_{L_2(\Omega)} + \|u - s_u\|_{W_2^{1/2}(\partial\Omega)}\right\}.$$

We look at both errors separately. Let $u_\rho \in B^\rho$ with

$$\rho = m/q,$$

i. e. Lemma 6.3 holds with m defined as in the proof. Due to (6.6), we know that $s_u = s_{u_\rho}$ holds. Using the sampling inequality (Theorem 2.33), the triangle inequality and

the fact that the differential operator is bounded, we obtain

$$\begin{aligned}\|Lu - Ls_u\|_{L_2(\Omega)} &\leq Ch_{X,\Omega}^{\beta-2}\|Lu - Ls_u\|_{W_2^{\beta-2}(\Omega)} \\ &\leq Ch_{X,\Omega}^{\beta-2}\left\{\|Lu - Lu_\rho\|_{W_2^{\beta-2}(\Omega)} + \|Lu_\rho - Ls_{u_\rho}\|_{W_2^{\beta-2}(\Omega)}\right\} \\ &\leq Ch_{X,\Omega}^{\beta-2}\left\{\|Lu - Lu_\rho\|_{W_2^{\beta-2}(\Omega)} + h_{X,\Omega}^{\sigma-\beta}\|Lu_\rho - Ls_{u_\rho}\|_{W_2^{\sigma-2}(\Omega)}\right\} \\ &\leq Ch_{X,\Omega}^{\beta-2}\left\{\|u - u_\rho\|_{W_2^{\beta}(\Omega)} + h_{X,\Omega}^{\sigma-\beta}\|u_\rho - s_{u_\rho}\|_{W_2^{\sigma}(\Omega)}\right\}.\end{aligned}$$

Now we turn to the boundary error. Similar to the proof of Theorem 4.9, we have for the boundary error

$$\|u - s_u\|_{W_2^{1/2}(\partial\Omega)} \leq Ch_{Y,\partial\Omega}^{\beta-1}\|u - s_u\|_{W_2^{\beta-1/2}(\partial\Omega)}.$$

As before, we deduce from the above inequality that

$$\begin{aligned}\|u - s_u\|_{W_2^{1/2}(\partial\Omega)} &\leq Ch_{Y,\partial\Omega}^{\beta-1}\left\{\|u - u_\rho\|_{W_2^{\beta-1/2}(\partial\Omega)} + \|u_\rho - s_{u_\rho}\|_{W_2^{\beta-1/2}(\partial\Omega)}\right\} \\ &\leq Ch_{Y,\partial\Omega}^{\beta-1}\left\{\|u - u_\rho\|_{W_2^{\beta-1/2}(\partial\Omega)} + h_{Y,\partial\Omega}^{\sigma-\beta}\|u_\rho - s_{u_\rho}\|_{W_2^{\sigma-1/2}(\partial\Omega)}\right\} \\ &\leq Ch_{Y,\partial\Omega}^{\beta-1}\left\{\|u - u_\rho\|_{W_2^{\beta}(\Omega)} + h_{Y,\partial\Omega}^{\sigma-\beta}\|u_\rho - s_{u_\rho}\|_{W_2^{\sigma}(\Omega)}\right\},\end{aligned}$$

where in the second step we have used the sampling inequality and in the last step the trace theorem (Lemma 4.6). Setting $h = \max\{h_{X,\Omega}, h_{Y,\partial\Omega}\} < 1$ and combining both error estimates, we find

$$\|u - s_u\|_{L_2(\Omega)} \leq Ch^{\beta-2}\left\{\|Eu - u_\rho\|_{W_2^{\beta}(\mathbb{R}^d)} + h^{\sigma-\beta}\|u_\rho - s_{u_\rho}\|_{W_2^{\sigma}(\mathbb{R}^d)}\right\}.$$

Again, we estimate the two terms separately. From Lemma 6.3, we know

$$\|Eu - u_\rho\|_{W_2^{\beta}(\mathbb{R}^d)} \leq 5\|Eu\|_{W_2^{\beta}(\mathbb{R}^d)} \leq C\|u\|_{W_2^{\beta}(\Omega)}$$

thus giving us a bound for the first term. For the second term, we first note that since $\rho \geq 1$

$$\begin{aligned}\|u_\rho\|_{W_2^{\sigma}(\mathbb{R}^d)}^2 &= (2\pi)^{-d/2}\int_{\|\omega\|_2\leq\rho}\frac{|\widehat{u_\rho}(\omega)|^2}{(1+\|\omega\|_2^2)^{-\sigma}}d\omega \\ &= (2\pi)^{-d/2}\int_{\|\omega\|_2\leq\rho}|\widehat{u_\rho}(\omega)|^2(1+\|\omega\|_2^2)^{\beta}(1+\|\omega\|_2^2)^{\sigma-\beta}d\omega \\ &\leq (2\pi)^{-d/2}(1+\rho^2)^{\sigma-\beta}\|u_\rho\|_{W_2^{\beta}(\mathbb{R}^d)}^2 \\ &\leq (2\pi)^{-d/2}2^{\sigma-\beta}\rho^{2\sigma-2\beta}\|u_\rho\|_{W_2^{\beta}(\mathbb{R}^d)}^2 \\ &= C\rho^{2\sigma-2\beta}\|u_\rho\|_{W_2^{\beta}(\mathbb{R}^d)}^2.\end{aligned}$$

This is the crucial inequality that states that for band-limited functions we can bound stronger norms by weaker ones. Employing optimality, the above result and inequality (6.7), we now find

$$\begin{aligned} h^{\sigma-\beta}\|u_\rho - s_{u_\rho}\|_{W_2^\sigma(\mathbb{R}^d)} &\le Ch^{\sigma-\beta}\|u_\rho\|_{W_2^\sigma(\mathbb{R}^d)} \\ &\le Ch^{\sigma-\beta}\rho^{\sigma-\beta}\|u_\rho\|_{W_2^\beta(\mathbb{R}^d)} \\ &\le 6Ch^{\sigma-\beta}\rho^{\sigma-\beta}\|Eu\|_{W_2^\beta(\mathbb{R}^d)} \\ &= Cm^{\sigma-\beta}\left(\frac{h}{q}\right)^{\sigma-\beta}\|Eu\|_{W_2^\beta(\mathbb{R}^d)} \\ &\le C\left(\frac{h}{q}\right)^{\sigma-\beta}\|u\|_{W_2^\beta(\Omega)}, \end{aligned}$$

where in the second to the last step we have made use of our specific choice of ρ. Putting everything together, we find the desired result

$$\begin{aligned} \|u - s_u\|_{L_2(\Omega)} &\le Ch^{\beta-2}\left\{1 + \left(\frac{h}{q}\right)^{\sigma-\beta}\right\}\|u\|_{W_2^\beta(\Omega)} \\ &= Ch^{\beta-2}\|u\|_{W_2^\beta(\Omega)}. \end{aligned}$$

The last step follows from our assumption that the mesh ratio h/q is bounded.

□

6.2 Multilevel Collocation

Now we turn to translation-invariant kernels that depend on a scale $\delta > 0$. We define

$$\Psi_\delta(\mathbf{x}) = \delta^{-d}\Psi(\mathbf{x}/\delta).$$

Then, by Corollary 1.2 we know that $\widehat{\Psi_\delta}(\boldsymbol{\omega}) = \widehat{\Psi}(\delta\boldsymbol{\omega})$ holds. Furthermore, Ψ_δ shall generate $H^\beta(\mathbb{R}^d)$ and Φ_δ shall generate $H^\sigma(\mathbb{R}^d)$. Our goal is to extend Lemma 6.3 to scaled kernels.

Lemma 6.5 *Let $u \in H^\beta(\Omega)$, $\beta > d/2+2$, solve (3.5). Furthermore let $X = X_1 \cup X_2$ be a finite subset where $X_1 \subset \Omega$ and $X_2 \subset \partial\Omega$ with a separation distance q_X. Let X_1 consist of n interior and X_2 of $N-n$ boundary points. Finally let $\delta \in (0,1]$ and $\rho \ge m\delta/q_X$, where $m \ge 1$ is defined as in the proof of Lemma 6.3. Then there exists a function $u_{\rho/\delta} \in B^{\rho/\delta}$ with*

1. *$\lambda_k(u) = \lambda_k(u_{\rho/\delta})$ for $1 \le k \le N$ and*
2. *$\|Eu - u_{\rho/\delta}\|_{\Psi_\delta} \le 5\|Eu\|_{\Psi_\delta}$.*

Proof. In order to simplify our notation, let us scale the extended solution to the PDE. Therefore, we define $v \in H^\beta(\mathbb{R}^d)$ by $v(\mathbf{x}) = \delta^{d/2} Eu(\delta \mathbf{x})$. The Fourier transform is given by $\widehat{v}(\boldsymbol{\omega}) = \delta^{-d/2} \widehat{Eu}(\boldsymbol{\omega}/\delta)$. Now we define a scaled data set of the form

$$Z = \{\mathbf{z}_1, \ldots, \mathbf{z}_N\} = X/\delta = \{\mathbf{x}/\delta \in X\},$$

which has a scaled separation distance $q_Z = q_X/\delta$ as well as a scaled differential operator

$$\widetilde{L} = \sum_{i,j=1}^{d} \widetilde{a}_{ij} \partial_{ij} + \sum_{i=1}^{d} \widetilde{b}_i \partial_i + c,$$

where

$$\widetilde{a}_{ij} = \frac{a_{ij}}{\delta^2} \qquad \text{and} \qquad \widetilde{b}_i = \frac{b_i}{\delta}.$$

The coefficients a_{ij}, b_i and c come from the differential operator (3.6). Since $v \in H^\beta(\mathbb{R}^d)$, Lemma 6.3 assures the existence of a $v_\rho \in B^\rho$ such that

$$\lambda_j^Z(v) = \lambda_j^Z(v_\rho) \quad \text{and} \quad \|v - v_\rho\|_{H^\beta(\mathbb{R}^d)} \leq 5 \|v\|_{H^\beta(\mathbb{R}^d)}, \tag{6.8}$$

where

$$\lambda_j^Z = \begin{cases} \delta_{\mathbf{z}_j} \circ \widetilde{L}, & 1 \leq j \leq n, \\ \delta_{\mathbf{z}_j}, & n+1 \leq j \leq N. \end{cases}$$

Now we define $u_{\rho/\delta}(\mathbf{x}) = \delta^{-d/2} v_\rho(\mathbf{x}/\delta)$ with Fourier transform $\widehat{u}_{\rho/\delta}(\boldsymbol{\omega}) = \delta^{d/2} \widehat{v_\rho}(\delta \boldsymbol{\omega})$. Since $v_\rho \in B^\rho$, we have $u_{\rho/\delta} \in B^{\rho/\delta}$. Furthermore, for $1 \leq k \leq n$ we compute

$$\begin{aligned}
L[u_{\rho/\delta}](\mathbf{x}_k) &= \delta^{-d/2} L[v_\rho(\cdot/\delta)](\mathbf{x}_k) \\
&= \delta^{-d/2} \left[\sum_{i,j=1}^{d} a_{ij}(\cdot/\delta) \partial_{ij}[v_\rho(\cdot/\delta)] + \sum_{i=1}^{d} b_i(\cdot/\delta) \partial_i[v_\rho(\cdot/\delta)] + c(\cdot/\delta) v_\rho(\cdot/\delta) \right] (\mathbf{x}_k) \\
&= \delta^{-d/2} \left[\sum_{i,j=1}^{d} \frac{a_{ij}}{\delta^2} \partial_{ij}[v_\rho] + \sum_{i=1}^{d} \frac{b_i}{\delta} \partial_i[v_\rho] + c v_\rho \right] (\mathbf{x}_k/\delta) \\
&= \delta^{-d/2} \widetilde{L}^Z[v_\rho](\mathbf{z}_k).
\end{aligned}$$

Now by (6.8), we find

$$\begin{aligned}
L[u_{\rho/\delta}](\mathbf{x}_k) = \delta^{-d/2} \widetilde{L}^Z[v](\mathbf{z}_k) &= \widetilde{L}^Z[Eu(\delta\cdot)](\mathbf{z}_k) \\
&= \left[\sum_{i,j=1}^{d} \widetilde{a}_{ij}(\delta\cdot) \partial_{ij}[Eu(\delta\cdot)] + \sum_{i=1}^{d} \widetilde{b}_i(\delta\cdot) \partial_i[Eu(\delta\cdot)] + c(\delta\cdot) Eu(\delta\cdot) \right] (\mathbf{z}_k) \\
&= \left[\sum_{i,j=1}^{d} a_{ij} \partial_{ij}[Eu] + \sum_{i=1}^{d} b_i \partial_i[Eu] + cEu \right] (\delta \mathbf{z}_k) \\
&= L[Eu](\mathbf{x}_k).
\end{aligned}$$

For the boundary functionals, i. e. $n+1 \le k \le N$, we deduce

$$u_{\rho/\delta}(\mathbf{x}_k) = \delta^{-d/2} v_\rho(\mathbf{x}_k/\delta) = \delta^{-d/2} v_\rho(\mathbf{z}_k) = \delta^{-d/2} v(\mathbf{z}_k) = Eu(\delta \mathbf{z}_k) = Eu(\mathbf{x}_k),$$

again by (6.8). That is, we have now proven the generalised interpolation property

$$\lambda_k(u_{\rho/\delta}) = \lambda_k(Eu)$$

for $1 \le k \le N$. The inequality in (6.8) yields the second assertion, once we can show that

$$\|v - v_\rho\|_{H^\beta(\mathbb{R}^d)} = \|Eu - u_{\rho/\delta}\|_{\Psi_\delta} \quad \text{and} \quad \|v\|_{H^\beta(\mathbb{R}^d)} = \|Eu\|_{\Psi_\delta}.$$

The first equality follows from

$$\begin{aligned}
\|v - v_\rho\|^2_{H^\beta(\mathbb{R}^d)} &= (2\pi)^{-d/2} \int_{\mathbb{R}^d} |\widehat{(v - v_\rho)}(\boldsymbol{\omega})|^2 \left(1 + \|\boldsymbol{\omega}\|_2^2\right)^\beta d\boldsymbol{\omega} \\
&= (2\pi)^{-d/2} \delta^{-d} \int_{\mathbb{R}^d} |\widehat{Eu}(\boldsymbol{\omega}/\delta) - \widehat{u_{\rho/\delta}}(\boldsymbol{\omega}/\delta)|^2 \left(1 + \|\boldsymbol{\omega}\|_2^2\right)^\beta d\boldsymbol{\omega} \\
&= (2\pi)^{-d/2} \int_{\mathbb{R}^d} |\widehat{Eu}(\boldsymbol{\omega}) - \widehat{u_{\rho/\delta}}(\boldsymbol{\omega})|^2 \left(1 + \delta^2\|\boldsymbol{\omega}\|_2^2\right)^\beta d\boldsymbol{\omega} \\
&= (2\pi)^{-d/2} \int_{\mathbb{R}^d} \frac{|\widehat{Eu}(\boldsymbol{\omega}) - \widehat{u_{\rho/\delta}}(\boldsymbol{\omega})|^2}{\widehat{\Psi}(\delta\boldsymbol{\omega})} d\boldsymbol{\omega} \\
&= \|Eu - u_{\rho/\delta}\|^2_{\Psi_\delta}
\end{aligned}$$

and similarly one obtains the second equality from

$$\begin{aligned}
\|v\|^2_{H^\beta(\mathbb{R}^d)} &= (2\pi)^{-d/2} \int_{\mathbb{R}^d} |\widehat{v}(\boldsymbol{\omega})|^2 \left(1 + \|\boldsymbol{\omega}\|_2^2\right)^\beta d\boldsymbol{\omega} \\
&= (2\pi)^{-d/2} \delta^{-d} \int_{\mathbb{R}^d} |\widehat{Eu}(\boldsymbol{\omega}/\delta)|^2 \left(1 + \|\boldsymbol{\omega}\|_2^2\right)^\beta d\boldsymbol{\omega} \\
&= (2\pi)^{-d/2} \int_{\mathbb{R}^d} |\widehat{Eu}(\boldsymbol{\omega})|^2 \left(1 + \delta^2\|\boldsymbol{\omega}\|_2^2\right)^\beta d\boldsymbol{\omega} \\
&= \|Eu\|^2_{\Psi_\delta}.
\end{aligned}$$

□

We need to be able to bound the Φ_δ norm by the Ψ_δ norm. In some sense this is an inverse error bound because the kernel Φ_δ corresponds to the smoother Sobolev space $H^\sigma(\mathbb{R}^d)$ and the kernel Ψ_δ to the rougher space $H^\beta(\mathbb{R}^d)$. The following lemma comes from [87, Lemma 5].

Lemma 6.6 *Under the assumptions and using the same notation of Lemma 6.5 with $q_X \le \delta$, we have*

$$\|u_{\rho/\delta}\|_{\Phi_\delta} \le C\rho^{\sigma-\beta}\|Eu\|_{\Psi_\delta}.$$

Finally we bound the L_2 error between numerical and analytical solution to the PDE in such a way that the dependences on the mesh norm and the scale become obvious. These results will be the key element in our convergence proof of the multilevel algorithm for rougher target functions. Note that the constant ρ that controls the support of the Fourier transform is dependent on the scale δ.

Theorem 6.7 *Let $\Omega \subseteq \mathbb{R}^d$ be a bounded domain with a $C^{k,s}$ boundary for $k \in \mathbb{N}_0$ and $s \in [0,1)$. Assume the mesh ratio h/q is bounded, $\rho = m\delta/q$ and $q \leq \delta$. Then*

$$\|u - s_u\|_{L_2(\Omega)} \leq Ch^{\beta-2}\delta^{-\beta}\|Eu\|_{\Psi_\delta}$$

for $h = \max\{h_{X,\Omega}, h_{Y,\partial\Omega}\}$.

Proof. Just as in the proof of Theorem 6.4, we obtain for $u_{\rho/\delta} \in B^{\rho/\delta}$

$$\|u - s_u\|_{L_2(\Omega)} \leq Ch^{\beta-2}\left\{\|Eu - u_{\rho/\delta}\|_{W_2^\beta(\mathbb{R}^d)} + h^{\sigma-\beta}\|u_{\rho/\delta} - s_{u_{\rho/\delta}}\|_{W_2^\sigma(\mathbb{R}^d)}\right\}.$$

This time we need to be a bit more careful when using the near-best approximation property. It actually holds only in the Ψ_δ norm. However, when using the norm equivalence between the Ψ_δ norm and the Sobolev norm we introduce a scale-dependent constant. More precisely, we obtain

$$\|u - s_u\|_{L_2(\Omega)} \leq Ch^{\beta-2}\left\{\delta^{-\beta}\|Eu - u_{\rho/\delta}\|_{\Psi_\delta} + h^{\sigma-\beta}\delta^{-\sigma}\|u_{\rho/\delta} - s_{u_{\rho/\delta}}\|_{\Phi_\delta}\right\}.$$

We can bound the first norm by Lemma 6.5, i. e.

$$\|Eu - u_{\rho/\delta}\|_{\Psi_\delta} \leq 5\|Eu\|_{\Psi_\delta}.$$

For the second norm, we deduce by optimality, Lemma 6.6 and our assumption on ρ that

$$\begin{aligned}
h^{\sigma-\beta}\delta^{-\sigma}\|u_{\rho/\delta} - s_{u_{\rho/\delta}}\|_{\Phi_\delta} &\leq h^{\sigma-\beta}\delta^{-\sigma}\|u_{\rho/\delta}\|_{\Phi_\delta} \\
&\leq Ch^{\sigma-\beta}\delta^{-\sigma}\rho^{\sigma-\beta}\|Eu\|_{\Psi_\delta} \\
&= Ch^{\sigma-\beta}\delta^{-\sigma}\left(m\frac{\delta}{q}\right)^{\sigma-\beta}\|Eu\|_{\Psi_\delta} \\
&= C\left(m\frac{h}{q}\right)^{\sigma-\beta}\delta^{-\beta}\|Eu\|_{\Psi_\delta}.
\end{aligned}$$

That is, combining both estimates we find that

$$\|u - s_u\|_{L_2(\Omega)} \leq Ch^{\beta-2}\delta^{-\beta}\left\{1 + \left(m\frac{h}{q}\right)^{\sigma-\beta}\right\}\|Eu\|_{\Psi_\delta}.$$

Finally the assertion follows since we assumed the mesh ratio h/q to be bounded. □

The proof of the above theorem implies in particular the following corollary.

Corollary 6.8 *Under the same asumptions as above we have*

$$\|u - s_u\|_{H^\beta(\Omega)} \leq \|Eu - s_{Eu}\|_{H^\beta(\mathbb{R}^d)} \leq C\delta^{-\beta} \left\{ 1 + \left(m\frac{h}{q} \right)^{\sigma-\beta} \right\} \|Eu\|_{\Psi_\delta}.$$

Proof. Optimality and the triangle inequality implies

$$\|Eu - s_{Eu}\|_{H^\beta(\mathbb{R}^d)} \leq \|Eu - u_{\rho/\delta}\|_{H^\beta(\mathbb{R}^d)} + \|u_{\rho/\delta} - s_{u_{\rho/\delta}}\|_{H^\sigma(\mathbb{R}^d)}.$$

Then we only need to follow the same steps as in the proof above. □

Now, we can state and prove the following convergence theorem for the multilevel algorithm for rougher target functions. The proof is similar to the proof for smooth target functions, see Theorem 4.10. The main difference is that we have to use our bound on the L_2 error obtained through the near-best approximation property since optimality in the smoother Φ norm is not available.

Theorem 6.9 *Assume $u \in W_2^\beta(\Omega)$ solves (3.5). Let $k := \lfloor \beta \rfloor > 2 + d/2$ and the domain Ω have a $C^{k,s}$ boundary with $\beta = k+s$ for $s \in [0,1)$. We define two point set sequences. Firstly, let $X_1, X_2, \ldots$ be a sequence of point sets in Ω with mesh norms $h_{X_1,\Omega}, h_{X_2,\Omega}, \ldots$ such that the X_j contain no singular point of the operator L and let $Y_1, Y_2, \ldots$ be a sequence of point sets in $\partial\Omega$ with mesh norms $h_{Y_1,\partial\Omega}, h_{Y_2,\partial\Omega}, \ldots$. Set $h_j = \max\{h_{X_j,\Omega}, h_{Y_j,\partial\Omega}\}$ and assume*

$$\gamma\mu h_j \leq h_{j+1} \leq \mu h_j \tag{6.9}$$

for $j = 1, 2, ...$ and some fixed $\mu \in (0,1)$ and $\gamma \in (0,1)$ as well as the quasi uniformity condition

$$q_j \leq h_j \leq cq_j$$

where $q_j = q_{X_j \cup Y_j}$ for $j = 1, 2, \ldots$ and $c > 0$. Let Φ be a kernel satisfying

$$c_1(1 + \|\boldsymbol{\omega}\|_2^2)^{-\sigma} \leq \widehat{\Phi}(\boldsymbol{\omega}) \leq c_2(1 + \|\boldsymbol{\omega}\|_2^2)^{-\sigma}, \quad \boldsymbol{\omega} \in \mathbb{R}^d,$$

with two fixed constants $0 < c_1 \leq c_2$. Define $\delta_j = \left(\frac{h_j}{\mu}\right)^{1-\frac{2}{\beta}}$ and

$$\Psi_j(\mathbf{x} - \mathbf{y}) = \Psi_{\delta_j}(\mathbf{x} - \mathbf{y}) = \delta_j^{-d}\Psi((\mathbf{x} - \mathbf{y})/\delta_j),$$

where Ψ is a kernel generating $H^\beta(\mathbb{R}^d)$, defined via its Fourier transform

$$\widehat{\Psi}(\boldsymbol{\omega}) = (1 + \|\boldsymbol{\omega}\|_2^2)^{-\beta}, \quad \boldsymbol{\omega} \in \mathbb{R}^d$$

with $\sigma \geq \beta > d/2 + 2$. Lastly, let $h_1 \leq \mu$ be sufficiently small. Then, there exists a constant C independent of μ, j and u such that

$$\|Ee_j\|_{\Psi_{j+1}} \leq \alpha\|Ee_{j-1}\|_{\Psi_j},$$

for $j = 1, 2, \ldots$ with $\alpha = C\mu^{\beta-2}$. Thus, we have the estimate

$$\|u - u_n\|_{L_2(\Omega)} \leq C\alpha^n \|Ee_n\|_{H^\beta(\Omega)}$$

and the multiscale approximation u_n converges to u in the L_2 norm if we choose μ so small that $\alpha = C_0\mu^{\beta-2} < 1$.

Proof. First we see that

$$\delta_j = \left(\frac{h_j}{\mu}\right)^{1-\frac{2}{\beta}} \leq \left(\frac{h_j h_{j-1}}{h_j}\right)^{1-\frac{2}{\beta}} < \left(\frac{h_{j-1}}{\mu}\right)^{1-\frac{2}{\beta}} = \delta_{j-1}.$$

That is $\delta_j < \delta_1 \leq 1$ since $h_1 \leq \mu$ and $1 - \frac{2}{\beta} > 0$ due to our assumptions. Hence we can apply Lemma 2.30. We use the definition of the native space norm to obtain

$$\|Ee_j\|^2_{\Psi_{j+1}} = \int_{\mathbb{R}^d} |\widehat{Ee_j(\boldsymbol{\omega})}|^2 (1 + \delta_{j+1}^2 \|\boldsymbol{\omega}\|_2^2)^\beta d\boldsymbol{\omega} =: I_1 + I_2$$

with

$$I_1 = \int_{\|\boldsymbol{\omega}\|_2 \leq 1/\delta_{j+1}} |\widehat{Ee_j}(\boldsymbol{\omega})|^2 (1 + \delta_{j+1}^2 \|\boldsymbol{\omega}\|_2^2)^\beta d\boldsymbol{\omega}$$
$$I_2 = \int_{\|\boldsymbol{\omega}\|_2 \geq 1/\delta_{j+1}} |\widehat{Ee_j}(\boldsymbol{\omega})|^2 (1 + \delta_{j+1}^2 \|\boldsymbol{\omega}\|_2^2)^\beta d\boldsymbol{\omega}.$$

For the first term I_1, we obtain

$$\begin{aligned}
I_1 &\leq 2^\beta \int_{\mathbb{R}^d} |\widehat{Ee_j}(\boldsymbol{\omega})|^2 d\boldsymbol{\omega} = 2^\beta \|Ee_j\|^2_{L_2(\mathbb{R}^d)} && \text{by Parseval's identity} \\
&\leq C\|e_j\|^2_{L_2(\Omega)} && \text{by definition of } E \\
&\leq C h_j^{2(\beta-2)} \delta_j^{-2\beta} \|Ee_{j-1}\|^2_{\Psi_j} && \text{by Theorem 6.7} \\
&= C\mu^{2(\beta-2)} \|Ee_{j-1}\|^2_{\Psi_j},
\end{aligned}$$

where in the last step we have used

$$\mu^{2(\beta-2)} = \frac{h_j^{2(\beta-2)}}{\delta_j^{2\beta}}.$$

For the second term I_2, we obtain

$$
\begin{aligned}
I_2 &\leq 2^\beta \delta_{j+1}^{2\beta} \int_{\|\boldsymbol{\omega}\|_2 \geq 1/\delta_{j+1}} |\widehat{Ee_j}(\boldsymbol{\omega})|^2 \|\boldsymbol{\omega}\|_2^{2\beta} d\boldsymbol{\omega} \\
&\leq 2^\beta \delta_{j+1}^{2\beta} \int_{\|\boldsymbol{\omega}\|_2 \geq 1/\delta_{j+1}} |\widehat{Ee_j}(\boldsymbol{\omega})|^2 (1 + \|\boldsymbol{\omega}\|_2^2)^\beta d\boldsymbol{\omega} \\
&\leq 2^\beta \delta_{j+1}^{2\beta} \|Ee_j\|_{W_2^\beta(\mathbb{R}^d)}^2 \\
&\leq C\delta_{j+1}^{2\beta} \|e_j\|_{W_2^\beta(\Omega)}^2 = C\delta_{j+1}^{2\beta} \|Ee_{j-1} - s_{Ee_{j-1}}\|_{W_2^\beta(\Omega)}^2 \\
&\leq C\delta_{j+1}^{2\beta} \|Ee_{j-1} - s_{Ee_{j-1}}\|_{W_2^\beta(\mathbb{R}^d)}^2 \\
&\leq C\delta_{j+1}^{2\beta} \delta_j^{-2\beta} \|Ee_{j-1}\|_{\Psi_j}^2 && \text{by Corollary 6.8} \\
&\leq C\mu^{2(\beta-2)} \|Ee_{j-1}\|_{\Psi_j}^2,
\end{aligned}
$$

where in the last step we have used

$$
\left(\frac{\delta_{j+1}}{\delta_j}\right)^{2\beta} = \left(\frac{h_{j+1}}{h_j}\right)^{2(\beta-2)} \leq \mu^{2(\beta-2)}.
$$

Thus, in total we have

$$
\|Ee_j\|_{\Psi_{j+1}} \leq C_0 \mu^{\beta-2} \|Ee_{j-1}\|_{\Psi_j} \leq \alpha \|Ee_{j-1}\|_{\Psi_j}, \tag{6.10}
$$

with $\alpha = C_0\mu^{\beta-2}$. From this we can conclude

$$
\begin{aligned}
\|u - u_n\|_{L_2(\Omega)} &= \|e_n\|_{L_2(\Omega)} \\
&\leq C h_n^{\beta-2} \delta_{n+1}^{-\beta} \|Ee_n\|_{\Psi_{n+1}} && \text{by Theorem 6.7} \\
&\leq C \|Ee_n\|_{\Psi_{n+1}},
\end{aligned}
$$

where we have used in the last step that

$$
\frac{h_n^{\beta-2}}{\delta_{n+1}^\beta} = \left(\frac{h_n}{h_{n+1}}\right)^{\beta-2} \mu^{\beta-2} \leq \left(\frac{1}{\gamma\mu}\right)^{\beta-2} \mu^{\beta-2} = \gamma^{2-\beta}.
$$

Now applying (6.10) n times, we find

$$
\|u - u_n\|_{L_2(\Omega)} \leq C\|Ee_n\|_{\Psi_{n+1}} \leq C\alpha^n \|Eu\|_{W_2^\beta(\mathbb{R}^d)} \leq C\alpha^n \|u\|_{W_2^\beta(\Omega)}.
$$

□

6.3 Numerical Examples

Finally, we present a numerical example. We would like to solve a Poisson problem with Dirichlet boundary conditions. However, this time the solution to the elliptic PDE is supposed to lie in a rougher space than the numerical solution. We achieve this by creating the right-hand side from the relatively rough basis function $\phi_{2,1}$, namely from the boundary value problem

$$\begin{aligned} \Delta u(x,y) &= \Delta\phi_{2,1}(r(x,y)) \qquad \text{in} \quad \Omega = (0,1)^2, \\ u(x,y) &= \phi_{2,1}(r(x,y)) \qquad \text{on} \quad \partial\Omega, \end{aligned} \tag{6.11}$$

where $r(x,y) = \sqrt{(x-x_0)^2 + (y-y_0)^2}/\gamma$ with $x_0 = y_0 = \gamma = 0.5$.

As we know from Theorem 2.31, $\Phi_{d,k}$ generates $H^\tau(\mathbb{R}^d)$ where $\tau = d/2 + k + 1/2$. Since

$$\begin{aligned} \|\Phi_{d,k}\|^2_{H^\alpha(\mathbb{R}^d)} &= \int_{\mathbb{R}^d} |\widehat{\Phi_{d,k}}(\boldsymbol{\omega})|^2 (1 + \|\boldsymbol{\omega}\|^2)^\alpha d\boldsymbol{\omega} \\ &\leq C \int_{\mathbb{R}^d} (1 + \|\boldsymbol{\omega}\|^2)^{-2\tau} (1 + \|\boldsymbol{\omega}\|^2)^\alpha d\boldsymbol{\omega} \\ &= C \int_0^\infty (1 + r^2)^{-2\tau} (1 + r^2)^\alpha r^{d-1} dr \\ &< \infty \end{aligned}$$

if $\alpha < 2\tau - d/2$, we see that the solution to (6.11), i. e. $u = \phi_{2,1}$, lies in $H^\alpha(\mathbb{R}^2)$ with $\alpha < 4$.

On the other hand, we choose as basis function for the numerical solution $\phi_{2,4} \in \mathcal{N}_{\phi_{2,4}}(\mathbb{R}^2) = H^{5.5}(\mathbb{R}^2)$ so that $u \notin \mathcal{N}_{\phi_{2,4}}(\mathbb{R}^2)$. Even though the theorem is only proven for a relationship which is arbitrarily close to

$$\delta = (h/\mu)^{1-2/\beta},$$

where we have set $\beta = \sup\{\alpha < 4\} = 4$, we choose for our example the relationship

$$\delta = (h/\mu)^{1-2/\sigma}$$

with $\sigma = 5.5$. Since in the second case the support radii shrink faster than in the first case, the condition numbers will be lower. Unfortunately, the convergence proof works only for the former relationship. This is due to the following observation. When examining I_1 in the proof of the convergence theorem, we need to be able to bound $h^{\beta-2}/\delta^\beta$, which for the second relationship yields

$$\frac{h^{\beta-2}}{\delta^\beta} = \mu^{\beta-2\beta/\sigma} h^{-2+2\beta/\sigma} = \mu^{\beta-2} \left(\frac{\mu}{h}\right)^{2\varepsilon/\sigma},$$

where we have set $\beta = \sigma - \varepsilon$ for some $\varepsilon > 0$. However, for fixed μ this will tend to infinity as h decreases. So as long as μ is smaller than the mesh norm on the

N	H	$\|e\|_{L_2(\overline{\Omega})}$	$\|e\|_{L_2(\Omega)}$	$\|e\|_{L_2(\partial\Omega)}$	$\|e\|_{H^1(\overline{\Omega})}$	$\|e\|_{L_\infty(\overline{\Omega})}$	cond(A)
9	2^{-1}	1.97e+0	1.99e0	5.05e-2	9.30e0	4.14e0	1.5e3
25	2^{-2}	6.51e-1	6.56e-1	6.73e-3	3.33e0	1.69e0	7.5e4
81	2^{-3}	9.65e-2	9.73e-2	6.52e-4	5.28e-1	3.13e-1	1.3e7
289	2^{-4}	1.34e-2	1.35e-2	8.01e-5	8.42e-2	5.01e-2	1.8e9
1089	2^{-5}	1.84e-3	1.85e-3	7.86e-6	1.50e-2	7.60e-3	1.6e11
4225	2^{-6}	2.40e-4	2.42e-4	6.17e-7	2.83e-3	1.11e-3	1.4e13
16641	2^{-7}	2.95e-5	2.98e-5	3.68e-8	5.24e-4	1.55e-4	1.3e15

Table 6.1: Convergence study for the Poisson problem (6.11) with basis function $\phi_{2,4}$ and support radii $\delta = \nu\,(h/\mu)^{1-2/5.5}$ for $\mu = 0.5$ and $\nu = 2.4$.

N	H	$\|e\|_{L_2(\overline{\Omega})}$	$\|e\|_{L_2(\Omega)}$	$\|e\|_{L_2(\partial\Omega)}$	$\|e\|_{H^1(\overline{\Omega})}$	$\|e\|_{L_\infty(\overline{\Omega})}$	cond(A)
25	2^{-2}	1.60	1.60	2.91	1.48	1.29	-5.69
81	2^{-3}	2.75	2.75	3.37	2.66	2.43	-6.53
289	2^{-4}	2.84	2.84	3.03	2.65	2.64	-7.03
1089	2^{-5}	2.87	2.87	3.35	2.49	2.72	-6.48
4225	2^{-6}	2.93	2.93	3.67	2.41	2.78	-6.51
16641	2^{-7}	3.02	3.02	4.07	2.43	2.83	-6.53

Table 6.2: Convergence order for the Poisson problem (6.11) with basis function $\phi_{2,4}$ and support radii $\delta = \nu\,(h/\mu)^{1-2/5.5}$ for $\mu = 0.5$ and $\nu = 2.4$.

finest level, the bound will not blow up. This seems to be the case in our numerical example. Using the second relationship between mesh norm and support radii we still obtain convergence – at least for all seven levels considered here.

The results can be seen in Tables 6.1 and 6.2. We achieve a decent convergence rate, which is comparable to the nonescape case. The final error and residual as well as the behaviour of the L_2 error and the condition number are depicted in Figure 6.1. The blue line corresponds to the unpreconditioned case and the red line to a Jacobi preconditioner.

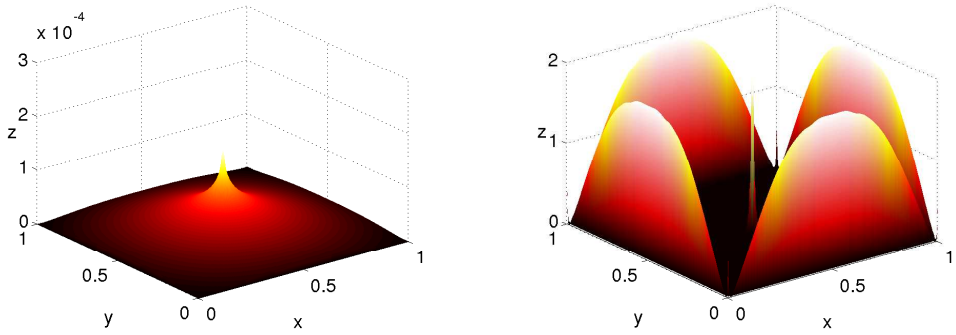

(a) Error on finest level

(b) Residual on finest level

(c) L_2 error

(d) Condition numbers

Figure 6.1: Multilevel approximation to (6.11) with basis function $\Phi_{2,4}$.

Chapter 7

Matrix-Valued Kernels

In this chapter, we introduce positive definite matrix-valued kernels, which we will eventually use to construct divergence-free kernels [65, 56, 57, 55, 36, 35]. Thus, this chapter serves mainly as an introduction to help us propose a numerical multilevel method for solving Darcy's problem subsequently. At the end, we prove the convergence of a multilevel method, which can be used to approximate divergence-free vector fields.

The theory for positive definite matrix-valued kernels was originally developed by Narcowich and Ward in [65]. We will follow an approach by Fuselier for introducing the theory [36, 35], which mimics some of the ideas from the scalar-valued case.

In the final two chapters, we will slightly deviate from earlier notation and denote with bold capital Greek letters matrix-valued and with lower-case Greek letters scalar-valued kernels. Previously, we used capital and lower-case letters to distinguish between kernels that take vectors or scalars as input.

7.1 Positive Definite Matrix-Valued Kernels

Let us start by making a reasonable generalisation of positive definite scalar-valued kernels.

Definition 7.1 *A continuous matrix-valued kernel* $\boldsymbol{\Phi}\colon \mathbb{R}^d \to \mathbb{R}^{n\times n}$ *is called* **positive definite** *if it is even,* $\boldsymbol{\Phi}(-\mathbf{x}) = \boldsymbol{\Phi}(\mathbf{x})$*, symmetric,* $\boldsymbol{\Phi}(\mathbf{x}) = \boldsymbol{\Phi}(\mathbf{x})^T$*, and if*

$$\sum_{j,k=1}^{N} \boldsymbol{\alpha}_j^T \boldsymbol{\Phi}(\mathbf{x}_j - \mathbf{x}_k)\boldsymbol{\alpha}_k > 0$$

for all pairwise distinct $\mathbf{x}_j \in \mathbb{R}^d$ *and all nonvanishing* $\boldsymbol{\alpha}_j \in \mathbb{R}^n$*.*

We will be mainly interested in two specific examples for matrix-valued positive definite kernels. Let $\phi, \psi\colon \mathbb{R}^d \to \mathbb{R}$ be positive definite functions and $\phi \in C^2(\mathbb{R}^d)$.

Then we define

$$\begin{aligned} &\boldsymbol{\Phi}_c\colon \mathbb{R}^d \to \mathbb{R}^{d\times d}, && \boldsymbol{\Phi}_c := -\nabla\nabla^T\phi \\ &\widetilde{\boldsymbol{\Phi}} : \mathbb{R}^d \to \mathbb{R}^{d\times d}, && \widetilde{\boldsymbol{\Phi}} := (-\Delta I + \nabla\nabla^T)\phi \\ &\boldsymbol{\Phi} : \mathbb{R}^d \to \mathbb{R}^{(d+1)\times(d+1)}, && \boldsymbol{\Phi} := \begin{pmatrix} \widetilde{\boldsymbol{\Phi}} & \mathbf{0} \\ \mathbf{0}^T & \psi \end{pmatrix} =: \widetilde{\boldsymbol{\Phi}} \otimes \psi, \end{aligned} \tag{7.1}$$

where Δ is the Laplacian, ∇ the gradient and I the d-dimensional identity matrix. The component-wise Fourier transforms of $\boldsymbol{\Phi}_c$ and $\widetilde{\boldsymbol{\Phi}}$ are given by

$$\widehat{\boldsymbol{\Phi}_c}(\boldsymbol{\omega}) = \boldsymbol{\omega}\boldsymbol{\omega}^T\widehat{\phi}(\boldsymbol{\omega}) \qquad \text{and} \qquad \widehat{\widetilde{\boldsymbol{\Phi}}}(\boldsymbol{\omega}) = \left(\|\boldsymbol{\omega}\|_2^2 I - \boldsymbol{\omega}\boldsymbol{\omega}^T\right)\widehat{\phi}(\boldsymbol{\omega}).$$

For just two space dimensions the kernel $\widetilde{\boldsymbol{\Phi}}$ takes the form

$$\boldsymbol{\Phi} = \begin{pmatrix} -\partial_{22} & \partial_{12} \\ \partial_{21} & -\partial_{11} \end{pmatrix}\phi = \begin{pmatrix} -\frac{x_2^2}{r^2}\phi''(r) - \frac{x_1^2}{r^3}\phi'(r) & \frac{x_1x_2}{r^2}\phi''(r) - \frac{x_1x_2}{r^3}\phi'(r) \\ \frac{x_1x_2}{r^2}\phi''(r) - \frac{x_1x_2}{r^3}\phi'(r) & -\frac{x_1^2}{r^2}\phi''(r) - \frac{x_2^2}{r^3}\phi'(r) \end{pmatrix},$$

where $r = \sqrt{x_1^2 + x_2^2}$. Therefore, it is obvious that these kernels are not radial. Nevertheless, they are commonly referred to as matrix-valued radial basis functions. All of the above kernels are indeed positive definite in the sense of Definition 7.1. The proof of the following theorem can partially be found in [35].

Theorem 7.2 *Let $\phi \in W_1^2(\mathbb{R}^d)\cap C^2(\mathbb{R}^d)$ and ψ be positive definite. Then the kernels $\boldsymbol{\Phi}_c$, $\widetilde{\boldsymbol{\Phi}}$ and $\boldsymbol{\Phi}$ are positive definite.*

Proof. We start with $\widetilde{\boldsymbol{\Phi}}$. We want to use the inverse Fourier transform theorem (Theorem 1.3). Any function can be recovered through the inverse Fourier transform if it is continuous and both the function and its Fourier transform are L_1 integrable. Since $\phi \in W_1^2(\mathbb{R}^d) \cap C^2(\mathbb{R}^d)$, we have $\partial_i\partial_j\phi \in L_1(\mathbb{R}^d) \cap C(\mathbb{R}^d)$ and in particular $-\Delta\phi \in L_1(\mathbb{R}^d) \cap C(\mathbb{R}^d)$. Additionally, the Fourier transform

$$\widehat{-\Delta\phi}(\boldsymbol{\omega}) = -\sum_{i=1}^d \widehat{\frac{\partial^2\phi}{\partial x_i^2}}(\boldsymbol{\omega}) = \sum_{i=1}^d \omega_i^2\widehat{\phi}(\boldsymbol{\omega}) = \|\boldsymbol{\omega}\|_2^2\widehat{\phi}(\boldsymbol{\omega})$$

is nonnegative and nonvanishing, which implies that $-\Delta\phi$ is positive definite. By Corollary 6.12 from [84], we deduce that $\widehat{-\Delta\phi} \in L_1(\mathbb{R}^d)$. Since

$$|\omega_i\omega_j\widehat{\phi}(\boldsymbol{\omega})| \le \|\boldsymbol{\omega}\|_2^2\widehat{\phi}(\boldsymbol{\omega})$$

we have that $\omega_i\omega_j\widehat{\phi}(\boldsymbol{\omega}) = \widehat{\partial_i\partial_j\phi} \in L_1(\mathbb{R}^d)$. Thus $\widetilde{\boldsymbol{\Phi}}$ can be recovered through its inverse Fourier transform.

Denoting with $(\cdot)^*$ the complex conjugate transpose, we can compute for $\mathbf{c}_j \in \mathbb{R}^d$

$$\sum_{j,k=1}^{N} \mathbf{c}_j^T \widetilde{\mathbf{\Phi}}(\mathbf{x}_j - \mathbf{x}_k)\mathbf{c}_k = (-2\pi)^{d/2} \sum_{j,k} \mathbf{c}_j^T \left(\int_{\mathbb{R}^d} \widehat{\widetilde{\mathbf{\Phi}}}(\boldsymbol{\omega}) e^{i\mathbf{x}_j^T\boldsymbol{\omega}} e^{-i\mathbf{x}_k^T\boldsymbol{\omega}} \right) \mathbf{c}_k d\boldsymbol{\omega}$$

$$= (-2\pi)^{d/2} \int_{\mathbb{R}^d} \left(\sum_j \mathbf{c}_j e^{-i\mathbf{x}_j^T\boldsymbol{\omega}} \right)^* \left(I - \frac{\boldsymbol{\omega}\boldsymbol{\omega}^T}{\|\boldsymbol{\omega}\|_2^2} \right) \widehat{\phi}(\boldsymbol{\omega}) \|\boldsymbol{\omega}\|_2^2 \left(\sum_k \mathbf{c}_k e^{-i\mathbf{x}_k^T\boldsymbol{\omega}} \right) d\boldsymbol{\omega}$$

$$= (-2\pi)^{d/2} \int_{\mathbb{R}^d} \left(\sum_j \mathbf{c}_j e^{-i\mathbf{x}_j^T\boldsymbol{\omega}} \right)^* \left(I - \frac{\boldsymbol{\omega}\boldsymbol{\omega}^T}{\|\boldsymbol{\omega}\|_2^2} \right)^2 \widehat{\phi}(\boldsymbol{\omega}) \|\boldsymbol{\omega}\|_2^2 \left(\sum_k \mathbf{c}_k e^{-i\mathbf{x}_k^T\boldsymbol{\omega}} \right) d\boldsymbol{\omega}$$

$$= (-2\pi)^{d/2} \int_{\mathbb{R}^d} \left\| \left(I - \frac{\boldsymbol{\omega}\boldsymbol{\omega}^T}{\|\boldsymbol{\omega}\|_2^2} \right) \left(\sum_j \mathbf{c}_j e^{-i\mathbf{x}_j^T\boldsymbol{\omega}} \right) \right\|_2^2 \widehat{\phi}(\boldsymbol{\omega}) \|\boldsymbol{\omega}\|_2^2 d\boldsymbol{\omega}$$

$$\geq 0.$$

We have used the fact that $\left(I - \frac{\boldsymbol{\omega}\boldsymbol{\omega}^T}{\|\boldsymbol{\omega}\|_2^2} \right)$ is a Hermitian projection matrix and hence satisfies for $\boldsymbol{\omega} \neq \mathbf{0}$

$$\left(I - \frac{\boldsymbol{\omega}\boldsymbol{\omega}^T}{\|\boldsymbol{\omega}\|_2^2} \right) = \left(I - \frac{\boldsymbol{\omega}\boldsymbol{\omega}^T}{\|\boldsymbol{\omega}\|_2^2} \right)^2 = \left(I - \frac{\boldsymbol{\omega}\boldsymbol{\omega}^T}{\|\boldsymbol{\omega}\|_2^2} \right)^* \left(I - \frac{\boldsymbol{\omega}\boldsymbol{\omega}^T}{\|\boldsymbol{\omega}\|_2^2} \right),$$

as well as the observation that by Corollary 1.2 the Fourier transform of the matrix-valued kernel $\widetilde{\mathbf{\Phi}}$ is given by

$$\widehat{\widetilde{\mathbf{\Phi}}}(\boldsymbol{\omega}) = i^2(-\|\boldsymbol{\omega}\|_2^2 I + \boldsymbol{\omega}\boldsymbol{\omega}^T)\widehat{\phi}(\boldsymbol{\omega}) = \left(I - \frac{\boldsymbol{\omega}\boldsymbol{\omega}^T}{\|\boldsymbol{\omega}\|_2^2} \right) \widehat{\phi}(\boldsymbol{\omega}) \|\boldsymbol{\omega}\|_2^2. \tag{7.2}$$

It remains to show that if the sum of quadratic forms is zero, then all coefficient vectors $\mathbf{c}_j$ are zero. By our previous calculations this reduces to showing that if the function $\mathbf{f}\colon \mathbb{R}^d \setminus \{\mathbf{0}\} \to \mathbb{C}^d$ defined by

$$\mathbf{f}(\boldsymbol{\omega}) := \left(I - \frac{\boldsymbol{\omega}\boldsymbol{\omega}^T}{\|\boldsymbol{\omega}\|_2^2} \right) \sum_{j=1}^{N} \mathbf{c}_j e^{-i\mathbf{x}_j^T\boldsymbol{\omega}}$$

is zero on $\mathbb{R}^d$ then all $\mathbf{c}_j = \mathbf{0}$ for $j = 1, \ldots, N$.

Consider some function $g\colon \mathbb{R}^d \to \mathbb{R}$ that can be recovered through Fourier inversion (that is $g \in C(\mathbb{R}^d) \cap L_1(\mathbb{R}^d)$ and $\widehat{g} \in L_1(\mathbb{R}^d)$). Additionally, the same shall be true for all second partial derivatives of g.

Then, we have

$$\begin{aligned}\mathbf{0} = \mathbf{f}(\boldsymbol{\omega}) = \mathbf{f}(\boldsymbol{\omega})\widehat{g}(\boldsymbol{\omega}) &= \sum_{j=1}^{N} \left(\|\boldsymbol{\omega}\|_2^2 I - \boldsymbol{\omega}\boldsymbol{\omega}^T\right) e^{-i\mathbf{x}_j^T\boldsymbol{\omega}} \widehat{g}(\boldsymbol{\omega})\mathbf{c}_j \\ &= \sum_{j=1}^{N} \left(\|\boldsymbol{\omega}\|_2^2 I - \boldsymbol{\omega}\boldsymbol{\omega}^T\right) \widehat{g(\cdot - \mathbf{x}_j)}(\boldsymbol{\omega})\mathbf{c}_j \\ &= -\left(\sum_{j=1}^{N} [\Delta I - \nabla\nabla^T] g(\cdot - \mathbf{x}_j)\mathbf{c}_j\right)\widehat{\ }(\boldsymbol{\omega}).\end{aligned}$$

Through Fourier inversion we obtain

$$h(\mathbf{x}) := \sum_{j=1}^{N} [\Delta I - \nabla\nabla^T] g(\mathbf{x} - \mathbf{x}_j)\mathbf{c}_j = \check{\mathbf{0}} = \mathbf{0}.$$

Denote with c_{ji} the ith component of the vector $\mathbf{c}_j$ and introduce a short-hand notation for the components of the operator matrix, namely let

$$(d_{jk})_{1\le j,k\le d} = \Delta I - \nabla\nabla^T.$$

Our goal is now to show that $c_{11} = 0$. The other components follow similarly. Up to now, we made only very few assumptions on g. Suppose g has compact support with support radius smaller than $\min_{j\neq k} \|\mathbf{x}_j - \mathbf{x}_k\|$ and additionally fulfills the d^2 Hermite-Birkhoff interpolation conditions

$$d_{k1} g(\mathbf{0}) = 1 \qquad \text{and} \qquad d_{kj} g(\mathbf{0}) = 0 \tag{7.3}$$

for all $k = 1, \ldots, d$ and $j = 2, \ldots, d$. Then we have due to the compact support

$$\mathbf{0} = h(\mathbf{x}_1) = \sum_{j=1}^{N} [\Delta I - \nabla\nabla^T] g(\mathbf{x}_1 - \mathbf{x}_j)\mathbf{c}_j = [\Delta I - \nabla\nabla^T] g(\mathbf{0})\mathbf{c}_1$$

or componentwise for any k

$$0 = \sum_{j=1}^{N} d_{kj} g(\mathbf{0}) c_{1j} = d_{k1} g(\mathbf{0}) c_{11} = c_{11},$$

where the last two equalities follow from our Hermite-Birkhoff interpolation conditions. The existence of such a function g follows from Hermite-Birkhoff theory [84, Theorems 16.4, 16.5]. The positive definiteness of $\boldsymbol{\Phi}_c$ can be shown analogously. For a proof see [35, Theorem 1].

Lastly $\boldsymbol{\Phi}$ is positive definite because $\widetilde{\boldsymbol{\Phi}}$ and ψ are. Let $\mathbf{c}_j = (\widetilde{\mathbf{c}}_j, c_j)^T \in \mathbb{R}^{d+1}$. Then

$$\sum_{j,k=1}^{N} \mathbf{c}_j^T \boldsymbol{\Phi}(\mathbf{x}_j - \mathbf{x}_k)\mathbf{c}_k = \sum_{j,k=1}^{N} \left\{ \widetilde{\mathbf{c}}_j^T \widetilde{\boldsymbol{\Phi}}(\mathbf{x}_j - \mathbf{x}_k)\widetilde{\mathbf{c}}_k + c_j \psi(\mathbf{x}_j - \mathbf{x}_k) c_k \right\} > 0.$$

□

We will call a vector-valued function $\mathbf{f}\colon \mathbb{R}^d \to \mathbb{R}^d$ *divergence-free* if

$$\operatorname{div}(\mathbf{f}) = \nabla \cdot \mathbf{f} = 0.$$

We will call it *curl-free* if there exists a scalar-valued function $f\colon \mathbb{R} \to \mathbb{R}$ such that

$$\operatorname{grad}(f) = \nabla f = \mathbf{f}.$$

In agreement with the previous definition we use the notation

$$\operatorname{curl}(\mathbf{f}) = \mathbf{0}$$

if such a function exists. If we take the gradient of the scalar-valued function $\partial_i \phi$ we obtain

$$\operatorname{grad}(\partial_i \phi) = \begin{pmatrix} \partial_{1i} \\ \vdots \\ \partial_{di} \end{pmatrix} \phi,$$

which is the ith column of $\mathbf{\Phi}_c$. This means that $\mathbf{\Phi}_c$ consists of curl-free columns. Similarly, if we form the divergence of the ith column of $\widetilde{\mathbf{\Phi}}$, we see that

$$\begin{aligned} \operatorname{div}(\widetilde{\mathbf{\Phi}}_i) &= \left[\partial_{1i1} + \ldots + \partial_{(i-1)i(i-1)} + \partial_i(-\Delta + \partial_{ii}) + \partial_{(i+1)i(i+1)} + \ldots + \partial_{did}\right] \phi \\ &= \left[\partial_i \Delta - \partial_i \Delta\right] \phi = 0. \end{aligned}$$

Thus, $\widetilde{\mathbf{\Phi}}$ has divergence-free columns.

7.1.1 Native Spaces for Matrix-Valued Kernels

We would like to introduce native spaces for matrix-valued kernels. We will follow here mostly ideas from [36]. It is possible to develop a similar Hilbert space theory as in the scalar-valued case. Define the function space

$$\mathbf{F}_{\mathbf{\Phi}}(\Omega) := \left\{ \sum_{j=1}^{N} \mathbf{\Phi}(\cdot - \mathbf{x}_j)\boldsymbol{\alpha}_j \mid \mathbf{x}_j \in \Omega, \boldsymbol{\alpha}_j \in \mathbb{R}^n \right\}$$

and equip it with the inner product

$$\left(\sum_{j=1}^{N} \mathbf{\Phi}(\cdot - \mathbf{x}_j)\boldsymbol{\alpha}_j, \sum_{k=1}^{M} \mathbf{\Phi}(\cdot - \mathbf{y}_k)\boldsymbol{\beta}_k \right)_{\mathbf{\Phi}} := \sum_{j=1}^{N} \sum_{k=1}^{M} \boldsymbol{\alpha}_j^T \Phi(\mathbf{x}_j - \mathbf{y}_k)\boldsymbol{\beta}_k.$$

Note that the bilinear form is indeed an inner product since Φ is assumed to be symmetric and positive definite.

There is also a kernel reproduction property. For $\mathbf{f} = \sum_{j=1}^{N} \mathbf{\Phi}(\cdot - \mathbf{x}_j)\boldsymbol{\alpha}_j \in \mathbf{F}_{\mathbf{\Phi}}(\Omega)$ and $\boldsymbol{\alpha} \in \mathbb{R}^n$ we find

$$\begin{aligned}(\mathbf{f}, \mathbf{\Phi}(\cdot - \mathbf{x})\boldsymbol{\alpha})_{\mathbf{\Phi}} &= \left(\sum_{j=1}^{N} \mathbf{\Phi}(\cdot - \mathbf{x}_j)\boldsymbol{\alpha}_j, \mathbf{\Phi}(\cdot - \mathbf{x})\boldsymbol{\alpha} \right)_{\mathbf{\Phi}} \\ &= \sum_{j=1}^{N} \boldsymbol{\alpha}_j^T \mathbf{\Phi}(\mathbf{x}_j - \mathbf{x})\boldsymbol{\alpha} \\ &= \sum_{j=1}^{N} \boldsymbol{\alpha}^T \mathbf{\Phi}(\mathbf{x}_j - \mathbf{x})^T \boldsymbol{\alpha}_j \\ &= \sum_{j=1}^{N} \boldsymbol{\alpha}^T \mathbf{\Phi}(\mathbf{x} - \mathbf{x}_j)\boldsymbol{\alpha}_j = \mathbf{f}(\mathbf{x})^T \boldsymbol{\alpha},\end{aligned} \tag{7.4}$$

where we have used the definition of the inner product as well as the fact that a positive definite $\mathbf{\Phi}$ is symmetric and even.

As in the scalar-valued case, we form the closure with respect to the norm induced by the inner product and denote it with $\mathcal{F}_{\mathbf{\Phi}}(\Omega)$, i. e.

$$\mathcal{F}_{\mathbf{\Phi}}(\Omega) := \overline{\mathbf{F}_{\mathbf{\Phi}}(\Omega)}^{\|\cdot\|_{\mathbf{\Phi}}}.$$

Again, it is not obvious what these abstract elements in the completion actually mean. But the scalar-valued case gives a good indication what to do. To interpret these elements as functions we define for an element $\mathbf{f} \in \mathcal{F}_{\mathbf{\Phi}}(\Omega)$ the function value

$$f_j(\mathbf{x}) := (\mathbf{f}, \mathbf{\Phi}(\cdot - \mathbf{x})\mathbf{e}_j)_{\mathbf{\Phi}}$$

where $\mathbf{e}_j$ denotes the jth canonical unit vector. Now we can interpret the abstract elements from the completion as continuous functions by defining a linear mapping $R\colon \mathcal{F}_{\mathbf{\Phi}}(\Omega) \to C(\Omega, \mathbb{R}^n)$, whose jth component $(1 \le j \le n)$ is given by

$$R(\mathbf{f})_j(\mathbf{x}) := f_j(\mathbf{x}) = (\mathbf{f}, \mathbf{\Phi}(\cdot - \mathbf{x})\mathbf{e}_j)_{\mathbf{\Phi}}\,.$$

We make several remarks. Firstly, $R(\mathbf{f})(\mathbf{x})$ defines actually a continuous function because for each component we find

$$\begin{aligned}|R(\mathbf{f})_j(\mathbf{x}) - R(\mathbf{f})_j(\mathbf{y})| &= (\mathbf{f}, (\mathbf{\Phi}(\cdot - \mathbf{x}) - \mathbf{\Phi}(\cdot - \mathbf{y}))\mathbf{e}_j)_{\mathbf{\Phi}} \\ &\le \|\mathbf{f}\|_{\mathbf{\Phi}} \|(\mathbf{\Phi}(\cdot - \mathbf{x}) - \mathbf{\Phi}(\cdot - \mathbf{y}))\mathbf{e}_j\|_{\mathbf{\Phi}},\end{aligned}$$

where

$$\|(\mathbf{\Phi}(\cdot - \mathbf{x}) - \mathbf{\Phi}(\cdot - \mathbf{y}))\mathbf{e}_j\|_{\mathbf{\Phi}}^2 = 2\mathbf{e}_j^T \mathbf{\Phi}(\mathbf{0})\mathbf{e}_j - 2\mathbf{e}_j^T \mathbf{\Phi}(\mathbf{x} - \mathbf{y})\mathbf{e}_j.$$

Thus as $\mathbf{x}$ tends to $\mathbf{y}$, $R(\mathbf{f})_j(\mathbf{x})$ tends to $R(\mathbf{f})_j(\mathbf{y})$ as $\mathbf{\Phi}$ is assumed to be continuous. Therefore each component of $R(\mathbf{f})$ is continuous, which implies that $R(\mathbf{f})$ defines a continuous function itself.

Furthermore, for $\mathbf{f} \in \mathbf{F}_\Phi(\Omega)$ we have

$$R(\mathbf{f})_j(\mathbf{x}) = (\mathbf{f}, \mathbf{\Phi}(\cdot - \mathbf{x})\mathbf{e}_j)_{\mathbf{\Phi}} = \mathbf{f}(\mathbf{x})^T\mathbf{e}_j \qquad \text{or} \qquad R(\mathbf{f}) = \mathbf{f} \tag{7.5}$$

by the kernel reproduction property for functions from $\mathbf{F}_\Phi(\Omega)$, see equation (7.4).

Lastly, we note that R is injective.

Lemma 7.3 *The mapping $R\colon \mathcal{F}_{\mathbf{\Phi}}(\Omega) \to C(\Omega, \mathbb{R}^n)$ is injective.*

Proof. For $\mathbf{f} \in \mathcal{F}_{\mathbf{\Phi}}(\Omega)$ consider $R(\mathbf{f}) = \mathbf{0}$. By the definition of the mapping we immediately deduce

$$(\mathbf{f}, \mathbf{\Phi}(\cdot - \mathbf{x})\mathbf{e}_j)_{\mathbf{\Phi}} = \mathbf{0}$$

for all $\mathbf{x} \in \Omega$ and $1 \leq j \leq n$. Thus $\mathbf{f}$ is perpendicular to the space $\mathbf{F}_{\mathbf{\Phi}}(\Omega)$. Since $\mathbf{f}$ lies in the closure of $\mathbf{F}_{\mathbf{\Phi}}(\Omega)$, we can find a sequence $\mathbf{f}_n$ in it that converges to $\mathbf{f}$. For each $\mathbf{f}_n \in \mathbf{F}_{\mathbf{\Phi}}(\Omega)$ the perpendicularity implies

$$0 = (\mathbf{f}, \mathbf{f}_n)_{\mathbf{\Phi}}\,.$$

After taking the limit and using the continuity of inner products, we then have $\|\mathbf{f}\|^2_{\mathbf{\Phi}} = 0$ or $\mathbf{f} = \mathbf{0}$. □

The injectivity means that $R\colon \mathcal{F}_{\mathbf{\Phi}}(\Omega) \to R(\mathcal{F}_{\mathbf{\Phi}}(\Omega)) \subseteq C(\Omega, \mathbb{R}^n)$ is actually a bijective mapping and we can identify each abstract element from $\mathcal{F}_{\mathbf{\Phi}}(\Omega)$ with a continuous function from $R(\mathcal{F}_{\mathbf{\Phi}}(\Omega))$. Just as in the scalar-valued case, this motivates us to define the native space as the image of R.

Definition 7.4 *The* **native space** *of a positive definite matrix-valued kernel $\mathbf{\Phi}$ is defined by*

$$\mathcal{N}_{\mathbf{\Phi}}(\Omega) := R(\mathcal{F}_{\mathbf{\Phi}}(\Omega)).$$

It is equipped with the inner product

$$(\mathbf{f}, \mathbf{g})_{\mathcal{N}_{\mathbf{\Phi}}(\Omega)} := \left(R^{-1}\mathbf{f}, R^{-1}\mathbf{g}\right)_{\mathbf{\Phi}}\,.$$

To simplify notation we will sometimes use $(\cdot,\cdot)_{\mathbf{\Phi}}$ instead of $(\cdot,\cdot)_{\mathcal{N}_{\mathbf{\Phi}}(\Omega)}$ and $\|\cdot\|_{\mathbf{\Phi}}$ instead of $\|\cdot\|_{\mathcal{N}_{\mathbf{\Phi}}(\Omega)}$. Since we work only with positive definite functions (and not conditionally positive definite functions) it should be clear what is meant.

As in the scalar-valued case, the native space is unique [35, Proposition 1]. We can also extend the kernel reproduction property (7.4) to the native space.

Lemma 7.5 (Kernel Reproduction Properties) *For $\mathbf{f} \in \mathcal{N}_{\mathbf{\Phi}}(\Omega), \boldsymbol{\alpha} \in \mathbb{R}^n$ and $\mathbf{x} \in \Omega$ we have*

$$\begin{aligned} \mathbf{\Phi}(\cdot - \mathbf{x})\boldsymbol{\alpha} &\in \mathcal{N}_{\mathbf{\Phi}}(\Omega), \\ (\mathbf{f}, \mathbf{\Phi}(\cdot - \mathbf{x})\boldsymbol{\alpha})_{\mathbf{\Phi}} &= \mathbf{f}(\mathbf{x})^T\boldsymbol{\alpha}. \end{aligned}$$

Proof. For the second property let $\mathbf{f} \in \mathcal{N}_{\mathbf{\Phi}}(\Omega)$ then there exists a unique $\mathbf{g} \in \mathcal{F}_{\mathbf{\Phi}}(\Omega)$ such that $R(\mathbf{g}) = \mathbf{f}$. We compute for $1 \leq j \leq n$

$$\begin{aligned}\mathbf{f}(\mathbf{x})^T\mathbf{e}_j = [R(\mathbf{g})(\mathbf{x})]^T\mathbf{e}_j = (\mathbf{g}, \mathbf{\Phi}(\cdot - \mathbf{x})\mathbf{e}_j)_{\mathbf{\Phi}} &= \left(R^{-1}\mathbf{f}, \mathbf{\Phi}(\cdot - \mathbf{x})\mathbf{e}_j\right)_{\mathbf{\Phi}} \\ &= (\mathbf{f}, \mathbf{\Phi}(\cdot - \mathbf{x})\mathbf{e}_j)_{\mathcal{N}_{\mathbf{\Phi}}(\Omega)},\end{aligned}$$

where in the last step we have used that R (and thus R^{-1} as well) leaves $\mathbf{\Phi}(\cdot - \mathbf{x})\mathbf{e}_j$ unaltered, see equation (7.5). This also immediately implies the first property. □

Thus the native space is a Hilbert space of continuous functions on the domain Ω with reproducing kernel $\mathbf{\Phi}$.

7.1.2 Alternative Characterisation of Native Spaces

In Chapter 2, we have seen that the native space of a scalar-valued translation-invariant kernel $\phi \in C(\mathbb{R}^d) \cap L_1(\mathbb{R}^d)$ can be characterised by

$$\mathcal{N}_\phi(\mathbb{R}^d) = \left\{ f \in L_2(\mathbb{R}^d) \cap C(\mathbb{R}^d) \mid \int_{\mathbb{R}^d} \frac{|\widehat{f}(\boldsymbol{\omega})|^2}{\widehat{\phi}(\boldsymbol{\omega})} d\boldsymbol{\omega} < \infty \right\},$$

equipped with an inner product

$$(f, g)_{\mathcal{N}_\phi(\mathbb{R}^d)} := (2\pi)^{-d/2} \int_{\mathbb{R}^d} \frac{\overline{\widehat{g}(\boldsymbol{\omega})}\widehat{f}(\boldsymbol{\omega})}{\widehat{\phi}(\boldsymbol{\omega})} d\boldsymbol{\omega}.$$

Unfortunately, the seemingly natural generalisation to matrix-valued kernel

$$(\mathbf{f}, \mathbf{g})_{\mathcal{N}_{\mathbf{\Phi}}(\mathbb{R}^d)} := (-2\pi)^{d/2} \int_{\mathbb{R}^d} \widehat{\mathbf{g}}(\boldsymbol{\omega})^* \widehat{\mathbf{\Phi}}(\boldsymbol{\omega})^{-1} \widehat{\mathbf{f}}(\boldsymbol{\omega}) d\boldsymbol{\omega}$$

would only work if $\widehat{\mathbf{\Phi}}(\boldsymbol{\omega})$ was invertible for all $\boldsymbol{\omega} \in \mathbb{R}^d$. However, since

$$\widehat{\widehat{\mathbf{\Phi}}}(\boldsymbol{\omega}) = \left(\|\boldsymbol{\omega}\|_2^2 I - \boldsymbol{\omega}\boldsymbol{\omega}^T\right) \widehat{\phi}(\boldsymbol{\omega}) \qquad \text{and} \qquad \widehat{\mathbf{\Phi}_c}(\boldsymbol{\omega}) = \boldsymbol{\omega}\boldsymbol{\omega}^T \widehat{\phi}(\boldsymbol{\omega})$$

have rank $d-1$ and 1 respectively, these matrices are not invertible for any $\boldsymbol{\omega} \in \mathbb{R}^d$. Therefore, Fuselier [36] suggested considering the Moore-Penrose inverse, which we denote with $\widehat{\mathbf{\Phi}}(\boldsymbol{\omega})^+$.

The Moore-Penrose inverse [39] for some matrix $A \in \mathbb{R}^{n \times m}$ is defined as the matrix $A^+ \in \mathbb{R}^{m \times n}$, which satisfies the following four conditions

1. $AA^+A = A$,
2. $A^+AA^+ = A^+$,
3. $(AA^+)^* = AA^+$,
4. $(A^+A)^* = A^+A$.

This generalised inverse always exists and is unique. With the help of the Moore-Penrose inverse, the inner product would be given by

$$(\mathbf{f},\mathbf{g})_{\mathcal{N}_\Phi(\mathbb{R}^d)} := (2\pi)^{-d/2}\int_{\mathbb{R}^d}\widehat{\mathbf{g}}(\boldsymbol{\omega})^*\widehat{\widetilde{\mathbf{\Phi}}}(\boldsymbol{\omega})^+\widehat{\mathbf{f}}(\boldsymbol{\omega})d\boldsymbol{\omega}. \tag{7.6}$$

Obviously we need to exclude those functions whose Fourier transforms are perpendicular to the columns of $\widehat{\widetilde{\mathbf{\Phi}}}(\boldsymbol{\omega})^+$. Otherwise the inner product would not be positive definite. It will turn out in the following discussion below that for the native space corresponding to the kernel $\widetilde{\mathbf{\Phi}}$ we will only allow divergence-free functions. On the other hand, for the native space belonging to $\mathbf{\Phi}_{\underline{c}}$ we only allow curl-free functions.

We compute the Moore-Penrose inverse for $\widehat{\widetilde{\mathbf{\Phi}}}(\boldsymbol{\omega})$. The properties of the Moore-Penrose inverse used in the following discussion can be found in [5]. Its singular value decomposition coincides with the eigenvalue decomposition, since it is a square, symmetric and positive semi-definite matrix, see (7.7) and (7.8). Thus there has to be a decomposition of the form

$$\widehat{\widetilde{\mathbf{\Phi}}}(\boldsymbol{\omega}) = U\Sigma U^T$$

where U is a $d\times d$ matrix that consists of eigenvectors $\mathbf{u}_i$ corresponding to non-negative eigenvalues σ_i, which Σ has as diagonal entries, i. e. $\Sigma = \operatorname{diag}(\sigma_1,\dots,\sigma_d)$. Note that in this special case we have $d = n$. It is relatively easy to compute the eigenvectors and their corresponding eigenvalues.

If $\boldsymbol{\omega} = \mathbf{0}$, then $\widehat{\widetilde{\mathbf{\Phi}}}(\boldsymbol{\omega})$ is the zero matrix, whose pseudo inverse is again the zero matrix. Let $\boldsymbol{\omega}\neq\mathbf{0}$. If we choose $d-1$ orthonormal vectors $\mathbf{u}_i$ that are perpendicular to $\boldsymbol{\omega}$, then we can compute

$$\widehat{\widetilde{\mathbf{\Phi}}}(\boldsymbol{\omega})\mathbf{u}_i = \left(\|\boldsymbol{\omega}\|_2^2 I - \boldsymbol{\omega}\boldsymbol{\omega}^t\right)\widehat{\phi}(\boldsymbol{\omega})\mathbf{u}_i = \widehat{\phi}(\boldsymbol{\omega})\|\boldsymbol{\omega}\|_2^2\mathbf{u}_i. \tag{7.7}$$

Therefore, the $\mathbf{u}_i$ are $d-1$ orthonormal eigenvectors with positive eigenvalues $\sigma_i = \widehat{\phi}(\boldsymbol{\omega})\|\boldsymbol{\omega}\|_2^2$ for $i = 1,\dots,d-1$. On the other hand, we have

$$\widehat{\widetilde{\mathbf{\Phi}}}(\boldsymbol{\omega})\boldsymbol{\omega} = \mathbf{0} \tag{7.8}$$

and hence $\mathbf{u}_d = \boldsymbol{\omega}/\|\boldsymbol{\omega}\|_2$ is a unit-norm eigenvector with corresponding eigenvalue $\sigma_d = 0$. Hence, we have

$$U = \left(\mathbf{u}_1,\dots,\mathbf{u}_{d-1},\boldsymbol{\omega}/\|\boldsymbol{\omega}\|_2\right).$$

Now, we are able to compute the Moore-Penrose inverse. Using the properties that for an invertible matrix $A^+ = A^{-1}$ and that $(AB)^+ = B^+A^+$ if either A has orthonormal columns or B has orthonormal rows, we compute

$$\widehat{\widetilde{\mathbf{\Phi}}}(\boldsymbol{\omega})^+ = \left(U\Sigma U^T\right)^+ = (U^T)^+\Sigma^+U^+ = U\Sigma^+U^T.$$

For a diagonal matrix we obtain the pseudo inverse by taking the reciprocal of each nonzero element, leaving zero elements unaltered. Hence we can proceed

$$\begin{aligned}
\widehat{\widetilde{\mathbf{\Phi}}}(\boldsymbol{\omega})^+ &= \frac{1}{\widehat{\phi}(\boldsymbol{\omega})\|\boldsymbol{\omega}\|_2^2} U \begin{pmatrix} 1 & & \\ & \ddots & \\ & & 1 \\ & & & 0 \end{pmatrix} \begin{pmatrix} \mathbf{u}_1^T \\ \vdots \\ \mathbf{u}_{d-1}^T \\ \boldsymbol{\omega}^T/\|\boldsymbol{\omega}\|_2 \end{pmatrix} = \frac{1}{\widehat{\phi}(\boldsymbol{\omega})\|\boldsymbol{\omega}\|_2^2} U \begin{pmatrix} \mathbf{u}_1^T \\ \vdots \\ \mathbf{u}_{d-1}^T \\ \mathbf{0}^T \end{pmatrix} \\
&= \frac{1}{\widehat{\phi}(\boldsymbol{\omega})\|\boldsymbol{\omega}\|_2^2} U \left[U^T - \begin{pmatrix} \mathbf{0}_1^T \\ \vdots \\ \mathbf{0}_{d-1}^T \\ \boldsymbol{\omega}^T/\|\boldsymbol{\omega}\|_2 \end{pmatrix} \right] \\
&= \frac{1}{\widehat{\phi}(\boldsymbol{\omega})\|\boldsymbol{\omega}\|_2^2} \left[I - \begin{pmatrix} \mathbf{u}_1, & \ldots, & \mathbf{u}_{d-1}, & \boldsymbol{\omega}/\|\boldsymbol{\omega}\|_2 \end{pmatrix} \begin{pmatrix} \mathbf{0}_1^T \\ \vdots \\ \mathbf{0}_{d-1}^T \\ \boldsymbol{\omega}^T/\|\boldsymbol{\omega}\|_2 \end{pmatrix} \right] \\
&= \frac{1}{\widehat{\phi}(\boldsymbol{\omega})\|\boldsymbol{\omega}\|_2^2} \left[I - \begin{pmatrix} \omega_1/\|\boldsymbol{\omega}\|_2^2 \boldsymbol{\omega}^T \\ \vdots \\ \omega_d/\|\boldsymbol{\omega}\|_2^2 \boldsymbol{\omega}^T \end{pmatrix} \right] = \frac{1}{\widehat{\phi}(\boldsymbol{\omega})\|\boldsymbol{\omega}\|_2^2} \left[I - \frac{\boldsymbol{\omega}\boldsymbol{\omega}^T}{\|\boldsymbol{\omega}\|_2^2} \right].
\end{aligned}$$

Thus, we have shown the first part of the following lemma.

Lemma 7.6 (Pseudo Inverses) *For $\boldsymbol{\omega} \neq \mathbf{0}$, we have*

$$\begin{aligned}
\widehat{\widetilde{\mathbf{\Phi}}}(\boldsymbol{\omega})^+ &= \frac{1}{\widehat{\phi}(\boldsymbol{\omega})\|\boldsymbol{\omega}\|_2^2} \left[I - \frac{\boldsymbol{\omega}\boldsymbol{\omega}^T}{\|\boldsymbol{\omega}\|_2^2} \right], \\
\widehat{\mathbf{\Phi}_c}(\boldsymbol{\omega})^+ &= \frac{1}{\widehat{\phi}(\boldsymbol{\omega})\|\boldsymbol{\omega}\|_2^2} \frac{\boldsymbol{\omega}\boldsymbol{\omega}^T}{\|\boldsymbol{\omega}\|_2^2}.
\end{aligned}$$

The second part can be shown analogously to the above. Finally, we can state two useful characterisations of the native spaces of $\widetilde{\mathbf{\Phi}}$ and $\mathbf{\Phi}_c$. The vector function space $\mathbf{L}_2(\mathbb{R}^d)$ and $\mathbf{C}(\mathbb{R}^d)$ mean that each component function lies in $L_2(\mathbb{R}^d)$ or $C(\mathbb{R}^d)$, respectively. A thorough definition follows in the Section 7.1.3.

Theorem 7.7 (Characterisation of Native Spaces) *Suppose the positive definite kernel ϕ lies in $W_1^2(\mathbb{R}^d) \cap C^2(\mathbb{R}^d)$. Then the native space of the divergence-free kernel is given by*

$$\mathcal{N}_{\widetilde{\mathbf{\Phi}}}(\mathbb{R}^d) = \left\{ \mathbf{f} \in \mathbf{L}_2(\mathbb{R}^d) \cap \mathbf{C}(\mathbb{R}^d) \mid \int_{\mathbb{R}^d} \frac{\|\widehat{\mathbf{f}}(\boldsymbol{\omega})\|_2^2}{\|\boldsymbol{\omega}\|_2^2 \widehat{\phi}(\boldsymbol{\omega})} d\boldsymbol{\omega} < \infty, \operatorname{div}(\mathbf{f}) = 0 \right\}$$

and the native space of the curl-free kernel is given by

$$\mathcal{N}_{\mathbf{\Phi}_c}(\mathbb{R}^d) = \left\{ \mathbf{f} \in \mathbf{L}_2(\mathbb{R}^d) \cap \mathbf{C}(\mathbb{R}^d) \mid \int_{\mathbb{R}^d} \frac{\|\widehat{\mathbf{f}}(\boldsymbol{\omega})\|_2^2}{\|\boldsymbol{\omega}\|_2^2 \widehat{\phi}(\boldsymbol{\omega})} d\boldsymbol{\omega} < \infty, \operatorname{curl}(\mathbf{f}) = 0 \right\}.$$

That means we have the same norm for both native spaces

$$\|\mathbf{f}\|^2_{\mathcal{N}_{\widetilde{\mathbf{\Phi}}}(\mathbb{R}^d)} = \|\mathbf{f}\|^2_{\mathcal{N}_{\mathbf{\Phi}_c}(\mathbb{R}^d)} = (2\pi)^{-d/2} \int_{\mathbb{R}^d} \frac{\|\widehat{\mathbf{f}}(\boldsymbol{\omega})\|_2^2}{\|\boldsymbol{\omega}\|_2^2 \widehat{\phi}(\boldsymbol{\omega})}.$$

Proofs of this can be found in [36, Theorem 2 and 3] as well as in [86, Theorem 3.4]. The spaces consist of different elements but are supplied with the same norm. Remember that we need to make sure that the bilinear form (7.6) is positive definite. Hence, we want to exclude the Fourier transforms of all nontrivial functions that lie in the nullspace of $\widehat{\mathbf{\Phi}}^+(\boldsymbol{\omega})$. In other words, we want to consider only those Fourier transformed functions for which $\widehat{\mathbf{\Phi}}^+(\boldsymbol{\omega})$ acts like the inverse, i. e.

$$\widehat{\mathbf{\Phi}}(\boldsymbol{\omega})\widehat{\mathbf{\Phi}}^+(\boldsymbol{\omega})\widehat{\mathbf{f}}(\boldsymbol{\omega}) = \widehat{\mathbf{f}}(\boldsymbol{\omega}).$$

The first native space in Theorem 7.7 consists only of divergence-free functions. In terms of Fourier transforms, that means these functions need to satisfy $\boldsymbol{\omega}^T\widehat{\mathbf{f}}(\boldsymbol{\omega}) = 0$. In this case the above identity indeed holds:

$$\widehat{\widetilde{\mathbf{\Phi}}}(\boldsymbol{\omega})\widehat{\widetilde{\mathbf{\Phi}}}^+(\boldsymbol{\omega})\widehat{\mathbf{f}}(\boldsymbol{\omega}) = \left(I - \frac{\boldsymbol{\omega}\boldsymbol{\omega}^T}{\|\boldsymbol{\omega}\|_2^2}\right)^2 \widehat{\mathbf{f}}(\boldsymbol{\omega}) = \left(I - \frac{\boldsymbol{\omega}\boldsymbol{\omega}^T}{\|\boldsymbol{\omega}\|_2^2}\right) \widehat{\mathbf{f}}(\boldsymbol{\omega}) = \widehat{\mathbf{f}}(\boldsymbol{\omega}).$$

On the other hand, the second native space consists only of curl-free functions. In terms of Fourier transforms, that means these functions need to satisfy $\widehat{\mathbf{f}}(\boldsymbol{\omega}) = \boldsymbol{\omega}\widehat{h}(\boldsymbol{\omega})$ for some scalar-valued function h. Again, we can compute

$$\widehat{\mathbf{\Phi}_c}(\boldsymbol{\omega})\widehat{\mathbf{\Phi}_c}^+(\boldsymbol{\omega})\widehat{\mathbf{f}}(\boldsymbol{\omega}) = \left(\frac{\boldsymbol{\omega}\boldsymbol{\omega}^T}{\|\boldsymbol{\omega}\|_2^2}\right)^2 \widehat{\mathbf{f}}(\boldsymbol{\omega}) = \left(\frac{\boldsymbol{\omega}\boldsymbol{\omega}^T}{\|\boldsymbol{\omega}\|_2^2}\right) \boldsymbol{\omega}\widehat{h}(\boldsymbol{\omega}) = \boldsymbol{\omega}\widehat{h}(\boldsymbol{\omega}) = \widehat{\mathbf{f}}(\boldsymbol{\omega}).$$

Lastly, we state a theorem that characterises matrix-valued kernels that have a tensor product nature. The theorem can be found in [86, Proposition 3.9].

Theorem 7.8 *Assume that $\phi, \psi\colon \mathbb{R}^d \to \mathbb{R}$ are positive definite and additionally let $\phi \in W_1^2(\mathbb{R}^d) \cap C^2(\mathbb{R}^d)$. Then, the native space of the kernel $\mathbf{\Phi} = \widetilde{\mathbf{\Phi}} \otimes \psi$, with $\widetilde{\mathbf{\Phi}}$ defined as in* (7.1)*, is given by*

$$\mathcal{N}_{\mathbf{\Phi}}(\mathbb{R}^d) = \mathcal{N}_{\widetilde{\mathbf{\Phi}}}(\mathbb{R}^d) \times \mathcal{N}_{\psi}(\mathbb{R}^d)$$

with its norm for some $\mathbf{f} = (\mathbf{f_u}, f_p)^T$ given by

$$\begin{aligned}\|\mathbf{f}\|^2_{\mathcal{N}_{\mathbf{\Phi}}(\mathbb{R}^d)} &= \|\mathbf{f_u}\|^2_{\mathcal{N}_{\widetilde{\mathbf{\Phi}}}(\mathbb{R}^d)} + \|f_p\|^2_{\mathcal{N}_{\psi}(\mathbb{R}^d)} \\ &= (2\pi)^{-d/2} \int_{\mathbb{R}^d} \left[\frac{\|\widehat{\mathbf{f_u}}(\boldsymbol{\omega})\|_2^2}{\|\boldsymbol{\omega}\|_2^2 \widehat{\phi}(\boldsymbol{\omega})} + \frac{|\widehat{f_p}(\boldsymbol{\omega})|^2}{\widehat{\psi}(\boldsymbol{\omega})} \right] d\boldsymbol{\omega}.\end{aligned}$$

7.1.3 Native Spaces as Sobolev Spaces

As in the scalar-valued case, it is possible to interpret the native space under some assumptions as some type of Sobolev space. From Chapter 2 we know that the native space of a scalar-valued function is norm-equivalent to a classical Sobolev space if the Fourier transform of the kernel has algebraic decay, see Corollary 2.29.

We define the vector-valued Sobolev space $\mathbf{W}_r^\sigma(\Omega)$ to consist of those vector functions $\mathbf{u} = (u_1, \dots, u_d)^T \colon \Omega \to \mathbb{R}^d$ for which each component lies in the scalar-valued Sobolev space $W_r^\sigma(\Omega)$. A norm on the vector-valued Sobolev space can be defined with the help of the scalar-valued Sobolev norm in the following way

$$\|\mathbf{u}\|_{\mathbf{W}_r^\sigma(\Omega)} = \begin{cases} \left(\sum_{j=1}^d \|u_j\|_{W_r^\sigma(\Omega)}^r\right)^{1/r} & \text{for } 1 \leq r < \infty, \\ \max_{1\leq j\leq d} \|u_j\|_{W_\infty^\sigma(\Omega)} & \text{for } r = \infty. \end{cases}$$

This means we take the discrete ℓ_r norm of the Sobolev norms of each component for the vector function $\mathbf{u}$. Furthermore, for $r = 2$ we will use the notation $\mathbf{H}^\sigma(\Omega) = \mathbf{W}_2^\sigma(\Omega)$. We introduce divergence-free and curl-free Sobolev spaces,

$$\mathbf{H}^\sigma(\mathbb{R}^d, \operatorname{div}) = \left\{ \mathbf{f} \in \mathbf{H}^\sigma(\mathbb{R}^d) \mid \operatorname{div}(\mathbf{f}) = 0 \right\},$$
$$\mathbf{H}^\sigma(\mathbb{R}^d, \operatorname{curl}) = \left\{ \mathbf{f} \in \mathbf{H}^\sigma(\mathbb{R}^d) \mid \operatorname{curl}(\mathbf{f}) = 0 \right\}.$$

With the help of the spaces we define

$$\widetilde{\mathbf{H}}^\sigma(\mathbb{R}^d) = \left\{ \mathbf{f} \in \mathbf{H}^\sigma(\mathbb{R}^d) \mid \int_{\mathbb{R}^d} \frac{\|\widehat{\mathbf{f}}(\boldsymbol{\omega})\|_2^2}{\|\boldsymbol{\omega}\|_2^2} (1 + \|\boldsymbol{\omega}\|_2^2)^{\sigma+1} d\boldsymbol{\omega} < \infty \right\},$$
$$\widetilde{\mathbf{H}}^\sigma(\mathbb{R}^d, \operatorname{div}) = \left\{ \mathbf{f} \in \mathbf{H}^\sigma(\mathbb{R}^d, \operatorname{div}) \mid \int_{\mathbb{R}^d} \frac{\|\widehat{\mathbf{f}}(\boldsymbol{\omega})\|_2^2}{\|\boldsymbol{\omega}\|_2^2} (1 + \|\boldsymbol{\omega}\|_2^2)^{\sigma+1} d\boldsymbol{\omega} < \infty \right\},$$
$$\widetilde{\mathbf{H}}^\sigma(\mathbb{R}^d, \operatorname{curl}) = \left\{ \mathbf{f} \in \mathbf{H}^\sigma(\mathbb{R}^d, \operatorname{curl}) \mid \int_{\mathbb{R}^d} \frac{\|\widehat{\mathbf{f}}(\boldsymbol{\omega})\|_2^2}{\|\boldsymbol{\omega}\|_2^2} (1 + \|\boldsymbol{\omega}\|_2^2)^{\sigma+1} d\boldsymbol{\omega} < \infty \right\}.$$

All the spaces introduced in this section are obviously related. Let us consider a divergence-free velocity $\mathbf{u}$, which lies in the space $\widetilde{\mathbf{H}}^\sigma(\mathbb{R}^d, \operatorname{div})$ for some $\sigma > 0$. This space, however, is a subspace of $\mathbf{H}^\sigma(\mathbb{R}^d)$. Therefore, we may sometimes write $\mathbf{u}$ in the $\mathbf{H}^\sigma(\mathbb{R}^d)$ norm as well. Moreover, the following lemma holds:

Lemma 7.9 (Relationship between different Sobolev Norms) *We can bound the* $\mathbf{H}^\sigma(\mathbb{R}^d)$ *norm as follows:*

$$\|\mathbf{u}\|_{\mathbf{H}^\sigma(\mathbb{R}^d)} \leq \|\mathbf{u}\|_{\widetilde{\mathbf{H}}^\sigma(\mathbb{R}^d)}.$$

Proof. Using the definition, we obtain

$$\begin{aligned}
\|\mathbf{u}\|^2_{\mathbf{H}^\sigma(\mathbb{R}^d)} &= \sum_{j=1}^n \|u_j\|^2_{H^\sigma(\mathbb{R}^d)} = \sum_{j=1}^n \int_{\mathbb{R}^d} |\widehat{u_j}(\boldsymbol{\omega})|^2 (1+\|\boldsymbol{\omega}\|_2^2)^\sigma d\boldsymbol{\omega} \\
&= \int_{\mathbb{R}^d} \sum_{j=1}^n |\widehat{u_j}(\boldsymbol{\omega})|^2 (1+\|\boldsymbol{\omega}\|_2^2)^\sigma d\boldsymbol{\omega} \\
&= \int_{\mathbb{R}^d} \|\widehat{\mathbf{u}}(\boldsymbol{\omega})\|_2^2 (1+\|\boldsymbol{\omega}\|_2^2)^\sigma d\boldsymbol{\omega} \\
&\leq \int_{\mathbb{R}^d} \frac{\|\widehat{\mathbf{u}}(\boldsymbol{\omega})\|_2^2}{\|\boldsymbol{\omega}\|_2^2} (1+\|\boldsymbol{\omega}\|_2^2)^{\sigma+1} d\boldsymbol{\omega} \\
&= \|\mathbf{u}\|_{\widetilde{\mathbf{H}}^\sigma(\mathbb{R}^d)},
\end{aligned}$$

where we have used that $1 \leq \frac{1+\|\boldsymbol{\omega}\|_2^2}{\|\boldsymbol{\omega}\|_2^2}$. □

Now we are able to state another characterisation of the native spaces that we discussed so far.

Theorem 7.10 (Native Spaces as Sobolev Spaces) *Let ϕ generate $H^{\sigma+1}(\mathbb{R}^d)$ and ψ generate $H^\tau(\mathbb{R}^d)$, i. e. $\mathcal{N}_\phi(\mathbb{R}^d) = H^{\sigma+1}(\mathbb{R}^d)$ and $\mathcal{N}_\psi(\mathbb{R}^d) = H^\tau(\mathbb{R}^d)$. Then, the native spaces can be characterised through*

$$\begin{aligned}
\mathcal{N}_{\widetilde{\mathbf{\Phi}}}(\mathbb{R}^d) &= \widetilde{\mathbf{H}}^\sigma(\mathbb{R}^d, \operatorname{div}), \\
\mathcal{N}_{\mathbf{\Phi}_c}(\mathbb{R}^d) &= \widetilde{\mathbf{H}}^\sigma(\mathbb{R}^d, \operatorname{curl}), \\
\mathcal{N}_{\mathbf{\Phi}}(\mathbb{R}^d) &= \widetilde{\mathbf{H}}^\sigma(\mathbb{R}^d, \operatorname{div}) \times H^\tau(\mathbb{R}^d).
\end{aligned}$$

Proofs can be found in [36, 86].

We finish this section by introducing a vector-valued extension operator since again we are mostly interested in bounded domains and therefore need to extend our locally defined Sobolev functions to functions defined on the whole Euclidean space. The following result is taken from [86, Proposition 3.8.]. We denote the scalar-valued extension operator, which we have introduced in Section 4.2.1, now with E_S to avoid confusion.

Proposition 7.11 (Extension Operator) *Suppose either $d = 2$ or $d = 3$. Let $\sigma, \tau \geq 0$ and let $\Omega \subseteq \mathbb{R}^d$ be a simply-connected domain with $C^{k,1}$ boundary, where $k \geq \sigma$ is some integer. Then there exists a continuous operator*

$$\mathbf{E} = (\widetilde{\mathbf{E}}_{\operatorname{div}}, E_S) \colon \mathbf{H}^\sigma(\Omega, \operatorname{div}) \times H^\tau(\Omega) \to \widetilde{\mathbf{H}}^\sigma(\mathbb{R}^d, \operatorname{div}) \times H^\tau(\mathbb{R}^d)$$

such that

1. $\mathbf{E}\mathbf{v}|_\Omega = \mathbf{v}|_\Omega \qquad$ *for all* $\qquad \mathbf{v} = (\mathbf{u}, p) \in \mathbf{H}^\sigma(\Omega, \operatorname{div}) \times H^\tau(\Omega)$,
2. $\|\widetilde{\mathbf{E}}_{\operatorname{div}}\mathbf{u}\|_{\widetilde{\mathbf{H}}^\sigma(\mathbb{R}^d, \operatorname{div})} + \|E_S p\|_{H^\tau(\mathbb{R}^d)} \leq C \left(\|\mathbf{u}\|_{\mathbf{H}^\sigma(\Omega, \operatorname{div})} + \|p\|_{H^\tau(\Omega)} \right)$,

for some $C > 0$.

7.1.4 Reconstruction Problem

The following discussion is well-known from the theory of scalar-valued kernels which can easily be extended to matrix-valued kernels [86]. We provide it nevertheless to remind us of some of the key results. Suppose we want to reconstruct data $\mathbf{f}_1, \ldots, \mathbf{f}_N \in \mathbb{R}^n$ at scattered data points $X = \{\mathbf{x}_1, \ldots, \mathbf{x}_N\} \subset \mathbb{R}^d$. For some coefficient vectors $\boldsymbol{\alpha}_j$, we can set up a vector-valued interpolant of the form

$$\mathbf{s}_{\mathbf{f},X} := \sum_{j=1}^{N} \boldsymbol{\Phi}(\cdot - \mathbf{x}_j)\boldsymbol{\alpha}_j \tag{7.9}$$

and apply to it the interpolation conditions

$$\mathbf{s}_{\mathbf{f},X}(\mathbf{x}_k) = \mathbf{f}_k \tag{7.10}$$

for $k = 1, \ldots, N$. This means we have to solve the $nN \times nN$ block matrix system

$$\begin{pmatrix} \boldsymbol{\Phi}(\mathbf{x}_1 - \mathbf{x}_1) & \ldots & \boldsymbol{\Phi}(\mathbf{x}_1 - \mathbf{x}_N) \\ \vdots & & \vdots \\ \boldsymbol{\Phi}(\mathbf{x}_N - \mathbf{x}_1) & \ldots & \boldsymbol{\Phi}(\mathbf{x}_N - \mathbf{x}_N) \end{pmatrix} \begin{pmatrix} \boldsymbol{\alpha}_1 \\ \vdots \\ \boldsymbol{\alpha}_N \end{pmatrix} = \begin{pmatrix} \mathbf{f}_1 \\ \vdots \\ \mathbf{f}_N \end{pmatrix}$$

or in abbreviated form

$$A_{\boldsymbol{\Phi},X}\boldsymbol{\alpha} = \mathbf{f}. \tag{7.11}$$

Note that for $\boldsymbol{\beta} = (\boldsymbol{\beta}_1, \ldots, \boldsymbol{\beta}_N)^T \in \mathbb{R}^{nN}$, we have

$$\boldsymbol{\beta}^T A_{\boldsymbol{\Phi},X}\boldsymbol{\beta} = \sum_{j,k=1}^{N} \boldsymbol{\beta}_j^T \boldsymbol{\Phi}(\mathbf{x}_j - \mathbf{x}_k)\boldsymbol{\beta}_k > 0,$$

since $\boldsymbol{\Phi}$ is a positive definite kernel. Therefore, the matrix is positive definite and the interpolant (7.9) with coefficient vectors determined by (7.11) exists and is unique.

Assuming the data are generated by $\mathbf{f}_j = \mathbf{f}(\mathbf{x}_j)$, the interpolant $\mathbf{s}_{\mathbf{f},X}$ is the best approximation in

$$\mathbf{V}_X = \left\{ \sum_{j=1}^{N} \boldsymbol{\Phi}(\cdot - \mathbf{x}_j)\boldsymbol{\beta}_j \mid \boldsymbol{\beta}_j \in \mathbb{R}^n \right\}.$$

This is a direct consequence from Lemma 7.5 because for any $\mathbf{g} = \sum_{j=1}^{N} \boldsymbol{\Phi}(\cdot - \mathbf{x}_j)\boldsymbol{\beta}_j \in \mathbf{V}_X$ we deduce the best approximation property

$$\begin{aligned} (\mathbf{f} - \mathbf{s}_{\mathbf{f},X}, \mathbf{g})_{\boldsymbol{\Phi}} &= \sum_{j=1}^{N} \left(\mathbf{f} - \mathbf{s}_{\mathbf{f},X}, \boldsymbol{\Phi}(\cdot - \mathbf{x}_j)\boldsymbol{\beta}_j\right)_{\boldsymbol{\Phi}} \\ &= \sum_{j=1}^{N} \left[\mathbf{f}(\mathbf{x}_j) - \mathbf{s}_{\mathbf{f},X}(\mathbf{x}_j)\right]^T \boldsymbol{\beta}_j = \mathbf{0}, \end{aligned}$$

where we have used the interpolation condition (7.10) in the last step. This best approximation property immediately implies two stability results. Namely,

$$\|\mathbf{f} - \mathbf{s}_{\mathbf{f},X}\|_{\mathbf{\Phi}} \leq \|\mathbf{f}\|_{\mathbf{\Phi}} \qquad \text{and} \qquad \|\mathbf{s}_{\mathbf{f},X}\|_{\mathbf{\Phi}} \leq \|\mathbf{f}\|_{\mathbf{\Phi}}.$$

The first inequality follows from the best approximation property for $\mathbf{g} = \mathbf{s}_{\mathbf{f},X}$ as well as the Cauchy-Schwarz inequality

$$\|\mathbf{f} - \mathbf{s}_{\mathbf{f},X}\|_{\mathbf{\Phi}}^2 = (\mathbf{f} - \mathbf{s}_{\mathbf{f},X}, \mathbf{f} - \mathbf{s}_{\mathbf{f},X})_{\mathbf{\Phi}} = (\mathbf{f} - \mathbf{s}_{\mathbf{f},X}, \mathbf{f})_{\mathbf{\Phi}} \leq \|\mathbf{f} - \mathbf{s}_{\mathbf{f},X}\|_{\mathbf{\Phi}} \|\mathbf{f}\|_{\mathbf{\Phi}}.$$

Similarly, we obtain the second inequality from

$$\|\mathbf{s}_{\mathbf{f},X}\|_{\mathbf{\Phi}}^2 = (\mathbf{s}_{\mathbf{f},X}, \mathbf{s}_{\mathbf{f},X})_{\mathbf{\Phi}} + (\mathbf{f} - \mathbf{s}_{\mathbf{f},X}, \mathbf{s}_{\mathbf{f},X})_{\mathbf{\Phi}} = (\mathbf{f}, \mathbf{s}_{\mathbf{f},X})_{\mathbf{\Phi}} \leq \|\mathbf{s}_{\mathbf{f},X}\|_{\mathbf{\Phi}} \|\mathbf{f}\|_{\mathbf{\Phi}}.$$

7.2 Multilevel Divergence-Free Interpolation

In this section, we develop the multilevel interpolation theory for matrix-valued kernels. Although for interpolation it would be enough to examine scaled versions of the kernel $\widetilde{\mathbf{\Phi}}$, we will now look at *combined* kernels. Discussing these more general kernels will be useful when we turn to solving Darcy's problem in the next chapter. The necessary results for this chapter are then obtained as a byproduct. As for scalar-valued kernels, we can define the scaled matrix-valued kernels

$$\mathbf{\Phi}_{\delta,\varepsilon} := \begin{pmatrix} \widetilde{\mathbf{\Phi}}_\delta & \mathbf{0} \\ \mathbf{0}^T & \psi_\varepsilon \end{pmatrix} : \mathbb{R}^d \to \mathbb{R}^{(d+1)\times(d+1)}, \tag{7.12}$$

where

$$\begin{aligned} &\widetilde{\mathbf{\Phi}}_\delta := (-\Delta I + \nabla\nabla^T)\phi_\delta, \\ &\phi_\delta(\mathbf{x}) = \delta^{-d}\phi(\mathbf{x}/\delta) \qquad \text{and} \qquad \psi_\varepsilon(\mathbf{x}) = \varepsilon^{-d}\psi(\mathbf{x}/\varepsilon). \end{aligned}$$

If both scales are in fact identical, i. e. $\delta = \varepsilon$, we will shorten the notation and write $\mathbf{\Phi}_\delta$ instead of $\mathbf{\Phi}_{\delta,\delta}$. For a start, we need to understand how the native space norm of a matrix-valued kernel that depends on a scale is related to the appropriate Sobolev norms. Assume we have two kernels $\phi, \psi \colon \mathbb{R}^d \to \mathbb{R}$ whose Fourier transforms satisfy for positive σ, τ the following algebraic decay conditions

$$c_1(1 + \|\boldsymbol{\omega}\|_2^2)^{-\sigma-1} \leq \widehat{\phi}(\boldsymbol{\omega}) \leq c_2(1 + \|\boldsymbol{\omega}\|_2^2)^{-\sigma-1}$$

and

$$c_3(1 + \|\boldsymbol{\omega}\|_2^2)^{-\tau} \leq \widehat{\psi}(\boldsymbol{\omega}) \leq c_4(1 + \|\boldsymbol{\omega}\|_2^2)^{-\tau}$$

for $c_1, c_2, c_3, c_4 > 0$. Hence, ϕ generates $H^{\sigma+1}(\mathbb{R}^d)$ and ψ generates $H^\tau(\mathbb{R}^d)$.

Lemma 7.12 (Norm Equivalence for Scaled Matrix-Valued Kernels) *Let $\delta, \varepsilon \in (0, \delta_c]$. Let ϕ generate $H^{\sigma+1}(\mathbb{R}^d)$ and ψ generate $H^\tau(\mathbb{R}^d)$. Then*

$$\mathcal{N}_{\widetilde{\mathbf{\Phi}}_\delta}(\mathbb{R}^d) \times \mathcal{N}_{\psi_\varepsilon}(\mathbb{R}^d) = \widetilde{\mathbf{H}}^\sigma(\mathbb{R}^d, \mathrm{div}) \times H^\tau(\mathbb{R}^d)$$

and for every $\mathbf{w} = (\mathbf{w_u}, w_p) \in \widetilde{\mathbf{H}}^\sigma(\mathbb{R}^d, \mathrm{div}) \times H^\tau(\mathbb{R}^d)$, we have

$$C_1 \left\{ \|\mathbf{w_u}\|^2_{\mathcal{N}_{\widetilde{\mathbf{\Phi}}_\delta}(\mathbb{R}^d)} + \|w_p\|^2_{\mathcal{N}_{\psi_\varepsilon}(\mathbb{R}^d)} \right\} \leq \|\mathbf{w_u}\|^2_{\widetilde{\mathbf{H}}^\sigma(\mathbb{R}^d,\mathrm{div})} + \|w_p\|^2_{H^\tau(\mathbb{R}^d)},$$
$$C_2 \left\{ \delta^{-2(\sigma+1)} \|\mathbf{w_u}\|^2_{\mathcal{N}_{\widetilde{\mathbf{\Phi}}_\delta}(\mathbb{R}^d)} + \varepsilon^{-2\tau} \|w_p\|^2_{\mathcal{N}_{\psi_\varepsilon}(\mathbb{R}^d)} \right\} \geq \|\mathbf{w_u}\|^2_{\widetilde{\mathbf{H}}^\sigma(\mathbb{R}^d,\mathrm{div})} + \|w_p\|^2_{H^\tau(\mathbb{R}^d)}$$

for two positive constants C_1, C_2.

Proof. We first consider the upper bound. If $\delta \leq 1$, then

$$(1 + \|\boldsymbol{\omega}\|_2^2)^{\sigma+1} = \delta^{-2(\sigma+1)} (\delta^2 + \|\delta\boldsymbol{\omega}\|_2^2)^{\sigma+1} \leq \delta^{-2(\sigma+1)} (1 + \|\delta\boldsymbol{\omega}\|_2^2)^{\sigma+1}.$$

On the other hand if $1 < \delta \leq \delta_c$, we can simply use

$$(1 + \|\boldsymbol{\omega}\|_2^2)^{\sigma+1} < (1 + \|\delta\boldsymbol{\omega}\|_2^2)^{\sigma+1} \leq \delta^{-2(\sigma+1)} \delta_c^{2(\sigma+1)} (1 + \|\delta\boldsymbol{\omega}\|_2^2)^{\sigma+1}.$$

With both estimates we can then deduce for $m = \max\{1, \delta_c^{\sigma+1}, \delta_c^\tau\}$

$$\begin{aligned}
&\|\mathbf{w_u}\|^2_{\widetilde{\mathbf{H}}^\sigma(\mathbb{R}^d,\mathrm{div})} + \|w_p\|^2_{H^\tau(\mathbb{R}^d)} \\
&= (2\pi)^{-d/2} \int_{\mathbb{R}^d} \left\{ \frac{\|\widehat{\mathbf{w_u}}(\boldsymbol{\omega})\|_2^2}{\|\boldsymbol{\omega}\|_2^2} (1 + \|\boldsymbol{\omega}\|_2^2)^{\sigma+1} + |\widehat{w_p}(\boldsymbol{\omega})|^2 (1 + \|\boldsymbol{\omega}\|_2^2)^\tau \right\} d\boldsymbol{\omega} \\
&\leq \frac{m^2}{(2\pi)^{d/2}} \int_{\mathbb{R}^d} \left\{ \frac{\|\widehat{\mathbf{w_u}}(\boldsymbol{\omega})\|_2^2}{\delta^{2(\sigma+1)} \|\boldsymbol{\omega}\|_2^2} (1 + \|\delta\boldsymbol{\omega}\|_2^2)^{\sigma+1} + \frac{|\widehat{w_p}(\boldsymbol{\omega})|^2}{\varepsilon^{2\tau}} (1 + \|\varepsilon\boldsymbol{\omega}\|_2^2)^\tau \right\} d\boldsymbol{\omega} \\
&\leq m^2 \max\{c_2, c_4\} (2\pi)^{-d/2} \int_{\mathbb{R}^d} \left\{ \delta^{-2(\sigma+1)} \frac{\|\widehat{\mathbf{w_u}}(\boldsymbol{\omega})\|_2^2}{\|\boldsymbol{\omega}\|_2^2 \widehat{\phi}(\delta\boldsymbol{\omega})} + \varepsilon^{-2\tau} \frac{|\widehat{w_p}(\boldsymbol{\omega})|^2}{\widehat{\psi}(\varepsilon\boldsymbol{\omega})} \right\} d\boldsymbol{\omega} \\
&= m^2 \max\{c_2, c_4\} (2\pi)^{-d/2} \int_{\mathbb{R}^d} \left\{ \delta^{-2(\sigma+1)} \frac{\|\widehat{\mathbf{w_u}}(\boldsymbol{\omega})\|_2^2}{\|\boldsymbol{\omega}\|_2^2 \widehat{\phi_\delta}(\boldsymbol{\omega})} + \varepsilon^{-2\tau} \frac{|\widehat{w_p}(\boldsymbol{\omega})|^2}{\widehat{\psi_\varepsilon}(\boldsymbol{\omega})} \right\} d\boldsymbol{\omega} \\
&= C_2 \left\{ \delta^{-2(\sigma+1)} \|\mathbf{w_u}\|^2_{\mathcal{N}_{\widetilde{\mathbf{\Phi}}_\delta}(\mathbb{R}^d)} + \varepsilon^{-2\tau} \|w_p\|^2_{\mathcal{N}_{\psi_\varepsilon}(\mathbb{R}^d)} \right\},
\end{aligned}$$

where $C_2 = m^2 \max\{c_2, c_4\}$. For the lower bound, again, we distinguish between two cases. If $\delta \leq 1$, then we have

$$(1 + \|\boldsymbol{\omega}\|_2^2)^{\sigma+1} \geq (1 + \|\delta\boldsymbol{\omega}\|_2^2)^{\sigma+1}.$$

On the other hand, for $1 < \delta \leq \delta_c$, we have

$$(1 + \|\boldsymbol{\omega}\|_2^2)^{\sigma+1} = \delta^{-2(\sigma+1)} (\delta^2 + \|\delta\boldsymbol{\omega}\|_2^2)^{\sigma+1} > \delta_c^{-2(\sigma+1)} (1 + \|\delta\boldsymbol{\omega}\|_2^2)^{\sigma+1}.$$

Similarly, for $k = \min\{1, \delta_c^{-\sigma-1}, \delta_c^{-\tau}\}$, we then find

$$\begin{aligned}
&\|\mathbf{w}_\mathbf{u}\|^2_{\widetilde{\mathbf{H}}^\sigma(\mathbb{R}^d,\mathrm{div})} + \|w_p\|^2_{H^\tau(\mathbb{R}^d)} \\
&\geq k^2(2\pi)^{-d/2} \int_{\mathbb{R}^d} \left\{ \frac{\|\widehat{\mathbf{w}_\mathbf{u}}(\boldsymbol{\omega})\|_2^2}{\|\boldsymbol{\omega}\|_2^2}(1+\|\delta\boldsymbol{\omega}\|_2^2)^{\sigma+1} + |\widehat{w_p}(\boldsymbol{\omega})|^2(1+\|\varepsilon\boldsymbol{\omega}\|_2^2)^\tau \right\} d\boldsymbol{\omega} \\
&\geq \min\{c_1, c_3\} k^2(2\pi)^{-d/2} \int_{\mathbb{R}^d} \left\{ \frac{\|\widehat{\mathbf{w}_\mathbf{u}}(\boldsymbol{\omega})\|_2^2}{\|\boldsymbol{\omega}\|_2^2 \widehat{\phi_\delta}(\boldsymbol{\omega})} + \frac{|\widehat{w_p}(\boldsymbol{\omega})|^2}{\widehat{\psi_\varepsilon}(\boldsymbol{\omega})} \right\} d\boldsymbol{\omega} \\
&= C_1 \left\{ \|\mathbf{w}_\mathbf{u}\|^2_{\mathcal{N}_{\widetilde{\boldsymbol{\Phi}}_\delta}(\mathbb{R}^d)} + \|w_p\|^2_{\mathcal{N}_{\psi_\varepsilon}(\mathbb{R}^d)} \right\},
\end{aligned}$$

where $C_1 = k^2 \min\{c_1, c_3\}$. □

We can adjust the previous lemma to our specific needs.

Lemma 7.13 *Let $\delta \in (0, \delta_c]$. Let both ϕ and ψ generate $H^{\sigma+1}(\mathbb{R}^d)$. Then $\mathcal{N}_{\widetilde{\boldsymbol{\Phi}}_\delta}(\mathbb{R}^d) \times \mathcal{N}_{\psi_\delta}(\mathbb{R}^d) = \widetilde{\mathbf{H}}^\sigma(\mathbb{R}^d, \mathrm{div}) \times H^{\sigma+1}(\mathbb{R}^d)$ and for every $\mathbf{w} = (\mathbf{w}_\mathbf{u}, w_p)$ that lies in the space $\widetilde{\mathbf{H}}^\sigma(\mathbb{R}^d, \mathrm{div}) \times H^{\sigma+1}(\mathbb{R}^d)$, there exist two positive constants C_1, C_2 such that*

$$\sqrt{C_1}\|\mathbf{w}\|_{\mathcal{N}_{\boldsymbol{\Phi}_\delta}(\mathbb{R}^d)} \leq \|\mathbf{w}_\mathbf{u}\|_{\widetilde{\mathbf{H}}^\sigma(\mathbb{R}^d,\mathrm{div})} + \|w_p\|_{H^{\sigma+1}(\mathbb{R}^d)} \leq \sqrt{2C_2}\delta^{-\sigma-1}\|\mathbf{w}\|_{\mathcal{N}_{\boldsymbol{\Phi}_\delta}(\mathbb{R}^d)}.$$

Proof. Lemma 7.12 yields

$$\sqrt{C_1}\|\mathbf{w}\|_{\mathcal{N}_{\boldsymbol{\Phi}_\delta}(\mathbb{R}^d)} \leq \sqrt{\|\mathbf{w}_\mathbf{u}\|^2_{\widetilde{\mathbf{H}}^\sigma(\mathbb{R}^d,\mathrm{div})} + \|w_p\|^2_{H^{\sigma+1}(\mathbb{R}^d)}} \leq \sqrt{C_2}\delta^{-\sigma-1}\|\mathbf{w}\|_{\mathcal{N}_{\boldsymbol{\Phi}_\delta}(\mathbb{R}^d)}.$$

Now we use the norm equivalence between the ℓ_1 and ℓ_2 norm, i. e. the fact that for $a, b > 0$ we have

$$\frac{1}{\sqrt{2}}(a+b) \leq \sqrt{a^2+b^2} \leq a+b.$$

□

If there is no scalar component in Lemma 7.12, we automatically obtain for $\mathbf{u} \in \widetilde{\mathbf{H}}^\sigma(\mathbb{R}^d, \mathrm{div})$ that

$$C_1\|\mathbf{u}\|_{\mathcal{N}_{\widetilde{\boldsymbol{\Phi}}_\delta}(\mathbb{R}^d)} \leq \|\mathbf{u}\|_{\widetilde{\mathbf{H}}^\sigma(\mathbb{R}^d,\mathrm{div})} \leq C_2\delta^{-(\sigma+1)}\|\mathbf{u}\|_{\mathcal{N}_{\widetilde{\boldsymbol{\Phi}}_\delta}(\mathbb{R}^d)}, \tag{7.13}$$

where C_1 and C_2 are again some positive constants independent of the scale δ.

Another ingredient of the multilevel convergence proof consists of sampling inequalities for vector-valued functions. In preparation for the next chapter we state two versions. Both come from and are proven in [86].

Lemma 7.14 (Vector-Valued Sampling Inequality for Interior) *Let $\Omega \subseteq \mathbb{R}^d$ be a domain with Lipschitz boundary. Furthermore, let $1 < r < \infty$ and $\sigma, \eta \in \mathbb{R}$ with $\sigma > d/2$ and $0 \leq \eta \leq \sigma - d(1/2 - 1/r)_+$. Assume that $\mathbf{u} \in \mathbf{H}^\sigma(\Omega)$ satisfies $\mathbf{u}|_X = \mathbf{0}$ on a discrete set $X \subseteq \Omega$ with a sufficiently small fill distance $h_{X,\Omega}$. Then,*

$$\|\mathbf{u}\|_{\mathbf{W}_r^\eta(\Omega)} \leq C h_{X,\Omega}^{\sigma-\eta-d(1/2-1/r)_+}\|\mathbf{u}\|_{\mathbf{H}^\sigma(\Omega)}$$

for some $C > 0$.

Lemma 7.15 (Vector-Valued Sampling Inequality for Boundary) *Let $\Omega \subseteq \mathbb{R}^d$ be a domain with a $C^{k,s}$ boundary for $k \in \mathbb{N}_0$ and $0 < s \leq 1$. Furthermore, let $1 < r < \infty$ and $\sigma := k + s > d/2$ and $0 \leq \eta \leq \sigma - 1/2 - (d-1)(1/2 - 1/r)_+$. Assume that $\mathbf{u} \in \mathbf{H}^\sigma(\Omega)$ satisfies $\mathbf{u}|_Y = \mathbf{0}$ on a discrete set $Y \subseteq \Omega$ with a sufficiently small fill distance $h_{Y,\partial\Omega}$. Then,*

$$\|\mathbf{u}\|_{\mathbf{W}_r^\eta(\partial\Omega)} \leq C h_{Y,\partial\Omega}^{\sigma-1/2-\eta-(d-1)(1/2-1/r)_+} \|\mathbf{u}\|_{\mathbf{H}^\sigma(\Omega)}$$

for some $C > 0$.

Finally, we need a lemma from [13].

Lemma 7.16 *Assume $\mathbf{u} \in \mathbf{H}^\sigma(\Omega, \mathrm{div})$ with $\sigma > 0$. Then*

$$\int_{\mathbb{R}^d} \frac{\|\widehat{\widetilde{\mathbf{E}}_{\mathrm{div}}\mathbf{u}}(\boldsymbol{\omega})\|_2^2}{\|\boldsymbol{\omega}\|_2^2} d\boldsymbol{\omega} \leq C \|\mathbf{u}\|_{\mathbf{L}_2(\Omega)}^2.$$

7.2.1 Symmetric Multilevel Interpolation Algorithm

Suppose we are given a sequence of point sets in Ω, namely $X_1, X_2, \ldots$, with decreasing mesh norms $h_{X_1,\Omega}, h_{X_2,\Omega}, \ldots$. From these mesh norms we construct support radii so that

$$\delta_j = \beta h_j^{\frac{\sigma}{\sigma+1}}$$

for some proportionality constant $\beta > 0$. In order to simplify the notation for the rest of the chapter, we drop the tilde and denote the divergence-free matrix-valued kernels by

$$\boldsymbol{\Phi} = (-\Delta I + \nabla\nabla^T)\phi.$$

This should not be confused with the combined kernel we have introduced earlier and we will use again in the next chapter. With this definition we define scaled kernels via $\boldsymbol{\Phi}_j = \boldsymbol{\Phi}_{\delta_j} = (-\Delta I + \nabla\nabla^T)\phi_\delta$ where $\phi_\delta(\mathbf{x}) = \delta^{-d}\phi(\mathbf{x}/\delta)$. The vector-valued divergence-free interpolants $\mathbf{s}_j$ come from the space

$$\mathbf{V}_j = \mathrm{span}\{\boldsymbol{\Phi}_j(\cdot - \mathbf{x}) | \mathbf{x} \in X_j\}.$$

Now, we can state the symmetric multilevel interpolation algorithm for matrix-valued kernels, which reconstructs some divergence-free target function $\mathbf{u}$ by a residual correction scheme.

Algorithm 7.17 (Symmetric Multilevel Interpolation Algorithm)

Input: Right-hand side $\mathbf{u}$ with $\mathrm{div}(\mathbf{u}) = 0$ and number of levels n

Set $\mathbf{u}_0 = \mathbf{0}$ and $\mathbf{e}_0 = \mathbf{u}$. For $j = 1, \ldots, n$ **do**

(i) Determine the local correction $\mathbf{s}_j \in \mathbf{V}_j$ to $\mathbf{e}_{j-1}$ on X_j

$$\mathbf{s}_j(\mathbf{x}) = \mathbf{e}_{j-1}(\mathbf{x}) \qquad \mathbf{x} \in X_j$$

(ii) Update the global approximation and the residuals

$$\mathbf{u}_j = \mathbf{u}_{j-1} + \mathbf{s}_j$$
$$\mathbf{e}_j = \mathbf{e}_{j-1} - \mathbf{s}_j$$

end

Output: Approximate solution $\mathbf{u}_n$ to $\mathbf{u}$

The residual in this case is in fact the error between the solution $\mathbf{u}$ and its jth multiscale approximation $\mathbf{u}_j$, i. e.

$$\mathbf{e}_j = \mathbf{u} - \mathbf{u}_j.$$

This algorithm converges indeed.

Theorem 7.18 (Convergence of Multilevel Interpolation Algorithm)
Let $\sigma > d/2$, $\mathbf{u} \in \mathbf{H}^\sigma(\Omega, \mathrm{div})$ and $X_1, X_2, \ldots$ be a sequence of point sets in Ω with mesh norms $h_{X_1,\Omega}, h_{X_2,\Omega}, \ldots$. Assume

$$\gamma\mu h_j \le h_{j+1} \le \mu h_j \tag{7.14}$$

for $j = 1, 2, \ldots$ and some fixed $\mu \in (0,1)$ and $\gamma \in (0,1)$. Suppose that the kernel $\mathbf{\Phi}$ is chosen such that $\mathcal{N}_{\mathbf{\Phi}}(\mathbb{R}^d) = \widetilde{\mathbf{H}}^\sigma(\mathbb{R}^d, \mathrm{div})$. This means in particular that ϕ generates $H^{\sigma+1}(\mathbb{R}^d)$. Define

$$\delta_j = \left(\frac{h_j}{\mu}\right)^{\frac{\sigma}{\sigma+1}} \quad \text{as well as} \quad \mathbf{\Phi}_j = \mathbf{\Phi}_{\delta_j} = (-\Delta I + \nabla\nabla^T)\phi_{\delta_j}$$

with $\phi_\delta = \delta^{-d}\phi(\cdot/\delta)$. Lastly, let $h_1 \le \mu$ be sufficiently small. Then, there exists a positive constant C independent of μ, j and u such that

$$\|\widetilde{\mathbf{E}}_{\mathrm{div}}\mathbf{e}_j\|_{\mathbf{\Phi}_{j+1}} \le \alpha \|\widetilde{\mathbf{E}}_{\mathrm{div}}\mathbf{e}_{j-1}\|_{\mathbf{\Phi}_j}, \tag{7.15}$$

for $j = 1, 2, \ldots$ with $\alpha = C\mu^\sigma$. Thus, we have the estimates

$$\|\mathbf{u} - \mathbf{u}_k\|_{\mathbf{L}_2(\Omega)} \le C\alpha^k \|\mathbf{u}\|_{\mathbf{H}^\sigma(\Omega)}$$

and in particular the multiscale approximation $\mathbf{u}_k$ converges to $\mathbf{u}$ in the L_2 norm if we choose μ so small that $\alpha < 1$.

Proof. It is easy to verify that the support radii are monotonically decreasing. We compute

$$\begin{aligned}
\|\mathbf{E}_{\mathrm{div}}\mathbf{e}_j\|^2_{\mathbf{\Phi}_{j+1}} &= (2\pi)^{-d/2} \int_{\mathbb{R}^d} \frac{\|\widehat{\mathbf{E}_{\mathrm{div}}\mathbf{e}_j}(\boldsymbol{\omega})\|_2^2}{\|\boldsymbol{\omega}\|_2^2 \widehat{\phi_{j+1}}(\boldsymbol{\omega})} d\boldsymbol{\omega} \\
&\le \frac{1}{c_1}(2\pi)^{-d/2} \int_{\mathbb{R}^d} \frac{\|\widehat{\mathbf{E}_{\mathrm{div}}\mathbf{e}_j}(\boldsymbol{\omega})\|_2^2}{\|\boldsymbol{\omega}\|_2^2} (1 + \|\delta_{j+1}\boldsymbol{\omega}\|_2^2)^{\sigma+1} d\boldsymbol{\omega} \\
&=: \frac{1}{c_1}(2\pi)^{-d/2}(I_1 + I_2),
\end{aligned}$$

where we introduced the notation

$$I_1 = \int\limits_{\|\boldsymbol{\omega}\|_2 \leq \frac{1}{\delta_{j+1}}} \frac{\|\widehat{\mathbf{E}_{\mathrm{div}}\mathbf{e}_j}(\boldsymbol{\omega})\|_2^2}{\|\boldsymbol{\omega}\|_2^2}(1+\|\delta_{j+1}\boldsymbol{\omega}\|_2^2)^{\sigma+1}d\boldsymbol{\omega}$$

$$I_2 = \int\limits_{\|\boldsymbol{\omega}\|_2 \geq \frac{1}{\delta_{j+1}}} \frac{\|\widehat{\mathbf{E}_{\mathrm{div}}\mathbf{e}_j}(\boldsymbol{\omega})\|_2^2}{\|\boldsymbol{\omega}\|_2^2}(1+\|\delta_{j+1}\boldsymbol{\omega}\|_2^2)^{\sigma+1}d\boldsymbol{\omega}.$$

To bound these two integrals we start with the following observation that

$$\begin{aligned}
\|\mathbf{e}_j\|_{\mathbf{H}^\sigma(\Omega)}^2 &= \|\mathbf{e}_{j-1} - \mathbf{s}_{\mathbf{e}_{j-1}}\|_{\mathbf{H}^\sigma(\Omega)}^2 \\
&= \|\mathbf{E}_{\mathrm{div}}\mathbf{e}_{j-1} - \mathbf{s}_{\mathbf{E}_{\mathrm{div}}\mathbf{e}_{j-1}}\|_{\mathbf{H}^\sigma(\Omega)}^2 \\
&\leq \|\mathbf{E}_{\mathrm{div}}\mathbf{e}_{j-1} - \mathbf{s}_{\mathbf{E}_{\mathrm{div}}\mathbf{e}_{j-1}}\|_{\mathbf{H}^\sigma(\mathbb{R}^d)}^2 \\
&\leq \|\mathbf{E}_{\mathrm{div}}\mathbf{e}_{j-1} - \mathbf{s}_{\mathbf{E}_{\mathrm{div}}\mathbf{e}_{j-1}}\|_{\widetilde{\mathbf{H}}^\sigma(\mathbb{R}^d)}^2 \\
&\leq C\delta_j^{-2(\sigma+1)}\|\mathbf{E}_{\mathrm{div}}\mathbf{e}_{j-1} - \mathbf{s}_{\mathbf{E}_{\mathrm{div}}\mathbf{e}_{j-1}}\|_{\boldsymbol{\Phi}_j}^2 \\
&\leq C\delta_j^{-2(\sigma+1)}\|\mathbf{E}_{\mathrm{div}}\mathbf{e}_{j-1}\|_{\boldsymbol{\Phi}_j}^2.
\end{aligned} \tag{7.16}$$

Here we have used the definition of $\mathbf{e}_j$, the facts that $\mathbf{E}_{\mathrm{div}}\mathbf{e}_{j-1} = \mathbf{e}_{j-1}$ on Ω and that the interpolant $\mathbf{s}_{\mathbf{e}_{j-1}}$ equals $\mathbf{s}_{\mathbf{E}_{\mathrm{div}}\mathbf{e}_{j-1}}$ as well as Lemma 7.9, Lemma 7.12 and the best approximation property of the interpolant.

For the first integral, I_1, we have $\delta_{j+1}\|\boldsymbol{\omega}\|_2 \leq 1$ and thus by Lemma 7.16, the sampling inequality (Lemma 7.14) and (7.16), it follows that

$$\begin{aligned}
I_1 &\leq 2^{\sigma+1}\int_{\|\boldsymbol{\omega}\|_2 \leq \frac{1}{\delta_{j+1}}} \frac{\|\widehat{\mathbf{E}_{\mathrm{div}}\mathbf{e}_j}(\boldsymbol{\omega})\|_2^2}{\|\boldsymbol{\omega}\|_2^2}d\boldsymbol{\omega} \\
&\leq C\|\mathbf{e}_j\|_{\mathbf{L}_2(\Omega)}^2 \\
&\leq Ch_j^{2\sigma}\|\mathbf{e}_j\|_{\mathbf{H}^\sigma(\Omega)}^2 \\
&\leq Ch_j^{2\sigma}\delta_j^{-2(\sigma+1)}\|\mathbf{E}_{\mathrm{div}}\mathbf{e}_{j-1}\|_{\boldsymbol{\Phi}_j}^2 \\
&= C_1\mu^{2\sigma}\|\mathbf{E}_{\mathrm{div}}\mathbf{e}_{j-1}\|_{\boldsymbol{\Phi}_j}^2,
\end{aligned}$$

using also that by definition we have

$$\frac{h_j^\sigma}{\delta_j^{\sigma+1}} = \mu^\sigma.$$

Now we turn to the second integral I_2. Since $\delta_{j+1}\|\boldsymbol{\omega}\|_2 \geq 1$, we find

$$(1+\delta_{j+1}^2\|\boldsymbol{\omega}\|_2^2)^{\sigma+1} \leq (2\delta_{j+1}^2\|\boldsymbol{\omega}\|_2^2)^{\sigma+1} \leq 2^{\sigma+1}\delta_{j+1}^{2(\sigma+1)}(1+\|\boldsymbol{\omega}\|_2^2)^{\sigma+1}$$

and consequently, using Proposition 7.11 and (7.16) once again, gives

$$\begin{aligned} I_2 &\leq 2^{\sigma+1}\delta_{j+1}^{2(\sigma+1)} \int_{\mathbb{R}^d} \frac{\|\mathbf{E}_{\mathrm{div}}\mathbf{e}_j(\boldsymbol{\omega})\|_2^2}{\|\boldsymbol{\omega}\|_2^2}(1+\|\boldsymbol{\omega}\|_2^2)^{\sigma+1}d\boldsymbol{\omega} \\ &= 2^{\sigma+1}\delta_{j+1}^{2(\sigma+1)}\|\mathbf{E}_{\mathrm{div}}\mathbf{e}_j\|_{\widetilde{\mathbf{H}}^\sigma(\mathbb{R}^d,\mathrm{div})} \\ &\leq C\delta_{j+1}^{2(\sigma+1)}\|\mathbf{e}_j\|_{\mathbf{H}^\sigma(\Omega)}^2 \\ &\leq C(\delta_{j+1}/\delta_j)^{2(\sigma+1)}\|\mathbf{E}_{\mathrm{div}}\mathbf{e}_{j-1}\|_{\boldsymbol{\Phi}_j}^2 \\ &\leq C_2\mu^{2\sigma}\|\mathbf{E}_{\mathrm{div}}\mathbf{e}_{j-1}\|_{\boldsymbol{\Phi}_j}^2. \end{aligned}$$

In the last step we have used

$$\left(\frac{\delta_{j+1}}{\delta_j}\right)^{\sigma+1} = \left(\frac{h_{j+1}}{\mu}\right)^{\sigma}\left(\frac{\mu}{h_j}\right)^{\sigma} = \left(\frac{h_{j+1}}{h_j}\right)^{\sigma} \leq \mu^\sigma.$$

Combining both estimates now yields (7.15) with

$$\alpha = \sqrt{\frac{1}{c_1}(2\pi)^{-d/2}}(C_1+C_2)^{1/2}\mu^\sigma = C\mu^\sigma.$$

It follows by the sampling inequality and Lemma 7.12 that

$$\begin{aligned} \|\mathbf{u}-\mathbf{u}_n\|_{\mathbf{L}_2(\Omega)}^2 = \|\mathbf{e}_n\|_{\mathbf{L}_2(\Omega)}^2 &\leq Ch_n^{2\sigma}\|\mathbf{e}_n\|_{\mathbf{H}^\sigma(\Omega)}^2 \\ &\leq Ch_n^{2\sigma}\delta_{n+1}^{-2(\sigma+1)}\|\mathbf{E}_{\mathrm{div}}\mathbf{e}_n\|_{\boldsymbol{\Phi}_{n+1}}^2 \\ &= C\|\mathbf{E}_{\mathrm{div}}\mathbf{e}_n\|_{\boldsymbol{\Phi}_{n+1}}^2, \end{aligned}$$

where we have used the fact that

$$\frac{h_n^\sigma}{\delta_{n+1}^{\sigma+1}} = \mu^\sigma\left(\frac{h_n}{h_{n+1}}\right)^\sigma \leq \mu^\sigma\left(\frac{1}{\mu\gamma}\right)^\sigma = \gamma^{-\sigma}.$$

Applying (7.15), n times we can conclude

$$\begin{aligned} \|\mathbf{u}-\mathbf{u}_n\|_{\mathbf{L}_2(\Omega)}^2 &\leq C\alpha^{2n}\|\mathbf{E}_{\mathrm{div}}\mathbf{e}_0\|_{\boldsymbol{\Phi}_1}^2 = C\alpha^{2n}\|\mathbf{E}_{\mathrm{div}}\mathbf{u}\|_{\boldsymbol{\Phi}_1}^2 \\ &\leq C\alpha^{2n}\|\mathbf{u}\|_{\mathbf{H}^\sigma(\Omega)}^2. \end{aligned}$$

□

In contrast to the multilevel interpolation with scalar-valued kernels from Section 4.1, the multilevel interpolation of divergence-free fields with matrix-valued kernels is shown to converge only for a (mildly) nonproportional relationship between mesh norm and support radius. In fact, as we will see in the next section, a proportional relationship does not lead to convergence. The nonproportionality is introduced via the native space norm for matrix-valued kernels (as can be seen in Lemma 7.12).

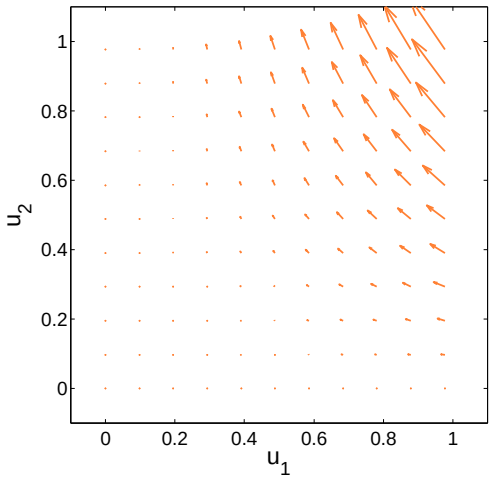

(a) Vector field $\mathbf{u}$

Figure 7.1: The divergence-free vector field (7.17) after seven levels, using a basis function $\phi_{2,3}$, $\mu = 0.5$ and $\nu = 2.5$.

7.2.2 Numerical Example

We run a numerical example for a divergence-free vector field of the form

$$\mathbf{u}(x, y) = \begin{pmatrix} -2x^3 y \\ 3x^2 y^2 \end{pmatrix} \tag{7.17}$$

on the closed unit square $\Omega = [0, 1]^2$. Note, that the vector field is indeed divergence-free. As for example (P2) in Chapter 4, we choose regular nested grids. As basis function we employ $\phi_{2,3}$ (i. e. $\sigma + 1 = 4.5$). Furthermore, we use a proportionality constant $\nu = 2.5$ and support radii of the form

$$\delta = \nu h^{\frac{\sigma}{\sigma+1}} = \nu h^{\frac{7}{9}} \tag{7.18}$$

for some $\nu > 0$. As the numerical results in Tables 7.1 and 7.2 show, the numerical solution converges. Note the number N is actually referring to the amount of data points. The systems that need to be solved are actually twice as big, since $\mathbf{u}$ consists of two components. The final multilevel interpolant and the errors are depicted in Figures 7.2 and 7.1.

Tables 7.3 and 7.4 show the results for the stationary case, i. e.

$$\delta = \nu h. \tag{7.19}$$

In this case, the algorithm eventually stagnates.

N	H	$\|\mathbf{e}\|_{\mathbf{L}_2(\Omega)}$	$\|\mathbf{e}\|_{\mathbf{H}^1(\Omega)}$	$\|\mathbf{e}\|_{\mathbf{L}_\infty(\Omega)}$	cond(A)
9	2^{-1}	1.83e-1	1.53e0	6.11e-1	1.3e2
25	2^{-2}	3.35e-2	5.00e-1	2.19e-1	9.2e2
81	2^{-3}	5.62e-3	1.65e-1	6.19e-2	5.5e3
289	2^{-4}	1.02e-3	6.13e-2	1.75e-2	2.4e4
1089	2^{-5}	1.91e-4	2.46e-2	4.80e-3	9.1e4
4225	2^{-6}	3.37e-5	1.02e-2	1.17e-3	2.9e5
16641	2^{-7}	5.29e-6	4.47e-3	2.81e-4	8.3e5

Table 7.1: Convergence study multilevel interpolation of divergence-free vector field (7.17) with basis function $\phi_{2,3}$ and support radii (7.18) where $\nu = 2.5$.

N	H	$\|\mathbf{e}\|_{\mathbf{L}_2(\Omega)}$	$\|\mathbf{e}\|_{\mathbf{H}^1(\Omega)}$	$\|\mathbf{e}\|_{\mathbf{L}_\infty(\Omega)}$	cond(A)
25	2^{-2}	2.45	1.61	1.48	-2.83
81	2^{-3}	2.57	1.60	1.83	-2.58
289	2^{-4}	2.46	1.43	1.83	-2.12
1089	2^{-5}	2.42	1.31	1.86	-1.93
4225	2^{-6}	2.50	1.27	2.04	-1.69
16641	2^{-7}	2.67	1.20	2.05	-1.50

Table 7.2: Orders for multilevel interpolation of divergence-free vector field (7.17) with basis function $\phi_{2,3}$ and support radii (7.18) where $\nu = 2.5$.

N	H	$\|\mathbf{e}\|_{\mathbf{L}_2(\Omega)}$	$\|\mathbf{e}\|_{\mathbf{H}^1(\Omega)}$	$\|\mathbf{e}\|_{\mathbf{L}_\infty(\Omega)}$	cond(A)
9	2^{-1}	2.00e-1	1.70e0	6.18e-1	9.4e1
25	2^{-2}	4.10e-2	6.11e-1	2.72e-1	2.3e2
81	2^{-4}	7.88e-3	2.28e-1	8.69e-2	3.9e2
289	2^{-4}	1.68e-3	9.77e-2	2.56e-2	5.2e2
1089	2^{-5}	5.44e-4	6.22e-2	7.00e-3	6.1e2
4225	2^{-6}	3.90e-4	8.54e-2	1.62e-3	6.7e2
16641	2^{-7}	4.15e-4	1.66e-2	9.85e-4	6.6e2

Table 7.3: Convergence study multilevel interpolation of divergence-free vector field (7.17) with basis function $\phi_{2,3}$ and support radii (7.19) where $\nu = 2.5$.

N	H	$\|\mathbf{e}\|_{\mathbf{L}_2(\Omega)}$	$\|\mathbf{e}\|_{\mathbf{H}^1(\Omega)}$	$\|\mathbf{e}\|_{\mathbf{L}_\infty(\Omega)}$	cond(A)
25	2^{-2}	2.28	1.47	1.18	-1.29
81	2^{-3}	2.38	1.42	1.65	-0.78
289	2^{-4}	2.23	1.22	1.76	-0.41
1089	2^{-5}	1.63	0.65	1.87	-0.23
4225	2^{-6}	0.48	-0.45	2.11	-0.12
16641	2^{-7}	-0.09	2.37	0.72	0.02

Table 7.4: Orders for multilevel interpolation of divergence-free vector field (7.17) with basis function $\phi_{2,3}$ and support radii (7.19) where $\nu = 2.5$.

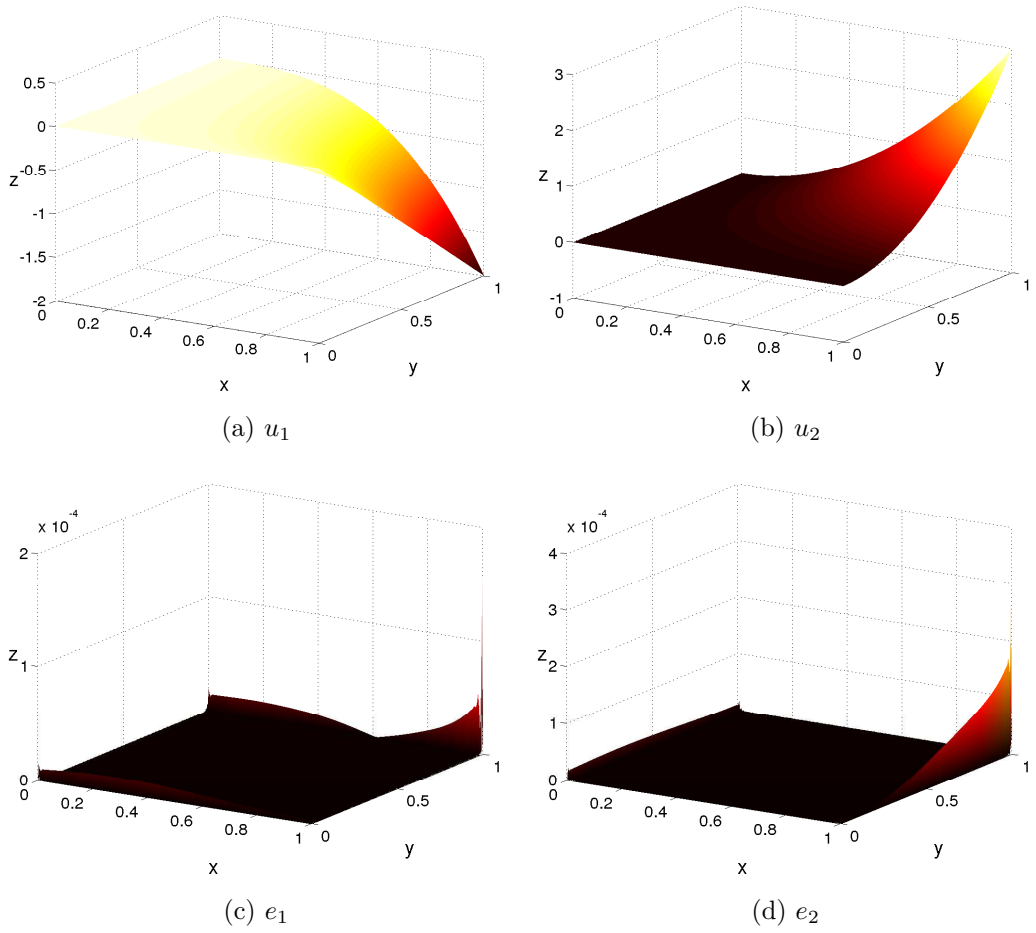

(a) u_1 (b) u_2

(c) e_1 (d) e_2

Figure 7.2: Both components of multilevel approximation and corresponding errors of divergence-free vector field (7.17) after seven levels, using a basis function $\phi_{2,3}$, $\mu = 0.5$ and $\nu = 2.5$.

Chapter 8

Darcy's Problem

After having introduced divergence-free kernels in the previous chapter, we study now a multilevel technique to solve Darcy's problem. Convergence is shown for smooth and rough target functions. Previous work has focussed on the one-shot error theory [74, 75], which we generalise to scale-dependent kernels here to prove the convergence of a meshless multilevel collocation algorithm. We give a short introduction to Darcy's problem based on ideas from [73].

8.1 Introduction to Darcy's Problem

Darcy's law is an empirical relationship used to describe fluid flow through porous media. It was derived by the French mathematician Henry Darcy in the middle of the 19th century. Through a series of experiments, Darcy made the observation that the flow rate Q (measured in m^3/s) of liquid through a pipe behaves like

$$Q = -KA\frac{h_2 - h_1}{L},$$

where K (in units m/s) is the hydraulic conductivity, A (in m^2) the cross-sectional area of the pipe, and L (in m) the length over which there exists a pressure drop from h_2 to h_1 (both measured in m). If we assume that $h_2 > h_1$, then the minus sign accounts for the fact that the liquid flows from the region of high pressure to the region of lower pressure.

More generally, we obtain

$$\mathbf{q} = -\frac{K}{\mu}\nabla p,$$

where K is the permeability tensor, which from a mathematical perspective can be represented as a matrix [1, 73]. It is possible to derive Darcy's law in its generalised form from the Navier-Stokes equations for anisotropic media [69]. This motivates the following problem, which we would like to solve numerically. We generalise Darcy's law even more by introducing a forcing term and supplement it with Neumann

boundary conditions, which ensures well-posedness for this first-order problem. Note also that we have absorbed the viscosity into the tensor.

Assume for some open bounded domain $\Omega \subseteq \mathbb{R}^d$, we are given the right-hand sides $\mathbf{f}$ and $\mathbf{g}$. We then want to determine the velocity field $\mathbf{u}\colon \overline{\Omega} \to \mathbb{R}$ and the pressure $p\colon \Omega \to \mathbb{R}$ that are governed by the equations

$$\mathbf{u} + K\nabla p = \mathbf{f} \qquad \text{in} \quad \Omega, \tag{8.1}$$

$$\mathbf{u} \cdot \mathbf{n} = \mathbf{g} \cdot \mathbf{n} \qquad \text{on} \quad \partial\Omega, \tag{8.2}$$

where $\mathbf{n}$ denotes the outer unit normal vector to the boundary $\partial\Omega$. Often we will abbreviate the first equation with

$$L\mathbf{v} = \mathbf{f},$$

where $\mathbf{v} = (\mathbf{u}, p)$. Since the pressure p is only determined up to a real constant, we will work in the quotient space $H^\sigma(\Omega)/\mathbb{R}$ and define the norm

$$\|p\|_{H^\sigma(\Omega)/\mathbb{R}} := \inf_{c\in\mathbb{R}} \|p + c\|_{H^\sigma(\Omega)}.$$

However, since this notation is rather tedious, we will often implicitly take a representer p such that

$$\|p\|_{H^\sigma(\Omega)/\mathbb{R}} = \|p\|_{H^\sigma(\Omega)}.$$

Furthermore, let us assume that the fluid flow is incompressible. From the conservation of mass one can derive the equivalent condition that the velocity vector field is incompressible, i. e.

$$\nabla \cdot \mathbf{u} = 0 \qquad \text{in} \quad \Omega. \tag{8.3}$$

Combining the equations, (8.1) and (8.3), yields *Darcy's problem*. Due to the divergence theorem, the incompressibility condition implies a compatibility condition

$$\int_{\partial\Omega} \mathbf{g} \cdot \mathbf{n} \, dS = 0.$$

The tensor $K\colon \Omega \to \mathbb{R}^{d\times d}$ shall be symmetric and strictly elliptic, in the sense that there exists a constant $c_0 > 0$ such that

$$\boldsymbol{\xi}^T K(\mathbf{x})\boldsymbol{\xi} \geq c_0 \|\boldsymbol{\xi}\|_2^2 \tag{8.4}$$

for $\boldsymbol{\xi} \in \mathbb{R}^d$ and $\mathbf{x} \in \Omega$.

Analogously to the continuous dependence on the data for second order elliptic differential operators, the right-hand side data for Darcy's problem also controls the solution in the following way. For a proof see [74].

Theorem 8.1 (Continuous Dependence on Data) *Let Ω be a bounded open subset of $\mathbb{R}^d$ with $C^{\lceil\sigma\rceil+1,1}$ boundary $\partial\Omega$. Assume that $\mathbf{f} \in \mathbf{W}_r^{\sigma+1}(\Omega)$ and that $\mathbf{g} \in \mathbf{W}_r^{\sigma+1-1/r}(\partial\Omega)$ for $1 < r < \infty$ and $\sigma \geq 0$ with $\int_{\partial\Omega} \mathbf{g}\cdot\mathbf{n}\, dS = 0$. Furthermore, let the*

permeability tensor $K = (K_{ij})$ *satisfy* (8.4), $K = K^T$ *and* $K_{ij} \in W_r^{\sigma+1}(\overline{\Omega})$. *Then, the velocity component of the solution to Darcy's problem* $\mathbf{u}$ *lies in* $\mathbf{W}_r^{\sigma+1}(\Omega)$ *and the pressure component* p *lies in* $W_r^{\sigma+2}(\Omega)/\mathbb{R}$. *The following relationship holds*

$$\|\mathbf{u}\|_{\mathbf{W}_r^{\eta+1}(\Omega)} + \|p\|_{W_r^{\eta+2}(\Omega)/\mathbb{R}} \leq C \left(\|\mathbf{f}\|_{\mathbf{W}_r^{\eta+1}(\Omega)} + \|\mathbf{g} \cdot \mathbf{n}\|_{\mathbf{W}_r^{\eta+1-1/r}(\partial\Omega)} \right)$$

for $0 \leq \eta \leq \sigma$ *and some* $C > 0$.

8.2 Generalised Interpolation for Matrix-Valued Kernels

We want to construct approximants to systems of partial differential equations. Therefore, we introduce generalised interpolation for matrix-valued kernels $\mathbf{\Phi}$.

We denote with $\mathcal{N}_{\mathbf{\Phi}}(\Omega)^*$ the dual space of the native space, i. e. the set of all continuous functionals mapping the native space to the real numbers. Suppose $\lambda \in \mathcal{N}_{\mathbf{\Phi}}(\Omega)^*$, then the Riesz representation theorem asserts that there exists a unique Riesz representer $\mathbf{g}_\lambda \in \mathcal{N}_{\mathbf{\Phi}}(\Omega)^*$ such that

$$\lambda(\mathbf{f}) = (\mathbf{f}, \mathbf{g}_\lambda)_{\mathbf{\Phi}}$$

for all $\mathbf{f} \in \mathcal{N}_{\mathbf{\Phi}}(\Omega)$. If we make the specific choice of $\mathbf{f} = \mathbf{\Phi}(\cdot - \mathbf{x})\boldsymbol{\alpha} \in \mathcal{N}_{\mathbf{\Phi}}(\Omega)$, then by the reproduction property (Lemma 7.5), we deduce from the above equation that

$$\lambda(\mathbf{\Phi}(\cdot - \mathbf{x})\boldsymbol{\alpha}) = \mathbf{g}_\lambda(\mathbf{x})^T \boldsymbol{\alpha}.$$

If we insert for $\boldsymbol{\alpha}$ the jth canonical unit basis vector $\mathbf{e}_j$, we see that the functional λ maps the jth column of the matrix $\mathbf{\Phi}(\cdot - \mathbf{x})$ to the jth component of the Riesz representer. Hence, if we define $\lambda^{\mathbf{y}}\mathbf{\Phi}(\mathbf{x} - \mathbf{y})$ as the application of the functional λ to each column, we readily see that $\mathbf{g}_\lambda = \lambda^{\mathbf{y}}\mathbf{\Phi}(\cdot - \mathbf{y})$ and

$$\lambda(\mathbf{f}) = (\mathbf{f}, \lambda^{\mathbf{y}}\mathbf{\Phi}(\cdot - \mathbf{y}))_{\mathbf{\Phi}},$$

which can be interpreted as a generalised reproduction property. From it we can, similarly to the scalar-valued case, derive an optimal recovery result [74, Proposition 2.6].

Theorem 8.2 *Let* $\mathbf{\Phi}\colon \Omega \subset \mathbb{R}^d \to \mathbb{R}^{n \times n}$ *be a positive definite, matrix-valued kernel. Furthermore, let* $\lambda_1, \ldots, \lambda_N \in \mathcal{N}_{\mathbf{\Phi}}(\Omega)^*$ *be linearly independent functionals and* $f_1, \ldots, f_N \in \mathbb{R}$ *given data. Then, the minimisation problem*

$$\min\{\|\mathbf{s}\|_{\mathcal{N}_{\mathbf{\Phi}}(\Omega)} \mid \mathbf{s} \in \mathcal{N}_{\mathbf{\Phi}}(\Omega), \lambda_j(\mathbf{s}) = f_j, 1 \leq j \leq N\}$$

has a unique solution, which is given by

$$\mathbf{s}_f = \sum_{j=1}^{N} \alpha_j \lambda_j^{\mathbf{y}} \mathbf{\Phi}(\cdot - \mathbf{y}).$$

The real coefficients α_j are uniquely determined by the generalised interpolation conditions

$$\lambda_k(\mathbf{s}_f) = f_k$$

for $1 \leq k \leq N$.

8.3 RBF Discretisation of Darcy's Problem

Now we would like to apply the rather general previous section to Darcy's problem. We choose interior points $X = \{\mathbf{x}_1, \dots, \mathbf{x}_N\} \subseteq \Omega$ and boundary points $Y = \{\mathbf{y}_1, \dots, \mathbf{y}_M\} \subseteq \partial\Omega$. For the combined vector $\mathbf{v} = (\mathbf{u}, p)$, we define interior functionals

$$\begin{aligned} \lambda_j^{(i)}(\mathbf{v}) &= u_i(\mathbf{x}_j) + (K\nabla p)_i(\mathbf{x}_j) \\ &= u_i(\mathbf{x}_j) + \sum_{k=1}^{d} K_{ik}(\mathbf{x}_j) \frac{\partial}{\partial x_k} p(\mathbf{x}_j) \end{aligned} \tag{8.5}$$

for the component index $1 \leq i \leq d$ and the data index $1 \leq j \leq N$. For the boundary, we define

$$\lambda_j^{(d+1)}(\mathbf{v}) = \sum_{k=1}^{d} u_k(\mathbf{y}_j) n_k(\mathbf{y}_j) \tag{8.6}$$

for $1 \leq j \leq M$. That means the norm-minimal interpolant from Theorem 8.2 is given by

$$\mathbf{s}_{\mathbf{v}}(\mathbf{x}) = \sum_{i=1}^{d} \sum_{j=1}^{N} \alpha_j^{(i)} (\lambda_j^{(i)})^{\mathbf{y}} \mathbf{\Phi}(\mathbf{x} - \mathbf{y}) + \sum_{j=1}^{M} \beta_j (\lambda_j^{(d+1)})^{\mathbf{y}} \mathbf{\Phi}(\mathbf{x} - \mathbf{y}). \tag{8.7}$$

Here, $\mathbf{\Phi}$ denotes the combined kernel from (7.1). For the theory to work, we need to know that the functionals are linearly independent. This is indeed true and not difficult to show, see the proof of Theorem 2.7 in [74]. We quote the theorem here as it summarises our knowledge thus far.

Theorem 8.3 *Let $\Omega \subset \mathbb{R}^d$ with a $C^{k,1}$ boundary, where $k \geq 1$. Assume that the functions $\phi, \psi \colon \mathbb{R}^d \to \mathbb{R}$ are positive definite and chosen such that $\mathcal{N}_{\mathbf{\Phi}}(\mathbb{R}^d) = \widetilde{\mathbf{H}}^{\sigma}(\mathbb{R}^d, \mathrm{div}) \times H^{\sigma+1}(\mathbb{R}^d)$ with $\sigma > d/2$. Then, the interpolant $\mathbf{s}_{\mathbf{v}} = (\mathbf{s}_{\mathbf{u}}, s_p)$ from (8.7) is well-defined and uniquely determined by the interpolation conditions (8.5) and (8.6). It satisfies $L\mathbf{s}_{\mathbf{v}}(\mathbf{x}_j) = \mathbf{f}(\mathbf{x}_j)$ with $L\mathbf{v} := \mathbf{u} + K\nabla p$ and $\mathbf{s}_{\mathbf{u}}(\mathbf{y}_j) \cdot \mathbf{n}(\mathbf{y}_j) = \mathbf{g}(\mathbf{y}_j) \cdot \mathbf{n}(\mathbf{y}_j)$ and is divergence-free in $\mathbb{R}^d$, $\nabla \cdot \mathbf{s}_{\mathbf{u}} = 0$.*

The error of this discretisation scheme has been discussed in [74]. We omit the details here as we will prove a more general result for scaled kernels, see Theorem 8.6.

Lastly, we focus on the two dimensional case, $d = 2$, and take the specific form of the kernel $\mathbf{\Phi}$ into account, see (7.1). The functionals for the first component, for example, take the form

$$(\lambda_j^{(1)})^{\mathbf{y}} \mathbf{\Phi}(\mathbf{x} - \mathbf{y}) = \begin{pmatrix} -\partial_{22}\phi(\mathbf{x} - \mathbf{x}_j) \\ \partial_{12}\phi(\mathbf{x} - \mathbf{x}_j) \\ (K\nabla_{\mathbf{y}}\psi)_1(\mathbf{x} - \mathbf{x}_j) \end{pmatrix}^T,$$

where $\nabla_{\mathbf{y}}$ is taken with respect to the second argument. Correspondingly, $\nabla_{\mathbf{x}}$ will be taken with respect to the first argument. For this two dimensional problem we interpret $\mathbf{v} = (\mathbf{u}^T, p)$ as a row vector. The interpolant then takes the form

$$\begin{aligned} \mathbf{s}_{(\mathbf{u}^T,p)}(\mathbf{x}) = &\sum_{j=1}^N \alpha_j^{(1)} \begin{pmatrix} -\partial_{22}\phi(\mathbf{x} - \mathbf{x}_j) \\ \partial_{12}\phi(\mathbf{x} - \mathbf{x}_j) \\ (K\nabla_{\mathbf{y}}\psi)_1(\mathbf{x} - \mathbf{x}_j) \end{pmatrix}^T + \sum_{j=1}^N \alpha_j^{(2)} \begin{pmatrix} \partial_{21}\phi(\mathbf{x} - \mathbf{x}_j) \\ -\partial_{11}\phi(\mathbf{x} - \mathbf{x}_j) \\ (K\nabla_{\mathbf{y}}\psi)_2(\mathbf{x} - \mathbf{x}_j) \end{pmatrix}^T \\ &+ \sum_{j=1}^M \beta_j \begin{pmatrix} -\partial_{22}\phi(\mathbf{x} - \mathbf{y}_j)n_1(\mathbf{y}_j) + \partial_{21}\phi(\mathbf{x} - \mathbf{y}_j)n_2(\mathbf{y}_j) \\ \partial_{12}\phi(\mathbf{x} - \mathbf{y}_j)n_1(\mathbf{y}_j) - \partial_{11}\phi(\mathbf{x} - \mathbf{y}_j)n_2(\mathbf{y}_j) \\ 0 \end{pmatrix}^T. \end{aligned}$$

We determine the coefficients from the interpolation conditions

$$L\mathbf{s}_{(\mathbf{u}^T,p)}(\mathbf{x}_k) = \mathbf{f}(\mathbf{x}_k) \qquad \text{and} \qquad \mathbf{s}_{\mathbf{u}}(\mathbf{y}_\ell) \cdot \mathbf{n}(\mathbf{y}_\ell) = \mathbf{g}(\mathbf{y}_\ell) \cdot \mathbf{n}(\mathbf{y}_\ell)$$

for $1 \le k \le N$ and $1 \le \ell \le M$, where we have set $L\mathbf{v} := \mathbf{u} + K\nabla p$. The first equation yields

$$\begin{aligned} L\mathbf{s}_{(\mathbf{u}^T,p)}(\mathbf{x}_k) = &\sum_{j=1}^N \alpha_j^{(1)} \begin{pmatrix} -\partial_{22}\phi(\mathbf{x}_k - \mathbf{x}_j) \\ \partial_{12}\phi(\mathbf{x}_k - \mathbf{x}_j) \end{pmatrix} + \sum_{j=1}^N \alpha_j^{(2)} \begin{pmatrix} \partial_{21}\phi(\mathbf{x}_k - \mathbf{x}_j) \\ -\partial_{11}\phi(\mathbf{x}_k - \mathbf{x}_j) \end{pmatrix} \\ &+ \sum_{j=1}^M \beta_j \begin{pmatrix} -\partial_{22}\phi(\mathbf{x}_k - \mathbf{y}_j)n_1(\mathbf{y}_j) + \partial_{21}\phi(\mathbf{x}_k - \mathbf{y}_j)n_2(\mathbf{y}_j) \\ \partial_{12}\phi(\mathbf{x}_k - \mathbf{y}_j)n_1(\mathbf{y}_j) - \partial_{11}\phi(\mathbf{x}_k - \mathbf{y}_j)n_2(\mathbf{y}_j) \end{pmatrix} \\ &+ K\nabla_{\mathbf{x}} \left(\sum_{j=1}^N \alpha_j^{(1)} (K\nabla_{\mathbf{y}}\psi)_1(\mathbf{x}_k - \mathbf{x}_j) + \sum_{j=1}^N \alpha_j^{(2)} (K\nabla_{\mathbf{y}}\psi)_2(\mathbf{x}_k - \mathbf{x}_j) \right) \\ &= \mathbf{f}(\mathbf{x}_k). \end{aligned}$$

The second equation follows similarly. That is, we need to solve a block system of the form

$$\begin{pmatrix} A_{11} & A_{12} & A_{13} \\ A_{21} & A_{22} & A_{23} \\ A_{31} & A_{32} & A_{33} \end{pmatrix} \begin{pmatrix} \boldsymbol{\alpha}_1 \\ \boldsymbol{\alpha}_2 \\ \boldsymbol{\beta} \end{pmatrix} = \begin{pmatrix} \mathbf{f}_1 \\ \mathbf{f}_2 \\ \mathbf{f}_3 \end{pmatrix}$$

with

$$
\begin{aligned}
A_{11} &= [-\partial_{22}\phi(\mathbf{x}_k - \mathbf{x}_j) + (K\nabla_{\mathbf{x}})_1(K\nabla_{\mathbf{y}}\psi)_1(\mathbf{x}_k - \mathbf{x}_j)]_{1\le k,j\le N} \\
A_{12} &= A_{21} = [\partial_{12}\phi(\mathbf{x}_k - \mathbf{x}_j) + (K\nabla_{\mathbf{x}})_1(K\nabla_{\mathbf{y}}\psi)_2(\mathbf{x}_k - \mathbf{x}_j)]_{1\le k,j\le N} \\
A_{22} &= [-\partial_{11}\phi(\mathbf{x}_k - \mathbf{x}_j) + (K\nabla_{\mathbf{x}})_2(K\nabla_{\mathbf{y}}\psi)_2(\mathbf{x}_k - \mathbf{x}_j)]_{1\le k,j\le N} \\
A_{13} &= A_{31}^T = [-\partial_{22}\phi(\mathbf{x}_k - \mathbf{y}_\ell)n_1(\mathbf{y}_\ell) + \partial_{21}\phi(\mathbf{x}_k - \mathbf{y}_\ell)n_2(\mathbf{y}_\ell)]_{1\le k\le N,1\le \ell\le M} \\
A_{23} &= A_{32}^T = [\partial_{12}\phi(\mathbf{x}_k - \mathbf{y}_\ell)n_1(\mathbf{y}_\ell) - \partial_{11}\phi(\mathbf{x}_k - \mathbf{y}_\ell)n_2(\mathbf{y}_\ell)]_{1\le k\le N,1\le \ell\le M} \\
A_{33} &= [n_1(\mathbf{y}_k)\left(-\partial_{22}\phi(\mathbf{y}_k - \mathbf{y}_\ell)n_1(\mathbf{y}_\ell) + \partial_{21}\phi(\mathbf{y}_k - \mathbf{y}_\ell)n_2(\mathbf{y}_\ell)\right) \\
&\quad + n_2(\mathbf{y}_k)\left(\partial_{12}\phi(\mathbf{y}_k - \mathbf{y}_\ell)n_1(\mathbf{y}_\ell) - \partial_{11}\phi(\mathbf{y}_k - \mathbf{y}_\ell)n_2(\mathbf{y}_\ell)\right)]_{1\le k,\ell\le M}
\end{aligned}
$$

as well as

$$
\boldsymbol{\alpha}_1 = (\alpha_{1j})_{1\le j\le N}, \boldsymbol{\alpha}_2 = (\alpha_{2j})_{1\le j\le N}, \boldsymbol{\beta} = (\beta_\ell)_{1\le \ell\le M}
$$

and

$$
\mathbf{f}_1 = (f_1(\mathbf{x}_k))_{1\le k\le N}, \mathbf{f}_2 = (f_2(\mathbf{x}_k))_{1\le k\le N}, \mathbf{f}_3 = (\mathbf{g}(\mathbf{y}_\ell)\cdot\mathbf{n}(\mathbf{y}_\ell))_{1\le \ell\le M}.
$$

We note that if the permeability tensor K is the identity and $\phi = \psi$, we automatically have two zero blocks, namely $A_{12} = A_{21}$ because the partial derivative with respect to y_2 introduces via the chain rule a minus sign.

8.4 Multilevel Theory

Now, we would like to develop the multilevel theory for Darcy's problem.

The goal is to find an error bound for the analytical solution and its collocation approximation of Darcy's problem if the underlying kernels depend on a scale $\delta > 0$. In order to estimate the overall error for Darcy's problem, we split it into a boundary and interior error and consider both errors separately. The following proposition generalises Proposition 3.4 from [74] by extending it to scaled kernels.

Proposition 8.4 (Interior Error for Darcy's Problem) *Let $\Omega \subseteq \mathbb{R}^d$ for $d = 2, 3$ be simply connected and open with a $C^{\lceil\sigma\rceil+1,1}$ boundary $\partial\Omega$ for some $\sigma > d/2$. Let the permeability tensor $K = (K_{ij})$ be strictly elliptic on Ω (i. e. satisfy (8.4)) with $K = K^T$ and components K_{ij} in $H^\sigma(\Omega)$. Assume that $\mathbf{f} \in \mathbf{H}^{\sigma+1}(\Omega)$, $\mathbf{g} \in \mathbf{H}^{\sigma+1/2}(\partial\Omega)$ and the compatability condition $\int_{\partial\Omega}\mathbf{g}\cdot\mathbf{n}dS = 0$. Suppose that the kernel $\mathbf{\Phi}_\delta$ is chosen such that $\mathcal{N}_{\mathbf{\Phi}_\delta}(\mathbb{R}^d) = \widetilde{\mathbf{H}}^\sigma(\mathbb{R}^d, \mathrm{div}) \times H^{\sigma+1}(\mathbb{R}^d)$. Then for $0 \le \eta \le \sigma - d(1/2 - 1/r)_+ - 1$ and for $1 < r < \infty$, we have*

$$
\begin{aligned}
&\|L\mathbf{v} - L\mathbf{s}_{\mathbf{v}}\|_{\mathbf{W}_r^{\eta+1}(\Omega)} \\
&\quad \le C\delta^{-\sigma-1}h_{X,\Omega}^{\sigma-\eta-1-d(1/2-1/r)_+}\|\mathbf{E}\mathbf{v} - \mathbf{s}_{\mathbf{E}\mathbf{v}}\|_{\mathcal{N}_{\mathbf{\Phi}_\delta}(\mathbb{R}^d)} \\
&\quad \le C\delta^{-\sigma-1}h_{X,\Omega}^{\sigma-\eta-1-d(1/2-1/r)_+}\|\mathbf{E}\mathbf{v}\|_{\mathcal{N}_{\mathbf{\Phi}_\delta}(\mathbb{R}^d)} \\
&\quad \le C\delta^{-\sigma-1}h_{X,\Omega}^{\sigma-\eta-1-d(1/2-1/r)_+}\left(\|\mathbf{f}\|_{\mathbf{H}^\sigma(\Omega)} + \|\mathbf{g}\cdot\mathbf{n}\|_{H^{\sigma-1/2}(\partial\Omega)}\right)
\end{aligned}
$$

for some $C > 0$ independent of the mesh norm as well as $\mathbf{u}$ and $\mathbf{s}_\mathbf{u}$.

Proof. We pick a representer p of the equivalence class that in a slight abuse of notation we call p as well so that

$$\|p\|_{H^{\sigma+1}(\Omega)} = \|p\|_{H^{\sigma+1}(\Omega)/\mathbb{R}}$$

and note that on Ω the generalised interpolant $\mathbf{s}_\mathbf{v}$ coincides with the generalised interpolant to the extended $\mathbf{E}\mathbf{v} = (\widetilde{\mathbf{E}}_{\mathrm{div}}\mathbf{u}, E_S p) \in \widetilde{\mathbf{H}}^\sigma(\mathbb{R}^d, \mathrm{div}) \times H^{\sigma+1}(\mathbb{R}^d)$. We compute

$$\begin{aligned}
\|L\mathbf{v} - L\mathbf{s}_\mathbf{v}\|_{\mathbf{H}^\sigma(\Omega)} &= \|L\mathbf{E}\mathbf{v} - L\mathbf{s}_{\mathbf{E}\mathbf{v}}\|_{\mathbf{H}^\sigma(\Omega)} \\
&\leq \|\widetilde{\mathbf{E}}_{\mathrm{div}}\mathbf{u} - \mathbf{s}_{\widetilde{\mathbf{E}}_{\mathrm{div}}\mathbf{u}}\|_{\mathbf{H}^\sigma(\mathbb{R}^d)} + \|K(\nabla E_S p - \nabla s_{E_S p})\|_{\mathbf{H}^\sigma(\mathbb{R}^d)} \\
&\leq \|\widetilde{\mathbf{E}}_{\mathrm{div}}\mathbf{u} - \mathbf{s}_{\widetilde{\mathbf{E}}_{\mathrm{div}}\mathbf{u}}\|_{\mathbf{H}^\sigma(\mathbb{R}^d)} + C\|E_S p - s_{E_S p}\|_{H^{\sigma+1}(\mathbb{R}^d)},
\end{aligned}$$

where we have used the Sobolev product theorem [59, Lemma 3.4 (ii)] several times, which states that if $\sigma > d/2$, we have for two scalar-valued functions u, v the inequality

$$\|uv\|_{H^\sigma(\mathbb{R}^d)} \leq C\|u\|_{H^\sigma(\mathbb{R}^d)}\|v\|_{H^\sigma(\mathbb{R}^d)}$$

for some constant $C > 0$ independent of u and v. Then we can deduce by Lemma 7.13, the optimality in the $\mathcal{N}_{\mathbf{\Phi}_\delta}(\mathbb{R}^d)$ norm, the continuous dependence on the data (Theorem 8.1) as well as properties of the extension operators that

$$\begin{aligned}
\|L\mathbf{v} - L\mathbf{s}_\mathbf{v}\|_{\mathbf{H}^\sigma(\Omega)} &\leq \|\widetilde{\mathbf{E}}_{\mathrm{div}}\mathbf{u} - \mathbf{s}_{\widetilde{\mathbf{E}}_{\mathrm{div}}\mathbf{u}}\|_{\widetilde{\mathbf{H}}^\sigma(\mathbb{R}^d,\mathrm{div})} + C\|E_S p - s_{E_S p}\|_{H^{\sigma+1}(\mathbb{R}^d)} \\
&\leq C\delta^{-\sigma-1}\|\mathbf{E}\mathbf{v} - \mathbf{s}_{\mathbf{E}\mathbf{v}}\|_{\mathcal{N}_{\mathbf{\Phi}_\delta}(\mathbb{R}^d)} \\
&\leq C\delta^{-\sigma-1}\|\mathbf{E}\mathbf{v}\|_{\mathcal{N}_{\mathbf{\Phi}_\delta}(\mathbb{R}^d)} \\
&\leq C\delta^{-\sigma-1}\left(\|\widetilde{\mathbf{E}}_{\mathrm{div}}\mathbf{u}\|_{\widetilde{\mathbf{H}}^\sigma(\mathbb{R}^d,\mathrm{div})} + \|E_S p\|_{H^{\sigma+1}(\mathbb{R}^d)}\right) \\
&\leq C\delta^{-\sigma-1}\left(\|\mathbf{u}\|_{\mathbf{H}^\sigma(\Omega)} + \|p\|_{H^{\sigma+1}(\Omega)}\right) \\
&\leq C\delta^{-\sigma-1}\left(\|\mathbf{f}\|_{\mathbf{H}^\sigma(\Omega)} + \|\mathbf{g}\cdot\mathbf{n}\|_{H^{\sigma-1/2}(\partial\Omega)}\right).
\end{aligned}$$

□

For the error on the boundary, we again start by taking the corresponding proposition (Proposition 3.6) from [74] and extend the result to scaled kernels.

Proposition 8.5 (Boundary Error for Darcy's Problem) *Let $d = 2, 3$ and $\sigma > d/2$. Assume that Ω, K, $\mathbf{f}$ and $\mathbf{g}$ satisfy the same smoothness assumptions as in Proposition 8.4. Suppose that the kernel $\mathbf{\Phi}_\delta$ is chosen such that $\mathcal{N}_{\mathbf{\Phi}_\delta}(\mathbb{R}^d) = \widetilde{\mathbf{H}}^\sigma(\mathbb{R}^d, \mathrm{div}) \times H^{\sigma+1}(\mathbb{R}^d)$.*

Then

$$\begin{aligned}
&\|(\mathbf{u}-\mathbf{s}_{\mathbf{u}})\cdot\mathbf{n}\|_{\mathbf{W}_r^{\eta+1-1/r}(\partial\Omega)}\\
&\quad\leq C\delta^{-\sigma-1}h_{Y,\partial\Omega}^{\sigma-\eta-1-1/2+1/r-(d-1)(1/2-1/r)_+}\|\mathbf{E}\mathbf{v}-\mathbf{s}_{\mathbf{E}\mathbf{v}}\|_{\mathcal{N}_{\boldsymbol{\Phi}_\delta}(\mathbb{R}^d)}\\
&\quad\leq C\delta^{-\sigma-1}h_{Y,\partial\Omega}^{\sigma-\eta-1-1/2+1/r-(d-1)(1/2-1/r)_+}\|\mathbf{E}\mathbf{v}\|_{\mathcal{N}_{\boldsymbol{\Phi}_\delta}(\mathbb{R}^d)}\\
&\quad\leq C\delta^{-\sigma-1}h_{Y,\partial\Omega}^{\sigma-\eta-1-1/2+1/r-(d-1)(1/2-1/r)_+}\left(\|\mathbf{f}\|_{\mathbf{H}^\sigma(\Omega)}+\|\mathbf{g}\cdot\mathbf{n}\|_{H^{\sigma-1/2}(\partial\Omega)}\right)
\end{aligned}$$

for some $C>0$ independent of the mesh norm as well as $\mathbf{u}$ and $\mathbf{s}_{\mathbf{u}}$ and $1<r<\infty$ and $0\leq\eta\leq\sigma-1/2-(d-1)(1/2-1/r)_+-1+1/r$.

Proof. Just as in the proof of Proposition 3.6 from [74] we derive

$$\|(\mathbf{u}-\mathbf{s}_{\mathbf{u}})\cdot\mathbf{n}\|_{\mathbf{W}_r^{\eta+1-1/r}(\partial\Omega)}\leq Ch_{Y,\partial\Omega}^{\sigma-\eta-1-1/2+1/r-(d-1)(1/2-1/r)_+}\|\mathbf{u}-\mathbf{s}_{\mathbf{u}}\|_{\mathbf{H}^\sigma(\Omega)}.$$

Now we can use the same reasoning as for the proof of Proposition 8.4 to conclude that

$$\begin{aligned}
\|\mathbf{u}-\mathbf{s}_{\mathbf{u}}\|_{\mathbf{H}^\sigma(\Omega)}&\leq C\delta^{-\sigma-1}\|\mathbf{E}\mathbf{v}-\mathbf{s}_{\mathbf{E}\mathbf{v}}\|_{\mathcal{N}_{\boldsymbol{\Phi}_\delta}(\mathbb{R}^d)}\\
&\leq C\delta^{-\sigma-1}\|\mathbf{E}\mathbf{v}\|_{\mathcal{N}_{\boldsymbol{\Phi}_\delta}(\mathbb{R}^d)}\\
&\leq C\delta^{-\sigma-1}\left(\|\mathbf{f}\|_{\mathbf{H}^\sigma(\Omega)}+\|\mathbf{g}\cdot\mathbf{n}\|_{H^{\sigma-1/2}(\partial\Omega)}\right).
\end{aligned}$$

□

Theorem 8.6 (Error for Darcy's Problem) *Let Ω be an open, bounded, simply connected subset of $\mathbb{R}^d$ with a $C^{\lceil\sigma\rceil+1,1}$ boundary $\partial\Omega$ where $d=2,3$ for some $\sigma>d/2$. Let the permeability tensor $K=(K_{ij})$ be strictly elliptic on Ω (i. e. satisfy (8.4)) with $K=K^T$ and components K_{ij} in $H^\sigma(\Omega)$. Assume that the data $\mathbf{f}\in\mathbf{H}^{\sigma+1}(\Omega)$, $\mathbf{g}\in\mathbf{H}^{\sigma+1/2}(\partial\Omega)$ and $\int_{\partial\Omega}\mathbf{g}\cdot\mathbf{n}dS=0$. Suppose that the kernel $\boldsymbol{\Phi}_\delta$ is chosen such that $\mathcal{N}_{\boldsymbol{\Phi}_\delta}(\mathbb{R}^d)=\widetilde{\mathbf{H}}^\sigma(\mathbb{R}^d,\mathrm{div})\times H^{\sigma+1}(\mathbb{R}^d)$. Then, we can bound the error between analytical solution and collocation approximant as follows*

$$\begin{aligned}
&\|\mathbf{u}-\mathbf{s}_{\mathbf{u}}\|_{\mathbf{W}_r^{\eta+1}(\Omega)}+\|p-s_p\|_{W_r^{\eta+2}(\Omega)/\mathbb{R}}\\
&\quad\leq C\delta^{-\sigma-1}\left(h_{X,\Omega}^{\sigma-\eta-1-d(1/2-1/r)_+}+h_{Y,\partial\Omega}^{\sigma-\eta-1-1/2+1/r-(d-1)(1/2-1/r)_+}\right)\\
&\qquad\times\|\mathbf{E}\mathbf{v}-\mathbf{s}_{\mathbf{E}\mathbf{v}}\|_{\mathcal{N}_{\boldsymbol{\Phi}_\delta}(\mathbb{R}^d)}\\
&\quad\leq C\delta^{-\sigma-1}\left(h_{X,\Omega}^{\sigma-\eta-1-d(1/2-1/r)_+}+h_{Y,\partial\Omega}^{\sigma-\eta-1-1/2+1/r-(d-1)(1/2-1/r)_+}\right)\\
&\qquad\times\|\mathbf{E}\mathbf{v}\|_{\mathcal{N}_{\boldsymbol{\Phi}_\delta}(\mathbb{R}^d)}\\
&\quad\leq C\delta^{-\sigma-1}\left(h_{X,\Omega}^{\sigma-\eta-1-d(1/2-1/r)_+}+h_{Y,\partial\Omega}^{\sigma-\eta-1-1/2+1/r-(d-1)(1/2-1/r)_+}\right)\\
&\qquad\times\left(\|\mathbf{f}\|_{\mathbf{H}^\sigma(\Omega)}+\|\mathbf{g}\cdot\mathbf{n}\|_{H^{\sigma-1/2}(\partial\Omega)}\right)
\end{aligned}$$

for $1 < r < \infty$ and $0 \le \eta \le \sigma - d(1/2 - 1/r)_+ - 1$ and some constant $C > 0$ that is independent of both mesh norms, the analytical solution as well as its collocation approximation. Note that optimality is not used for the first inequality.

Proof. Theorem 8.1 asserts

$$\begin{aligned}&\|\mathbf{u} - \mathbf{s_u}\|_{\mathbf{W}_r^{\eta+1}(\Omega)} + \|p - s_p\|_{W_r^{\eta+2}(\Omega)/\mathbb{R}} \\ &\quad \le C \left(\|L(\mathbf{v} - \mathbf{s_v})\|_{\mathbf{W}_r^{\eta+1}(\Omega)} + \|(\mathbf{u} - \mathbf{s_u}) \cdot \mathbf{n}\|_{\mathbf{W}_r^{\eta+1-1/r}(\partial\Omega)} \right).\end{aligned}$$

Using Propositions 8.4 and 8.5, completes the proof. □

Corollary 8.7 *Under the same assumptions as above, $r = 2$ and $h := h_{X,\Omega} \approx h_{Y,\partial\Omega}$, the above result simplifies to*

$$\begin{aligned}\|\mathbf{u} - \mathbf{s_u}\|_{\mathbf{H}^{\eta+1}(\Omega)} + \|p - s_p\|_{H^{\eta+2}(\Omega)/\mathbb{R}} &\\ \le C\delta^{-\sigma-1} h^{\sigma-\eta-1} \|\mathbf{E}\mathbf{v} - \mathbf{s}_{\mathbf{E}\mathbf{v}}\|_{\mathcal{N}_{\mathbf{\Phi}_\delta}(\mathbb{R}^d)} &\\ \le C\delta^{-\sigma-1} h^{\sigma-\eta-1} \|\mathbf{E}\mathbf{v}\|_{\mathcal{N}_{\mathbf{\Phi}_\delta}(\mathbb{R}^d)} &\\ \le C\delta^{-\sigma-1} h^{\sigma-\eta-1} \left(\|\mathbf{f}\|_{\mathbf{H}^\sigma(\Omega)} + \|\mathbf{g} \cdot \mathbf{n}\|_{H^{\sigma-1/2}(\partial\Omega)} \right).\end{aligned}$$

Symmetric Multilevel Collocation Algorithm

Suppose we are given a sequence of point sets in Ω, namely $X_1, X_2, \ldots$, with decreasing mesh norms $h_{X_1,\Omega}, h_{X_2,\Omega}, \ldots$ as well as a sequence of point sets on $\partial\Omega$ denoted by $Y_1, Y_2, \ldots$ with corresponding decreasing mesh norms $h_{Y_1,\partial\Omega}, h_{Y_2,\partial\Omega}, \ldots$. Set $h_j = \max\{h_{X_j,\Omega}, h_{Y_j,\partial\Omega}\}$. With these mesh norms we construct support radii of the form

$$\delta_j = \beta h_j^{\frac{\sigma-1}{\sigma+1}}$$

for some proportionality constant $\beta > 0$ and define scaled matrix-valued kernels $\mathbf{\Phi}_j = \mathbf{\Phi}_{\delta_j}$ as in (7.12), where $\mathbf{\Phi}$ denotes the combined kernel (7.1). Then we can define interpolants $\mathbf{s}_j$ from the space

$$L\mathbf{V}_{X_j} + \mathbf{V}_{Y_j} = \operatorname{span}\{L_2\mathbf{\Phi}_j(\cdot - \mathbf{x}) | \mathbf{x} \in X_j\} + \operatorname{span}\{\mathbf{\Phi}_j(\cdot - \mathbf{y}) | \mathbf{y} \in Y_j\}.$$

Here L_2 denotes action with respect to the second argument.

Algorithm 8.8 (Multilevel Algorithm for Darcy's Problem)

Input: Right-hand sides $\mathbf{f}$ and $\mathbf{g} \cdot \mathbf{n}$, number of levels n

Set $\mathbf{v}_0 = \mathbf{0}, \mathbf{f}_0 = \mathbf{f}, \mathbf{g}_0 \cdot \mathbf{n} = \mathbf{g} \cdot \mathbf{n}$ and for $j = 1, \ldots, n$ **do**

(i) Determine $\mathbf{s}_j \in L\mathbf{V}_{X_j} + \mathbf{V}_{Y_j}$ to $\mathbf{f}_{j-1}$ on X_j and $\mathbf{g}_{j-1} \cdot \mathbf{n}$ on Y_j, i. e,

$$\begin{aligned}L\mathbf{s}_j(\mathbf{x}) &= \mathbf{f}_{j-1}(\mathbf{x}), && \mathbf{x} \in X_j \\ (\mathbf{s}_j \cdot \mathbf{n})(\mathbf{y}) &= (\mathbf{g}_{j-1} \cdot \mathbf{n})(\mathbf{y}), && \mathbf{y} \in Y_j\end{aligned}$$

(ii) Update the global approximation and the residuals

$$\begin{aligned} \mathbf{v}_j &= \mathbf{v}_{j-1} + \mathbf{s}_j \\ \mathbf{f}_j &= \mathbf{f}_{j-1} - L(\mathbf{s}_j|_\Omega) \\ (\mathbf{g}_j \cdot \mathbf{n}) &= (\mathbf{g}_{j-1} \cdot \mathbf{n}) - (\mathbf{s}_j \cdot \mathbf{n})|_{\partial\Omega} \end{aligned}$$

end

Output: Approximate solution $\mathbf{v}_n$ to $\mathbf{v} = (\mathbf{u}, p)$

We define the error between the solution $\mathbf{v} = (\mathbf{u}, p)$ and its jth multiscale approximation $\mathbf{v}_j$ through

$$\mathbf{e}_j = \mathbf{v} - \mathbf{v}_j.$$

With $\mathbf{e}_{\mathbf{u},j}$ and $e_{p,j}$ we denote the velocity component and the pressure component of the error at level j. We show that the algorithm converges.

Theorem 8.9 (Convergence of Multilevel Collocation Algorithm)
Let $d = 2, 3$ and $\sigma > d/2$. Assume that Ω, K, $\mathbf{f}$ and $\mathbf{g}$ satisfy the same smoothness assumptions as in Theorem 8.6. We define two point set sequences. Firstly, let $X_1, X_2, \ldots$ be a sequence of point sets in Ω with mesh norms $h_{X_1,\Omega}, h_{X_2,\Omega}, \ldots$ and secondly let $Y_1, Y_2, \ldots$ be a sequence of point sets on $\partial\Omega$ with mesh norms $h_{Y_1,\partial\Omega}, h_{Y_2,\partial\Omega}, \ldots$. Set $h_j = \max\{h_{X_j,\Omega}, h_{Y_j,\partial\Omega}\}$ and assume

$$\gamma\mu h_j \leq h_{j+1} \leq \mu h_j \tag{8.8}$$

for $j = 1, 2, \ldots$ and some fixed $\mu \in (0, 1)$ and $\gamma \in (0, 1)$. Suppose that the kernel $\mathbf{\Phi}$ from (7.1) is chosen such that $\mathcal{N}_{\mathbf{\Phi}}(\mathbb{R}^d) = \widetilde{\mathbf{H}}^\sigma(\mathbb{R}^d, \mathrm{div}) \times H^{\sigma+1}(\mathbb{R}^d)$. This means in particular that the functions ϕ and ψ are positive definite and both functions generate $H^{\sigma+1}(\mathbb{R}^d)$. Define

$$\delta_j = \left(\frac{h_j}{\mu}\right)^{\frac{\sigma-1}{\sigma+1}} \quad \text{as well as} \quad \mathbf{\Phi}_j = \mathbf{\Phi}_{\delta_j}.$$

Lastly, let $h_1 \leq \mu$ be sufficiently small. Then, there exists a constant C independent of μ, j and u such that

$$\|\mathbf{E}\mathbf{e}_j\|_{\mathbf{\Phi}_{j+1}} \leq \alpha \|\mathbf{E}\mathbf{e}_{j-1}\|_{\mathbf{\Phi}_j}, \tag{8.9}$$

for $j = 1, 2, \ldots$ with $\alpha = C\mu^{\sigma-1}$. Thus, we have the estimates

$$\|\mathbf{v} - \mathbf{v}_k\|_{\mathbf{L}_2(\Omega)} \leq C\alpha^k \left(\|\mathbf{u}\|_{\mathbf{H}^\sigma(\Omega)} + \|p\|_{H^{\sigma+1}(\Omega)}\right)$$

and in particular the multiscale approximation $\mathbf{v}_k$ converges to $\mathbf{v}$ in the L_2 norm if we choose μ so small that $\alpha < 1$.

Remark 8.10 *Since $d = 2, 3$ and $\sigma > d/2$, we have*

$$0 < \sigma - 1.$$

Therefore, it is indeed possible to find a $\mu \in (0, 1)$ such that $\alpha < 1$.

Proof. The support radii are monotonically decreasing. Instead of working with equivalence classes, we pick a representer for the pressure component and denote it with p as well. We compute

$$\begin{aligned}
\|\mathbf{E}\mathbf{e}_j\|^2_{\mathcal{N}_{\mathbf{\Phi}_{j+1}}(\mathbb{R}^d)} &= (2\pi)^{-d/2} \int_{\mathbb{R}^d} \left\{ \frac{\|\widehat{\widetilde{\mathbf{E}}_{\mathrm{div}}\mathbf{e}_{\mathbf{u},j}}(\boldsymbol{\omega})\|_2^2}{\|\boldsymbol{\omega}\|_2^2 \widehat{\phi_{j+1}}(\boldsymbol{\omega})} + \frac{|\widehat{E_S e_{p,j}}(\boldsymbol{\omega})|^2}{\widehat{\psi_{j+1}}(\boldsymbol{\omega})} \right\} d\boldsymbol{\omega} \\
&\leq \max\left\{ \frac{1}{c_1}, \frac{1}{c_3} \right\} \\
&\qquad (2\pi)^{-d/2} \int_{\mathbb{R}^d} \left\{ \frac{\|\widehat{\widetilde{\mathbf{E}}_{\mathrm{div}}\mathbf{e}_{\mathbf{u},j}}(\boldsymbol{\omega})\|_2^2}{\|\boldsymbol{\omega}\|_2^2} + |\widehat{E_S e_{p,j}}(\boldsymbol{\omega})|^2 \right\} (1 + \|\delta_{j+1}\boldsymbol{\omega}\|_2^2)^{\sigma+1} d\boldsymbol{\omega} \\
&=: C(2\pi)^{-d/2}(I_1 + I_2),
\end{aligned}$$

where we introduced the notation

$$\begin{aligned}
I_1 &= \int\limits_{\|\boldsymbol{\omega}\|_2 \leq \frac{1}{\delta_{j+1}}} \left\{ \frac{\|\widehat{\widetilde{\mathbf{E}}_{\mathrm{div}}\mathbf{e}_{\mathbf{u},j}}(\boldsymbol{\omega})\|_2^2}{\|\boldsymbol{\omega}\|_2^2} + |\widehat{E_S e_{p,j}}(\boldsymbol{\omega})|^2 \right\} (1 + \|\delta_{j+1}\boldsymbol{\omega}\|_2^2)^{\sigma+1} d\boldsymbol{\omega} \\
I_2 &= \int\limits_{\|\boldsymbol{\omega}\|_2 \geq \frac{1}{\delta_{j+1}}} \left\{ \frac{\|\widehat{\widetilde{\mathbf{E}}_{\mathrm{div}}\mathbf{e}_{\mathbf{u},j}}(\boldsymbol{\omega})\|_2^2}{\|\boldsymbol{\omega}\|_2^2} + |\widehat{E_S e_{p,j}}(\boldsymbol{\omega})|^2 \right\} (1 + \|\delta_{j+1}\boldsymbol{\omega}\|_2^2)^{\sigma+1} d\boldsymbol{\omega}.
\end{aligned}$$

For the first integral we have $\delta_{j+1}\|\boldsymbol{\omega}\|_2 \leq 1$. We combine this estimate with Lemma 7.16, Parseval's identity and Corollary 8.7.

We can then compute

$$
\begin{aligned}
I_1 &\leq 2^{\sigma+1} \int_{\|\boldsymbol{\omega}\|_2 \leq \frac{1}{\delta_{j+1}}} \left\{ \frac{\|\widehat{\widetilde{\mathbf{E}}_{\mathrm{div}} \mathbf{e}_{\mathbf{u},j}}(\boldsymbol{\omega})\|_2^2}{\|\boldsymbol{\omega}\|_2^2} + |\widehat{E_S e_{p,j}}(\boldsymbol{\omega})|^2 \right\} d\boldsymbol{\omega} \\
&\leq C \left\{ \|\mathbf{e}_{\mathbf{u},j}\|_{\mathbf{L}_2(\Omega)}^2 + \|\widehat{E_S e_{p,j}}\|_{L_2(\mathbb{R}^d)}^2 \right\} \\
&= C \left\{ \|\mathbf{e}_{\mathbf{u},j}\|_{\mathbf{L}_2(\Omega)}^2 + \|E_S e_{p,j}\|_{L_2(\mathbb{R}^d)}^2 \right\} \\
&\leq C \left\{ \|\mathbf{e}_{\mathbf{u},j}\|_{\mathbf{L}_2(\Omega)}^2 + \|e_{p,j}\|_{L_2(\Omega)}^2 \right\} \\
&\leq C \left\{ \|\mathbf{e}_{\mathbf{u},j}\|_{\mathbf{H}^1(\Omega)}^2 + \|e_{p,j}\|_{H^2(\Omega)}^2 \right\} \\
&\leq C \left\{ \|\mathbf{e}_{\mathbf{u},j}\|_{\mathbf{H}^1(\Omega)} + \|e_{p,j}\|_{H^2(\Omega)} \right\}^2 \\
&= C \left\{ \|\mathbf{e}_{\mathbf{u},j-1} - \mathbf{s}_{\mathbf{e}_{\mathbf{u},j-1}}\|_{\mathbf{H}_1(\Omega)} + \|e_{p,j-1} - s_{e_{p,j-1}}\|_{H^2(\Omega)} \right\}^2 \\
&\leq C\delta_j^{-2(\sigma+1)} h_j^{2(\sigma-1)} \|\mathbf{E}\mathbf{e}_{j-1} - \mathbf{s}_{\mathbf{E}\mathbf{e}_{j-1}}\|_{\mathcal{N}_{\boldsymbol{\Phi}_j}(\mathbb{R}^d)}^2 \\
&\leq C\delta_j^{-2(\sigma+1)} h_j^{2(\sigma-1)} \|\mathbf{E}\mathbf{e}_{j-1}\|_{\mathcal{N}_{\boldsymbol{\Phi}_j}(\mathbb{R}^d)}^2 \\
&= C_1 \mu^{2(\sigma-1)} \|\mathbf{E}\mathbf{e}_{j-1}\|_{\mathcal{N}_{\boldsymbol{\Phi}_j}(\mathbb{R}^d)}^2.
\end{aligned}
$$

We have used the fact that the interpolant is norm-minimal with respect to the $\mathcal{N}_{\boldsymbol{\Phi}_j}$ norm. Since $\delta_{j+1}\|\boldsymbol{\omega}\|_2 \geq 1$, we find

$$
(1 + \delta_{j+1}^2 \|\boldsymbol{\omega}\|_2^2)^{\sigma+1} \leq (2\delta_{j+1}^2 \|\boldsymbol{\omega}\|_2^2)^{\sigma+1} \leq 2^{\sigma+1} \mu^{2(\sigma-1)} (1 + \delta_j^2 \|\boldsymbol{\omega}\|_2^2)^{\sigma+1}
$$

and consequently

$$
\begin{aligned}
I_2 &\leq C\mu^{2(\sigma-1)} \|\mathbf{E}\mathbf{e}_j\|_{\mathcal{N}_{\boldsymbol{\Phi}_j}(\mathbb{R}^d)}^2 \\
&= C\mu^{2(\sigma-1)} \|\mathbf{E}\mathbf{e}_{j-1} - \mathbf{s}_{\mathbf{E}\mathbf{e}_{j-1}}\|_{\mathcal{N}_{\boldsymbol{\Phi}_j}(\mathbb{R}^d)}^2 \\
&\leq C_2 \mu^{2(\sigma-1)} \|\mathbf{E}\mathbf{e}_{j-1}\|_{\mathcal{N}_{\boldsymbol{\Phi}_j}(\mathbb{R}^d)}^2.
\end{aligned}
$$

In the last step we have used again the fact that the interpolant is norm-minimal in the $\mathcal{N}_{\boldsymbol{\Phi}_j}$ norm. Combining both estimates now yields (8.9) with

$$
\alpha = \sqrt{C(2\pi)^{-d/2}} (C_1 + C_2)^{1/2} \mu^{\sigma-1} = C\mu^{\sigma-1}.
$$

With the help of this monotonicity result and Corollary 8.7, we can bound

$$\begin{aligned}
\|\mathbf{v}-\mathbf{v}_n\|^2_{\mathbf{L}_2(\Omega)} &= \|\mathbf{e}_{n-1}-\mathbf{s}_n\|^2_{\mathbf{L}_2(\Omega)} \\
&= \|\mathbf{e}_{n-1}-\mathbf{s}_{\mathbf{e}_{n-1}}\|^2_{\mathbf{L}_2(\Omega)} \\
&\leq \|\mathbf{e}_{n-1}-\mathbf{s}_{\mathbf{e}_{n-1}}\|^2_{\mathbf{H}^1(\Omega)} \\
&= \|\mathbf{e}_{\mathbf{u},n-1}-\mathbf{s}_{\mathbf{e}_{\mathbf{u},n-1}}\|^2_{\mathbf{H}^1(\Omega)} + \|e_{p,n-1}-s_{e_{p,n-1}}\|^2_{H^1(\Omega)} \\
&\leq \|\mathbf{e}_{\mathbf{u},n-1}-\mathbf{s}_{\mathbf{e}_{\mathbf{u},n-1}}\|^2_{\mathbf{H}^1(\Omega)} + \|e_{p,n-1}-s_{e_{p,n-1}}\|^2_{H^2(\Omega)} \\
&\leq \left(\|\mathbf{e}_{\mathbf{u},n-1}-\mathbf{s}_{\mathbf{e}_{\mathbf{u},n-1}}\|_{\mathbf{H}^1(\Omega)} + \|e_{p,n-1}-s_{e_{p,n-1}}\|_{H^2(\Omega)}\right)^2 \\
&\leq C\delta_{n+1}^{-\sigma-1}h_n^{\sigma-1}\|\mathbf{E}\mathbf{e}_{n-1}-\mathbf{s}_{\mathbf{E}\mathbf{e}_{n-1}}\|^2_{\mathcal{N}_{\mathbf{\Phi}_{\delta_{n+1}}}(\mathbb{R}^d)} \\
&= C\|\mathbf{E}\mathbf{e}_{n-1}-\mathbf{s}_{\mathbf{E}\mathbf{e}_{n-1}}\|^2_{\mathcal{N}_{\mathbf{\Phi}_{\delta_{n+1}}}(\mathbb{R}^d)} \\
&= C\|\mathbf{E}\mathbf{e}_n\|_{\mathcal{N}_{\mathbf{\Phi}_{\delta_{n+1}}}(\mathbb{R}^d)},
\end{aligned}$$

where we have used the fact that

$$\frac{h_n^{\sigma-1}}{\delta_{n+1}^{\sigma+1}} = \mu^{\sigma-1}\left(\frac{h_n}{h_{n+1}}\right)^{\sigma-1} \leq \mu^{\sigma-1}\left(\frac{1}{\mu\gamma}\right)^{\sigma-1} = \gamma^{1-\sigma}.$$

Then picking a representer p such that $\|p\|_{H^{\sigma+1}(\Omega)} = \|p\|_{H^{\sigma+1}(\Omega)/\mathbb{R}}$, we obtain

$$\begin{aligned}
\|\mathbf{v}-\mathbf{v}_n\|^2_{\mathbf{L}_2(\Omega)} &\leq C\|\mathbf{E}\mathbf{e}_n\|^2_{\mathcal{N}_{\mathbf{\Phi}_{\delta_{n+1}}}(\mathbb{R}^d)} \\
&\leq C\alpha^{2n}\|\mathbf{E}\mathbf{e}_0\|^2_{\mathcal{N}_{\mathbf{\Phi}_{\delta_1}}(\mathbb{R}^d)} \\
&= C\alpha^{2n}\|\mathbf{E}\mathbf{v}\|^2_{\mathcal{N}_{\mathbf{\Phi}_{\delta_1}}(\mathbb{R}^d)} \\
&\leq C\alpha^{2n}\left(\|\widetilde{\mathbf{E}}_{\mathrm{div}}\mathbf{u}\|_{\widetilde{\mathbf{H}}^\sigma(\mathbb{R}^d,\mathrm{div})} + \|E_S p\|_{H^{\sigma+1}(\mathbb{R}^d)}\right)^2 \\
&\leq C\alpha^{2n}\left(\|\mathbf{u}\|_{\widetilde{\mathbf{H}}^\sigma(\Omega,\mathrm{div})} + \|p\|_{H^{\sigma+1}(\Omega)}\right)^2 \\
&\leq C\alpha^{2n}\left(\|\mathbf{u}\|_{\mathbf{H}^\sigma(\Omega)} + \|p\|_{H^{\sigma+1}(\Omega)}\right)^2.
\end{aligned}$$

□

8.5 Multilevel Escape Theory

As in previous chapters, it is possible to generalise these ideas to the case where the approximant and the solution to Darcy's problem lie in different spaces. We use the one-shot theory developed by Schräder and Wendland in [75].

We define the kernel K^s through its Fourier transform given by

$$\widehat{K^s}(\boldsymbol{\omega}) := (1+\|\boldsymbol{\omega}\|_2^2)^{-s},$$

which is thus the canonical reproducing kernel for $H^s(\mathbb{R}^d)$. For two kernels K^t and K^s, we can again introduce a scaled matrix-valued kernel

$$\mathbf{K}_\delta^{s,t} := \begin{pmatrix} \widetilde{\mathbf{K}}_\delta^s & \mathbf{0} \\ \mathbf{0}^T & K_\delta^t \end{pmatrix} : \mathbb{R}^d \to \mathbb{R}^{(d+1)\times(d+1)},$$

with

$$\widetilde{\mathbf{K}}_\delta^s := (-\Delta I + \nabla\nabla^T) K_\delta^{s+1} \qquad \text{and} \qquad K_\delta^t := \delta^{-d} K^t(\cdot/\delta).$$

We extend the spaces of band-limited functions to vector-valued functions

$$\begin{aligned}
\mathbf{B}^\rho &:= \left\{ \mathbf{f} \in \mathbf{L}_2(\mathbb{R}^d) \mid \operatorname{supp} \widehat{\mathbf{f}} \subseteq B(\mathbf{0}, \rho) \right\}, \\
\widetilde{\mathbf{B}}^\rho &:= \left\{ \mathbf{f} \in \mathbf{B}^\rho \mid \int_{\mathbb{R}^d} \frac{\|\widehat{\mathbf{f}}(\boldsymbol{\omega})\|_2^2}{\|\boldsymbol{\omega}\|_2^2} d\boldsymbol{\omega} < \infty \right\}, \\
\widetilde{\mathbf{B}}_{\mathrm{div}}^\rho &:= \left\{ \mathbf{f} \in \widetilde{\mathbf{B}}^\rho \mid \boldsymbol{\omega}^T \mathbf{f}(\boldsymbol{\omega}) = 0 \right\}.
\end{aligned}$$

The following lemma in the form below is from [75] and comes originally from [36, Lemma 2].

Lemma 8.11 *Let $q_X = 1/2 \min_{j\neq k} \|\mathbf{x}_j - \mathbf{x}_k\|_2$ be the separation radius of the discrete set $X = \{\mathbf{x}_1, \ldots, \mathbf{x}_N\}$. Let $\mathbf{g} = \sum_{j=1}^N \widetilde{\mathbf{K}}^\sigma(\cdot - \mathbf{x}_j)\boldsymbol{\alpha}_j$ and $\sigma > d/2$. Define $\mathbf{g}_\rho$ by $\widehat{\mathbf{g}_\rho} = \widehat{\mathbf{g}}\chi_\rho$, where χ_ρ is the characteristic function of the ball $B(\mathbf{0}, \rho)$. Then, there exists a constant $\kappa \geq 24 \left(\frac{\pi(d+2)(d+3)d}{4(d-1)} \Gamma^2(\frac{d+2}{d}) \right)^{1/(d+1)} =: \widetilde{C}$, which is independent of X and all $\boldsymbol{\alpha}_j$, such that for $\rho = \kappa/q_X$ we have*

$$I_\rho := \|\mathbf{g} - \mathbf{g}_\rho\|_{\widetilde{\mathbf{H}}^\sigma(\mathbb{R}^d)} \leq \frac{1}{2} \|\mathbf{g}\|_{\widetilde{\mathbf{H}}^\sigma(\mathbb{R}^d)}.$$

Theorem 8.12 (Band-limited Approximation of Darcy Solution) *Let $X \subseteq \Omega$ denote the interior collocation points and $Y \subseteq \partial\Omega$ the boundary collocation points. Let $\rho_{\mathbf{u}}, \rho_p > \widetilde{C}\delta/q$, where $\widetilde{C}$ is chosen as in Lemma 8.11 and $q = q_{X\cup Y}$. Then, for $\mathbf{v} = (\mathbf{u}, p) \in \widetilde{\mathbf{H}}^\tau(\mathbb{R}^d, \mathrm{div}) \times H^\sigma(\mathbb{R}^d)$ there exists a function $\mathbf{v}_{\boldsymbol{\rho}/\delta} = (\mathbf{u}_{\rho_{\mathbf{u}}/\delta}, p_{\rho_{\mathbf{u}}/\delta}) \in \widetilde{\mathbf{B}}_{\mathrm{div}}^{\rho_{\mathbf{u}}/\delta} \times B^{\rho_p/\delta}$ such that*

1. $L\mathbf{v}|_X = L\mathbf{v}_{\boldsymbol{\rho}/\delta}|_X, \qquad (\mathbf{u}\cdot\mathbf{n})|_Y = (\mathbf{u}_{\rho_{\mathbf{u}}/\delta}\cdot\mathbf{n})|_Y,$
2. $\delta^{-2}\|\mathbf{u} - \mathbf{u}_{\rho_{\mathbf{u}}/\delta}\|^2_{\mathcal{N}_{\widetilde{\mathbf{K}}_\delta^\tau}(\mathbb{R}^d)} + \|p - p_{\rho_p/\delta}\|^2_{\mathcal{N}_{K_\delta^\sigma}(\mathbb{R}^d)}$
$$\leq 25 \left(\delta^{-2}\|\mathbf{u}\|^2_{\mathcal{N}_{\widetilde{\mathbf{K}}_\delta^\tau}(\mathbb{R}^d)} + \|p\|^2_{\mathcal{N}_{K_\delta^\sigma}(\mathbb{R}^d)} \right).$$

Proof. Define $\mathbf{w}(\mathbf{x}) = \delta^{d/2}\mathbf{v}(\delta\mathbf{x}) \in \widetilde{\mathbf{H}}^\tau(\mathbb{R}^d, \mathrm{div}) \times H^\sigma(\mathbb{R}^d)$, then its Fourier transform satisfies $\widehat{\mathbf{w}}(\boldsymbol{\omega}) = \delta^{-d/2}\widehat{\mathbf{v}}(\boldsymbol{\omega}/\delta)$. Now define a scaled data set

$$Z = Z_1 + Z_2 = (X \cup Y)/\delta = \{\mathbf{s}/\delta \mid \mathbf{s} \in X \cup Y\},$$

which implies $q_Z = q_{X\cup Y}/\delta = q/\delta$ and thus $\rho_{\mathbf{u}}, \rho_p > \widetilde{C}\delta/q = \widetilde{C}/q_Z$, as well as a scaled operator

$$\widetilde{L}(\mathbf{u}, p) := \mathbf{u} + \widetilde{K}\nabla p := \mathbf{u} + 1/\delta K\nabla p,$$

where K is the permeability tensor from (8.1). By Theorem 3.5 from [75] we know that there is a $\mathbf{w}_{\boldsymbol{\rho}} = (\mathbf{u}_{\rho_{\mathbf{u}}}, p_{\rho_p}) \in \widetilde{\mathbf{B}}^{\rho_{\mathbf{u}}}_{\mathrm{div}} \times B^{\rho_p}$ such that

$$\widetilde{L}\mathbf{w}|_{Z_1} = \widetilde{L}\mathbf{w}_{\boldsymbol{\rho}}|_{Z_1}, \qquad (\mathbf{w}_{\mathbf{u}} \cdot \mathbf{n})|_{Z_2} = (\mathbf{u}_{\rho_{\mathbf{u}}} \cdot \mathbf{n})|_{Z_2}, \qquad \text{and} \tag{8.10}$$

$$\|\mathbf{w} - \mathbf{w}_{\boldsymbol{\rho}}\|_{\widetilde{\mathbf{H}}^{\tau}(\mathbb{R}^d,\mathrm{div})\times H^{\sigma}(\mathbb{R}^d)} \leq 5\left(\|\mathbf{w}_{\mathbf{u}}\|^2_{\widetilde{\mathbf{H}}^{\tau}(\mathbb{R}^d,\mathrm{div})} + \|w_p\|^2_{H^{\sigma}(\mathbb{R}^d)}\right)^{1/2}. \tag{8.11}$$

We define $\mathbf{v}_{\boldsymbol{\rho}/\delta} \equiv (\mathbf{u}_{\rho_{\mathbf{u}}/\delta}, p_{\rho_p/\delta}) := \delta^{-d/2}\mathbf{w}_{\boldsymbol{\rho}}(\cdot/\delta)$ which lies per definition $\widetilde{\mathbf{B}}^{\rho_{\mathbf{u}}/\delta}_{\mathrm{div}} \times B^{\rho_p/\delta}$ and with Fourier transform $\widehat{\mathbf{v}_{\boldsymbol{\rho}/\delta}}(\boldsymbol{\omega}) = \delta^{\delta/2}\widehat{\mathbf{w}_{\boldsymbol{\rho}}}(\delta\boldsymbol{\omega})$. Now we check the interpolation properties. For $1 \leq k \leq N$ we have

$$\begin{aligned}
L[\mathbf{v}_{\boldsymbol{\rho}/\delta}](\mathbf{x}_k) &= \delta^{-d/2} L\left[\mathbf{w}_{\boldsymbol{\rho}}(\cdot/\delta)\right](\mathbf{x}_k) \\
&= \delta^{-d/2}\left[\mathbf{u}_{\rho_{\mathbf{u}}}(\cdot/\delta) + K(\cdot/\delta)\nabla p_{\rho_p}(\cdot/\delta)\right](\mathbf{x}_k) \\
&= \delta^{-d/2}\left[\mathbf{u}_{\rho_{\mathbf{u}}} + 1/\delta K\nabla p_{\rho_p}\right](\mathbf{x}_k/\delta) \\
&= \delta^{-d/2}\widetilde{L}\left[\mathbf{w}_{\boldsymbol{\rho}}\right](\mathbf{z}_k).
\end{aligned}$$

Now by (8.10), we find

$$\begin{aligned}
L[\mathbf{v}_{\boldsymbol{\rho}/\delta}](\mathbf{x}_k) &= \delta^{-d/2}\widetilde{L}\left[\mathbf{w}\right](\mathbf{z}_k) = \widetilde{L}\left[\mathbf{v}(\delta\cdot)\right](\mathbf{z}_k) \\
&= \left[\mathbf{u}(\delta\cdot) + \widetilde{K}(\delta\cdot)\nabla p(\delta\cdot)\right](\mathbf{z}_k) \\
&= \left[\mathbf{u} + K\nabla p\right](\delta\mathbf{z}_k) \\
&= L\left[\mathbf{v}\right](\mathbf{x}_k).
\end{aligned}$$

Similarly, we have for the boundary

$$(\mathbf{u}_{\boldsymbol{\rho}_{\mathbf{u}}/\delta} \cdot \mathbf{n})|_Y = \delta^{-d/2}(\mathbf{u}_{\boldsymbol{\rho}_{\mathbf{u}}} \cdot \mathbf{n})(\cdot/\delta)|_Y = \delta^{-d/2}(\mathbf{w}_{\mathbf{u}} \cdot \mathbf{n})|_{Z_2} = (\mathbf{u} \cdot \mathbf{n})(\delta\cdot)|_{Z_2} = (\mathbf{u} \cdot \mathbf{n})|_Y.$$

We are done once we can show that the near-best approximation property holds. It follows from (8.11).

We compute

$$
\begin{aligned}
\|\mathbf{w}-\mathbf{w}_{\boldsymbol{\rho}}\|^2_{\widetilde{\mathbf{H}}^\tau(\mathbb{R}^d,\mathrm{div})\times H^\sigma(\mathbb{R}^d)} &= \|\mathbf{w}_{\mathbf{u}}-\mathbf{u}_{\rho_{\mathbf{u}}}\|^2_{\widetilde{\mathbf{H}}^\tau(\mathbb{R}^d,\mathrm{div})} + \|w_p-p_{\rho_p}\|^2_{H^\sigma(\mathbb{R}^d)} \\
&= (2\pi)^{-d/2}\int_{\mathbb{R}^d}\left\{\frac{\|\widehat{(\mathbf{w}_{\mathbf{u}}-\mathbf{u}_{\rho_{\mathbf{u}}})}(\boldsymbol{\omega})\|_2^2}{\|\boldsymbol{\omega}\|_2^2(1+\|\boldsymbol{\omega}\|_2^2)^{-\tau-1}} + \frac{|\widehat{(w_p-p_{\rho_p})}(\boldsymbol{\omega})|^2}{(1+\|\boldsymbol{\omega}\|_2^2)^{-\sigma}}\right\}d\boldsymbol{\omega} \\
&= (2\pi)^{-d/2}\delta^{-d}\int_{\mathbb{R}^d}\left\{\frac{\|\widehat{(\widehat{\mathbf{u}}-\mathbf{u}_{\rho_{\mathbf{u}}/\delta})}(\boldsymbol{\omega}/\delta)\|_2^2}{\|\boldsymbol{\omega}\|_2^2(1+\|\boldsymbol{\omega}\|_2^2)^{-\tau-1}} + \frac{|\widehat{(\widehat{p}-p_{\rho_p/\delta})}(\boldsymbol{\omega}/\delta)|^2}{(1+\|\boldsymbol{\omega}\|_2^2)^{-\sigma}}\right\}d\boldsymbol{\omega} \\
&= (2\pi)^{-d/2}\int_{\mathbb{R}^d}\left\{\frac{\|\widehat{(\widehat{\mathbf{u}}-\mathbf{u}_{\rho_{\mathbf{u}}/\delta})}(\boldsymbol{\omega})\|_2^2}{\|\delta\boldsymbol{\omega}\|_2^2(1+\|\delta\boldsymbol{\omega}\|_2^2)^{-\tau-1}} + \frac{|\widehat{(\widehat{p}-p_{\rho_p/\delta})}(\boldsymbol{\omega})|^2}{(1+\|\delta\boldsymbol{\omega}\|_2^2)^{-\sigma}}\right\}d\boldsymbol{\omega} \\
&= (2\pi)^{-d/2}\int_{\mathbb{R}^d}\left\{\frac{\|\widehat{(\widehat{\mathbf{u}}-\mathbf{u}_{\rho_{\mathbf{u}}/\delta})}(\boldsymbol{\omega})\|_2^2}{\|\delta\boldsymbol{\omega}\|_2^2\widehat{K^{\tau+1}}(\delta\boldsymbol{\omega})} + \frac{|\widehat{(\widehat{p}-p_{\rho_p/\delta})}(\boldsymbol{\omega})|^2}{\widehat{K^\sigma}(\delta\boldsymbol{\omega})}\right\}d\boldsymbol{\omega} \\
&= (2\pi)^{-d/2}\int_{\mathbb{R}^d}\left\{\frac{\|\widehat{(\widehat{\mathbf{u}}-\mathbf{u}_{\rho_{\mathbf{u}}/\delta})}(\boldsymbol{\omega})\|_2^2}{\|\delta\boldsymbol{\omega}\|_2^2\widehat{K_\delta^{\tau+1}}(\boldsymbol{\omega})} + \frac{|\widehat{(\widehat{p}-p_{\rho_p/\delta})}(\boldsymbol{\omega})|^2}{\widehat{K_\delta^\sigma}(\boldsymbol{\omega})}\right\}d\boldsymbol{\omega} \\
&= \delta^{-2}\|\mathbf{u}-\mathbf{u}_{\rho_{\mathbf{u}}/\delta}\|^2_{\mathcal{N}_{\widetilde{\mathbf{K}}_\delta^\tau}(\mathbb{R}^d)} + \|p-p_{\rho_p/\delta}\|^2_{\mathcal{N}_{K_\delta^\sigma}(\mathbb{R}^d)}.
\end{aligned}
$$

In the same fashion we derive

$$
\|\mathbf{w}\|^2_{\widetilde{\mathbf{H}}^\tau(\mathbb{R}^d,\mathrm{div})\times H^\sigma(\mathbb{R}^d)} = \delta^{-2}\|\mathbf{u}\|^2_{\mathcal{N}_{\widetilde{\mathbf{K}}_\delta^\tau}(\mathbb{R}^d)} + \|p\|^2_{\mathcal{N}_{K_\delta^\sigma}(\mathbb{R}^d)}
$$

and thus combining both results, we find

$$
\delta^{-2}\|\mathbf{u}-\mathbf{u}_{\rho_{\mathbf{u}}/\delta}\|^2_{\mathcal{N}_{\widetilde{\mathbf{K}}_\delta^\tau}(\mathbb{R}^d)} + \|p-p_{\rho_p/\delta}\|^2_{\mathcal{N}_{K_\delta^\sigma}(\mathbb{R}^d)} \leq 25\left(\delta^{-2}\|\mathbf{u}\|^2_{\mathcal{N}_{\widetilde{\mathbf{K}}_\delta^\tau}(\mathbb{R}^d)} + \|p\|^2_{\mathcal{N}_{K_\delta^\sigma}(\mathbb{R}^d)}\right).
$$

□

We need an inverse estimate to establish our main result, a bound on the error between analytical solution and its multilevel collocation approximation. This again generalises and is closely related to work done in [74].

Lemma 8.13 (Inverse Estimate) *Let ϕ and ψ generate $H^{\sigma+1}(\mathbb{R}^d)$ and $\sigma \geq \beta > d/2$. Then, for $\boldsymbol{\rho} = (\rho_{\mathbf{u}}, \rho_p)$ with $\min\{\rho_{\mathbf{u}}, \rho_p\} \geq 1$, we have*

$$
\|\mathbf{v}_{\boldsymbol{\rho}/\delta}\|_{\mathcal{N}_{\boldsymbol{\Phi}_\delta}(\mathbb{R}^d)} \leq C\left(\rho_{\mathbf{u}}^{\sigma-\beta}\|[\mathbf{v}_{\boldsymbol{\rho}/\delta}]_{\mathbf{u}}\|_{\mathcal{N}_{\widetilde{\mathbf{K}}_\delta^\beta}(\mathbb{R}^d)} + \rho_p^{\sigma-\beta}\|[\mathbf{v}_{\boldsymbol{\rho}/\delta}]_p\|_{\mathcal{N}_{K_\delta^{\beta+1}}(\mathbb{R}^d)}\right).
$$

Proof. We compute

$$\begin{aligned}
&\|\mathbf{v}_{\boldsymbol{\rho}/\delta}\|^2_{\mathcal{N}_{\boldsymbol{\Phi}_\delta}(\mathbb{R}^d)} \\
&= (2\pi)^{-d/2}\left(\int_{\|\boldsymbol{\omega}\|_2\le\rho_{\mathbf{u}}/\delta}\frac{\|\widehat{[\mathbf{v}_{\boldsymbol{\rho}/\delta}]_{\mathbf{u}}}(\boldsymbol{\omega})\|_2^2}{\|\boldsymbol{\omega}\|_2^2\widehat{\phi_\delta}(\boldsymbol{\omega})}d\boldsymbol{\omega}+\int_{\|\boldsymbol{\omega}\|_2\le\rho_p/\delta}\frac{|\widehat{[\mathbf{v}_{\boldsymbol{\rho}/\delta}]_p}(\boldsymbol{\omega})|^2}{\widehat{\psi_\delta}(\boldsymbol{\omega})}d\boldsymbol{\omega}\right)\\
&= (2\pi)^{-d/2}\left(\int_{\|\boldsymbol{\omega}\|_2\le\rho_{\mathbf{u}}/\delta}\frac{\|\widehat{[\mathbf{v}_{\boldsymbol{\rho}/\delta}]_{\mathbf{u}}}(\boldsymbol{\omega})\|_2^2}{\|\boldsymbol{\omega}\|_2^2\widehat{\phi}(\delta\boldsymbol{\omega})}d\boldsymbol{\omega}+\int_{\|\boldsymbol{\omega}\|_2\le\rho_p/\delta}\frac{|\widehat{[\mathbf{v}_{\boldsymbol{\rho}/\delta}]_p}(\boldsymbol{\omega})|^2}{\widehat{\psi}(\delta\boldsymbol{\omega})}d\boldsymbol{\omega}\right)\\
&\le C(2\pi)^{-d/2}\left(\int_{\|\boldsymbol{\omega}\|_2\le\rho_{\mathbf{u}}/\delta}\frac{\|\widehat{[\mathbf{v}_{\boldsymbol{\rho}/\delta}]_{\mathbf{u}}}(\boldsymbol{\omega})\|_2^2}{\|\boldsymbol{\omega}\|_2^2}(1+\|\delta\boldsymbol{\omega}\|_2^2)^{\sigma+1}d\boldsymbol{\omega}\right.\\
&\qquad\left.+\int_{\|\boldsymbol{\omega}\|_2\le\rho_p/\delta}|\widehat{[\mathbf{v}_{\boldsymbol{\rho}/\delta}]_p}(\boldsymbol{\omega})|^2(1+\|\delta\boldsymbol{\omega}\|_2^2)^{\sigma+1}d\boldsymbol{\omega}\right).
\end{aligned}$$

Now we use twice the fact that if $\|\delta\boldsymbol{\omega}\|_2^2\le r^2$ for some $r\ge 1$, we can deduce

$$\begin{aligned}
(1+\|\delta\boldsymbol{\omega}\|_2^2)^{\sigma+1} &= (1+\|\delta\boldsymbol{\omega}\|_2^2)^{\sigma-\beta}1/\widehat{K}^{\beta+1}(\delta\boldsymbol{\omega}) = (1+\|\delta\boldsymbol{\omega}\|_2^2)^{\sigma-\beta}1/\widehat{K}_\delta^{\beta+1}(\boldsymbol{\omega})\\
&\le (1+r^2)^{\sigma-\beta}1/\widehat{K}_\delta^{\beta+1}(\boldsymbol{\omega}) \le 2^{\sigma-\beta}r^{2(\sigma-\beta)}1/\widehat{K}_\delta^{\beta+1}(\boldsymbol{\omega}).
\end{aligned}$$

This leads to

$$\|\mathbf{v}_{\boldsymbol{\rho}/\delta}\|^2_{\mathcal{N}_{\boldsymbol{\Phi}_\delta}(\mathbb{R}^d)} \le C\left(\rho_{\mathbf{u}}^{2(\sigma-\beta)}\|[\mathbf{v}_{\boldsymbol{\rho}/\delta}]_{\mathbf{u}}\|^2_{\mathcal{N}_{\widetilde{\mathbf{K}}_\delta^\beta}(\mathbb{R}^d)}+\rho_p^{2(\sigma-\beta)}\|[\mathbf{v}_{\boldsymbol{\rho}/\delta}]_p\|^2_{\mathcal{N}_{K_\delta^{\beta+1}}(\mathbb{R}^d)}\right).$$

The assertion follows from the norm equivalence between the ℓ_1 and the ℓ_2 norm. □

Theorem 8.14 (Error for Multilevel Collocation Approximation to Darcy's Problem in Escape Case) *Let $\delta\le 1$ and Ω be a bounded, simply connected, open subset of $\mathbb{R}^d$, for $d=2,3$, with a $C^{\lceil\beta\rceil+1,1}$ boundary $\partial\Omega$. Suppose that the kernel $\boldsymbol{\Phi}_\delta$ is chosen such that its native space $\mathcal{N}_{\boldsymbol{\Phi}_\delta}(\mathbb{R}^d)=\widetilde{\mathbf{H}}^\sigma(\mathbb{R}^d,\mathrm{div})\times H^{\sigma+1}(\mathbb{R}^d)$ and the permeability tensor $K=(K_{ij})$ satisfies (8.4), $K=K^T$ and $K_{ij}\in H^\beta(\Omega)$. Furthermore, assume that the data satisfy $\mathbf{f}\in\mathbf{H}^{\beta+1}(\Omega),\mathbf{g}\in\mathbf{H}^{\beta+1/2}(\partial\Omega)$ and $\int_{\partial\Omega}\mathbf{g}\cdot\mathbf{n}dS=0$ with $\sigma\ge\beta>d/2$. Lastly, let $\rho_{\mathbf{u}}=\rho_p=(\widetilde{C}+\varepsilon)\delta/q>1$ for some $\varepsilon>0$ (independent of δ and q) and $\widetilde{C}$ chosen as in Lemma 8.11 and $q=q_{X\cup Y}$ for the interior collocation set X and the boundary collocation set Y.*

Then, the error between collocation approximation and the analytical solution can be bounded by

$$\begin{aligned}
&\|\mathbf{u}-\mathbf{s}_{\mathbf{u}}\|_{\mathbf{W}_r^{\eta+1}(\Omega)}+\|p-s_p\|_{W_r^{\eta+2}(\Omega)/\mathbb{R}}\\
&\quad\le C\delta^{-\beta-1}\left(h_{X,\Omega}^{\beta-\eta-1-d(1/2-1/r)_+}+h_{Y,\partial\Omega}^{\beta-\eta-1-1/2+1/r-(d-1)(1/2-1/r)_+}\right)\\
&\qquad\left(1+\frac{h_{X,\Omega}^{\sigma-\beta}+h_{Y,\partial\Omega}^{\sigma-\beta}}{q^{\sigma-\beta}}\right)\left(\delta^{-1}\|\widetilde{\mathbf{E}_{\mathrm{div}}\mathbf{u}}\|_{\mathcal{N}_{\widetilde{\mathbf{K}}_\delta^{\beta+1}(\mathbb{R}^d)}}+\|E_S p\|_{\mathcal{N}_{K_\delta^\beta}(\mathbb{R}^d)}\right)
\end{aligned}$$

for $1<r<\infty$ and $0\le\eta\le\beta-d(1/2-1/r)_+-1$.

Proof. Let $\mathbf{v} = (\mathbf{u}, p)$ be the combined vector of velocity and pressure and p a representer for the pressure such that $\|p\|_{W_r^{\eta+2}(\Omega)} = \|p\|_{W_r^{\eta+2}(\Omega)/\mathbb{R}}$.

Using the solution's continuous dependence on the given data (Theorem 8.1), we can derive for the difference $\mathbf{v} - \mathbf{s_v}$

$$\begin{aligned}\|\mathbf{u} - \mathbf{s_u}\|_{\mathbf{W}_r^{\eta+1}(\Omega)} + \|p - s_p\|_{W_r^{\eta+2}(\Omega)} \\ \leq C \left(\|L\mathbf{v} - L\mathbf{s_v}\|_{\mathbf{W}_r^{\eta+1}(\Omega)} + \|(\mathbf{u} - \mathbf{s_u}) \cdot \mathbf{n}\|_{W_r^{\eta+1-1/r}(\partial\Omega)} \right)\end{aligned}$$

for all $0 \leq \eta \leq \beta$. Since we have

$$(L\mathbf{v} - L\mathbf{s_v})|_X = \mathbf{0} \qquad \text{and} \qquad [(\mathbf{u} - \mathbf{s_u}) \cdot \mathbf{n}]|_Y = 0,$$

we can employ the corresponding sampling inequalities for the interior of the domain (Lemma 7.14) and for its boundary (Lemma 7.15). We will start with the interior error. The sampling inequality yields

$$\|L\mathbf{v} - L\mathbf{s_v}\|_{\mathbf{W}_r^{\eta+1}(\Omega)} \leq C h_{X,\Omega}^{\beta-\eta-1-d(1/2-1/r)_+} \|L\mathbf{v} - L\mathbf{s_v}\|_{\mathbf{H}^\beta(\Omega)}.$$

Since we have already shown in the proof of Proposition 8.4 that $\|K\nabla p\|_{H^\beta(\Omega)} \leq C\|p\|_{H^{\beta+1}(\Omega)}$, we deduce

$$\begin{aligned}\|L\mathbf{v} - L\mathbf{s_v}\|_{\mathbf{H}^\beta(\Omega)} &\leq C(\|\mathbf{u} - \mathbf{s_u}\|_{\mathbf{H}^\beta(\Omega)} + \|p - s_p\|_{H^{\beta+1}(\Omega)}) \\ &\leq C\|\mathbf{v} - \mathbf{s_v}\|_{\mathbf{H}^\beta(\Omega)\times H^{\beta+1}(\Omega)}.\end{aligned}$$

The last step follows from the norm equivalence between the ℓ_1 and the ℓ_2 norm. Now, with the help of the extension operator we extend the function $\mathbf{v}$ to $\mathbf{Ev} \in \widetilde{\mathbf{H}}^\beta(\mathbb{R}^d, \operatorname{div}) \times H^{\beta+1}(\mathbb{R}^d)$. By Theorem 8.12, we find a band-limited approximation $\mathbf{v}_{\boldsymbol{\rho}/\delta}$ to $\mathbf{Ev}$, which helps us to establish the bound

$$\begin{aligned}\|\mathbf{v} - \mathbf{s_v}\|_{\mathbf{H}^\beta(\Omega)\times H^{\beta+1}(\Omega)} \\ &= \|\mathbf{Ev} - \mathbf{s_{Ev}}\|_{\mathbf{H}^\beta(\Omega)\times H^{\beta+1}(\Omega)} \\ &\leq \|\mathbf{Ev} - \mathbf{v}_{\boldsymbol{\rho}/\delta}\|_{\mathbf{H}^\beta(\Omega)\times H^{\beta+1}(\Omega)} + \|\mathbf{v}_{\boldsymbol{\rho}/\delta} - \mathbf{s_{Ev}}\|_{\mathbf{H}^\beta(\Omega)\times H^{\beta+1}(\Omega)}. \qquad (8.12)\end{aligned}$$

We estimate both terms on the right-hand side separately. We start with the first term on the right-hand side.

By Lemma 7.13 and the near-best approximation property (Theorem 8.12), we obtain

$$\begin{aligned}
\|\mathbf{E}\mathbf{v} - \mathbf{v}_{\boldsymbol{\rho}/\delta}\|_{\mathbf{H}^\beta(\Omega)\times H^{\beta+1}(\Omega)} &= \left(\|\widetilde{\mathbf{E}}_{\mathrm{div}}\mathbf{u} - \mathbf{u}_{\rho_{\mathbf{u}}/\delta}\|^2_{\mathbf{H}^\beta(\Omega)} + \|E_S p - p_{\rho_p/\delta}\|^2_{H^{\beta+1}(\Omega)}\right)^{1/2} \\
&\leq \|\widetilde{\mathbf{E}}_{\mathrm{div}}\mathbf{u} - \mathbf{u}_{\rho_{\mathbf{u}}/\delta}\|_{\mathbf{H}^\beta(\mathbb{R}^d)} + \|E_S p - p_{\rho_p/\delta}\|_{H^{\beta+1}(\mathbb{R}^d)} \\
&\leq \sqrt{2C_2}\delta^{-\beta-1}\|\mathbf{E}\mathbf{v} - \mathbf{v}_{\boldsymbol{\rho}/\delta}\|_{\mathcal{N}_{\mathbf{K}^\beta,\beta+1}(\mathbb{R}^d)} \\
&\leq \sqrt{2C_2}\delta^{-\beta-1}\left(\delta^{-2}\|\widetilde{\mathbf{E}}_{\mathrm{div}}\mathbf{u} - \mathbf{u}_{\rho_{\mathbf{u}}/\delta}\|^2_{\mathcal{N}_{\widetilde{\mathbf{K}}^\beta_\delta}(\mathbb{R}^d)} + \|E_S p - p_{\rho_p/\delta}\|^2_{\mathcal{N}_{K^{\beta+1}_\delta}(\mathbb{R}^d)}\right)^{1/2} \\
&\leq 5\sqrt{2C_2}\delta^{-\beta-1}\left(\delta^{-2}\|\widetilde{\mathbf{E}}_{\mathrm{div}}\mathbf{u}\|^2_{\mathcal{N}_{\widetilde{\mathbf{K}}^\beta_\delta}(\mathbb{R}^d)} + \|E_S p\|^2_{\mathcal{N}_{K^{\beta+1}_\delta}(\mathbb{R}^d)}\right)^{1/2} \\
&\leq C\delta^{-\beta-1}\left(\delta^{-1}\|\widetilde{\mathbf{E}}_{\mathrm{div}}\mathbf{u}\|_{\mathcal{N}_{\widetilde{\mathbf{K}}^\beta_\delta}(\mathbb{R}^d)} + \|E_S p\|_{\mathcal{N}_{K^{\beta+1}_\delta}(\mathbb{R}^d)}\right).
\end{aligned} \tag{8.13}$$

Now we turn to the other term in (8.12). Since $\mathbf{v}_{\boldsymbol{\rho}/\delta}$ interpolates $\mathbf{v}$ in the sense that

$$L\mathbf{v}_{\boldsymbol{\rho}/\delta}|_X = L\mathbf{v}|_X \qquad \text{and} \qquad (\mathbf{v}_{\boldsymbol{\rho}/\delta}\cdot\mathbf{n})|_Y = (\mathbf{v}\cdot\mathbf{n})|_Y,$$

we can deduce that the collocation approximations of $\mathbf{v}_{\boldsymbol{\rho}/\delta}$ and the extended $\mathbf{E}\mathbf{v}$ are the same, i. e. $\mathbf{s}_{\mathbf{v}_{\boldsymbol{\rho}/\delta}} = \mathbf{s}_{\mathbf{E}\mathbf{v}}$. Therefore we can employ Theorem 8.6, to obtain the following result

$$\begin{aligned}
\|\mathbf{v}_{\boldsymbol{\rho}/\delta} - \mathbf{s}_{\mathbf{E}\mathbf{v}}\|_{\mathbf{H}^\beta(\Omega)\times H^{\beta+1}(\Omega)} &= \|\mathbf{v}_{\boldsymbol{\rho}/\delta} - \mathbf{s}_{\mathbf{v}_{\boldsymbol{\rho}/\delta}}\|_{\mathbf{H}^\beta(\Omega)\times H^{\beta+1}(\Omega)} \\
&\leq C\delta^{-\sigma-1}\left(h^{\sigma-\beta}_{X,\Omega} + h^{\sigma-\beta}_{Y,\partial\Omega}\right)\|\mathbf{v}_{\boldsymbol{\rho}/\delta}\|_{\mathcal{N}_{\boldsymbol{\Phi}_\delta(\mathbb{R}^d)}}.
\end{aligned}$$

Now we can use our inverse estimates (Lemma 8.13), our assumptions on $\rho_{\mathbf{u}}$ and ρ_p as well as Theorem 8.12 to bound the left-hand side to derive

$$\begin{aligned}
\|\mathbf{v}_{\boldsymbol{\rho}/\delta}\|_{\mathcal{N}_{\boldsymbol{\Phi}_\delta(\mathbb{R}^d)}} &\leq C(\rho^{\sigma-\beta}_{\mathbf{u}}\|\mathbf{u}_{\rho_{\mathbf{u}}/\delta}\|_{\mathcal{N}_{\widetilde{\mathbf{K}}^\beta_\delta}(\mathbb{R}^d)} + \rho^{\sigma-\beta}_p\|p_{\rho_p/\delta}\|_{\mathcal{N}_{K^{\beta+1}_\delta}(\mathbb{R}^d)}) \\
&= Cq^{\beta-\sigma}\delta^{\sigma-\beta}(\|\mathbf{u}_{\rho_{\mathbf{u}}/\delta}\|_{\mathcal{N}_{\widetilde{\mathbf{K}}^\beta_\delta}(\mathbb{R}^d)} + \|p_{\rho_p/\delta}\|_{\mathcal{N}_{K^{\beta+1}_\delta}(\mathbb{R}^d)}) \\
&\leq Cq^{\beta-\sigma}\delta^{\sigma-\beta}(\delta^{-1}\|\mathbf{u}_{\rho_{\mathbf{u}}/\delta}\|_{\mathcal{N}_{\widetilde{\mathbf{K}}^\beta_\delta}(\mathbb{R}^d)} + \|p_{\rho_p/\delta}\|_{\mathcal{N}_{K^{\beta+1}_\delta}(\mathbb{R}^d)}) \\
&\leq 6Cq^{\beta-\sigma}\delta^{\sigma-\beta}(\delta^{-1}\|\widetilde{\mathbf{E}}_{\mathrm{div}}\mathbf{u}\|_{\mathcal{N}_{\widetilde{\mathbf{K}}^\beta_\delta}(\mathbb{R}^d)} + \|E_S p\|_{\mathcal{N}_{K^{\beta+1}_\delta}(\mathbb{R}^d)}).
\end{aligned}$$

where we have used the fact that $\delta \leq 1$. Combining both estimates, we have

$$\begin{aligned}
&\|L\mathbf{v} - L\mathbf{s}_{\mathbf{v}}\|_{\mathbf{H}^\beta(\Omega)} \\
&\quad\leq C\delta^{-\beta-1}\left(1 + \frac{h^{\sigma-\beta}_{X,\Omega} + h^{\sigma-\beta}_{Y,\partial\Omega}}{q^{\sigma-\beta}}\right)\left(\delta^{-1}\|\widetilde{\mathbf{E}}_{\mathrm{div}}\mathbf{u}\|_{\mathcal{N}_{\widetilde{\mathbf{K}}^\beta_\delta}(\mathbb{R}^d)} + \|E_S p\|_{\mathcal{N}_{K^{\beta+1}_\delta}(\mathbb{R}^d)}\right).
\end{aligned}$$

For the boundary part, we note as in [74, Proof of Proposition 3.6] that the normal unit vector can be extended to the interior of Ω by a function $\widetilde{\mathbf{n}} \in H^{\lceil\beta\rceil}(\Omega)$ that additionally satisfies $\widetilde{\mathbf{n}}|_{\partial\Omega} = \mathbf{n}|_{\partial\Omega}$. Thus, we can deduce with the sampling inequality for the boundary of Ω that

$$\|(\mathbf{u}-\mathbf{s_u})\cdot\mathbf{n}\|_{W_r^{\eta+1-1/r}(\partial\Omega)} \leq C h_{Y,\partial\Omega}^{\beta-\eta-1-1/2+1/r-(d-1)(1/2-1/r)_+} \|(\mathbf{u}-\mathbf{s_u})\cdot\widetilde{\mathbf{n}}\|_{H^\beta(\Omega)}.$$

Since by [74, Proof of Proposition 3.6], we also have

$$\begin{aligned}\|(\mathbf{u}-\mathbf{s_u})\cdot\widetilde{\mathbf{n}}\|_{H^\beta(\Omega)} &\leq \|\widetilde{\mathbf{n}}\|_{\mathbf{H}^\beta(\Omega)}\|\mathbf{u}-\mathbf{s_u}\|_{\mathbf{H}^\beta(\Omega)} \leq C\|\mathbf{u}-\mathbf{s_u}\|_{\mathbf{H}^\beta(\Omega)} \\ &\leq C\|\mathbf{v}-\mathbf{s_v}\|_{\mathbf{H}^\beta(\Omega)\times H^{\beta+1}(\Omega)},\end{aligned}$$

we can employ the same steps as for the interior part to derive

$$\begin{aligned}&\|\mathbf{v}-\mathbf{s_v}\|_{\mathbf{H}^\beta(\Omega)\times H^{\beta+1}(\Omega)} \\ &\quad\leq \delta^{-\beta-1}\left(1+\frac{h_{X,\Omega}^{\sigma-\beta}+h_{Y,\partial\Omega}^{\sigma-\beta}}{q^{\sigma-\beta}}\right)\left(\delta^{-1}\|\widetilde{\mathbf{E}}_{\mathrm{div}}\mathbf{u}\|_{\mathcal{N}_{\widetilde{\mathbf{K}}_\delta^\beta}(\mathbb{R}^d)}+\|E_S p\|_{\mathcal{N}_{K_\delta^{\beta+1}}(\mathbb{R}^d)}\right),\end{aligned}$$

which finishes the proof. □

Corollary 8.15 *Under the same assumptions as above let the ratio*

$$\frac{h_{X,\Omega}^{\sigma-\beta}+h_{Y,\partial\Omega}^{\sigma-\beta}}{q^{\sigma-\beta}}$$

be bounded and $h = h_{X,\Omega} \approx h_{Y,\partial\Omega}$. *Then*

$$\|\mathbf{u}-\mathbf{s_u}\|_{\mathbf{H}^1(\Omega)} + \|p-s_p\|_{H^2(\Omega)/\mathbb{R}} \leq C\delta^{-\beta-2}h^{\beta-1}\|\mathbf{E}\mathbf{v}\|_{\mathcal{N}_{\mathbf{K}_\delta^{\beta,\beta+1}(\mathbb{R}^d)}}.$$

Comparing the bound on the error with our previous error estimate Corollary 8.7, we note that there is an additional scale δ, which leads to a slightly different scaling in the following convergence theorem compared to Theorem 8.9. Also, in the proof we need that $\beta-2$ is positive hence our condition on β becomes slightly stronger than in the nonescape case. The additional scale was introduced when approximating the solution to Darcy's problem with a band-limited function, Theorem 8.12.

Theorem 8.16 (Convergence of Multilevel Collocation Algorithm in Escape Case) *Let* $d = 2, 3$ *and* Ω *be a bounded, simply connected, open subset of* $\mathbb{R}^d$ *with a* $C^{\lceil\beta\rceil+1,1}$ *boundary. Let the permeability tensor* $K = (K_{ij})$ *be strictly elliptic on* Ω *(i. e. satisfy* (8.4)*) with* $K = K^T$ *and components* K_{ij} *in* $H^\beta(\overline{\Omega})$. *Assume that the data satisfy* $\mathbf{f} \in \mathbf{H}^{\beta+1}(\Omega)$, $\mathbf{g} \in \mathbf{H}^{\beta+1/2}(\partial\Omega)$ *and* $\int_{\partial\Omega}\mathbf{g}\cdot\mathbf{n}\,dS = 0$, *where* $\sigma \geq \beta > 1+\varepsilon+d/2$ *for* $\varepsilon > 0$ *arbitrarily small. We define two point set sequences. Firstly, let* $X_1, X_2, \ldots$ *be a sequence of point sets in* Ω *with mesh norms* $h_{X_1,\Omega}, h_{X_2,\Omega}, \ldots$ *and secondly let*

$Y_1, Y_2, \ldots$ be a sequence of point sets on $\partial\Omega$ with mesh norms $h_{Y_1,\partial\Omega}, h_{Y_2,\partial\Omega}, \ldots$. Set $h_j = \max\{h_{X_j,\Omega}, h_{Y_j,\partial\Omega}\}$ and assume

$$\gamma\mu h_j \leq h_{j+1} \leq \mu h_j \tag{8.14}$$

for $j = 1, 2, ...$ and some fixed $\mu \in (0,1)$ and $\gamma \in (0,1)$ as well as

$$q_j \leq h_j \leq c q_j$$

for $c > 0$ and $q_j = q_{X_j \cup Y_j}$ with $j = 1, 2, \ldots$. Suppose that the kernel $\mathbf{\Phi}$ from (7.1) is chosen such that $\mathcal{N}_{\mathbf{\Phi}}(\mathbb{R}^d) = \widetilde{\mathbf{H}}^\sigma(\mathbb{R}^d, \mathrm{div}) \times H^{\sigma+1}(\mathbb{R}^d)$. This means in particular that the functions ϕ and ψ are positive definite and both functions generate $H^{\sigma+1}(\mathbb{R}^d)$. Define

$$\delta_j = \left(\frac{h_j}{\mu}\right)^{\frac{\beta-1}{\beta+2}} \quad \text{as well as} \quad \mathbf{K}_j = \mathbf{K}_{\delta_j}^{\beta,\beta+1} \quad \text{and} \quad K_j = K_{\delta_j}^{\beta+1}.$$

Lastly, let $h_1 \leq \mu$ be sufficiently small. Then, there exists a constant C independent of μ, j and u such that

$$\|\mathbf{E}\mathbf{e}_j\|_{\mathbf{K}_{j+1}} \leq \alpha \|\mathbf{E}\mathbf{e}_{j-1}\|_{\mathbf{K}_j}, \tag{8.15}$$

for $j = 1, 2, ...$ with $\alpha = C\mu^{\frac{(\beta-1)(\beta-2)}{\beta+2}}$. Thus, we have the estimates

$$\|\mathbf{v} - \mathbf{v}_k\|_{\mathbf{L}_2(\Omega)} \leq C\alpha^k \left(\|\mathbf{u}\|_{\mathbf{H}^\beta(\Omega)} + \|p\|_{H^{\beta+1}(\Omega)} \right)$$

and in particular the multiscale approximation $\mathbf{v}_k$ converges to $\mathbf{v}$ in the L_2 norm if we choose μ so small that $\alpha < 1$.

Proof. The support radii are monotonically decreasing. Instead of working with equivalence classes, we pick a representer for the pressure component and denote it with p as well. We compute

$$\begin{aligned}
\|\mathbf{E}\mathbf{e}_j\|_{\mathbf{K}_{j+1}}^2 &= (2\pi)^{-d/2} \int_{\mathbb{R}^d} \left\{ \frac{\|\widehat{\widetilde{\mathbf{E}}_{\mathrm{div}}\mathbf{e}_{\mathbf{u},j}}(\boldsymbol{\omega})\|_2^2}{\|\boldsymbol{\omega}\|_2^2 \widehat{K_{j+1}}(\boldsymbol{\omega})} + \frac{|\widehat{E_S e_{p,j}}(\boldsymbol{\omega})|^2}{\widehat{K_{j+1}}(\boldsymbol{\omega})} \right\} d\boldsymbol{\omega} \\
&= (2\pi)^{-d/2} \int_{\mathbb{R}^d} \left\{ \frac{\|\widehat{\widetilde{\mathbf{E}}_{\mathrm{div}}\mathbf{e}_{\mathbf{u},j}}(\boldsymbol{\omega})\|_2^2}{\|\boldsymbol{\omega}\|_2^2} + |\widehat{E_S e_{p,j}}(\boldsymbol{\omega})|^2 \right\} (1 + \|\delta_{j+1}\boldsymbol{\omega}\|_2^2)^{\beta+1} d\boldsymbol{\omega} \\
&=: C(2\pi)^{-d/2}(I_1 + I_2)
\end{aligned}$$

where we introduced the notation

$$I_1 = \int\limits_{\|\mathbf{w}\|_2 \leq \frac{1}{\delta_{j+1}}} \left\{ \frac{\|\widehat{\widetilde{\mathbf{E}}_{\mathrm{div}}\mathbf{e}_{\mathbf{u},j}}(\boldsymbol{\omega})\|_2^2}{\|\boldsymbol{\omega}\|_2^2} + |\widehat{E_S e_{p,j}}(\boldsymbol{\omega})|^2 \right\} (1 + \|\delta_{j+1}\boldsymbol{\omega}\|_2^2)^{\beta+1} d\boldsymbol{\omega}$$

$$I_2 = \int\limits_{\|\mathbf{w}\|_2 \geq \frac{1}{\delta_{j+1}}} \left\{ \frac{\|\widehat{\widetilde{\mathbf{E}}_{\mathrm{div}}\mathbf{e}_{\mathbf{u},j}}(\boldsymbol{\omega})\|_2^2}{\|\boldsymbol{\omega}\|_2^2} + |\widehat{E_S e_{p,j}}(\boldsymbol{\omega})|^2 \right\} (1 + \|\delta_{j+1}\boldsymbol{\omega}\|_2^2)^{\beta+1} d\boldsymbol{\omega}.$$

For the first integral we use $\delta_{j+1}\|\boldsymbol{\omega}\|_2 \leq 1$ and thus by Lemma 7.16, Parseval's identity, Corollary 8.15

$$\begin{aligned}
I_1 &\leq 2^{\beta+1} \int_{\|\mathbf{w}\|_2 \leq \frac{1}{\delta_{j+1}}} \left\{ \frac{\|\widehat{\widetilde{\mathbf{E}}_{\mathrm{div}}\mathbf{e}_{\mathbf{u},j}}(\boldsymbol{\omega})\|_2^2}{\|\boldsymbol{\omega}\|_2^2} + \widehat{E_S e_{p,j}}(\boldsymbol{\omega}) \right\} d\boldsymbol{\omega} \\
&\leq C \left\{ \|\mathbf{e}_{\mathbf{u},j}\|_{\mathbf{L}_2(\Omega)}^2 + \|\widehat{E_S e_{p,j}}\|_{L_2(\mathbb{R}^d)}^2 \right\} \\
&= C \left\{ \|\mathbf{e}_{\mathbf{u},j}\|_{\mathbf{L}_2(\Omega)}^2 + \|E_S e_{p,j}\|_{L_2(\mathbb{R}^d)}^2 \right\} \\
&\leq C \left\{ \|\mathbf{e}_{\mathbf{u},j}\|_{\mathbf{L}_2(\Omega)}^2 + \|e_{p,j}\|_{L_2(\Omega)}^2 \right\} \\
&\leq C \left\{ \|\mathbf{e}_{\mathbf{u},j}\|_{\mathbf{H}^1(\Omega)}^2 + \|e_{p,j}\|_{H^2(\Omega)}^2 \right\} \\
&\leq C \left\{ \|\mathbf{e}_{\mathbf{u},j}\|_{\mathbf{H}^1(\Omega)} + \|e_{p,j}\|_{H^2(\Omega)} \right\}^2 \\
&= C \left\{ \|\mathbf{e}_{\mathbf{u},j-1} - \mathbf{s}_{\mathbf{e}_{\mathbf{u},j-1}}\|_{\mathbf{H}^1(\Omega)} + \|e_{p,j-1} - s_{e_{p,j-1}}\|_{H^2(\Omega)} \right\}^2 \\
&\leq C\delta_j^{-2(\beta+2)} h_j^{2(\beta-1)} \|\mathbf{E}\mathbf{e}_{j-1}\|_{\mathbf{K}_j}^2 \\
&= C_1 \mu^{2(\beta-1)} \|\mathbf{E}\mathbf{e}_{j-1}\|_{\mathbf{K}_j}^2.
\end{aligned}$$

Note that in the nonescape case we were able to use the optimality in native space norm. Here we need Theorem 8.14, which relied on the near-best approximation property for band-limited functions. Since $\delta_{j+1}\|\boldsymbol{\omega}\|_2 \geq 1$, we find

$$(1 + \delta_{j+1}^2\|\boldsymbol{\omega}\|_2^2)^{\beta+1} \leq 2^{\beta+1}\delta_{j+1}^{2(\beta+1)}\|\boldsymbol{\omega}\|_2^{2(\beta+1)} \leq 2^{\beta+1}\delta_{j+1}^{2(\beta+1)}(1 + \|\boldsymbol{\omega}\|_2^2)^{\beta+1}.$$

Consequently by Theorem 8.14, the quasi-uniformity assumption and the fact that $\delta_j \leq 1$ we deduce

$$\begin{aligned}
I_2 &\leq 2^{\beta+1}\delta_{j+1}^{2(\beta+1)} \int_{\mathbb{R}^d} \left\{ \frac{\|\widehat{\widetilde{\mathbf{E}}_{\mathrm{div}}\mathbf{e}_{\mathbf{u},j}}(\boldsymbol{\omega})\|_2^2}{\|\boldsymbol{\omega}\|_2^2} + |\widehat{E_S e_{p,j}}|^2 \right\} (1 + \|\boldsymbol{\omega}\|_2^2)^{\beta+1} d\boldsymbol{\omega} \\
&\leq C\delta_{j+1}^{2(\beta+1)} \left\{ \|\widetilde{\mathbf{E}}_{\mathrm{div}}\mathbf{e}_{\mathbf{u},j}\|_{\widetilde{\mathbf{H}}^\beta(\mathbb{R}^d)}^2 + \|E_S e_{p,j}\|_{H^{\beta+1}(\mathbb{R}^d)}^2 \right\} \\
&\leq C\delta_{j+1}^{2(\beta+1)} \left\{ \|\mathbf{e}_{\mathbf{u},j}\|_{\widetilde{\mathbf{H}}^\beta(\Omega)}^2 + \|e_{p,j}\|_{H^{\beta+1}(\Omega)}^2 \right\} \\
&= C\delta_{j+1}^{2(\beta+1)} \left\{ \|\mathbf{e}_{\mathbf{u},j-1} - \mathbf{s}_{\mathbf{e}_{\mathbf{u},j-1}}\|_{\widetilde{\mathbf{H}}^\beta(\Omega)}^2 + \|e_{p,j-1} - s_{e_{p,j-1}}\|_{H^{\beta+1}(\Omega)}^2 \right\} \\
&\leq C\delta_{j+1}^{2(\beta+1)}\delta_j^{-2(\beta-1)} \left(1 + \left(\frac{h_j}{q_j} \right)^{\sigma-\beta} \right) \left\{ \delta_j^{-2}\|\widetilde{\mathbf{E}}_{\mathrm{div}}\mathbf{e}_{\mathbf{u},j-1}\|_{\widetilde{\mathbf{K}}_{\delta_j}^\beta}^2 + \|E_S e_{p,j-1}\|_{K_{\delta_j}^{\beta+1}}^2 \right\} \\
&\leq C\delta_{j+1}^{2(\beta+1)}\delta_j^{-2(\beta-2)} \|\mathbf{E}\mathbf{e}_{j-1}\|_{\mathbf{K}_j}^2 \\
&\leq C\mu^{\frac{2(\beta-1)(\beta-2)}{\beta+2}} \|\mathbf{E}\mathbf{e}_{j-1}\|_{\mathbf{K}_j}^2,
\end{aligned}$$

using that for $h_{j+1}/\mu \leq h_j \leq 1$ we have

$$\frac{\delta_{j+1}^{\beta+1}}{\delta_j^{\beta-2}} = \frac{\left[(h_{j+1}/\mu)^{\frac{\beta-1}{\beta+2}}\right]^{\beta+1}}{\left[(h_j/\mu)^{\frac{\beta-1}{\beta+2}}\right]^{\beta-2}} \leq \left[\frac{(h_{j+1}/\mu)^{\frac{\beta-1}{\beta+2}}}{(h_j/\mu)^{\frac{\beta-1}{\beta+2}}}\right]^{\beta-2} \leq \mu^{\frac{(\beta-1)(\beta-2)}{\beta+2}}.$$

Note that for $d = 2$ or $d = 3$

$$\beta - 2 = \beta - 1 - 1 > d/2 + \varepsilon - 1 \geq \varepsilon > 0.$$

Hence, we have

$$\mu^{\beta-1} \leq \mu^{\frac{(\beta-1)(\beta-2)}{\beta+2}}.$$

Combining both estimates now yields (8.15) with

$$\alpha = \sqrt{C(2\pi)^{-d/2}}(C_1 + C_2)^{1/2}\mu^{\frac{(\beta-1)(\beta-2)}{\beta+2}} = C\mu^{\frac{(\beta-1)(\beta-2)}{\beta+2}}.$$

By Theorem 8.6, we can bound

$$\begin{aligned}
\|\mathbf{v} - \mathbf{v}_n\|_{\mathbf{L}_2(\Omega)}^2 &= \|\mathbf{e}_{n-1} - \mathbf{s}_n\|_{\mathbf{L}_2(\Omega)}^2 \\
&= \|\mathbf{e}_{n-1} - \mathbf{s}_{\mathbf{e}_{n-1}}\|_{\mathbf{L}_2(\Omega)}^2 \\
&\leq \|\mathbf{e}_{n-1} - \mathbf{s}_{\mathbf{e}_{n-1}}\|_{\mathbf{H}^1(\Omega)}^2 \\
&= \|\mathbf{e}_{\mathbf{u},n-1} - \mathbf{s}_{\mathbf{e}_{\mathbf{u},n-1}}\|_{\mathbf{H}^1(\Omega)}^2 + \|e_{p,n-1} - s_{e_{p,n-1}}\|_{H^1(\Omega)}^2 \\
&\leq \|\mathbf{e}_{\mathbf{u},n-1} - \mathbf{s}_{\mathbf{e}_{\mathbf{u},n-1}}\|_{\mathbf{H}^1(\Omega)}^2 + \|e_{p,n-1} - s_{e_{p,n-1}}\|_{H^2(\Omega)}^2 \\
&\leq \left(\|\mathbf{e}_{\mathbf{u},n-1} - \mathbf{s}_{\mathbf{e}_{\mathbf{u},n-1}}\|_{\mathbf{H}^1(\Omega)} + \|e_{p,n-1} - s_{e_{p,n-1}}\|_{H^2(\Omega)}\right)^2 \\
&\leq C\delta_{n+1}^{-2(\beta+2)} h_n^{2(\beta-1)} \|\mathbf{E}\mathbf{e}_{n-1} - \mathbf{s}_{\mathbf{E}\mathbf{e}_{n-1}}\|_{\mathbf{K}_{n+1}(\mathbb{R}^d)}^2 \\
&= C\|\mathbf{E}\mathbf{e}_{n-1} - \mathbf{s}_{\mathbf{E}\mathbf{e}_{n-1}}\|_{\mathbf{K}_{n+1}(\mathbb{R}^d)}^2 \\
&= C\|\mathbf{E}\mathbf{e}_n\|_{\mathbf{K}_{n+1}(\mathbb{R}^d)},
\end{aligned}$$

where we have used the fact that

$$\frac{h_n^{\beta-1}}{\delta_{n+1}^{\beta+2}} = \mu^{\beta-1}\left(\frac{h_n}{h_{n+1}}\right)^{\beta-1} \leq \mu^{\beta-1}\left(\frac{1}{\mu\gamma}\right)^{\beta-1} = \gamma^{1-\beta}.$$

Then picking a representer p such that $\|p\|_{H^{\beta+1}(\Omega)} = \|p\|_{H^{\beta+1}(\Omega)/\mathbb{R}}$, we obtain

$$\begin{aligned}
\|\mathbf{v} - \mathbf{v}_n\|_{\mathbf{L}_2(\Omega)}^2 &\leq C\|\mathbf{E}\mathbf{e}_n\|_{\mathbf{K}_{n+1}(\mathbb{R}^d)}^2 \\
&\leq C\alpha^{2n}\|\mathbf{E}\mathbf{v}\|_{\mathbf{K}_1(\mathbb{R}^d)}^2 \\
&\leq C\alpha^{2n}\left(\|\widetilde{\mathbf{E}}_{\mathrm{div}}\mathbf{u}\|_{\widetilde{\mathbf{H}}^\beta(\mathbb{R}^d,\mathrm{div})} + \|E_S p\|_{H^{\beta+1}(\mathbb{R}^d)}\right)^2 \\
&\leq C\alpha^{2n}\left(\|\mathbf{u}\|_{\widetilde{\mathbf{H}}^\beta(\Omega,\mathrm{div})} + \|p\|_{H^{\beta+1}(\Omega)}\right)^2 \\
&\leq C\alpha^{2n}\left(\|\mathbf{u}\|_{\mathbf{H}^\beta(\Omega)} + \|p\|_{H^{\beta+1}(\Omega)}\right)^2.
\end{aligned}$$

□

In this chapter, we have discussed the convergence of a multilevel algorithm for smooth solutions of Darcy's problem and one for rough solutions of Darcy's problem. The relationship between mesh norm and support radius differs in both cases. Hence, we examine numerical test problems to provide us with an insight of how relevant the new scaling for rough target functions is.

8.6 Numerical Examples

8.6.1 Multilevel Collocation

On the unit square $\Omega = (0,1)^2$, we solve the following special case of Darcy's problem numerically

$$\begin{aligned} \mathbf{u}(x,y) - \nabla p(x,y) &= (-2x^3y + 3x^2y^2, 3x^2y^2 + 2x^3y)^T \quad \text{in} \quad \Omega, \\ \nabla \cdot \mathbf{u} &= 0 \quad \text{in} \quad \Omega, \\ \mathbf{u}(x,y) \cdot \mathbf{n}(x,y) &= -2x^3y^2 n_1(x,y) + 3x^2y^2 n_2(x,y) \quad \text{on} \quad \partial\Omega. \end{aligned} \tag{8.16}$$

The analytic solution is given by

$$\mathbf{u}(x,y) = \begin{pmatrix} -2x^3y^2 \\ 3x^2y^2 \end{pmatrix} \qquad \text{and} \qquad p(x,y) = x^3y^2 + c,$$

where c is some real number. We use $\phi_{2,3} = \phi = \psi$, which generates $H^{4.5}(\mathbb{R}^d)$. That is, $\sigma + 1 = 4.5$ or $\sigma = 3.5$. This means that

$$\delta = \nu(h/\mu)^{\frac{\sigma-1}{\sigma+1}} = \nu(h/\mu)^{5/9}.$$

We use uniform and more arbitrary data sets. For the latter, we start with a Halton point set on the finest level and construct nested data sets using the Farthest Point Algorithm, just as done before in Chapter 4. As Halton points in 1D are distributed quite uniformly anyway, we use uniform data points on the boundary. The results can be found in Tables 8.1 and 8.2 as well as 8.3 and 8.4.

Figures 8.1 and 8.2 show the multilevel collocation approximation after seven levels on uniform data sets.

8.6.2 Multilevel Escape Collocation

We choose $\mathbf{f}$ and $\mathbf{g}$ in this example such that the true solution of the velocity and the pressure are

$$\mathbf{u}(x,y) = \begin{pmatrix} -\partial_y \\ \partial_x \end{pmatrix} \phi_{2,1}(r), \qquad \text{and} \qquad p(x,y) = x^3y^2 + c, \tag{8.17}$$

where $c > 0$ and $r = \sqrt{(x-x_0)^2 + (y-y_0)^2}/\gamma$ with $x_0 = y_0 = \gamma = 0.5$. In this example the permeability tensor K shall be given by the identity matrix. We

N	H	$\|\mathbf{e_u}\|_{\mathbf{L_2}}$	$\|\mathbf{e_u}\|_{\mathbf{L}_\infty}$	$\|\mathbf{e_u}\|_{\mathbf{H^1}}$	$\|\nabla e_p\|_{L_2}$	$\|\nabla e_p\|_{L_\infty}$	$\kappa(A)$
10	2^{-1}	4.86e-1	2.17e-0	2.78e-0	7.23e-1	2.86e-0	1.4e3
34	2^{-2}	1.68e-1	1.27e-0	1.80e-0	3.21e-1	2.17e-0	2.2e4
130	2^{-3}	4.60e-2	5.84e-1	9.45e-1	9.88e-2	1.24e-1	3.0e5
514	2^{-4}	1.02e-2	2.11e-1	4.08e-1	2.30e-2	5.36e-1	4.6e6
2050	2^{-5}	1.89e-3	6.13e-2	1.48e-1	4.37e-3	1.81e-1	6.3e7
8194	2^{-6}	3.12e-4	1.48e-2	4.70e-2	7.30e-4	5.05e-2	6.5e8
32770	2^{-7}	4.83e-5	3.09e-3	1.38e-2	1.15e-4	1.19e-2	6.3e9

Table 8.1: Convergence study for Darcy's problem with basis function $\phi_{2,3}$ and support radii $\delta = \nu(h/\mu)^{5/9}$ for $\mu = 0.5$ and $\nu = 4$ on uniform data sets.

N	H	$\|\mathbf{e_u}\|_{\mathbf{L_2}}$	$\|\mathbf{e_u}\|_{\mathbf{L}_\infty}$	$\|\mathbf{e_u}\|_{\mathbf{H^1}}$	$\|\nabla e_p\|_{L_2}$	$\|\nabla e_p\|_{L_\infty}$	$\kappa(A)$
34	2^{-2}	1.53	0.77	0.62	1.17	0.40	-4.04
130	2^{-3}	1.87	1.12	0.93	1.70	0.81	-3.75
514	2^{-4}	2.18	1.48	1.21	2.10	1.21	-3.92
2050	2^{-5}	2.43	1.78	1.46	2.40	1.56	-3.78
8194	2^{-6}	2.60	2.05	1.65	2.58	1.85	-3.37
32770	2^{-7}	2.69	2.26	1.77	2.66	2.08	-3.27

Table 8.2: Approximation orders for Darcy's problem with basis function $\phi_{2,3}$ and support radii $\delta = \nu(h/\mu)^{5/9}$ for $\mu = 0.5$ and $\nu = 4$ on uniform data sets.

N	h	$\|\mathbf{e_u}\|_{\mathbf{L_2}}$	$\|\mathbf{e_u}\|_{\mathbf{L}_\infty}$	$\|\mathbf{e_u}\|_{\mathbf{H^1}}$	$\|\nabla e_p\|_{L_2}$	$\|\nabla e_p\|_{L_\infty}$	$\kappa(A)$
9	3.54e-1	5.21e-1	2.21e-0	2.86e-0	7.82e-1	2.91e-0	1.3e3
27	1.77e-1	1.58e-1	1.25e-0	1.80e-0	2.91e-1	2.04e-0	2.4e4
96	8.84e-2	4.23e-2	5.75e-1	9.20e-1	7.79e-2	1.07e-0	8.1e4
358	4.42e-2	8.14e-3	1.99e-1	3.65e-1	1.49e-2	4.02e-1	2.8e6
1369	2.21e-2	1.27e-3	5.50e-2	1.14e-1	2.57e-3	1.14e-1	1.9e7
5227	1.10e-2	2.10e-4	1.44e-2	3.61e-2	4.05e-4	3.21e-2	2.9e8
19345	5.52e-3	2.34e-5	2.68e-3	8.39e-3	7.17e-4	8.94e-3	2.9e9

Table 8.3: Convergence study for Darcy's problem with basis function $\phi_{2,3}$ and support radii $\delta = \nu(h/\mu)^{5/9}$ for $\mu = 0.5$ and $\nu = 4$. The data sets are constructed from Halton points.

N	h	$\|\mathbf{e_u}\|_{\mathbf{L_2}}$	$\|\mathbf{e_u}\|_{\mathbf{L}_\infty}$	$\|\mathbf{e_u}\|_{\mathbf{H^1}}$	$\|\nabla e_p\|_{L_2}$	$\|\nabla e_p\|_{L_\infty}$	$\kappa(A)$
27	3.54e-1	1.72	0.82	0.66	1.43	0.51	-4.20
96	1.77e-1	1.90	1.12	0.97	1.90	0.93	-1.74
358	8.84e-2	2.38	1.53	1.33	2.39	1.41	-5.12
1369	4.42e-2	2.69	1.85	1.68	2.53	1.81	-2.75
5227	2.21e-2	2.59	1.94	1.66	2.67	1.83	-3.96
19345	5.52e-3	3.16	2.43	2.10	2.50	1.84	-3.32

Table 8.4: Approximation orders for Darcy's problem with basis function $\phi_{2,3}$ and support radii $\delta = \nu(h/\mu)^{5/9}$ for $\mu = 0.5$ and $\nu = 4$. The data sets are constructed from Halton points.

N	H	$\|\mathbf{e_u}\|_{\mathbf{L_2}}$	$\|\mathbf{e_u}\|_{\mathbf{L}_\infty}$	$\|\mathbf{e_u}\|_{\mathbf{H^1}}$	$\|\nabla e_p\|_{L_2}$	$\|\nabla e_p\|_{L_\infty}$	$\kappa(A)$
10	2^{-1}	1.72e0	4.23e0	1.80e1	6.92e-1	2.98e0	1.4e3
34	2^{-2}	1.38e0	3.00e0	1.53e1	1.09e0	3.79e0	2.2e4
130	2^{-3}	1.19e-1	6.44e-1	3.19e0	1.26e-1	1.52e0	3.0e5
514	2^{-4}	1.74e-2	1.62e-1	8.75e-1	2.77e-2	6.37e-1	4.6e6
2050	2^{-5}	2.83e-3	4.05e-2	2.56e-1	5.14e-3	2.09e-1	6.3e7
8194	2^{-6}	4.20e-4	9.40e-3	7.24e-2	8.45e-4	5.71e-2	6.5e8
32770	2^{-7}	5.84e-5	2.35e-3	2.07e-2	1.32e-4	1.33e-2	6.3e9

Table 8.5: Convergence study for Darcy's problem with basis function $\phi_{2,3}$ and support radii $\delta = \nu(h/\mu)^{5/9}$ for $\mu = 0.5$ and $\nu = 4$ on uniform data sets. We approximate a rough solution in $\mathbf{H}^{\beta+1}(\Omega)$ with $\beta < 2$.

N	H	$\|\mathbf{e_u}\|_{\mathbf{L_2}}$	$\|\mathbf{e_u}\|_{\mathbf{L}_\infty}$	$\|\mathbf{e_u}\|_{\mathbf{H^1}}$	$\|\nabla e_p\|_{L_2}$	$\|\nabla e_p\|_{L_\infty}$	$\kappa(A)$
34	2^{-2}	0.32	0.50	0.24	-0.65	-0.35	-4.04
130	2^{-3}	3.53	2.22	2.26	3.11	1.32	-3.75
514	2^{-4}	2.78	1.99	1.87	2.19	1.25	-3.93
2050	2^{-5}	2.62	2.00	1.77	2.43	1.61	-3.78
8194	2^{-6}	2.75	2.11	1.82	2.60	1.87	-3.37
32770	2^{-7}	2.84	2.00	1.81	2.68	2.10	-3.27

Table 8.6: Approximation orders for Darcy's problem with basis function $\phi_{2,3}$ and support radii $\delta = \nu(h/\mu)^{5/9}$ for $\mu = 0.5$ and $\nu = 4$ on uniform data sets. We approximate a rough solution in $\mathbf{H}^{\beta+1}(\Omega)$ with $\beta < 2$.

recall from Chapter 6, that $\phi_{2,1}$ lies in $H^\alpha(\mathbb{R}^d)$ with $\alpha < 2\tau - d/2$, where $\tau := d/2 + k + 1/2 = 2.5$. That is, due to the derivative in our definition of the solution to Darcy's problem, we have $\mathbf{u} \in \mathbf{H}^{\beta+1}(\Omega)$ for $\beta < 2$.

In this case, Theorem 8.16 guarantees convergence for

$$\delta = \nu h^{\frac{\beta-1}{\beta+2}}.$$

Choosing the supremum $\beta = 2$, we would have an exponent of $1/4$. However, we try the scaling from the previous, nonescape case, namely

$$\delta = \nu h^{\frac{\sigma-1}{\sigma+1}}.$$

Since $\sigma + 1 = 4.5$, this yields an exponent of $5/9$. Tables 8.5 and 8.6 show the results. Here, the errors for the velocity and pressure are given by $\mathbf{e_u} = \mathbf{u} - \mathbf{s_u}$ and $e_p = p - s_p$, respectively. Even though we use a weaker scaling, in the sense that the support radii tend faster to zero than Theorem 8.16 suggests, we still seem to obtain convergence.

Figures 8.3 and 8.4 show the multilevel collocation approximation after seven levels.

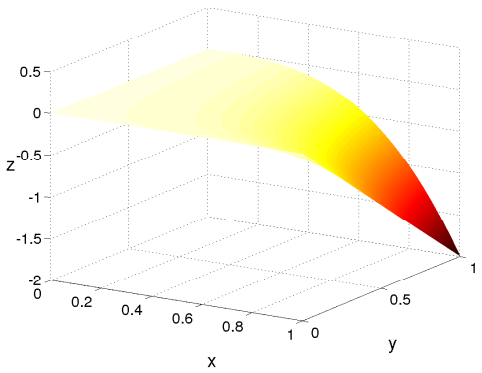

(a) u_1

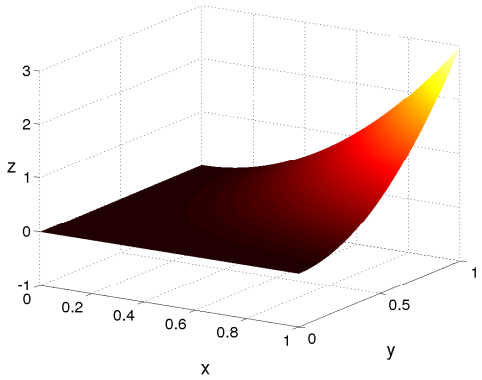

(b) u_2

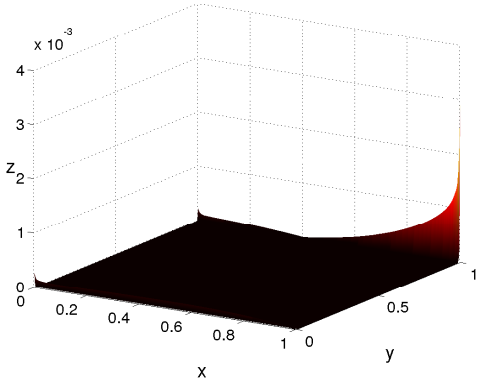

(c) e_1

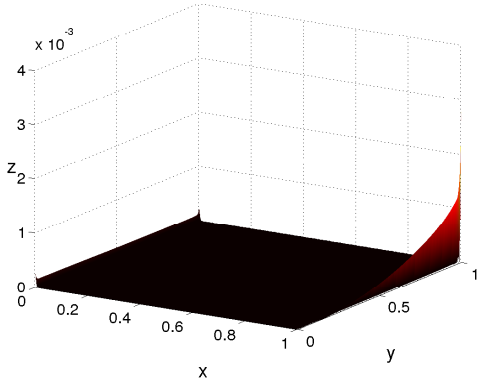

(d) e_2

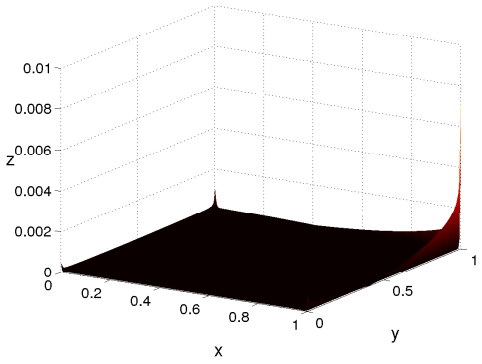

(e) $(L\mathbf{u})_1$

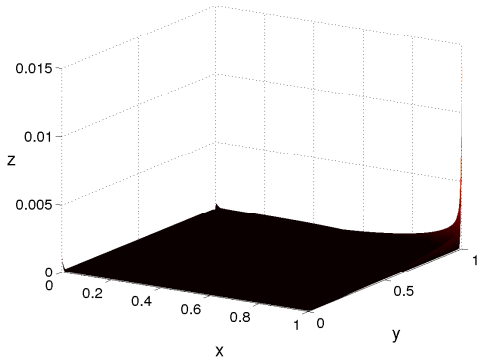

(f) $(L\mathbf{u})_2$

Figure 8.1: Both components of multilevel approximation, corresponding errors and residuals of Darcy's problem (8.16) after seven levels, using a basis function $\phi_{2,3}$, $\mu = 0.5$ and $\nu = 4$ on uniform data.

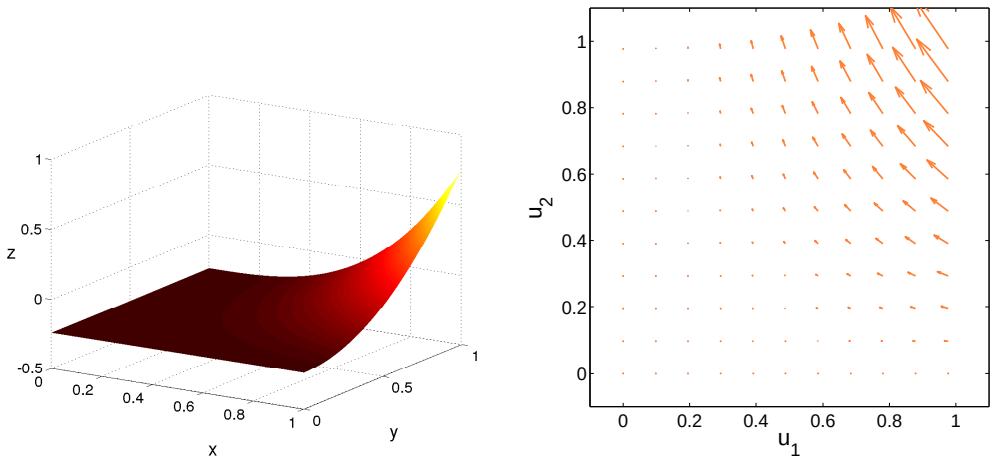

(a) Pressure p (b) Vector field $\mathbf{u}$

Figure 8.2: Pressure p and vector field $\mathbf{u}$ of Darcy's problem (8.16) after seven levels, using a basis function $\phi_{2,3}$, $\mu = 0.5$ and $\nu = 4$ on uniform data.

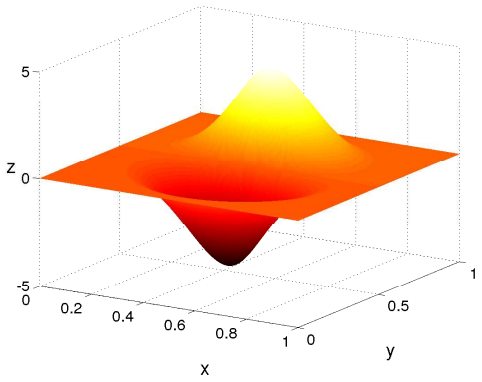

(a) u_1

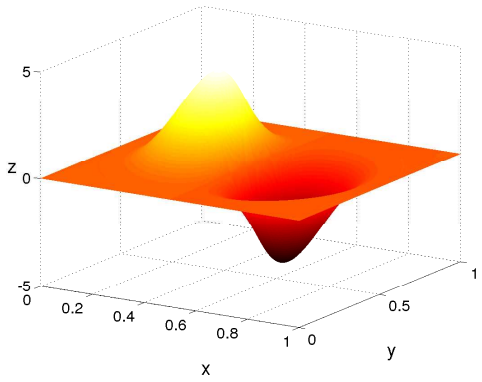

(b) u_2

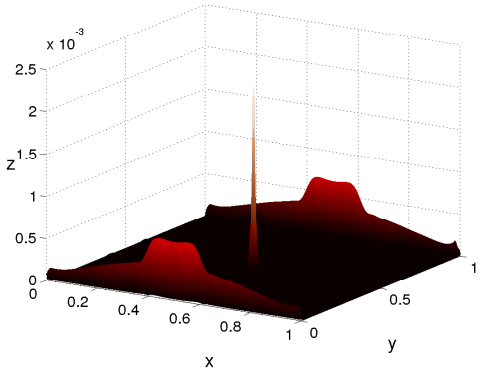

(c) e_1

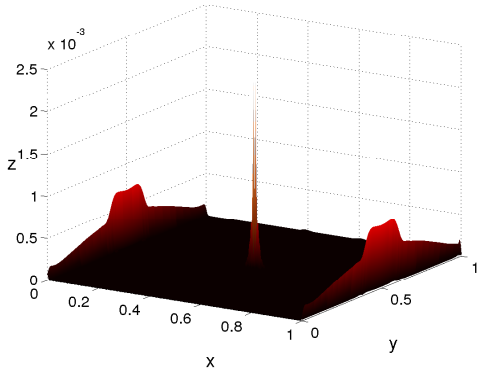

(d) e_2

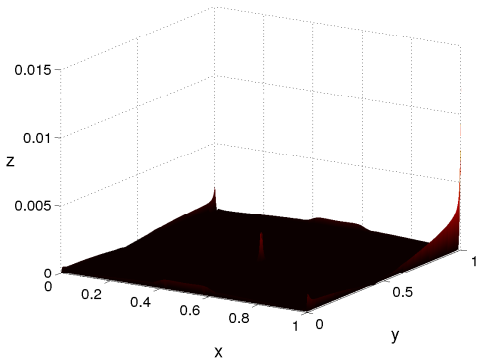

(e) $(L\mathbf{u})_1$

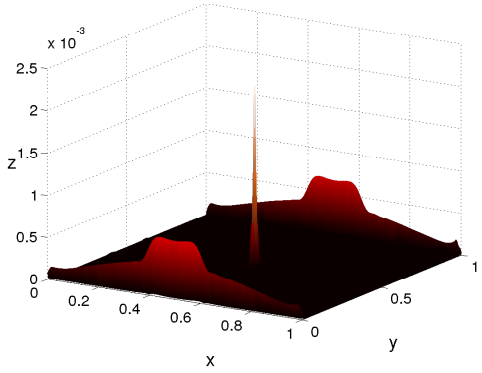

(f) $(L\mathbf{u})_2$

Figure 8.3: Both components of multilevel approximation, corresponding errors and residuals of Darcy's problem with data generated from (8.17) after seven levels, using a basis function $\phi_{2,3}$, $\mu = 0.5$ and $\nu = 4$ on uniform data.

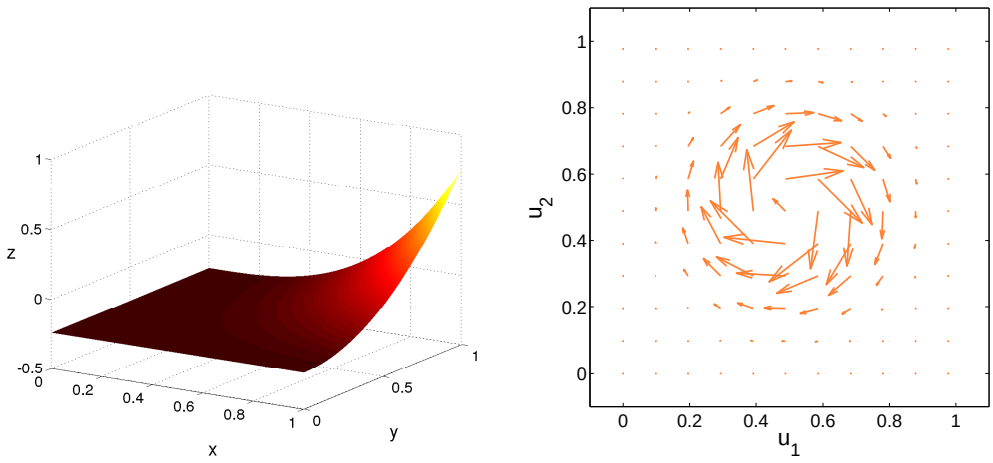

(a) Pressure p (b) Vector field $\mathbf{u}$

Figure 8.4: Pressure p and vector field $\mathbf{u}$ of Darcy's problem with data generated from (8.17) after seven levels, using a basis function $\phi_{2,3}$, $\mu = 0.5$ and $\nu = 4$ on uniform data.

Chapter 9

Summary and Future Work

In this thesis, we have analysed a multilevel collocation approach involving compactly supported radial basis functions from a theoretical as well as numerical point of view. The key idea is to approximate the residual on increasinlgly finer levels. After introducing the necessary theory of reproducing kernel Hilbert spaces, we focussed on linear second-order elliptic boundary problems as well as Darcy's problem, often used in physical applications to model groundwater flow. Whereas in the former case we used scalar-valued positive definite kernels for constructing multilevel approximants, in the latter case we used divergence-free matrix-valued kernels. We then developed a multilevel theory and were able to show convergence results. A similar result was presented for interpolating divergence-free vector fields.

Even though it had been observed more than a decade ago that the stationary setting, i. e. when the support radii shrink as fast as the mesh norm, does not lead to convergence, it was up to now an open question how the support radii should depend on the mesh norm to ensure convergence. For each of the above cases this question has been answered.

As opposed to multilevel interpolation schemes, the condition numbers of multilevel collocation matrices are not independent of the scale. We gave explicit bounds on their growth and focused on three improvements. Firstly, a diagonal preconditioner helped to significantly improve the theoretical and numerical results for the condition numbers. Secondly, we generalised Wahba's regularisation theory to the case where several smoothing parameters (here one for the boundary and one for the interior) are involved. This also led to better bounds for the condition numbers – in fact this regularisation technique could be interpreted as a special preconditioning strategy. And lastly, we used the alternating projection method to approximate the block collocation matrix by alternating between two smaller systems.

The standard multilevel convergence results require the solution to the PDE and its numerical approximation to be in the same Sobolev space. This might be undesirable if the smoothness of the PDE is not known a priori. Therefore, so-called *escape* results were investigated and proven to converge. The numerical results corroborate (where possible) the theoretical findings.

Finally, we discuss future research areas. There are several possibilities to extend the work in this thesis:

(1) Even though we were able to show convergence of the multilevel collocation methods presented in this thesis, theoretically verifying the numerically observed approximation orders remains still an open problem.

(2) The diagonal preconditioner investigated in Chapter 5 was shown to improve the condition number considerably. Yet, there is still room for improvement. For example, one could try a sparse approximate inverse preconditioner [40]. Possibly this could be combined with a completely different approach by Jerome and Fasshauer. In [25], they introduce a smoothing operator, which might be used to overcome the difficulty that the differential operator leads to a nonproportional relationship between mesh norm and support radius.

(3) RBFs have been successfully used for advection problems [4, 90]. One advantage of the collocation method presented here is that even problems where convection dominates diffusion would be approximated by discrete symmetric and positive definite linear systems. Hence, numerically challenging problems like boundary layers theoretically could be solved by a relatively well-behaved system – unlike for finite difference or finite element methods, which run into difficulties here. This could be exploited. But possibly even then an adaptive strategy is needed.

(4) So far the angle in the alternating projection method was only shown to be nonzero. However, it would be more useful to have a closed expression of the angle or at least reliable bounds.

(5) One could also discuss the stability of the level matrices for multilevel collocation for Darcy's problem. But since one-shot results are readily available in [74], it should be possible to extend these to multilevel collocation matrices. Since Darcy's problem is a first-order PDE system, the bound on the condition number should be slightly better than for second-order elliptic collocation. This I could already verify with numerical results. However, the analysis will be complicated by the fact that the multilevel collocation method for Darcy's problem is based on matrix-valued kernels.

Bibliography

[1] J. Bear, *Dynamics of Fluids in Porous Media*, American Elsevier Publishing Company, New York, 1972.

[2] R. K. Beatson, W. A. Light, and S. Billings, *Fast Solution of the Radial Basis Function Interpolation Equations: Domain Decomposition Methods*, SIAM J. Sci. Comput. **22** (2000), no. 5, 1717–1740.

[3] R. Beatson, H.-Q. Bui, and J. Levesley, *Embeddings of Beppo-Levi Spaces in Hölder-Zygmund Spaces, and a New Method for Radial Basis Function Interpolation Error Estimates*, J. Approx. Theory **137** (2005), no. 2, 166–178.

[4] J. Behrens and A. Iske, *Grid-free Adaptive Semi-Lagrangian Advection Using Radial Basis Functions*, Comput. Math. Appl. **43** (2002), 319–327.

[5] A. Ben-Israel and T. Greville, *Generalized Inverses: Theory and Applications*, CMS Books in Mathematics, Springer, Berlin, 2003.

[6] D. Braess, *Finite Elemente*, 4 ed., Springer, Berlin, 2007.

[7] S. C. Brenner and L. R. Scott, *The Mathematical Theory of Finite Element Methods*, 3rd ed., Texts in Applied Mathematics, vol. 15, Springer, New York, 2008.

[8] R. Brownlee and W. Light, *Approximation Orders for Interpolation by Surface Splines to Rough Functions*, IMA J. Numer. Anal. **24** (2004), no. 2, 179–192.

[9] M. D. Buhmann, *Radial Basis Functions: Theory and Implementations*, Cambridge Monographs on Applied and Computational Mathematics, vol. 12, Cambridge University Press, Cambridge, 2003.

[10] D. Busby, C. L. Farmer, and A. Iske, *Hierarchical Nonlinear Approximation for Experimental Design and Statistical Data Fitting*, SIAM J. Sci. Comput. **29** (2007), no. 1, 49–69.

[11] R. Chen and Z. Wu, *Solving Hyperbolic Conservation Laws Using Multiquadric Quasi-Interpolation*, Numer. Methods Partial Differential Equations **22** (2006), no. 4, 776–796.

[12] R. Chen and Z. Wu, *Solving Partial Differential Equation by Using Multiquadric Quasi-Interpolation*, Appl. Math. Comput. **186** (2007), no. 2, 1502–1510.

[13] A. Chernih and Q. T. L. Gia, *Multiscale Methods with Compactly Supported Radial Basis Functions for the Stokes Problem on Bounded Domains*, preprint (2013).

[14] A. Chernih and S. Hubbert, *Closed Form Representations and Properties of the Generalised Wendland Functions*, J. Approx. Theory **177** (2014), 17–33.

[15] F. Cucker and D. X. Zhou, *Learning Theory: An Approximation Theory Viewpoint*, Cambridge University Press, Cambridge, 2007.

[16] O. Davydov and D. T. Oanh, *On the Optimal Shape Parameter for Gaussian Radial Basis Function Finite Difference Approximation of the Poisson Equation*, Comput. Math. Appl. **62** (2011), no. 5, 2143–2161.

[17] P. Deuflhard and M. Weiser, *Adaptive Numerical Solution of PDEs*, Walter de Gruyter & Co., Hawthorne, 2012.

[18] N. Dyn and A. Ron, *Radial Basis Function Approximation: From Gridded Centers to Scattered Centers*, Proc. London Math Soc. **71** (1995), 76–108.

[19] H. C. Elman, D. J. Silvester, and A. J. Wathen, *Finite Elements and Fast Iterative Solvers: with Applications in Incompressible Fluid Dynamics*, Numerical Mathematics and Scientific Computation, Oxford University Press, Oxford, 2005.

[20] L. C. Evans, *Partial Differential Equations*, Graduate Studies in Mathematics, vol. 19, American Mathematical Society, Providence, 1998.

[21] C. L. Farmer, *Bayesian Field Theory Applied to Scattered Data Interpolation and Inverse Problems*, Algorithms for Approximation (A. Iske and J. Levesley, eds.), Springer, 2007, 147–166.

[22] P. Farrell and H. Wendland, *RBF Multiscale Collocation for Second Order Elliptic Boundary Value Problems*, SIAM J. Numer. Anal. **51** (2013), no. 4, 2403–2425.

[23] G. E. Fasshauer, *Solving Differential Equations with Radial Basis Functions: Multilevel Methods and Smoothing*, Adv. Comput. Math. **11** (1999), no. 2-3, 139–159.

[24] G. E. Fasshauer, *Meshfree Approximation Methods with MATLAB*, Interdisciplinary Mathematical Sciences, vol. 6, World Scientific Publishing, Hackensack, 2007.

[25] G. E. Fasshauer and J. W. Jerome, *Multistep Approximation Algorithms: Improved Convergence Rates through Postconditioning with Smoothing Kernels*, Adv. Comput. Math. **10** (1999), no. 1, 1–27.

[26] T. Feder and D. Greene, *Optimal Algorithms for Approximate Clustering*, Proceedings of the Twentieth Annual ACM Symposium on Theory of Computing (New York, USA), STOC '88, ACM, 1988, 434–444.

[27] M. S. Floater and A. Iske, *Multistep Scattered Data Interpolation using Compactly Supported Radial Basis Functions*, J. Comput. Appl. Math. **73** (1996), no. 1-2, 65–78.

[28] N. Flyer and G. B. Wright, *Transport Schemes on a Sphere using Radial Basis Functions.*, J. Comput. Physics **226** (2007), no. 1, 1059–1084.

[29] N. Flyer, G. B. Wright, and B. Fornberg, *Radial Basis Function-Generated Finite Differences: A Mesh-free Method for Computational Geosciences*, Handbook of Geomathematics (W. Freeden, Z. Nashed, and T. Sonar, eds.), Springer, 2nd ed., 2014 (in press).

[30] B. Fornberg and E. Lehto, *Stabilization of RBF-generated Finite Difference Methods for Convective PDEs*, J. Comput. Phys. **230** (2011), no. 6, 2270–2285.

[31] B. Fornberg and C. Piret, *On Choosing a Radial Basis Function and a Shape Parameter when Solving a Convective PDE on a Sphere*, J. Comput. Phys. **227** (2008), no. 5, 2758–2780.

[32] C. Franke and R. Schaback, *Solving Partial Differential Equations by Collocation Using Radial Basis Functions*, Adv. Comput. Math. **93** (1998), no. 1, 73–82.

[33] C. Franke and R. Schaback, *Convergence Order Estimates of Meshless Collocation Methods Using Radial Basis Functions.*, Adv. Comput. Math. **8** (1998), no. 4, 381–399.

[34] R. Franke, *A Critical Comparison of Some Methods for Interpolation of Scattered Data*, Final report, Defense Technical Information Center, Naval Postgraduate School Monterey, 1979.

[35] E. J. Fuselier, *Improved Stability Estimates and a Characterization of the Native Space for Matrix-Valued RBFs*, Adv. Comput. Math. **29** (2008), no. 3, 269–290.

[36] E. J. Fuselier, *Sobolev-Type Approximation Rates for Divergence-Free and Curl-Free RBF Interpolants.*, Math. Comput. **77** (2008), no. 263, 1407–1423.

[37] P. Giesl and H. Wendland, *Meshless Collocation: Error Estimates with Application to Dynamical Systems*, SIAM J. Numer. Anal. **45** (2007), no. 4, 1723–1741.

[38] D. Gilbarg and N. S. Trudinger, *Elliptic Partial Differential Equations of Second Order*, Classics in Mathematics, Springer, Berlin, 2001, Reprint of the 1998 edition.

[39] G. H. Golub and C. F. Van Loan, *Matrix Computations*, 3 ed., Johns Hopkins University Press, Baltimore, 1996.

[40] M. J. Grote and T. Huckle, *Parallel Preconditioning with Sparse Approximate Inverses*, SIAM J. Sci. Comput. **18** (1997), no. 3, 838–853.

[41] S. J. Hales and J. Levesley, *Error Estimates for Multilevel Approximation Using Polyharmonic Splines*, Numer. Algorithms **30** (2002), no. 1, 1–10.

[42] J. Halton, *On the Efficiency of Certain Quasi-Random Sequences of Points in Evaluating Multi-Dimensional Integrals*, Numer. Math. **2** (1960), no. 1, 84–90.

[43] Y. Hon and R. Schaback, *On Unsymmetric Collocation by Radial Basis Functions*, Appl. Math. Comput. **119** (2001), no. 2-3, 177–186.

[44] A. Iske, *Multiresolution Methods in Scattered Data Modelling*, Lecture Notes in Computational Science and Engineering, vol. 37, Springer, Berlin, 2004.

[45] A. Iske and J. Levesley, *Multilevel Scattered Data Approximation by Adaptive Domain Decomposition*, Numer. Algorithms **39** (2005), no. 1-3, 187–198.

[46] E. Kansa, *Multiquadrics - A Scattered Data Approximation Scheme with Applications to Computational Fluid-Dynamics I Surface Approximations and Partial Derivative Estimates*, Comput. Math. Appl. **19** (1990), no. 8-9, 127–145.

[47] P. Knabner and L. Angermann, *Numerical Methods for Elliptic and Parabolic Partial Differential Equations*, Texts in Applied Mathematics, vol. 44, Springer, New York, 2003.

[48] E. Larsson and B. Fornberg, *A Numerical Study of Some Radial Basis Function Based Solution Methods for Elliptic PDEs*, Comput. Math. Appl. **46** (2003), 891–902.

[49] Q. T. Le Gia, I. H. Sloan, and H. Wendland, *Multiscale Analysis in Sobolev Spaces on the Sphere.*, SIAM J. Numer. Anal. **48** (2010), no. 6, 2065–2090.

[50] Q. T. Le Gia, I. H. Sloan, and H. Wendland, *Multiscale RBF Collocation for Solving PDEs on Spheres*, Numer. Math. **121** (2012), no. 1, 99–125.

[51] R. J. LeVeque, *Finite-Volume Methods for Hyperbolic Problems*, Cambridge University Press, Cambridge, 2002.

[52] J. Levesley and X. Sun, *Approximation in Rough Native Spaces by Shifts of Smooth Kernels on Spheres*, J. Approx. Theory **133** (2005), no. 2, 269–283.

[53] J. Levesley and X. Sun, *Corrigendum to and Two Open Questions Arising from the Article: Approximation in Rough Native Spaces by Shifts of Smooth Kernels on Spheres*, J. Approx. Theory **138** (2006), no. 1, 124–127.

[54] J. Li, A. H.-D. Cheng, and C.-S. Chen, *A Comparison of Efficiency and Error Convergence of Multiquadric Collocation Method and Finite Element Method*, Eng. Anal. Bound. Elem. **27** (2003), no. 3, 251–257.

[55] S. Lowitzsch, *A Density Theorem for Matrix-Valued Radial Basis Functions*, Numer. Algorithms **39** (2005), no. 1-3, 253–256.

[56] S. Lowitzsch, *Error Estimates for Matrix-Valued Radial Basis Function Interpolation*, J. Approx. Theory **137** (2005), no. 2, 238–249.

[57] S. Lowitzsch, *Matrix-Valued Radial Basis Functions: Stability Estimates and Applications*, Adv. Comput. Math. **23** (2005), no. 3, 299–315.

[58] W. R. Madych and S. A. Nelson, *Multivariate Interpolation and Conditionally Positive Definite Functions. II*, Math. Comp. **54** (1990), no. 189, 211–230.

[59] A. Majda and A. Bertozzi, *Vorticity and Incompressible Flow*, Cambridge Texts in Applied Mathematics, Cambridge University Press, Cambridge, 2002.

[60] G. Matheron, *Principles of Geostatistics*, Economic Geology **58** (1963), no. 8, 1246–1266.

[61] K. W. Morton and D. F. Mayers, *Numerical Solution of Partial Differential Equations: An Introduction*, Cambridge University Press, Cambridge, 2005.

[62] F. Narcowich and J. Ward, *Scattered-Data Interpolation on $\mathbb{R}^d$: Error Estimates for Radial Basis and Band-Limited Functions*, SIAM J. Math. Anal. **36** (2004), no. 1, 284–300.

[63] F. J. Narcowich, *Recent Developments in Error Estimates for Scattered-Data Interpolation via Radial Basis Functions*, Numer. Algorithms **39** (2005), no. 1-3, 307–315.

[64] F. J. Narcowich, R. Schaback, and J. D. Ward, *Multilevel Interpolation and Approximation*, Appl. Comput. Harmon. Anal. **7** (1999), no. 3, 243–261.

[65] F. J. Narcowich and J. D. Ward, *Generalized Hermite Interpolation Via Matrix-Valued Conditionally Positive Definite Functions*, Math. Comp. **63** (1994), no. 208, 661–687.

[66] F. J. Narcowich and J. D. Ward, *Scattered Data Interpolation on Spheres: Error Estimates and Locally Supported Basis Functions*, SIAM J. Math. Anal. **33** (2002), no. 6, 1393–1410.

[67] F. J. Narcowich, J. D. Ward, and H. Wendland, *Sobolev Bounds on Functions with Scattered Zeros, with Applications to Radial Basis Function Surface Fitting*, Math. Comp. **74** (2005), no. 250, 743–763.

[68] F. J. Narcowich, J. D. Ward, and H. Wendland, *Sobolev Error Estimates and a Bernstein Inequality for Scattered Data Interpolation via Radial Basis Functions*, Constr. Approx. **24** (2006), no. 2, 175–186.

[69] S. Neuman, *Theoretical Derivation of Darcy's Law*, Acta Mech. **25** (1977), no. 3-4, 153–170.

[70] C. Piret, *The Orthogonal Gradients Method: A Radial Basis Functions Method for Solving Partial Differential Equations on Arbitrary Surfaces*, J. Comput. Phys. **231** (2012), no. 14, 4662–4675.

[71] M. J. D. Powell, *The Theory of Radial Basis Function Approximation in 1990*, Advances in Numerical Analysis: Volume II: Wavelets, Subdivision Algorithms, and Radial Basis Functions (W. A. Light, ed.), Oxford University Press, Oxford, 1992, 105–210.

[72] R. Schaback, *Error Estimates and Condition Numbers for Radial Basis Function Interpolation*, Adv. Comput. Math. **3** (1995), no. 3, 251–264.

[73] D. Schräder, *Analytically Divergence-Free Discretization Methods for Darcy's Problem*, Ph.D. thesis, University of Sussex, 2009.

[74] D. Schräder and H. Wendland, *A High-Order, Analytically Divergence-Free Discretization Method for Darcy's Problem.*, Math. Comput. **80** (2011), no. 273, 263–277.

[75] D. Schräder and H. Wendland, *An Extended Error Analysis for a Meshfree Discretization Method of Darcy's Problem.*, SIAM J. Numer. Anal. **50** (2012), no. 2, 838–857.

[76] K. Smith, D. Solmon, and S. Wagner, *Practical and Mathematical Aspects of the Problem of Reconstructing Objects from Radiographs*, Bull. Amer. Math. Soc. **83** (1977), 1227–1270.

[77] E. M. Stein, *Singular Integrals and Differentiability Properties of Functions*, Princeton Mathematical Series, No. 30, Princeton University Press, Princeton, 1970.

[78] M. Stein, *Interpolation of Spatial Data: Some Theory for Kriging*, Springer Series in Statistics, Springer, Berlin, 1999.

[79] L. N. Trefethen, *Spectral Methods in MATLAB*, Society for Industrial and Applied Mathematics, Philadelphia, 2000.

[80] G. Wahba, *Spline Models for Observational Data*, CBMS-NSF Regional Conference Series in Applied Mathematics, vol. 59, Society for Industrial and Applied Mathematics, Philadelphia, 1990.

[81] H. Wendland, *Piecewise Polynomial, Positive Definite and Compactly Supported Radial Functions of Minimal Degree*, Adv. Comput. Math. **4** (1995), no. 4, 389–396.

[82] H. Wendland, *Meshless Galerkin Methods using Radial Basis Functions*, Math. Comput. **68** (1999), no. 228, 1521–1531.

[83] H. Wendland, *Solving Large Generalized Interpolation Problems Efficiently*, Advances in Constructive Approximation, Nashboro Press, 2004, 509–518.

[84] H. Wendland, *Scattered Data Approximation*, Cambridge Monographs on Applied and Computational Mathematics, vol. 17, Cambridge University Press, Cambridge, 2005.

[85] H. Wendland, *On the Stability of Meshless Symmetric Collocation for Boundary Value Problems*, BIT **47** (2007), no. 2, 455–468.

[86] H. Wendland, *Divergence-Free Kernel Methods for Approximating the Stokes Problem*, SIAM J. Numer. Anal. **47** (2009), no. 4, 3158–3179.

[87] H. Wendland, *Multiscale Analysis of Sobolev Spaces on Bounded Domains*, Numer. Math. **116** (2010), no. 3, 493–517.

[88] H. Wendland and C. Rieger, *Approximate Interpolation with Applications to Selecting Smoothing Parameters*, Numer. Math **101** (2005), 643–662.

[89] J. Wloka, *Partial Differential Equations*, Cambridge University Press, Cambridge, 1987.

[90] G. B. Wright, N. Flyer, and D. A. Yuen, *A Hybrid Radial Basis Function-Pseudospectral Method for Thermal Convection in a 3-D Spherical Shell*, Geochemistry, Geophysics, Geosystems **11** (2010), no. 7, Q07003.

[91] K. Yosida, *Functional Analysis*, 6th ed., Grundlehren der Mathematischen Wissenschaften, vol. 123, Springer, Berlin, 1980.